UNIVERSITY
of
GLASGOW

Molecular Analysis of Rat A_3 Adenosine Receptor Regulation

Gail Ferguson BSc. MSc.

This thesis is presented for the degree of
Doctor of Philosophy
May 2001

Institute of Biomedical and Life Sciences
University of Glasgow

Acknowledgements

I would like to thank the following people for the help and support they have given me throughout this project:

My supervisor, Dr Tim Palmer, for guidance and advice in writing this thesis and the unique manner in which he gives constructive criticism. Grateful thanks also go to Prof. Graeme Milligan for making available the facilities of the Department of Biochemistry and Molecular Biology, and for being so generous in the early days of my research. I also acknowledge the British Heart Foundation for funding this project.

Thanks also go to past and present members of the Department. For fear of missing someone out I will refrain from naming you all, but thanks for the banter guys!

Lastly, special thanks go to my parents and family for putting up with my moods and without whose love and support this work would not have been possible.

Abbreviations

^{125}I-AB-MECA	^{125}I-4-aminobenzyl-5'-N-methylcarboxamidoadenosine
2Cl-IB-MECA	2-chloro-IB-MECA
5-HT	5-hydroxytrptamine
α_{1B} AdR	alpha 1B adrenergic receptor
A23187	Calcimycin, ionophore highly selective for Ca^{2+}
aa	amino acid
AC	adenylyl cyclase
ACE	angiotensin converting enzyme
ADA	adenosine deaminase
ADP	adenosine diphosphate
Ala	alanine
AMP	adenosine monophosphate
AngI	angiotensin I
AngII	angiotensin II
AP	adapter protein
APNEA	N-[2-(4-aminophenyl)ethyl]adenosine
AR	adenosine receptor
ATP	adenosine triphosphate
β-AdR	beta adrenergic receptor
β-ARK	beta adrenergic receptor kinase
βARK-CT	aa's 495-689 of β-ARK
BCA	bichinchonic acid
B_{max}	maximum expression level
BSA	bovine serum albumin
Ca^{2+}	calcium ion
cAMP	adenosine-3',5'- monophosphate
CCPA	2-chloro-N^6-cyclopentyladenosine
CCV	clathrin coated vesicle
cDNA	complementary deoxy ribonucleic acid
cGMP	guanosine-3',5'- monophospahte
CHAPS	3-[(3-Cholamidopropyl)-dimethylammonio]-1-propane sulfonate

CHO	Chinese Hamster Ovary
CPA	N^6-cyclopentyladenosine
cpm	counts per minute
CSC	8-(3-chlorostyryl)caffeine
C-terminal	Carboxyl/COOH-terminal
CTX	Cholera toxin
Cys	cysteine
Da	Dalton
DCC	deleted in colorectal cancer
DEAE-dextran	(diethylaminoethyl)-dextran
DMEM	Dulbecco's Modified Eagle's Medium
DMSO	dimethyl sulphoxide
dNTP	deoxynucleoside triphosphate
DPCPX	1,3-dipropyl-8-cyclopentylxanthine
D_1R	Dopamine 1 receptor
DRY	Asp-Arg-Tyr
DTT	dithiothreitol
E1	ubiquitin activating enzyme
E2	ubiquitin carrier protein
E3	ubiquitin protein-ligase
EC_{50}	concentration of the competitor required to compete for half the specific binding
ECL	enhanced chemiluminescence
EDTA	diaminoethanetetra-acetic acid disodium salt
EGFP	enhanced green flourescent protein
EGFR	epidermal growth factor receptor
EHNA	erythro-9(2-hydroxy-3-nonyl)adenine
ER	endoplasmic reticulum
ERK	extracellular regulated kinase
ET	Endothelin
FBS	foetal bovine serum
FRET	flouresence resonance energy transfer
G protein	guanine nucleotide binding regulatory protein
Gab1	Grb2-associated binding protein 1

GABA	γ-amino butyric acid
GDP	guanosine diphosphate
GFP	green fluorescent protein
G_i	G protein originally identified as inhibitor of adenylyl cyclase
GnRHR	gonadotrophin releasing hormone receptor
GPCR	G protein-coupled receptor
Grb2	growth factor receptor-binding protein
GRK	G protein-coupled receptor kinase
G_s	stimulatory G protein of adenylyl cyclase
GST	glutathione-S-transferase
GTP	guanine triphosphate
HA	haemagglutinin
HDAT	Human dopamine transporter
HEK 293	Human Embryonic Kidney 293
HEPES	N-2-hydroxyethylpiperazine-N'-2-ethanosulfonic acid
HRP	horseradish peroxidase
IB-MECA	N6-(3-iodobenzyl)-5'-(N-methylcarbomoyl)adenosine
IC_{50}	concentration of the competitor required to inhibit half the specific binding
IGF	insulin derived growth factor
IgG	immunoglobulin G
IL-8	interleukin-8
IP_3	inositol trisphosphate
JNK	c-Jun N-terminal kinase
Kan	kanomycin
K_d	concentration of ligand that will bind to half the receptors at equilibrium
K_i	affinity of the receptor for the competing drug
KRHB	Krebs-Ringer-HEPES -BSA
L-268605	(3-(4-methoxyphenyl)-5-amino-7-oxo thiazolo[3,2]pyrimidine)
LDL	low density lipoprotein
LH	leutenising hormone

mAchR	muscarinic acetylcholine receptor
MAPK	mitogen-activated protein kinase
mGluR	metabotropic glutamate receptor
mRNA	messenger ribonucleic acid
MRS1523	5-propyl-2-ethyl-4-propyl-3-(ethylsulfanylcarbonyl)-6-
mSOS	mammalian son-of-sevenless
MT	microtubule
NBCS	new-born calf serum
NECA	5'-N-ethylcarboxamidoadenosine
N-terminal	amino/NH_2-terminal
ORFs	open reading frames
p21Ras	product from the *ras* family of genes coding for 21kDa GTP-binding proteins
PBS	phosphate buffered saline
PBS-CM	PBS supplemented with 0.1mM $CaCl_2$ and 1mM $MgCl_2$
PC12	rat pheochromocytoma 12 cell line
PCR	polymerase chain reaction
PDE	phosphodiesterase
PH	pleckstrin homology
PKA	protein kinase A
PKC	protein kinase C
PLA_2	phospholipase A_2
PLC	phospholipase C
PM	plasma membrane
PMA	phorbol 12-myristate 13-acetate
PMSF	phenylmethylsulphonylfluoride
PTX	Pertussis toxin
RBL-2H3	rat basophilic leukaemia cells
RIPA	radioimmunoprecipitation buffer
RIPA-AMS	RIPA supplemented with 2M ammonium sulphate
RK	rhodopsin kinase
(R)-PIA	R-N^6-(phenylisopropyl)adenosine
RTK	receptor tyrosine kinase

SAH	S-adenosylhomocysteine
SAM	S-adenosyl methionine
SDS-PAGE	sodium dodecyl sulfate-polyacrylamide gel electrophoresis
SE	standard error
Ser	Serine
SH	Src homology
Shc	Src homology 2 domain containing protein
$t_{½}$	time required to see 50% effect
TAE	tris-acetate-EDTA
TEMED	N,N,N',N'-tetramethylethylenediamine
Tfn	transferrin
TGN	trans-Golgi network
Thr	threonine
TM	transmembrane
TRHR	thyrotropin releasing hormone receptor
Tyr	tyrosine
UDP	uridine diphosphate
UV	ultraviolet
V_2R	vasopressin 2 receptor
VSV	vesicular stomatitis virus
WT	wild type
XAC	xanthine amine conger
ZM 241385	4-(2-[7-amino-2-(2-furyl)[1,2,4]triazolo[2,3-α][1,3,5]triazin-5-ylamino]ethyl)phenol

Standard one and three letter amino acids codes have been used throughout.

Contents

Page No.

Chapter 1 Introduction

List of Figures

List of Tables

Abstract

The regulatory effects of adenosine are dependent upon its ability to bind four distinct adenosine receptor (AR) subtypes termed A_1, A_{2A}, A_{2B} and A_3 (Ralevic and Burnstock, 1998). Despite coupling to the same class of inhibitory guanine nucleotide-binding regulatory protein (G-protein) and binding the same physiological ligand, the A_1 and A_3ARs are subject to distinct regulatory events following agonist exposure. Rapid termination of G protein-coupled receptor (GPCR) signalling is typically regulated by their phosphorylation by second messenger-activated and/or G protein-coupled receptor kinases (GRKs). Upon phosphorylation by G protein-coupled receptor kinases (GRKs), many GPCRs bind arrestin proteins that serve to uncouple activated receptors from G-proteins leading to a functional desensitisation of G protein-linked signalling, cluster activated receptors to clathrin-coated vesicles (CCVs) and recruit and activate Src family tyrosine kinases ultimately resulting in the activation of the mitogen activated protein kinase (MAPK) cascade. It is thought that receptors proceed from CCVs to endosomes where they may be dephosphorylated and recycled back to the plasma membrane or degraded and down-regulated.

In this study, by employing the use of epitope and fluorescently tagged receptors, we show that agonist activation is required for A_3AR phosphorylation and internalisation and that this process can be blocked by an A_3AR-selective antagonist MRS 1523. We have characterised rates of A_3AR internalisation and recycling and shown that it is dynamically controlled by three phosphorylation sites Thr 307, 318 and 319 and two presumed palmitoylation sites Cys 302 and 305 in its carboxyl-terminal (C) tail. Mutation of the Thr sites renders the receptor resistant to phosphorylation by GRKs, ultimately resulting in a loss of receptor sequestration compared to WT A_3AR. In contrast, mutation of the Cys residues produces an increase in the rate of receptor internalisation compared to wild type (WT), a phenomenon not observed by the introduction of a similar mutation in the WT A_1AR (Cys^{309}Ala, data not shown).

By the use of confocal microscopy, we reveal that despite their differences in trafficking rates, both WT and (C-A)A_3ARs co-localise with transferrin (Tfn) receptor-positive early endosomes. We also demonstrate that this accumulation is dependent upon receptor phosphorylation as the non-internalising A_1AR can be directed through this endosomal pathway by replacing the C-terminal tail with the

GRK-phosphorylatable 14 amino acids of the A_3AR (A_1CT3AR). The process of receptor phosphorylation also dictates the pattern of arrestin distribution following agonist stimulation. A_1AR activation caused a re-distribution of arrestin3 to distinct spots at the plasma membrane whereas WT A_3AR, (C-A)A_3AR and A_1CT3 produced an accumulation of arrestin3 at both the plasma membrane and diffusely within the cytoplasm

This study also demonstrates that long-term agonist exposure causes a down-regulation in total A_3AR number *via* an as yet undefined pathway and may be directed by the C-terminal region of the receptor (Tsao and von Zastrow 2000b). Consequently, we have presented initial confocal images to suggest that recovery from down-regulation requires newly synthesised receptor to be transported from the Golgi apparatus to the plasma membrane.

Chapter 1

Introduction

1.1 Adenosine History

The first documentation of the physiological effects of adenosine and adenosine monophosphate (AMP) was in 1929, when Drury and Szent-Györgyi showed that extracts from heart muscle, brain, kidney and spleen had pronounced biological effects including arterial dilation, lowering of blood pressure and inhibition of intestinal contraction. Early investigation (Gillespie, 1934) drew attention to the structure-activity relationships of adenosine compounds showing that de-amination and removal of phosphate groups influenced not only the potency of the compound but also the type of response illustrated. Diverse responses to extracellular purines have now been documented for a wide range of biological systems including smooth muscle contraction, neurotransmission, inflammation and modulation of cardiac function.

1.1.1 Adenosine: Structure, Synthesis and Metabolism

Nucleotides consist of three distinct functional groups: (1) a heterocyclic nitrogenous base; (2) a pentose sugar and (3) a phosphoryl group, of which the nucleotide bases belong to two groups, purines and pyrimidines. The heterocyclic nitrogenous bases of purines are a 6-membered pyrimidine ring fused to a 5-membered imidazole ring and are termed adenine, guanine and hypoxanthine (Fig. 1.1). Purine nucleotides can be synthesised in three ways: *de novo* synthesis, reconstruction from purine bases through the addition of the ribose phosphate moiety, or phosphorylation of nucleosides, with the first two being the most important quantitatively (Zubay, 1998). A schematic representation of the pathways by which cells synthesise, interconvert and catabolise various purine nucleotides can be found in Fig. 1.2.

Adenosine is a by-product of adenosine triphosphate (ATP) metabolism that is released from cells into the surrounding tissue when oxygen demand exceeds supply (Bardenheur, 1986). Ischaemia, defined as the scenario whereby inadequate blood flow leads to tissue hypoxia, is one of the most potent stimuli that trigger the degradation of adenine nucleotides and the consequent formation of adenosine. Adenosine metabolism involves at least four different enzymes that can form adenosine (cytosolic 5'-nucleotidase, ecto 5'-nucleotidase, alkaline phosphatase and S-adenosylhomocysteinehydrolase) and another two enzymes (adenosine kinase,

Figure 1.1 Chemical structure of adenosine

Shown opposite is a schematic representation of the purine nucleoside adenosine. The purine bases consist of a 6-membered pyrimidine ring fused to a 5-membered imidazole ring, the fused system containing four nitrogen atoms. In purine nucleotides the glycosidic linkage is between N-9 of the purine and C-1 of the pentose sugar.

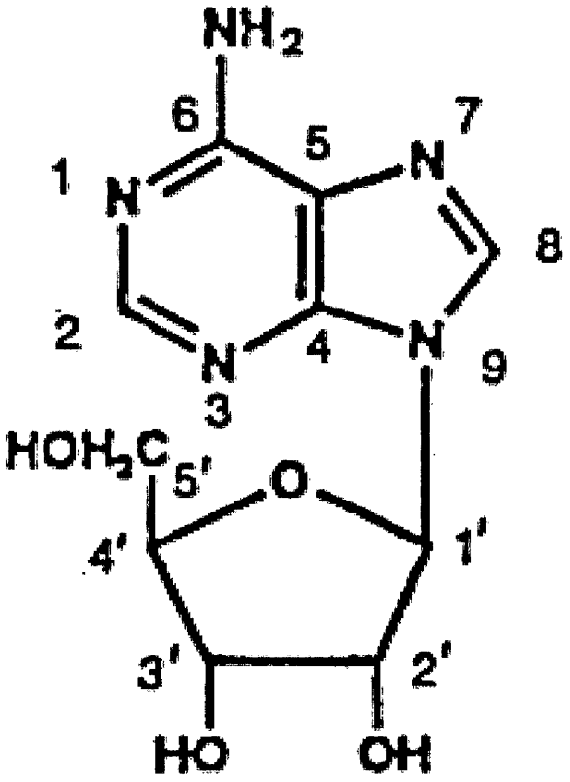

adenosine

Figure 1.2 Pathways of adenosine metabolism

Shown opposite is a representation of the pathways undertaken by cells to synthesise, interconvert and catabolise various purine nucleotides. Double-headed arrows indicate reversible enzymatic reactions and separate arrows in opposite directions between metabolites indicate a different enzyme is required in each direction. The diagram is arranged in tiers with purines, nucleosides and nucleoside mono-, di- and tri-phosphates in ascending order.

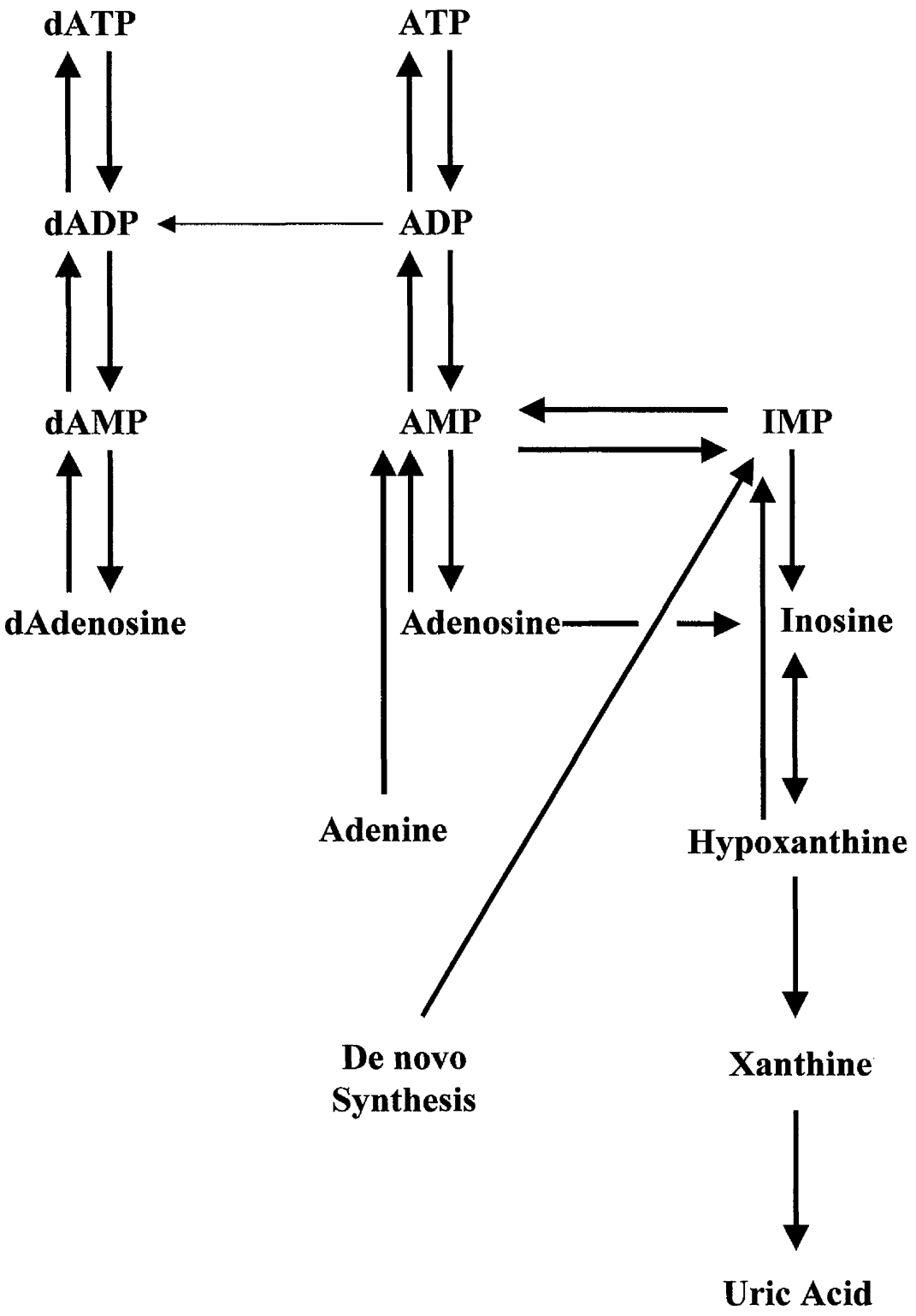
dATP
ATP
dADP
ADP
dAMP
AMP
IMP
dAdenosine
Adenosine
Inosine
Adenine
Hypoxanthine
De novo
Synthesis
Xanthine
Uric Acid

adenosine deaminase (ADA)) which lead to its metabolism to inosine and finally uric acid (Fig. 1.3). The biological effects documented by Drury and Szent- Györgyi are produced *via* a specific transport step which carries adenosine across the cell membrane. Various types of receptors have been cloned, although the most common and best characterised are those known as GPCRs.

1.2 G-protein coupled Receptors

Transduction of extracellular signals across the plasma membrane to the intracellular environment is achieved by the interaction of regulatory molecules with specific membrane-spanning cell-surface receptors. Structural and functional criteria has led to the definition of three broad categories of cell surface receptors: (1) receptors involved in cellular adhesion processes; (2) receptors which capture and convey ligands to appropriate intracellular destinations and (3) receptors which initiate a sequence of intracellular transducing signals when activated by their ligand. Examples of receptors that are components of the third class of receptors include cytokine receptors, ligand-gated ion channels and GPCRs. GPCRs can be divided into three distinct classes distinguishable by their amino acid (aa) sequences. Class I GPCRs can be further subdivided into a, b and c subtypes and includes odorants, rhodopsin and beta-adrenergic receptors (βAdRs) that are activated by ligand binding to the amino-terminal (N) domain and extracellular loops. Class II GPCRs comprise receptors for hormones such as glucagons and secretin. They share a similar morphology to Class Ic receptors but show no sequence homology. They have been shown to bind ligand *via* their long N-terminal domain. The third class of GPCRs includes the metabotropic glutamate receptors (mGlu), Ca^{2+}-sensing and γ-amino butyric acid (GABA) receptors. These receptors also possess a large extracellular domain (Bockaert and Pin, 1999).

G-protein coupled receptors (GPCRs) are integral membrane proteins that comprise the largest protein superfamily, consisting of greater than 1000 members. All members of the GPCR superfamily comprise a single polypeptide chain typically comprising seven stretches of hydrophobic transmembrane-spanning (TM) α-helices linked by hydrophilic extracellular N- and intracellular C-terminal domains of varying lengths (Ji et al., 1998; Fig. 1.4). The organisation of the membrane-spanning domains is such that they form a central pore accessible to the extracellular

Figure 1.3 Schematic representation of adenosine metabolism

Pathway of adenosine and homocysteine production from the transmethylation pathway. This involves the transfer of a methyl group of adenosyl methionine (SAM) to a variety of methyl acceptors. In a metabolic steady state, the S-adenosylhomocysteine (SAH) formed by this pathway is continuously removed by SAH-hydrolase such that adenosine formation *via* this pathway is equivalent to the transmethylation rate from SAM to SAH. The transmethylation pathway is essentially oxygen insensitive, while degradation of adenine nucleotides to adenosine is critically dependent on tissue oxygenation. Therefore when adenosine formation is accelerated by hypoxia, the net flux of adenosine from the transmethylation pathway back into adenine nucleotides is reversed.

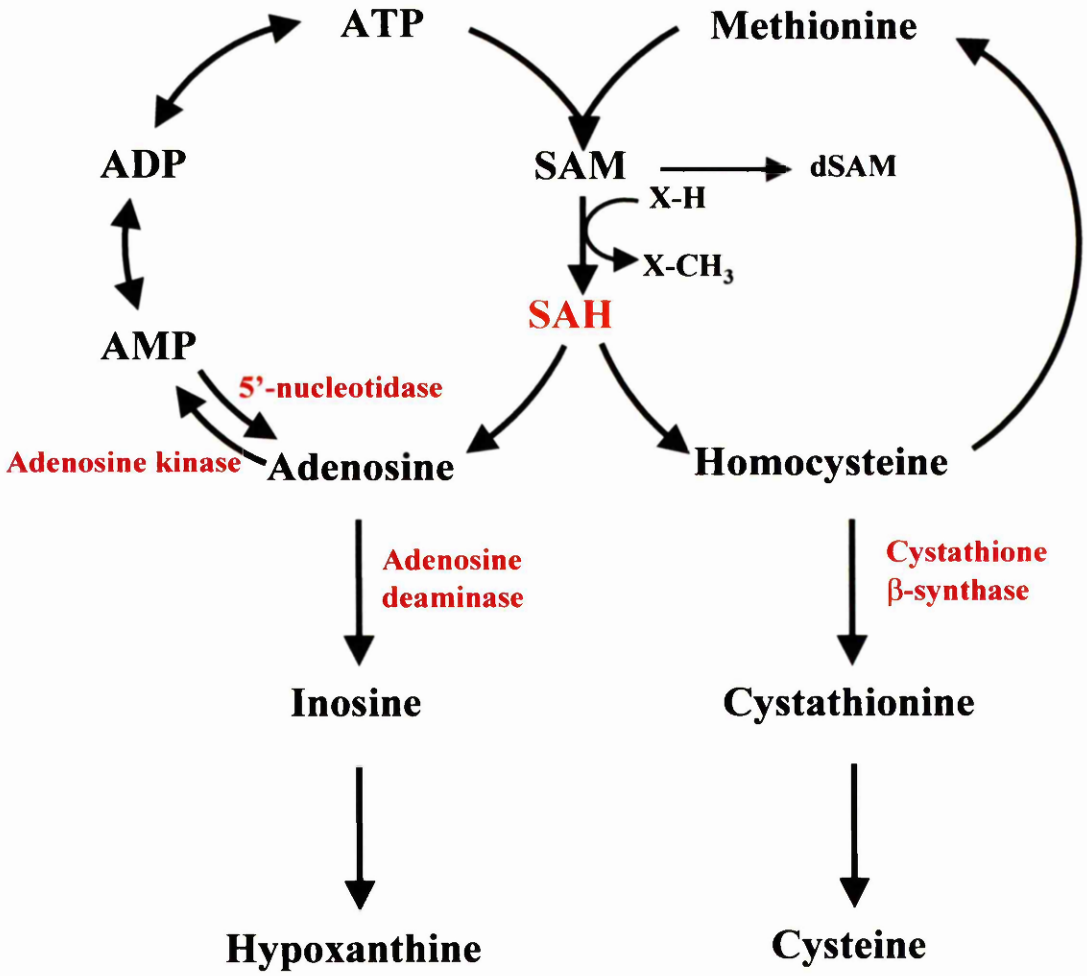
ATP
Methionine
ADP
SAM
dSAM
X-H
X-CH3
SAH
AMP
5'-nucleotidase
Adenosine kinase
Adenosine
Homocysteine
Adenosine deaminase
Cystathione β-synthase
Inosine
Cystathionine
Hypoxanthine
Cysteine

Figure 1.4 Schematic representation of a G-protein coupled receptor

G-protein coupled receptors (GPCRs) are integral membrane proteins that display a similar topography across differing species. They comprise a single polypeptide chain with an extracellular N- and intracellular C-terminus (black) linked by seven hydrophobic transmembrane (TM) spanning domains (blue). The TM domains display a relatively uniform size with the greatest variation in the receptors found within the extracellular and intracellular tails. GPCRs also contain several sites of lipid modification involved in receptor expression, ligand binding activity and G-protein interaction. Shown opposite is a schematic representation of a typical GPCR embedded within the plasma membrane.

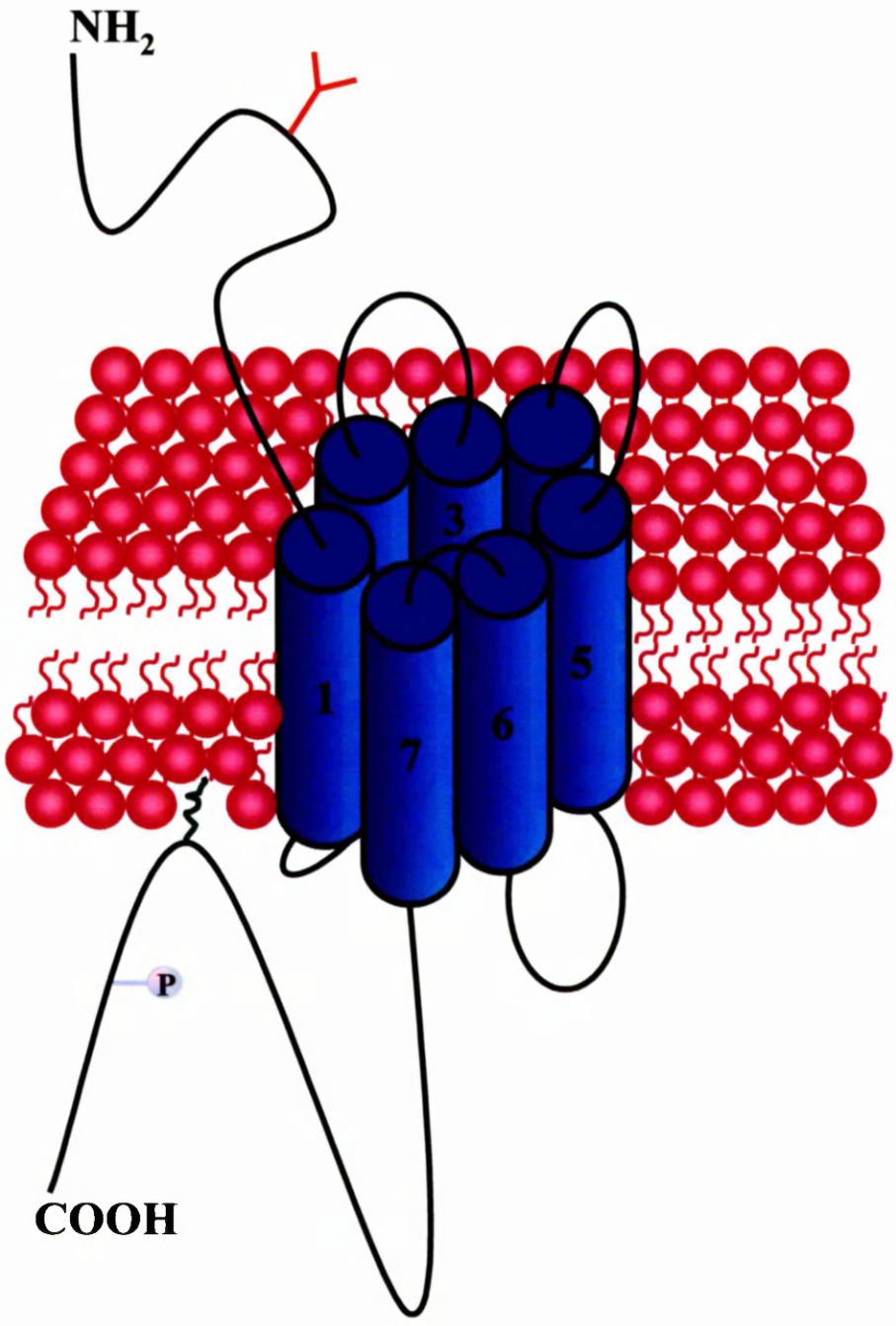
NH2
3
1
5
7
6
P
COOH

surface that can bind the appropriate ligand. Signal transduction *via* GPCRs is initiated by the interaction of the receptor with an extracellular ligand. These compounds initiate an intracellular response by causing a conformational change within the cytoplasmic loops of the receptor which are responsible for coupling and activation of G-proteins that in turn, act upon effector molecules (Gilman, 1987). The structure of these receptors was originally deduced by studies of bovine rhodopsin and beta2-adrenergic receptors (β_2AdR) (Henderson et al., 1990; Dixon et al., 1986) with further studies identifying key features that appear to be conserved throughout all GPCRs

1.2.1 Structural Features of GPCRs

The TM domains of GPCRs display a relatively constant length with variation in the members of this superfamily seen primarily in the N- and C-terminal domains. The N-terminal domain has been shown to range from between 340-450 residues in mature glycoprotein hormone receptors (Dias et al., 1992) to less than 10 residues in the A_{2A} (Furlong et al., 1992) and A_{2B}ARs (Pierce et al., 1992). The C-terminal domain comprises 359aa in the metabotropic glutamate receptor 1a (mGluR1a, Masu et al., 1991) compared to as little as 2aa in the gonadotrophin releasing hormone receptor (GnRHR, Brooks et al., 1993). Size variability is also seen in the third intracellular loop that ranges from 239aa in the m3 mucarinic acetylcholine receptor (mAchR, Peralta et al., 1987) to approximately 15aa in the human complement C5a receptor (Gerard and Gerard, 1991).

In most receptors, the N-terminal domain contains potential sites of Asp-linked (N-linked) glycosylation, represented by the sequence Asn-X-Ser/Thr (Hubbard and Ivatt, 1981). It has not been established whether all potential N-linked glycosylation sites are functional, but there is evidence of their requirement for receptor expression and ligand binding activity of GPCRs (Segaloff and Ascoli, 1993; Liu et al, 1993). Class II GPCRs such as receptors for endothelin A, B (ET_A, ET_B) and thrombin also contain an N-terminal hydrophobic leader sequence or signal peptide (Haendler et al., 1992; Zhong et al., 1992). This sequence directs newly synthesised receptor to the plasma membrane from the endoplasmic reticulum and is cleaved off to generate the mature receptor (Von Heijne, 1990). Almost all GPCRs contain Cys residues in the first and second extracellular loops that form disulphide bonds between each other. These bonds are critical for maintaining the tertiary

structure of the receptor as mutations of these residues in the rhodopsin (Karnik, 1998), β_2Ad (Dixon, 1987) and mAch receptors (Hulme, 1990) resulted in reduced expression levels, aberrant ligand binding properties and altered receptor functional activation in response to agonist. In addition, Dohlman and co-workers (1990) showed that mutation of these Cys residues in other receptor families, resulted in low levels of radioligand binding.

Both the C-terminal domain and third intracellular loop of GPCRs contain numerous Ser and Thr residues which are potential sites of receptor regulation *via* phosphorylation by kinases such as G-protein-coupled receptor kinases (GRK), protein kinase A (PKA) and protein kinase C isoforms (PKC) (Dohlman, 1991; Kobilka, 1992). These residues have significance in receptor desensitisation and initiation of internalisation (see section 1.4.1). Most GPCRs also contain a conserved Cys residue at the N-terminal region of the cytoplasmic tail. This has been shown in the β_2Ad (O'Dowd, 1989) and the rhodopsin receptor (Ovchinnikov et al., 1998) to be the site of palmitoylation. Palmitate is a 16-carbon fatty acid chain that can attach to Cys residues through a labile, reversible thioester linkage, regulation of which can be determined by the activation state of the receptor (Wedegaertner et al., 1995). Frequently, sites of palmitoylation are found to be close to other lipid modifications such as myristate or prenyl groups or to stretches of hydrophobic amino acids such as those found in the transmembrane domains of GPCRs (Mumby, 1997). This anchorage introduces an additional intracellular loop to the molecular structure of the receptor that may affect the interaction of the receptor with the G-protein (Milligan et al., 1995). Chemical removal of the palmitate from rhodopsin has been reported to enhance coupling of the receptor to the G-protein transducin (Morrison, 1991), whereas mutation of Cys 322 or 323 to Ser has no effect on activation of transducin (Karnik et al., 1993). In contrast, a β_2AdR with mutation of Cys 341 to Ala or Gly (Glycine) resulted in a receptor displaying a dramatic impairment in functional coupling to G_s (O'Dowd et al., 1989; Moffett et al., 1993). $Cys^{341}Gly$ was also observed to have an increased phosphorylation level in the absence of agonist and displayed no increase in either phosphorylation levels or uncoupling from G_s (stimulatory) upon agonist stimulation. The properties of the mutant β_2AdR resembled those of WT receptors that had undergone agonist-induced desensitisation (see Section 1.4.1), suggesting a role for palmitoylation in regulating

the accessibility of the C-terminal region to the action of protein kinases. This data implies that a universal role for palmitoylcysteines is unlikely. However, it is possible that these Cys residues have varying functions in receptor regulation from interaction with G-proteins to receptor turnover, expression and subcellular localisation (Kennedy and Limbird, 1993; Eason et al., 1994).

The greatest degree of amino acid similarity among GPCRs is found in the TM regions. Sequence similarity varies between 20-90% with the greatest conservation of sequence observed between subtypes of receptor families (Probst et al., 1992). Particularly well conserved throughout the GPCR superfamily are Pro residues occurring in TM regions 4, 5, 6 and 7. These residues are thought to be important for formation of the ligand binding pocket in receptors such as the mACh receptors and also for expression of the β_2AdR receptor at the cell surface (Strader, 1989). The sequence Asp-Arg-Tyr (DRY) occurring at the intracellular side of transmembrane region 3 is very highly conserved. The arginine residue is invariant, with the Asp and Tyr being only conservatively replaced in some receptors. For almost all GPCRs, this region along with the membrane proximal region of the second intracellular loop, is thought to be involved in receptor-G-protein coupling.

1.2.2 Receptor and G-protein interactions

Mutagenesis and biochemical experiments using a variety of GPCRs suggests that receptor activation by a ligand causes changes in the orientation of TM helices 3 and 6. These changes affect the conformation of the intracellular loops of the receptors and uncover previously masked G-protein binding sites (Farrens et al., 1996, Bourne, 1997). Deletion and site-directed mutagenesis studies have established that receptor-G-protein interaction relies on the receptor's third cytoplasmic loop, and in particular, the regions of the loop lying immediately adjacent to TM regions 5 and 6 (Savarese and Fraser, 1992).

Although much is known about the structural features of GPCRs involved in ligand recognition and G-protein binding, the mechanisms underlying ligand activation and subsequent G-protein coupling remains unclear. The DRY motif is a highly conserved triplet of amino acids located at the transmembrane region of helix three and the second intracellular loop (Probst et al., 1992). The Arg residue is the only fully conserved residue in the sequence. Mutations of this residue in the M1 muscarinic receptor and alpha 1B adrenergic receptor (α_{1B}AdR) have resulted in

receptors with impaired signal transduction properties and it is therefore thought to be a key residue required for interaction of receptor with G-protein (Zhu et al., 1994; Jones et al., 1995;Schee et al., 1996). The importance of this sequence in the second intracellular loop has also been described for rhodopsin, the angiotensin II (Ang II) receptor and more recently the interleukin-8 receptor (Konig et al., 1989; Ohyama et al., 1992; Damaj et al., 1996). Analysis of several gain-of-function mutant receptors that result in constitutive receptor activity have shown that multiple regions of the receptor including the extracellular, intracellular and TM domains may be involved in molecular mechanisms that keep the receptor in a constrained state in the absence of agonist (Leff, 1995; Lefkowitz, 1993; Lefkowitz et al., 1993). In the presence of agonist, conformational changes in the receptor lead to a disruption of complex intramolecular interactions that constrain the receptor in the inactive state. This causes rearrangement of the TM domains and exposure of the cytoplasmic regions to the G-protein whereby ligand binding triggers signal transduction *via* GPCRs (Ulloa-Aguirre et al., 1999). Taken together, these structural features determine the GPCRs ligand binding and G protein coupling characteristics.

1.2.3 Adenosine Receptors

Purines and pyrimidines mediate their effects by interactions with distinct cell-surface purine receptors (Ralevick and Burnstock, 1998). There are two main families of purine receptors: P_1, or adenosine receptors (ARs) and P_2, receptors that primarily recognise adenosine triphosphate, adenosine diphosphate (ADP), uridine triphosphate (UTP) and uridine diphosphate (UDP). P_1/ARs can be further divided into four subtypes, A_1, A_{2A}, A_{2B} and A_3 (Tucker and Linden, 1993) which all couple to G-proteins, while P_2 receptors have been divided into P2X, ligand-gated ion channels (Benham and Tsien, 1987) and P2Y, GPCRs (Abbracchio and Burnstock, 1994; Fredholm et al., 1994).

In common with other GPCRs, ARs consist of an extracellular N- and intracellular C-termini linked by 7 hydrophobic TM regions (Palmer and Stiles, 1995a). The ARs also display several common structural features that are conserved throughout the GPCR superfamily, such as glycosylation and phosphorylation sites. All four subtypes have been cloned from rat and human sources (Fig.1.5).

Figure 1.5 Sequence alignment of rat adenosine receptors

Shown opposite is a sequence alignment of rat A_1, A_{2A}, A_{2B} and A_3 adenosine receptors. Residues conserved in at least two of the four sequences are highlighted in yellow with the predicted transmembrane spanning domains indicated by a black line above the appropriate region. Conserved Cys residues possibly involved in receptor palmitoylation are indicated by (*).

This comparison was obtained using the MegaAlign programme within the Dnastar molecular biology analysis suite.

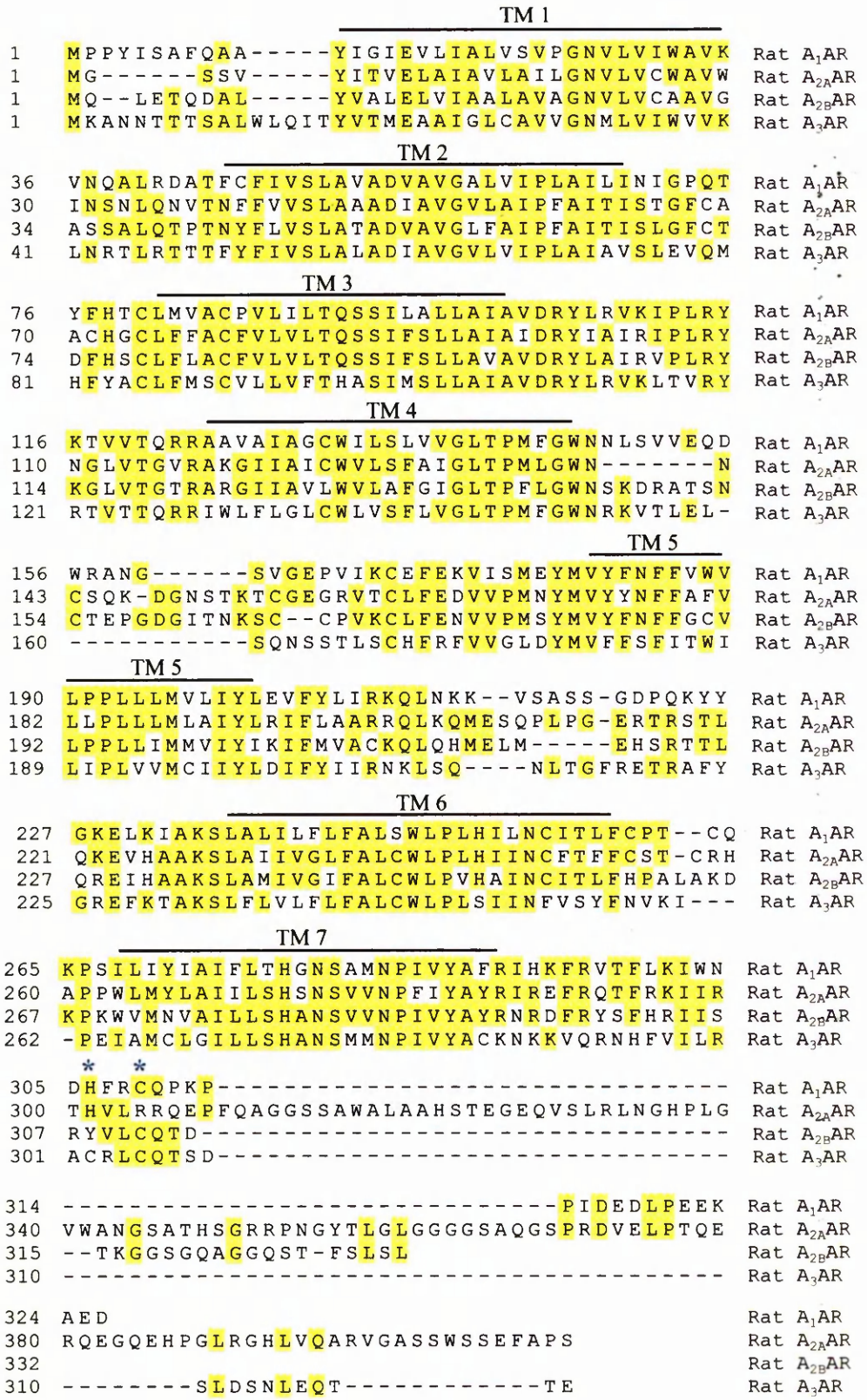
TM 1
TM 2
TM 3
TM 4
TM 5
TM 5
TM 6
TM 7
1 MPPYISAFQAA-----YIGIEVLIALVSVPGNVLVIWAVK Rat A1AR
1 MG------SSV-----YITVELAIAVLAILGNVLVCWAVW Rat A2AAR
1 MQ--LETQDAL-----YVALELVIAALAVAGNVLVCAAVG Rat A2BAR
1 MKANNTTTSALWLQITYVTMEAAIGLCAVVGNMLVIWVVK Rat A3AR
36 VNQALRDATFCFIVSLAVADVAVGALVIPLAILINIGPQT Rat A1AR
30 INSNLQNVTNFFVVSLAAADIAVGVLAIPFAITISTGFCA Rat A2AAR
34 ASSALQTPTNYFLVSLATADVAVGLFAIPFAITISLGFCT Rat A2BAR
41 LNRTLRTTTFYFIVSLALADIAVGVLVIPLAIAVSLEVQM Rat A3AR
76 YFHTCLMVACPVLILTQSSILALLAIAVDRYLRVKIPLRY Rat A1AR
70 ACHGCLFFACFVLVLTQSSIFSLLAIAIDRYIAIRIPLRY Rat A2AAR
74 DFHSCLFLACFVLVLTQSSIFSLLAVAVDRYLAIRVPLRY Rat A2BAR
81 HFYACLFMSCVLLVFTHASIMSLLAIAVDRYLRVKLTVRY Rat A3AR
116 KTVVTQRRAAVAIAGCWILSLVVGLTPMFGWNNLSVVEQD Rat A1AR
110 NGLVTGVRAKGIIAICWVLSFAIGLTPMLGWN-------N Rat A2AAR
114 KGLVTGTRARGIIAVLWVLAFGIGLTPFLGWNSKDRATSN Rat A2BAR
121 RTVTTQRRIWLFLGLCWLVSFLVGLTPMFGWNRKVTLEL- Rat A3AR
156 WRANG------SVGEPVIKCEFEKVISMEYMVYFNFFVWV Rat A1AR
143 CSQK-DGNSTKTCGEGRVTCLFEDVVPMNYMVYYNFFAFV Rat A2AAR
154 CTEPGDGITNKSC--CPVKCLFENVVPMSYMVYFNFFGCV Rat A2BAR
160 ----------SQNSSTLSCHFRFVVGLDYMVFFSFITWI Rat A3AR
190 LPPLLLMVLIYLEVFYLIRKQLNKK--VSASS-GDPQKYY Rat A1AR
182 LLPLLLMLAIYLRIFLAARRQLKQMESQPLPG-ERTRSTL Rat A2AAR
192 LPPLLIMMVIYIKIFMVACKQLQHMELM-----EHSRTTL Rat A2BAR
189 LIPLVVMCIIYLDIFYIIRNKLSQ----NLTGFRETRAFY Rat A3AR
227 GKELKIAKSLALILFLFALSWLPLHILNCITLFCPT--CQ Rat A1AR
221 QKEVHAAKSLAIIVGLFALCWLPLHIINCFTFFCST-CRH Rat A2AAR
227 QREIHAAKSLAMIVGIFALCWLPVHAINCITLFHPALAKD Rat A2BAR
225 GREFKTAKSLFLVLFLFALCWLPLSIINFVSYFNVKI--- Rat A3AR
265 KPSILIYIAIFLTHGNSAMNPIVYAFRIHKFRVTFLKIWN Rat A1AR
260 APPWLMYLAIILSHSNSVVNPFIYAYRIREFRQTFRKIIR Rat A2AAR
267 KPKWVMNVAILLSHANSVVNPIVYAYRNRDFRYSFHRIIS Rat A2BAR
262 -PEIAMCLGILLSHANSMMNPIVYACKNKKVQRNHFVILR Rat A3AR
305 DHFRCQPKP---------- Rat A1AR
300 THVLRRQEPFQAGGSSAWALAAHSTEGEQVSLRLNGHPLG Rat A2AAR
307 RYVLCQTD---------- Rat A2BAR
301 ACRLCQTSD---------- Rat A3AR
314 ----------PIDEDLPEEK Rat A1AR
340 VWANGSATHSGRRPNGYTLGLGGGGSAQGSPRDVELPTQE Rat A2AAR
315 --TKGGSGQAGGQST-FSLSL Rat A2BAR
310 ---------- Rat A3AR
324 AED Rat A1AR
380 RQEGQEHPGLRGHLVQARVGASSWSSEFAPS Rat A2AAR
332 Rat A2BAR
310 --------SLDSNLEQT----------TE Rat A3AR

As with most GPCRs, the TM regions of the ARs are highly conserved. TM regions 2, 3 and 5 show particularly long stretches of homology between the four subtypes (Palmer and Stiles, 1995a) and it is residues within these transmembrane regions that have been shown to be crucial for ligand binding and specificity (Olah et al., 1994, 1995). Early work by Klotz et al. (1988) implicated multiple His residues in the agonist and antagonist binding specificity of the A_1AR. These residues have also been linked to A_{2A} receptor ligand binding (Jacobson et al., 1992a). A_1, A_{2A}, and A_{2B} contain only two His residues in the TM domains, one at position 256 in TM region 6 and the other at position 274 in TM region 7. Individual mutations of these residues in the bovine A_1AR abolished both agonist and antagonist binding and replacement of His 256 with Leu resulted in a 4-fold decrease in affinity for antagonist, supporting a role of these residues in ligand binding (Olah et al., 1992).

Other features of GPCRs that are conserved in ARs are the presence of Cys residues in the extracellular loops. As stated previously, these residues contribute to the formation of disulfide bonds, which may confer conformational stability to GPCRs once inserted into the plasma membrane (PM). ARs also display consensus sites of N-linked glycosylation (N-X-Ser/Thr; Olah et al., 1990; Barrington et al., 1990; Palmer et al., 1992). These sites are found primarily on the second extracellular loops of the ARs with the A_3AR possessing an additional site within its N-terminal domain. As has been shown with other GPCRs, the exact role of ARs N-linked glycosylation remains unclear.

ARs initiate their effects through interaction of agonist-occupied receptors with G-proteins (Gilman, 1987). As with most other GPCRs, ARs contain a DRY motif in their second intracellular loop, which has been suggested to be a site of G-protein interaction (Fraser et al., 1988). Short amino acid sequences containing the motif BBXB or BBXXB, where B is a basic residue and X is any amino acid, can also be found in the intracellular regions of A_{2A}, A_{2B} and A_3ARs. As with the DRY motif, these sites have been documented as being involved in receptor-G-protein coupling (Okamoto and Nishimoto, 1992). The presence of a B/X motif is not compulsory for G-protein binding as canine and bovine A_1ARs do not possess such sequences within their cytoplasmic tails. However, they do contain clusters of basic residues in the third cytoplasmic loop and regions of the C-terminal tail in close contact to the membrane. In contrast, the A_{2A}AR contains two such B/X motifs in its

intracellular region, one in the third cytoplasmic loop and the other proximal to TM 7 in the C-terminal domain.

The C-terminal regions of ARs contain numerous sites of interest. A_1, A_{2B} and A_3ARs have conserved Cys residues in their C-terminal tails (Fig. 1.5). Previous studies on the β_2AdR and rhodopsin have suggested this residue to be a site of receptor palmitoylation (O'Dowd et al., 1989; Ovchinnikov et al., 1988). When this residue is mutated, these receptors display phosphorylation at a basal level prior to agonist stimulation. A_{2A}ARs do not possess an analogous Cys residue, suggesting that these residues have an important, albeit not conserved role in receptor signalling (Wedegaertner et al., 1995). It has also been suggested that the C-terminal tail of many receptors play a regulatory role in receptor signalling (Parent et al., 1999). The presence of multiple Ser and Thr residues in the C-terminal domains of the A_{2A} and A_3ARs suggests this is a site of regulation *via* receptor phosphorylation. Palmer et al., (1994) and Ramkumar et al., (1991) have noted that the A_{2A}ARs undergo a rapid agonist-induced functional desensitisation that is associated with receptor phosphorylation (Palmer et al., 1997). The significance of these predicted palmitoylation and phosphorylation sites in A_3AR activation will be discussed elsewhere. Receptors from each of the four distinct subtypes have been cloned from a variety of species and characterised by expression in various cell types.

1.2.4 Adenosine Receptor subtypes

(a) A_1AR

A_1ARs have been cloned from several species including rat (Mahan et al., 1991; Reppert et al., 1991), cow (Olah et al., 1992; Tucker et al., 1992) and man (Libert et al., 1992; Townsend-Nicholson et al., 1992; Ren and Stiles, 1994). These each encode open reading frames (ORFs) of 326 aa with a corresponding protein size of ~36,700 Daltons (Da). A_1ARs across the different species display ~87% amino acid identity, with this value rising to 92% within the TM regions. mRNA analysis has shown the A_1AR to be expressed in brain, testis (Mahan et al., 1991; Reppert et al., 1991), heart and kidney (Olah et al., 1992). A_1ARs have classically been associated with the inhibition of adenylyl cyclase (AC) and activation of phospholipase C (PLC) leading to a decrease in cyclic AMP (cAMP) levels and mobilisation of intracellular Ca^{2+} *via* the inhibitory (G_i/G_o) family of G-proteins (van Calker et al., 1979; Londos et al., 1980; Freissmuth et al., 1991; Munshi et al., 1991).

(b) A_{2A}AR

A_{2A}ARs have been cloned from numerous species including dog (Maenhaut et al., 1990), rat (Fink et al., 1992) man (Furlong et al., 1992), rabbit, sheep and mouse. They show an overall sequence identity of 84% between rat and human and 82% between rat and canine. These receptors are 410-412 aa in length (~ 45,000 Da) with approximately 120 of these aa's constituting the carboxyl terminal tail (Olah et al., 1997; Barrington et al., 1990). A_{2A}ARs are most commonly known to signal through the G_s-linked family of G-proteins leading to the activation of AC (Daly et al., 1983), but can also activate p21Ras and extracellular regulated kinase (ERK) in endothelial cells and protein kinase Cζ (PKCζ) in PC12 cells (Huang et al., 2001). A_{2A}ARs have a broad distribution including the immune system, platelets, vascular smooth muscle and endothelial cells. Within the brain, the highest levels of A_{2A}ARs are found in regions that are rich in dopamine including the striatum, nucleus accumbens and olfactory tubercle (Ongini and Fredholm, 1996).

(c) A_{2B}AR

A_{2B}ARs have been cloned from human hippocampus (Pierce et al., 1992), rat brain (Rivkees and Reppert, 1992; Stehle et al., 1992) and mouse bone marrow-derived mast cells (Marquardt et al., 1994). The C-terminal tail of the A_{2B} receptor contains ~80 aa fewer than that of the A_{2A} receptor and is therefore similar to the A_1 and A_3ARs in size (36-37 kDa). A_{2B}ARs have been reported to couple to different signalling pathways dependent upon species. These include activation of AC, coupling to PLC *via* the G_q/G_{11} family leading to an Inositol trisphosphate (IP_3)-dependent increase in Ca^{2+} when expressed in human mast cells (Feokstitov and Biaggioni, 1995) and coupling to PLC in Xenopus oocytes (Yakel et al., 1993). Recently, the A_{2B}AR has been shown to be involved in netrin-dependent growth of axons in the dorsal spinal cord *via* interaction with DCC protein (deleted in colorectal cancer; Corset et al., 2000). This suggests a novel role for these receptors in the nervous system distinct from their activities in neurotransmission.

(d) A_3AR

The A_3AR was cloned by the use of polymerase chain reaction (PCR) with degenerate nucleotide primers directed towards the conserved third and sixth transmembrane regions of GPCRs (Zhou, 1992). A resulting 226 aa fragment was

used to screen a rat brain copy DNA (cDNA) library and found to be closely related to A_1 and A_2ARs, with 58% and 57% homology respectively in putative TM domains (Zhou, 1992). This clone was identical to one obtained previously from a rat testis cDNA library which encoded a GPCR with greater than 40% sequence homology to canine A_1 and A_{2A}ARs (Meyerhof et al., 1991). Homologues of rat A_3AR have been cloned from sheep (Linden et al., 1993) and humans (Salvatore et al., 1993) and display a 72% overall amino acid identity to the rat receptor. A splice variant of the rat A_3AR containing a 17 amino acid insertion in the second intracellular loop has also been cloned and characterised (Sajjadi et al., 1996). Experimental analysis of the receptor transfected into Chinese hamster ovary (CHO) cells indicated that it inhibited AC (Zhou et al., 1992; Abbracchio et al., 1995) through interaction with a pertussis toxin-sensitive (PTX) G-protein, G_i and to a lesser extent $G_{q/11}$ (Palmer et al., 1995). Although widely distributed in humans, the physiological roles of the A_3AR are still under investigation. It has, however, been implicated in the release of histamine from mast cells (Ramkumar et al., 1993) and in the cardioprotective effect of adenosine following ischaemia reperfusion injury (Auchampach et al., 1997; Stambaugh et al., 1997). A_3AR mRNA is found expressed in testis, lung, kidney, heart, brain, mast cells, eosinophils and spleen depending on the species examined (see Table 1.1). Highest levels are found in the testis (Linden et al., 1993; Salvatore et al., 1993) lung (Salvatore et al., 1993) and spleen (Linden at al., 1993) for rat, human and sheep respectively.

1.3 G-Proteins

The term G-protein refers to a heterotrimeric plasma membrane-associated GTP binding protein which functions as an intermediary in transmembrane signalling pathways to transduce signals across the plasma membrane from activated receptors to effector enzymes or ion channels (Gilman, 1987). Evidence for the existence of G-proteins first came from Rodbell and Birnbaumer (1971) who described the stimulation of AC to be dependent upon the presence of guanosine triphosphate (GTP). It was not until 1981 (Sternweis et al) that the first G-protein was purified and initially described as 'a GTP-binding regulatory component of AC'. This 45 kDa protein is now better known as the stimulatory G-protein α-subunit $G_{s\alpha}$ (Gilman, 1987). Another G-protein was soon described as the inhibitory regulatory

Table 1.1 Distribution of adenosine receptor mRNA expression

All ARs exhibit overlapping distribution throughout the different species examined. The table opposite illustrates the expression of each AR subtype in cloned species.

Table 1.1

Receptor Subtype	Species	Location
A_1AR	Rat Bovine Human	Cortex, cerebellum, thalamus hippocampus, spinal cord, fat, testis, heart, kidney
$A_{2A}AR$	Canine Rat Human	Striatum, nucleus accumbens, olfactory tubercule, cortex, heart, kidney, lung, blood vessels, immune tissues
$A_{2B}AR$	Rat Human	Large intestine, brain, spinal cord, lung, aorta, airway smooth muscle, endothelium, mast cells
A_3AR	Rat Sheep Human	Testis, lung, kidney, heart, cardiac myocytes, brain, eosinophils, mast cells

component of AC and termed G_i (Bokoch et al., 1983). G-proteins consist of distinct heterotrimeric subunits, namely α, β and γ of which there are known to be 20-α, 6-β and 12-γ genes cloned to date (Hamm, 1998). These subunits participate in a complex activation-deactivation cycle in which the α-subunit dissociates and re-associates with the βγ-subunit in a guanine nucleotide-dependent manner (Gilman, 1987).

It is proposed that an equilibrium state exists between two forms of a receptor. The inactive form (R) can bind ligands (H) but cannot bind G-protein (G). The presence of ligand pushes the equilibrium toward the active form of ligand-receptor (H-R*) and the presence of G-protein pushes the equilibrium toward interaction of activated receptor (R*) with G-protein (R*-G). The active form of receptor has a greater affinity for ligand than the inactive form (R). In normal receptor systems, in the presence of G-protein but absence of ligand, there is a preponderance of the inactive form of the receptor (Baldwin, 1994). In an inactive form, guanosine diphosphate (GDP) is bound to the α subunit of the G-protein. Receptor activation by ligand produces changes in the orientation of the TM helices of the GPCR which in turn affects the conformation of the intracellular loops interacting with the G-protein (Altenbach et al., 1996; Farrens et al., 1996). At this point, the GDP bound to the α-subunit is exchanged for GTP and the G_α and $G_{\beta\gamma}$ subunits dissociate. Multiple receptors can converge on a single G-protein and in some cases, a single receptor can activate more than one G-protein, thereby modulating a plethora of intracellular signals (Bourne, 1997, Fig. 1.6).

1.3.1 G_α-subunits

G_α subunits contain an intrinsic GTPase activity that determines the lifetime of the active, dissociated state of the G-protein heterotrimer (Morris and Scarlata, 1997). The members of this family can be subdivided into four groups, each of which controls multiple effectors:

Figure 1.6 Regulatory cycle of G-protein activation/deactivation

The figure opposite depicts the mechanism by which ligand activates G-protein by interaction with receptor. Receptor mediates the exchange of GDP for GTP on the α-subunit leading to activation of the heterotrimer and dissociation of the α-GTP from βγ. The dissociated subunits can activate the appropriate effector enzymes, a process that is turned off by the intrinsic GTPase activity of the α-subunit, allowing reassociation of α-GDP with βγ to initiate another cycle.

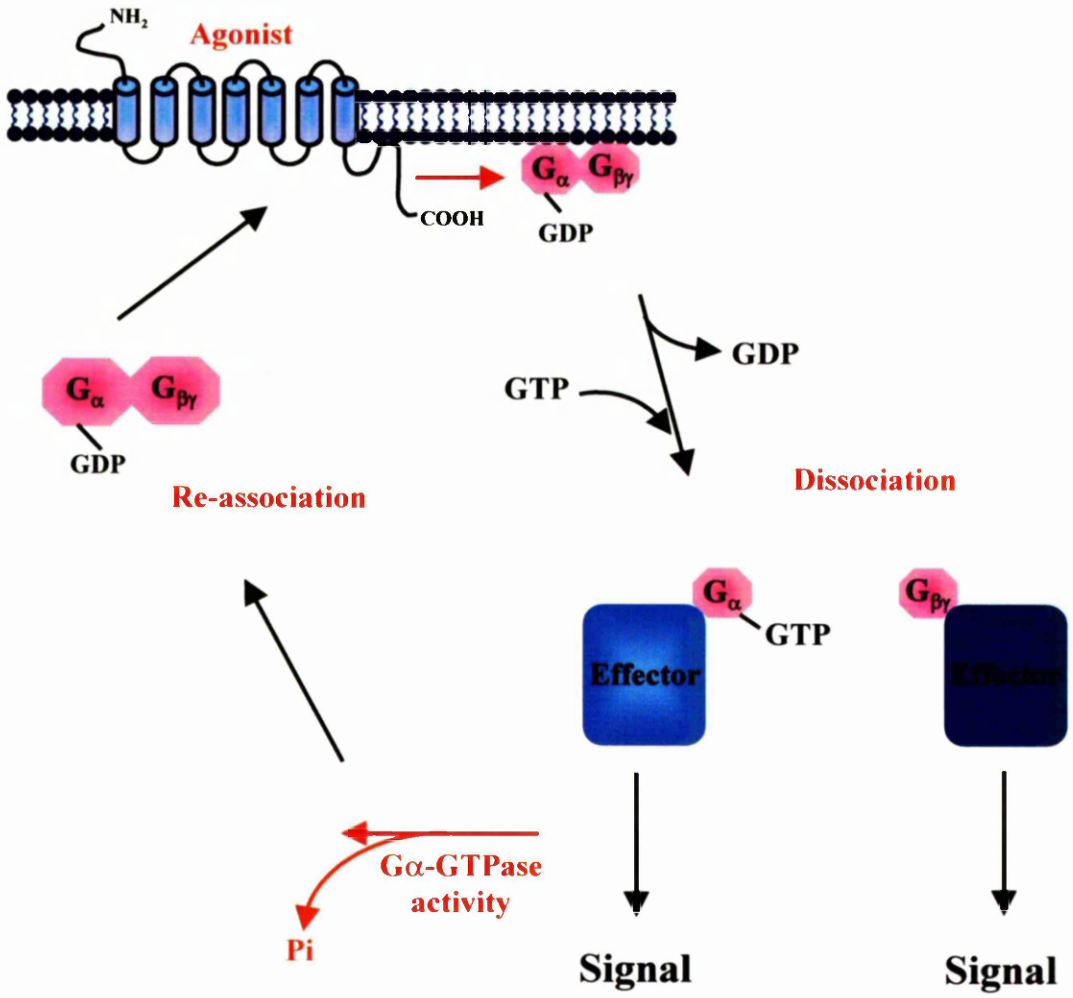
NH2
Agonist
COOH
Gα
Gβγ
GDP
GTP
GDP
Dissociation
Re-association
Gα
Gβγ
GDP
Effector
Gα
GTP
Gβγ
Effector
Gα-GTPase
activity
Pi
Signal
Signal

G_s family G_s is defined functionally by its ability to stimulate AC and open Ca^{2+} channels and contains two major isoforms of 45 and 52 kDa (Northup et al., 1980 and Sternweis et al., 1981) resulting from four splice variants of the same gene. Members of this family are ubiquitously expressed and are sensitive to cholera toxin (CTX) which adenosine diphosphate-ribosylates (ADP) the α-subunit at Arg 201, inactivating its GTPase activity causing persistent activation of $G_{s\alpha}$ (Bourne et al., 1991).

G_i family G_i is divided into three subtypes: G_{i-1}, G_{i-2} and G_{i-3} which range in size from 40-41 kDa and mediate the inhibition of cAMP synthesis (Gilman, 1987). It has been suggested that phosphorylation of the β_2AdR is a crucial molecular switch to subsequently allow G_i-mediated activation of ERK (Daaka et al., 1997). Similarly, G_i is involved in IGF-induced neuronal MAPK activation, required for neuronal development and reorganisation (Hallak et al., 2000). This family also includes two 'o' subtypes, G_{o1} and G_{o2}, of 39-41 kDa (Hsu et al., 1990). One possible function of the G_o-subtypes includes stimulation of PLC (Moriarty et al., 1990). The G_i family is sensitive to PTX that causes ADP-ribosylation of a Cys residue in the C-terminus of G_i/G_o, causing inactivation of GTPase activity with GDP being bound. This increases the affinity of the α-subunit for βγ and inactivates G_i/G_o by preventing the interaction of the α-subunit with receptors (Katada et al., 1984). This family also includes the PTX- and CTX-sensitive transducins G_{t1} and G_{t2} which couple to rhodopsin to activate retinal cGMP-phosphodiesterase (PDE, Stryer, 1986).

G_q family This family comprises of G_q, G_{11}, G_{14}, G_{15} and G_{16} (Pang and Sternweis, 1990). It is a toxin-insensitive family and has been implicated in the PTX-insensitive activation of some of the 6 PLC subtypes (Park et al., 1992). Suggestions of 'cross-talk' or co-stimulation of the G_q and G_i families can lead to augmentation of physiological responses such as muscle contraction (Selbie and Hill, 1998) by increasing PLC and PKC activity within cells.

G_{12} family The 44 kDa proteins G_{12} and G_{13} which make up this family are responsible for functions including the activation of JNK (c-Jun N-terminal kinase) and reorganisation of the cytoskeleton (Prasad et al., 1995; Buhl et al., 1995).

They have also been indicated in the regulation of small molecular weight G-proteins and Na^+-H^+ exchange (Milligan and Rees, 1999). They are expressed ubiquitously, are toxin-insensitive and their primary structure varies significantly from the other G-proteins by greater than 50% (Simon et al., 1991).

1.3.2 $G_{\beta\gamma}$-subunits

Less is known about the 35-36 kDa β-subunits and the 8-9 kDa γ-subunits. Despite this fact, $G_{\beta\gamma}$ has been shown to directly bind and activate a number of effectors such as phospholipase A_2 (PLA_2; Kim et al., 1989), PLC (Pang and Sternweis, 1990; Wilkie et al., 1991) and AC (Tang and Gilman, 1991 and Federman et al., 1992). The 20-α, 6-β and 12-γ subunits theoretically provide 1440 αβγ combinations. Alternatively, while α, β and γ can form any combination, it has been speculated that GPCRs recognise and interact exclusively with only one combination of α, β and γ which helps to explain the specificity of GPCR signalling (Lefkowitz, 1992). As each α, β and γ subunit interacts with distinct and specific effectors, the heterotrimeric nature of G-proteins increases the number of control mechanisms or effector molecules activated *via* ligand binding to GPCRs (Clapham and Neer, 1997).

Although the βγ-subunit is a heterodimer, functionally it is a monomer, as these two subunits cannot be dissociated except by denaturation (Clapham and Neer, 1997). The $G_{\beta\gamma}$-subunit induces conformational changes on the G_α when they come together to form the heterotrimer, increasing G_α affinity for GDP (Brandt and Ross, 1985) and enhancing binding of G_α to its appropriate receptor (Higashijima et al., 1987; Heithier, 1992 and Phillips, 1992). The C-terminal region of the G_γ-subunit contains a CAAX motif that directs prenylation of the molecule (Resh, 1996). Prenylation involves attachment of either a 15-carbon farnesyl or 20-carbon geranylgeranyl isoprenoid to a conserved Cys residue of proteins (Casey, 1994). $G_{\beta\gamma}$ subunits containing G_γ in which the Cys has been mutated to Ser, results in the prevention of prenylation and expression of the mutated βγ-subunits in the cytosol rather than being membrane bound (Muntz et al., 1992 and Simonds et al., 1991). This suggests that one function of the prenyl group is to form a membrane attachment to anchor the heterodimer at the plasma membrane. It has also been suggested that G_β can become phosphorylated on a His residue by an enzyme that uses GTP as a substrate (Wieland et al., 1993). This led to the hypothesis that the

phosphate group of the GTP could be transferred from His to GDP, leading to an alternative pathway for G_α-subunit activation (Kowluru et al., 1996). This has since been shown not to occur in biological systems (Hohenegger et al., 1996).

1.4 GPCR Regulation

In order to respond to the rapid changes in agonist concentration, receptors must be inactivated and restored to the cell surface for further stimulation. Chronic exposure of GPCRs to their agonists triggers multiple cellular changes leading to receptor desensitisation (seconds), sequestration (minutes) and down-regulation (hours-days). The best characterised of these systems is the β_2AdR and the light activated rhodopsin which have been shown to follow the three steps outlined above.

1.4.1 Desensitisation

(a) Phosphorylation

Desensitisation has traditionally been defined as the process whereby a GPCR-initiated response reaches a plateau and then diminishes despite the sustained presence of agonist. The phenomenon of desensitisation can be subdivided depending on the nature of the causative stimulus. *Homologous* desensitisation is agonist specific and occurs only at agonist-stimulated receptors. Consequently, only the activated receptor itself becomes desensitised. In contrast, *heterologous* desensitisation is a process where activation of one type of receptor causes desensitisation of other receptor types also. Heterologous desensitisation involves phosphorylation of GPCRs by second messenger-activated kinases such as cAMP-dependent protein kinase and PKC. Phosphorylation by these kinases impairs the ability of receptors to stimulate their associated G-proteins (Benovic et al., 1985 and (Pitcher et al., 1992). Investigation into the homologous desensitisation of β_2AdR and rhodopsin, showed that agonist-stimulated β_2AdR phosphorylation occurred even in the absence of cAMP-dependent protein kinase (Stadel et al., 1983 and Strasser et al., 1986). The enzyme responsible for this activity was purified from bovine brain (Benovic et al., 1987a) and termed β-adrenergic receptor kinase (βARK), later renamed as G-protein coupled receptor kinase-2 (GRK2). Rhodopsin

kinase (GRK1) is the enzyme responsible for phosphorylating light-activated rhodopsin in rod outer segments (Shichi and Somers, 1978).

Six mammalian GRKs have been cloned to date: GRK1 (rhodopsin kinase, Lorenz et al., 1991); GRK2 (β-adrenergic receptor kinase-1, Benovic et al., 1991a); GRK3 (β-adrenergic receptor kinase-2, Benovic et al., 1991); GRK4 (IT-11, Ambrose et al., 1992); GRK5 (Kunapuli and Benovic, 1993 and Premont et al., 1994) and GRK6 (Benovic and Gomez, 1993). With the exceptions of GRK1 (retina) and GRK4 (testis), GRKs are ubiquitously expressed (Freedman and Lefkowitz, 1996), suggesting a role for these kinases in a multitude of diverse signalling pathways.

(b) Structural features of GRKs

Structurally, GRKs contain a centrally located catalytic domain of 263-266 amino acids flanked by large amino- and carboxyl-terminal regulatory domains (Fig. 1.7). The amino-terminal domains are of common size, approximately 185 aa's, and demonstrate a good degree of structural homology. The C-terminal domains, in contrast, are highly variable in length, ranging from 100-230 aa's, and structure, which include many post-translational modifications (Krupnick and Benovic, 1998). GRKs do however exhibit several common characteristics in that they: 1) preferentially phosphorylate agonist-occupied receptors; 2) interact with their activated receptor substrates which potently activates these enzymes and 3) GRK-mediated GPCR phosphorylation requires the participation of regulatory mechanisms responsible for the localisation and receptor targeting of these enzymes (Pitcher et al., 1998). GRKs do not appear to bind to a clear consensus sequence in their substrates. However, they have been shown to bind preferentially to residues containing pairs of acidic (GRK1 and 2, Fredericks et al., 1996) or basic (GRK5 and 6, Kunapuli et al., 1994) residues located N-terminally to the last phosphorylated residue in the GPCR sequence.

GRKs 2 and 3 contain a pleckstrin homology (PH) domain within their carboxyl terminal. Pleckstrin, the major protein kinase C substrate in platelets, contains two PH domains that are thought to be involved in protein-protein interactions. This region of sequence has been described in more than 70 proteins so far and has been proposed to function as a mediator of protein/protein and protein/membrane interactions. Several different ligands for PH domains have been

Figure 1.7 **Domain architecture of G-protein coupled receptor kinases (GRKs)**

The sequence of the 6 known mammalian GRKs is shown opposite. GRKs contain a central catalytic domain flanked by an approximate 180 aa N-terminal domain and a highly conserved region. The carboxyl-terminal domains are variable in length and contain many post-translational modifications. Rhodopsin kinase (RK, GRK1) is farnesylated, βARK and βARK2 (GRKs 2 and 3) contain a βγ binding domain, GRKs 4 and 6 are palmitoylated and GRK5 contains a basic phospholipid binding domain.

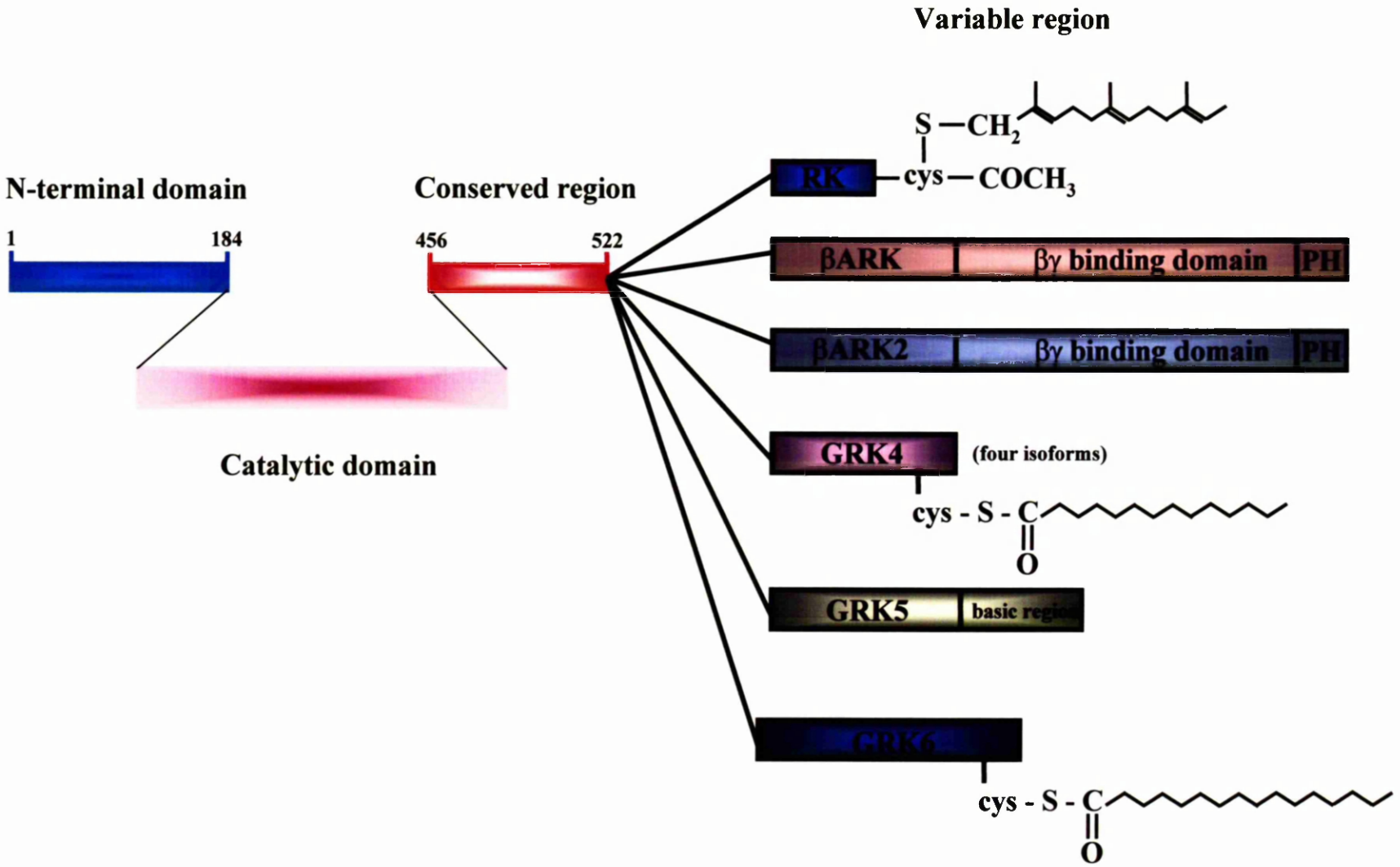
Variable region
S—CH2
cys—COCH3
N-terminal domain
1
184
Conserved region
456
522
RK
βARK
βγ binding domain
PH
βARK2
βγ binding domain
PH
Catalytic domain
GRK4
(four isoforms)
cys - S - C
O
GRK5
basic regio
cys - S - C
O

identified including PKC, IP_3 and the βγ-subunit of heterotrimeric G-proteins (Shaw, 1996). Although GRK 2 was initially described to be a soluble, cytosolic enzyme that translocated to the membrane upon receptor activation (Daaka et al., 1997a), recent data have indicated that several pools of GRK2 exist inside cells: cytosolic, membrane bound and microsomal membrane bound (Murga, et al., 1996; 1997). GRK2 activity is regulated upon interaction with several lipids and proteins present within the three cellular pools and translocation to the PM is facilitated by its interaction with free βγ-subunits released upon receptor activation (Premont et al., 1995). It was shown that $G_{\beta\gamma}$ bound the C-terminal tail of these enzymes and so led to the redistribution of the GRKs to the membrane (Pitcher et al., 1992 and Koch et al., 1993). This association dramatically enhanced GRK2-mediated phosphorylation of activated GPCRs such as the β_2AdR and the m2 muscarinic AchR (Pitcher et al., 1992 and 1995). On the basis of this, it has been proposed that receptor stimulation leads to activation of a heterotrimeric G-protein and the subsequent dissociation of the α- and βγ-subunits. The membrane-localised $G_{\beta\gamma}$ interacts with GRK2 and targets this enzyme to interact with its membrane-bound receptor substrate (Daaka et al., 1997). Recent studies have shown that GRKs can be regulated *via* interaction with many cellular components including actin (GRK5; Freeman et al., 1998), caveolin (GRK1-6; Carmen et al., 1999) and phospholipids (GRK 2,3,5; Carman et al., 2000). However to date, GRK2 and 3 are the only $G_{\beta\gamma}$-regulated GRKs to be identified (Pitcher et al., 1998; Carman et al., 2000).

1.4.2 Sequestration

(a) Arrestins

The interaction of GRK with activated receptor not only brings about receptor phosphorylation, but also serves to attract arrestin molecules to the plasma membrane. Arrestins are a class of protein that function in concert with GRKs to stop or 'arrest' intracellular signalling. Arrestins uncouple activated receptors from G-proteins leading to a functional desensitisation and promotion of clustering of activated receptors to clathrin-coated pits prior to sequestration away from the PM. There are currently four known mammalian arrestins: rod arrestin, (arrestin1, Shinohara et al., 1986), βarrestin (arrestin2, Lohse et al., 1990), βarrestin2 (arrestin3, Gurevich et al., 1993) and cone arrestin (arrestin4, Murakami et al., 1993; Fig. 1.8).

Figure 1.8 Domain architecture of arrestin proteins

The sequence of the four known mammalian arrestins is represented schematically. The solid lines are regions of invariant amino acid sequence and the divergence near the C-terminus represents divergence in sequence between the visual (arrestin-1 and arrestin-4) and non-visual (arrestin-2 and arrestin-3) arrestins.

A	activation recognition domain
P	phosphorylation recognition domain
S	secondary hydrophobic interaction domain
C	clathrin binding domain
+	basic amino terminus
-	acidic C-terminus

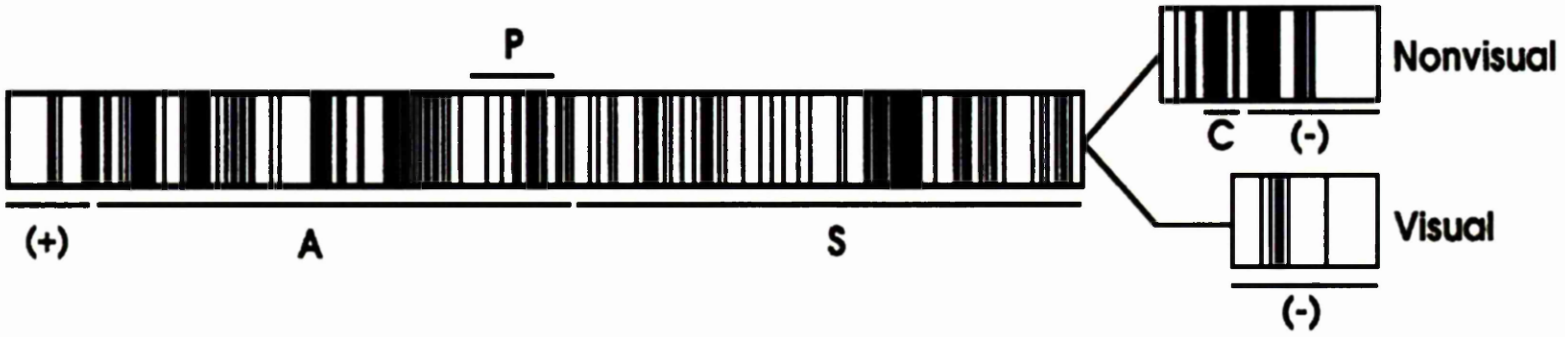
P
Nonvisual
C
(-)
Visual
(-)
(+)
A
S

The prototypic arrestin is a 48 kDa protein, initially termed S-antigen, first identified as the causative agent of a degenerative eye disease. It was subsequently demonstrated that this protein quenched light-dependent signal transduction in rod photoreceptor cells and was named visual arrestin (Pfister et al., 1985). More recently, a second retinal-specific arrestin with ~ 50% homology to visual arrestin was cloned. This arrestin was found to be restricted to cone photoreceptors and was therefore termed cone arrestin (Murakami et al., 1993 and Craft et al., 1994). It was postulated that the rhodopsin signal was quenched by arrestin *via* direct competition between arrestin and transducin for binding of phosphorylated light-activated rhodopsin (Kuhn et al., 1984). This has since been confirmed by direct binding studies with purified arrestin, transducin preparations and rod outer segments (Krupnick et al., 1997b). In 1987, Benovic and co-workers discovered a related protein that enhanced the inactivating effects of GRK2 on the β_2AdR and was postulated to be an arrestin-like protein. The protein was cloned by Lohse et al., (1990) by screening of a bovine brain library with a 1262bp cDNA probe comprising the entire coding sequence of visual arrestin. A positive clone was found to encode a 418aa protein with high homology to visual arrestin, originally termed 'β-arrestin' since it blunted βAdR signalling and it was subsequently named arrestin2. A second non-visual arrestin (arrestin3) was cloned from bovine brain (Sterne-Marr et al., 1993), human thyroid (Rapoport et al., 1992) and rat brain (Attramadal et al., 1992) using comparable screening strategies. Overall, the arrestins are 45% identical and show 70% similarity between residues 16 and 349 of the visual arrestins. Arrestins2 and 3 are ubiquitously expressed, and as such, have been suggested to regulate a wide variety of GPCRs.

(b) Requirement for arrestin in sequestration

A role for arrestins in homologous desensitisation has been shown for many receptors including β_2AdR (Pippig et al., 1993), β_1AdR (Freedman et al., 1995), α_{1B}AdR (Diviani et al., 1996) and odorant receptors (Dawson et al., 1993). Co-expression of these receptors with arrestin2 or arrestin3 showed that arrestin enhanced the rate of receptor desensitisation following agonist stimulation, suggesting that arrestin could discriminate between agonist-activated and non-agonist activated states of GPCRs. From this observation, the concept has arisen that

arrestins contain distinct domains that would interact specifically with GPCRs in their activated state. Analysis of several truncation mutants of visual and non-visual arrestins provided evidence that this region, called the 'activation-recognition region', was located within the N-terminal half of the arrestin molecule (Gurevich and Benovic, 1992; Gurevich et al., 1993 and 1995). In addition, direct binding studies using various receptor-GST (glutathione-S-transferase) fusion constructs demonstrated that the third cytoplasmic loop of the m2 and m3 muscarinic Ach and α_2AdR specifically bound to non-visual arrestins (Wu et al., 1997). Arrestins could discriminate between activated and non-activated receptors suggesting that they contained a recognition sequence specific to the area of the GPCR that is phosphorylated upon agonist exposure (Palczewski et al., 1991). This 'phosphorylation-recognition region' was determined once again by utilising truncated arrestin molecules. Mutants of visual arrestin and arrestin2 and 3 were shown to retain the ability to bind phosphorylated rhodopsin (Gurevich and Benovic, 1992) and the m2 mAChR (Gurevich et al., 1993, 1995).

(c) Arrestins as scaffolding proteins

Many GPCRs have been shown to activate the ERK/MAPK cascade *via* termination of membrane receptor signalling by sequestration (Luttrell et al., 1997; Della Rocca et al., 1999) or by stimulation of tyrosine kinase signalling cascades (van Biesen et al., 1996b; Gutkind, 1998). GPCR-mediated activation of ERK requires tyrosine phosphorylation and assembly of a membrane-associated Ras activation complex. Stimulation of receptors coupled to the G_i and G_q classes of G-protein α-subunit induces rapid tyrosine phosphorylation of the Shc and Gab1 adapter or 'scaffold' proteins followed by Grb2-dependent recruitment of the Ras guanine nucleotide exchange factor mSOS, leading to ERK activation (Luttrell et al., 1999a). Arrestin has been shown to redistribute to the plasma membrane with activated Src (c-Src), a kinase which mediates tyrosine phosphorylation of Shc and Gab1, in cells expressing β_2Ad receptors following agonist stimulation (Luttrell et al., 1999). In the absence of arrestin, c-Src was no longer able to associate with the β_2AdR. This suggested a role for arrestins as a scaffold, able to complex other small molecules for initiation of distinct signalling events. In support of this, expression of dominant-negative mutants of arrestin and dynamin, which block receptor

endocytosis, have been shown to block the activation of MAPK (Lin et al., 1998; Ahn et al., 1999) *via* receptors including the β_2Ad, thrombin and 5-hydroxytryptamine 1A receptor (5-HT_{1A}, Luttrell et al., 1997; Della Rocca et al., 1999). However, this is not universal to clathrin-sequestered receptors as the κ opioid receptor can still activate the MAPK cascade without being internalised (Li et al., 1999).

(d) Clathrin-coated vesicles

Numerous studies have demonstrated that agonist activation of GPCRs leads to translocation of these receptors from the cell surface to distinct intracellular vesicles. One mechanism by which GPCRs internalise is *via* clathrin-coated pits (Von Zastrow and Kobilka, 1992). Clathrin is a triskelion made up of three 190 kDa heavy chains, each with an associated light chain radiating from a central hub (Pearse, 1976, Fig. 1.9). Each leg is ~ 475 Å in length and has a uniform thickness of ~20Å. The coat is made up of triskelions which come together to form a lattice of pentagons and hexagons that curve round each other to enclose a bilayer vesicle (Kanaseki and Kadota, 1969, Fig. 1.9). CCVs are found in all nucleated cells from yeast to humans and are a means of transporting proteins and lipids from the plasma membrane to internal compartments (endosomes). They are also responsible for the transport of newly synthesised proteins from the trans-Golgi network (TGN) to the endosomes. Having shown that GRKs and arrestins were involved in receptor desensitisation, Krupnick et al. (1997b) suggested that non-visual arrestins contained a clathrin-binding domain that targeted desensitised GPCRs for sequestration. Using chimeric proteins containing the N-terminal region of visual arrestin and the carboxyl-terminal region of arrestin2, and *vice versa*, it was shown that the non-visual arrestins were able to interact with clathrin through their C-terminal domains. The site of interaction was further localised to between residues 367 and 385 of arrestin3. Analysis of the C-terminal domains of the four mammalian arrestins showed that arrestin2 and 3 had greater than 80% homology in this region. In contrast, visual arrestins lacked a significant portion of this region and showed less than 30% homology in the remaining residues (Krupnick et al., 1997b). These data put forward a putative clathrin-binding domain present in the non-visual arrestins (Fig. 1.10).

Figure 1.9 **Components of clathrin triskelions and 3D structure of a clathrin coat**

(A) The "height" of clathrin is 200 Å, and the distance between the terminal domains ranges between 300 and 400 Å. Each leg of the triskelion is 475 Å in length, and are of relatively uniform thickness (20 Å). A strongly curved region near the middle of the leg imparts a regular swirl to the trimer, and the somewhat straighter segments of the leg to either side of this curve are known as the distal and proximal domains, respectively.

(B) Representation of a clathrin barrel lattice. The N-terminal domains, which face inward toward the enclosed membrane, are in close contact with the adaptors (not shown). Each edge of a pentagon or a hexagon is made of two proximal segments belonging to two adjacent triskelions and two distal segments from two other, nonadjacent triskelions.

A

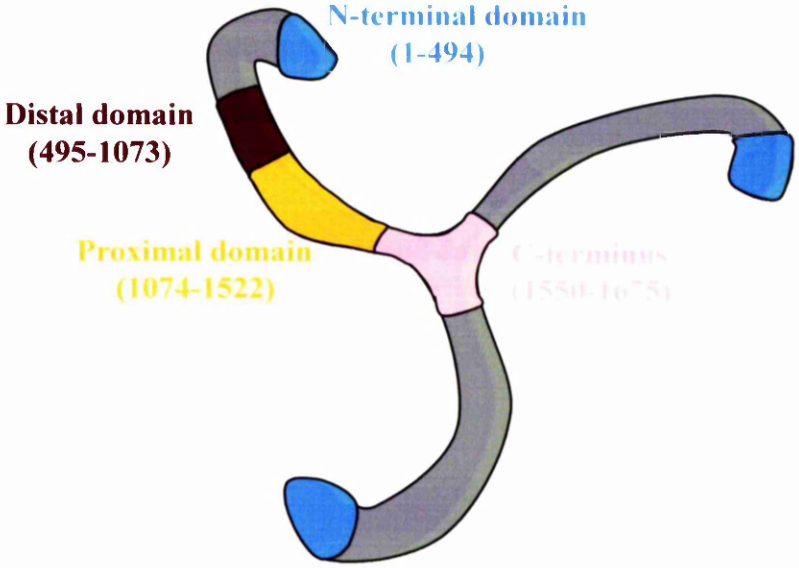
N-terminal domain
(1-494)
Distal domain
(495-1073)
Proximal domain
(1074-1522)

B

Figure 1.10 Alignment of bovine arrestins clathrin binding domain

Bovine arrestin-3 was aligned with the clathrin binding domains (residues 346-391) of bovine visual arrestin, cone arrestin and arrestin-2. Shaded areas denote the residues involved in clathrin binding.

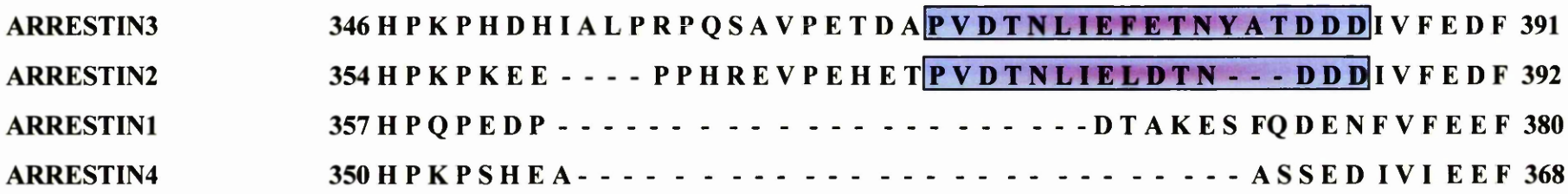
ARRESTIN3 346 H P K P H D H I A L P R P Q S A V P E T D A P V D T N L I E F E T N Y A T D D D I V F E D F 391
ARRESTIN2 354 H P K P K E E - - - - P P H R E V P E H E T P V D T N L I E L D T N - - - D D D I V F E D F 392
ARRESTIN1 357 H P Q P E D P - D T A K E S F Q D E N F V F E E F 380
ARRESTIN4 350 H P K P S H E A - A S S E D I V I E E F 368

(e) Cytosolic 'helper' proteins

A second major constituent of CCVs is the adapter protein (AP) complex. AP complexes form two subtypes, AP1 and AP2, which play multiple roles in controlling coated-vesicle formation (Pearse and Robinson, 1990). They are selectively targeted to either the TGN (AP1) or the plasma membrane (AP2) and direct the formation of clathrin-coated vesicles by acting as a connector between the activated receptor and the clathrin triskelions (Pearse and Bretscher, 1981).

The binding of clathrin is the first step in the initiation of a complex pathway that brings about receptor sequestration. *In vitro* data has shown that the assembly of clathrin coat proteins is insufficient in itself to drive receptor sequestration. Additional cytosolic proteins as well as ATP and GTP hydrolysis are required (Schmid and Damke, 1995). The final membrane fusion event leading to vesicle budding requires both ATP and GTP hydrolysis. ATPases involved in the budding stage have yet to be identified, however, the small GTPase dynamin has been shown to have a role (Van der Bliek et al., 1993; Herskovitz et al., 1993 and Damke et al., 1994). Dynamin is a 100 kDa protein originally purified from bovine brain and characterised as a microtubule (MT)-stimulated GTPase with MT-bundling activity (Shpetner and Vallee, 1989). The effect of dynamin on endocytosis was first observed in *Drosophila*. Temperature sensitive *Drosophila shibire* mutants were seen to undergo paralysis after shift to the restricted temperature (Koenig and Ikeda, 1989) and accumulated a high number of clathrin-coated and uncoated pits. The role of dynamin was confirmed in mammalian cells by the expression of GTPase deficient dynamin mutants which lead to inhibition of endocytosis (Van der Bliek et al., 1993 and Herkovits et al., 1993). Mammalian dynamin occurs in 3 different isoforms: dynamin-1, expressed exclusively in neurones and 70% identical to *shibire* dynamin; dynamin-2, ubiquitously expressed and dynamin-3, expressed in the testis (Van Deurs et al., 1989 and Vallee and Okamoto, 1995). As well as its N-terminal GTPase domain, dynamin contains a cluster of proline-rich sequences at its C-terminus which have the potential to interact with various Src homology (SH) 3 domains (Gout et al., 1993 and Okamoto et al., 1997). SH3 domains are found commonly in signal transduction and cytoskeletal proteins and mediate protein-protein interactions by binding to proline-rich sequences. Amphiphysin is a highly acidic, hydrophilic protein which can be found in soluble and particulate fractions of brain homogenates (David et al., 1996). There are two isoforms of amphiphysin,

Amph1 and Amph2 which share 49% amino acid sequence identity (Owen et al., 1998) and contain SH3 domains in their C-terminal regions (Lichte et al., 1992). Recent work suggested that amphiphysins are major physiological binding partners for dynamin in clathrin-mediated endocytosis (Wigge and McMahon, 1998).

By the use of numerous GTPase defective dynamin mutants (Van der Bliek et al., 1993 and Herskovits et al., 1993) and the introduction of SH3 domains into live cells (Wigge et al., 1997), a specific role for dynamin in endocytosis has been demonstrated (Damke et al., 1996). In this model, dynamin is GDP-bound (inactive) and targeted to the clathrin-coated pit by interaction with: 1) AP2 complexes (Wang et al., 1995) and 2) the SH3-domain containing protein amphiphysin (David et al., 1996) *via* a Pro-Arg-rich C-terminal domain. Amphiphysin binds the clathrin adapter AP2 *via* a region distinct from its SH3 domain resulting in an efficient recruitment of dynamin to the CCVs. GTP/GDP exchange triggers the re-distribution of dynamin from the clathrin lattice allowing it to self-assemble into helical rings at the neck of the coated pit. Intrinsic GTPase activity of dynamin results in a conformational change that closes the collar of the pit and pinches the CCV away from the membrane. The GDP-bound form of dynamin would then be disassembled and recycled (Damke, 1996).

1.4.3 Down-regulation

Prolonged agonist exposure over a period of hours results in receptor down-regulation, being defined as an overall decrease in receptor number (Gagnon et al., 1998). Using the β_2AdR as a model, it has been suggested that sequestered receptors traffick from early endosomes to lysosomes where they undergo degradation. Many GPCRs including the thrombin (Hein et al., 1994), thyrotropin (Petrou et al., 1997) and cholecystokinin (Tarasova et al., 1997) receptors have been shown to be sorted to lysosomes in an agonist-dependent manner.

After receptors and their ligands have been sequestered *via* CCVs, the vesicles are uncoated and the internalised molecules are delivered to 'early' or 'sorting' endosomes (Braell et al., 1984; Rothman and Schmid, 1986; Al-Awqati, 1986; Tycko and Maxfield, 1982). Due to the acidic pH in the early endosomes, the receptors and ligands are dissociated and the receptors are recycled back to the membrane for another round of agonist activation (Davis et al., 1987; DiPaolo and Maxfield, 1984; Yamashiro and Maxfield, 1987). The remaining molecules are

destined for degradation *via* late endosomes or lysosomes (Fig. 1.11). Not all receptor-ligand partnerships follow this pathway. Receptors such as Tfn remain associated with their ligand and traffic *via* the same route as low-density lipoprotein (LDL) receptors (Dautry-Varsat et al., 1983) i.e. they recycle from early endosomes, and although most receptors recycle back to the PM, some can be degraded after internalisation (Felder et al., 1990; Herbst et al., 1994). A variety of experimental techniques including biochemical purification and morphological analysis by microscopy, have been used to characterise endocytic organelles.

(a) Lysosomal degradation

Lysosomes are membrane–bound cytoplasmic organelles that serve as a major degradative compartment in eukaryotic cells (de Deuve, 1963; Kornfeld and Mellman, 1989 and Hunziker and Geuze, 1996). Both endogenous and exogenous molecules can be delivered to lysosomes where they are degraded by acid-dependent hydrolases contained within the lysosomal lumen (de Duve, 1963). Lysosomes are morphologically heterogeneous and often resemble organelles of the endocytic and secretory pathways (Kornfeld and Mellman, 1989). They can however be distinguished by their appearance under the electron microscope. Lysosomes appear as an electron-dense organelle and are therefore known as 'dense bodies', enclosed by a single membrane. They can also be seen to show a clear region just below the membrane ('halo'). This halo is rich in carbohydrates and is thought to protect the lysosomal membrane protein from degradation from its own acidic hydrolases.

(b) Ubiquitination

Another pathway of down-regulation involves the ubiquitin system. In this pathway, proteins are targeted for degradation by ligation to ubiquitin, a highly conserved 76 aa residue protein. The ligation of ubiquitin to the internalised proteins happens in three stages: 1) the C-terminal Gly residue of ubiquitin is activated in an ATP-requiring step by an activating enzyme E1; 2) activated ubiquitin is then transferred to a ubiquitin-carrier protein, E2, on an active Cys residue; 3) ubiquitin is linked by an amide isopeptide linkage to an amino group of the substrate protein's lysine (Lys) residues by a ubiquitin-protein ligase, E3. The ubiquitin pathway of degradation has been implicated in the immune response (Cox et al., 1995 and Dick

Figure 1.11 **Diagrammatic view of receptor transport pathways**

Upon ligand binding, receptors undergo sequestration *via* many pathways of which clathrin is the best studied. The clathrin vesicles are uncoated and receptors are delivered to acidic sorting endosomes where receptor and ligand are dissociated in preparation for recycling back to the membrane or down-regulation. A schematic representation of receptor transport pathways is shown opposite.

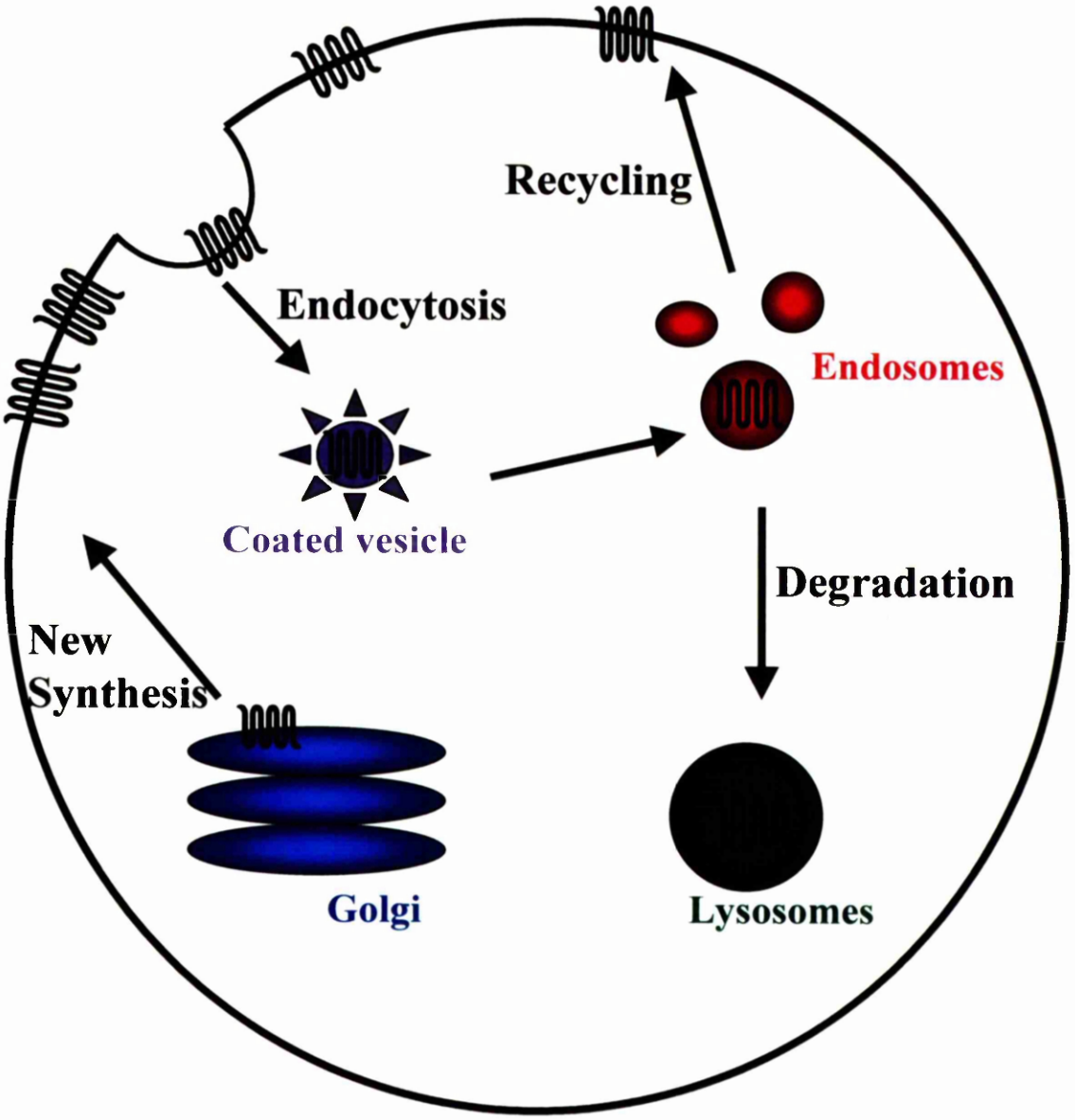
Recycling
Endocytosis
Endosomes
Coated vesicle
Degradation
New
Synthesis
Golgi
Lysosomes

et al., 1994), programmed cell death (Schwartz et al., 1990) as well as receptor down-regulation (Mori et al., 1995).

1.4.4 Tools of the Trade

In order to study the pathways of sequestration and down-regulation, numerous mutants and fluorescently labelled proteins involved in the pathways have been utilised (Chapter 4). One of the most common fluorescent tags used is that of green fluorescent protein (GFP).

GFP from the jellyfish *Aequorea victoria,* was first discovered in 1969 by Shimomura and Johnson and has since been utilised by many as a marker to visualise numerous cellular functions. Shimomura and Johnson noted that the purified protein "gave solutions a slightly greenish look in sunlight, and exhibited a very bright greenish fluorescence in the ultraviolet" (UV). The same group soon published the emission spectrum of GFP that peaked at 508nm when excited at 470nm. Morise et al, in 1974, purified and crystallised GFP and in 1978, Prendergast and Mann obtained the first estimate for the monomer molecular weight.

GFP is a single chain polypeptide of 238 amino acids with a calculated molecular weight of approximately 27kDa. Although GFP was crystallised in 1974, Ormö et al and Yang et al independently solved the first structure in 1996. GFP is an 11-stranded β-barrel threaded by an α-helix running up the axis of the cylinder (Fig. 1.12). The chromophore of GFP is covalently bound and is formed by modification of a Ser-Tyr-Gly sequence at aa's 65-67 in the native protein. It is attached to the α-helix and buried almost perfectly in the centre of the cylinder. Due to this structure, the chromophore is stable when exposed to a variety of harsh treatments including heat, extreme pH and chemical denaturants (Bokman and Ward, 1981) and the fluorescence survives glutaraldehyde and formaldehyde fixatives (Chalfie et al., 1994). The GFP most commonly used to date is an enhanced form which contains mutations of Ser to Thr at position 65 and phenylalanine (Phe) to Leu at position 64 giving a improved fluorescence over WT GFP. It is also encoded by a gene with human optimised codons (Cormack et al., 1996;1996 and Yang et al.,1996).

Figure 1.12 **Three-dimensional structure of green fluorescent protein (GFP)**

GFP consists of a single polypeptide chain forming an 11 β-stranded hollow cylinder through which is threaded an α-helix bearing the chromophore, shown in ball-and-stick representation opposite. Mutations in the chromophore are responsible for producing spectrum-shifted mutants that show enhanced or altered emission wavelengths.

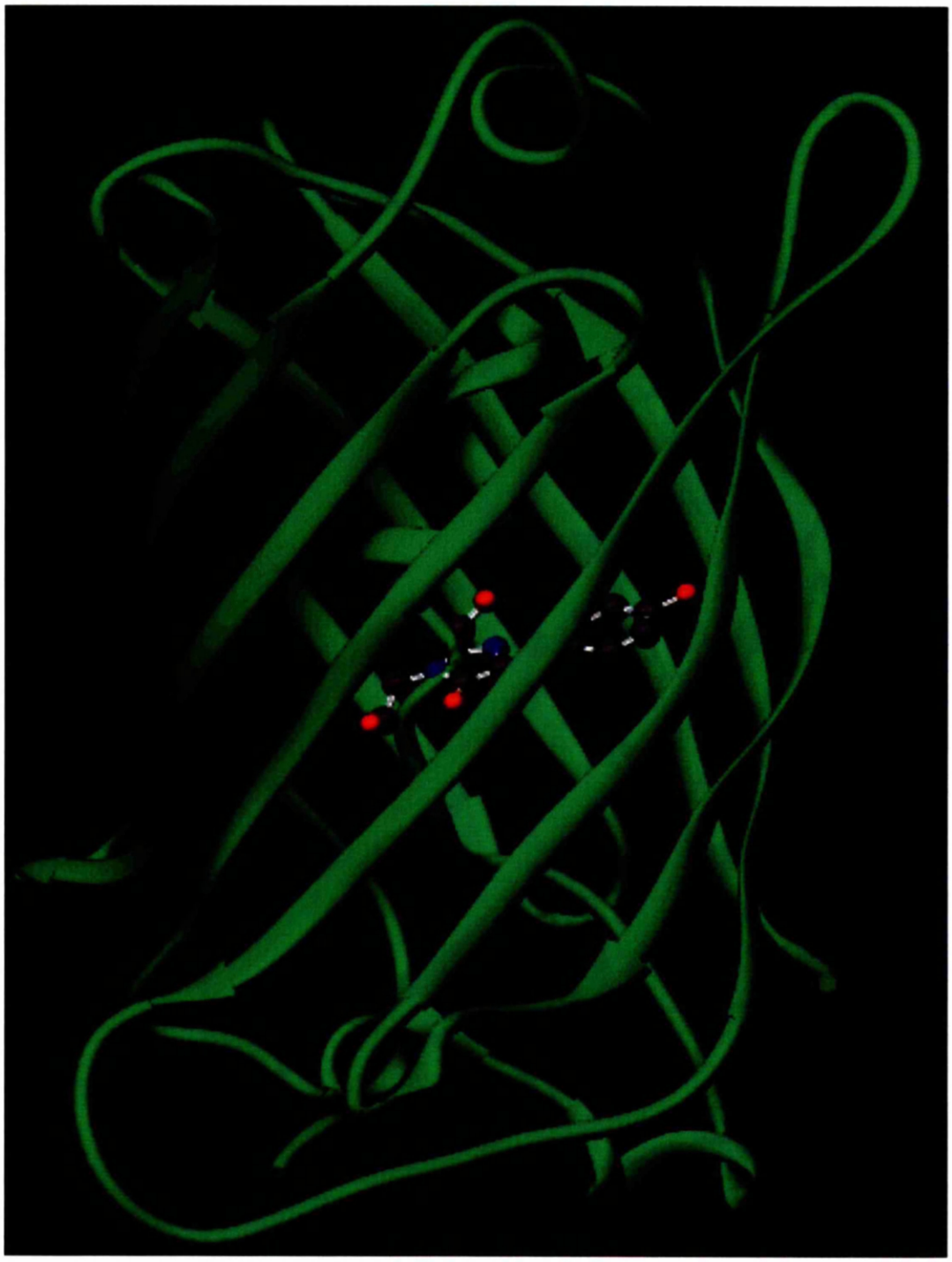

This enhanced form of GFP (EGFP) absorbs blue light at 488nm and emits green light at 509nm (Tsien, 1998).

GFP has many cell biological applications in which it is used as a tag or indicator. The most successful use of GFP has been as a genetic fusion partner to proteins of interest to monitor their cellular localisation and fate. One of the most well-known fusion strategies is that of GFP fusion with the C-terminal of GPCRs. Expression of these GPCR-GFP fusions in various cell types and systems has allowed the visualisation of receptor trafficking in response to agonist stimulation. These receptors include the β_2AdR (Barak et al., 1997a), cholecystokinin A receptor (Tarasova et al., 1997), TRHR (Drmota et al., 1998 and 1999), α_{1A} and α_{1B}AdR (Hirasawa et al., 1997), vasopressin V_2R (Schulein et al., 1998), ET_A and $_B$ receptors (Abe et al., 2000) and the A_1 and A_3ARs (unpublished data).

Mutations in GFP cDNA have resulted in the production of many 'fluorescently shifted' proteins (Table 1.2). These range from the UV through the visible spectrum of light and have dramatically increased the applications of fluorescent proteins. One way to exploit these biochemically enhanced GFPs is to use fluorescence resonance energy transfer or FRET. FRET occurs when two fluorophores are in molecular proximity (<100Å apart) and the emission spectrum of one fluorophore, the donor, overlaps the excitation spectrum of the second fluorophore, the acceptor (Tsien et al., 1993). The light emitted can be used to detect the interaction of the two labelled proteins. In principal the use of FRET offers advantages and disadvantages over other current methods for detecting protein-protein interactions (Tsien, 1998). The biggest disadvantage is the high level of background obtained as the donor emission has a tail that extends into the acceptor's emission band and the acceptor excitation has a tail that extends into the donor's excitation band. For this reason, FRET is best used at later stages of analysis when the two host proteins have been biochemically and molecularly well characterised and only the dynamics of their interaction is to be determined.

The process of sequestration has been subject to many disruptions. A subtle way of interfering in this system is by the use of mutant proteins. As previously stated, GRKs, arrestin, amphiphysin and dynamin are important in the initiation and 'pinching-off' of CCVs. Numerous truncations and mutations have been made of these proteins and all have unique effects on receptor sequestration (Chapter 4).

Table 1.2 Table of GFP chromophore mutations

The table opposite illustrates some of the 'fluorescently shifted' GFP molecules obtained by mutation of the centrally located chromophore (Ser-Tyr-Gly). These GFPs range from the UV through the visible spectrum of light.

Table 1.2

Amino Acid Change	Excitation / Emission	Effects
S65G	513/527nm	Red-shifted FP
S65T	488/511nm	Shifted emission maximum a few nm, increased fluorescence yield
Y66H	382/448nm	Blue FP, extremely dim
Y66F	N/A	Non-fluorescent
V68L	513/527nm	Red-shifted FP
S72A	513/527nm	Red-shifted FP
S205	N/A	Hydrogen bonds with E222
E222G	485/506nm	Single excitation peak, hydrogen bonds shown to be important in UV vs blue excitation photoisomers

1.5 Adenosine receptors and their ligands

Adenosine acting on its cell-surface receptors can elicit numerous responses within varying organ systems. ARs can be activated *via* endogenous adenosine when local levels rise due to stress in situations such as cardiac hypoxia (Fenton and Dobson, 1987) and ischaemia (Hagberg et al., 1987), or by externally administered adenosine and its analogues. The regulation of AR activation has therefore been recognised as having possible therapeutic functions.

1.5.1 AR Agonists

Agonists can be defined as compounds that act on receptors to elicit a response. Modifications of the N^6 and C2 positions of the adenine ring and the 5'-position of the ribose moiety produce analogues of adenosine which are more stable than adenosine itself, and have been used extensively to characterise the ARs (Ralevic and Burnstock, 1998). Agonists such as NECA (N-ethylcarboxamidoadenosine, Williams, 1989), APNEA (N-[2-(4-aminophenyl)ethyl]adenosine, Fozard and Carruthers, 1993) and ^{125}I-AB-MECA (^{125}I-aminobenzyl)-5'-N-methylcarboxamidoadenosine, Olah et al., 1994) do not show selectivity between AR subtypes (Fig. 1.13).

(a) A_1AR Agonists

Certain N^6-substituted adenosine derivatives including N^6-cyclopentyladenosine (CPA) and N^6-cyclohexyladenosine (CHA) and (R)N^6-phenylisopropyladenosine ((R)-PIA) are selective agonists of A_1ARs (Jacobson et al., 1992a). Substitutions at both the N^6 and C2 positions has produced a 2-chloro-CPA (CCPA) which has been found to be 1500-fold more potent at the A_1AR than the A_2AR following ligand binding studies using rat brain (Lohse et al., 1988; Jacobson et al., 1992b; Fig. 1.13).

(b) A_{2A}AR Agonists

Generally, A_{2A}ARs do not bind to N^6-substituted analogues but show a preference for derivatives that have been modified at the second position of the adenine ring. Bulky substitutions at this position have been shown to selectively enhance binding to A_{2A}ARs, leading to several A_{2A}-selective agonists being

produced (Jacobson et al., 1992b; Siddiqi et al., 1995). The C2-substituted derivative of NECA, CGS 21680, has been shown to be 140-fold more selective for A_{2A} than A_1ARs (Hutchison et al., 1990) but has very low affinity for A_{2B}ARs. This allows CGS 21680 to be used as a screen to discriminate between A_{2A} and A_{2B} receptor subtypes (Jarvis et al., 1989; Lupica et al., 1990). Although NECA itself is almost equipotent at A_1 and A_2 receptors, it can be used in characterisation of A_{2A}ARs providing that the A_1-selective ligands used do not show equivalent effects. It should be noted however, that most of the agonist studies have been carried out in species other than human, with the human A_{2A}ARs showing a much lower binding affinity for CGS 21680 and other AR agonists.

(c) A_{2B}AR Agonists

Selective agonists for the A_{2B}AR have, as yet, failed to be found. In order to determine the presence of A_{2B}ARs, accumulation of AC in membranes is used as long as a lack of activity/ binding of A_1, A_{2A} and A_3-selective agonists is confirmed (Ralevic and Burnstock, 1998). As with A_{2A}-selective agonists, A_{2B}ARs show preference for derivatives with substitution at the C2 position of the adenine ring. So far, NECA is the most potent adenosine analogue, even though it shows only low micromolar affinity for the receptor (Brackett and Daly, 1994). In a recent study netrin-1, a laminin-related secreted protein critical for controlling axon elongation, has been shown to bind to A_{2B}ARs and induce cAMP accumulation. This could suggest a second physiological ligand and possible selective agonist for these receptors (Corset et al., 2000).

(d) A_3AR Agonists

As observed with A_1ARs, the main class of A_3-selective adenosine analogues contains a substitution at the N^6 position of the adenine ring (Fig. 1.13). IB-MECA, (N6-(3-iodobenzyl)-5'-(N-methylcarbamoyl)adenosine), is 50-fold more selective for rat brain A_3ARs than A_1 or A_{2A} (Gallo-Rodriguez et al., 1994) and the iodinated radioligand ^{125}I-AB-MECA has been shown to bind A_3ARs with nanomaolar affinity. Selectivity of these ligands can be enhanced by substitution at the C2 position of these compounds, forming for example, 2-chloro-IB-MECA (2Cl-B-MECA) which has a 2500- and 1400-fold greater selectivity for A_3ARs over A_1 and A_{2A}ARs respectively (Kim et al., 1994).

Figure 1.13 **Chemical structure of non-selective adenosine receptor agonists**

Shown opposite are representations of the chemical structures of the adenosine analogues N-ethylcarboxamidoadenosine (NECA), R-N^6-(phenylisopropyl)adenosine ((R)-PIA) and (^{125}I-4-aminobenzyl-5'-N-methylcarboxamidoadenosine) [^{125}I]AB-MECA. These compounds are non-selective agonists for the adenosine receptors.

A

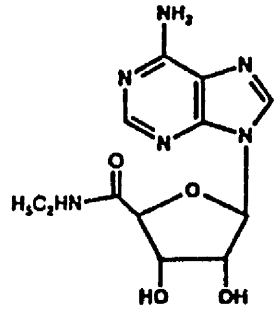

NECA

B

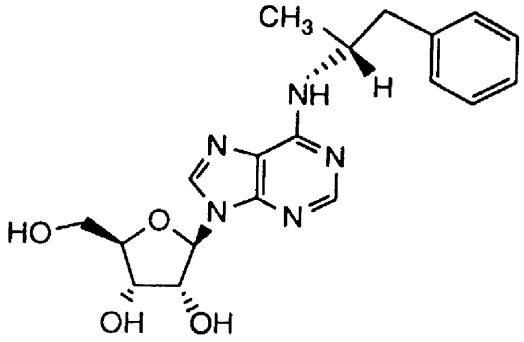

R-PIA

C

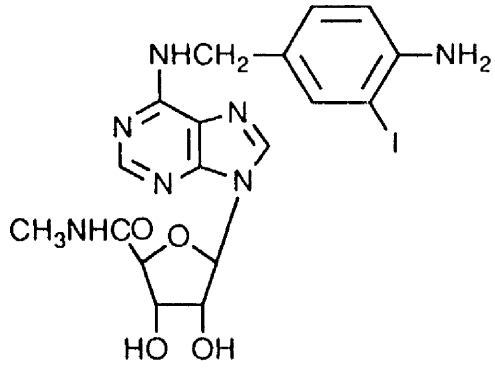

[^{125}I]AB-MECA

1.5.2 AR Antagonists

Xanthines and their derivatives, including natural derivatives such as caffeine, are non-selective, although not universal, AR antagonists. Antagonists can be defined as ligands that inhibit the action of agonists, binding to the R and R* states of a receptor with equal affinity.

(a) A_1AR Antagonists

Substitutions into position 8 of the xanthine ring have yielded potent and selective A_1AR antagonists for example DPCPX (1,3-dipropyl-8-cyclopentylxanthine) and XAC (xanthine amine conger). Of these compounds, DPCPX has the greatest affinity for the rat A_1ARs (Bruns et al., 1987; Lohse et al., 1987) with a lower affinity for human A_1 receptors (Libert et al., 1992; Klotz et al., 1998). Some non-xanthine antagonists have also been described which show reasonable affinity and selectivity for A_1ARs.

(b) A_{2A}AR Antagonists

Several A_{2A}AR antagonists have been described and synthesised. CSC (8-(3-chlorostyryl)caffeine) is a potent A_{2A}-selective antagonist often used in radioligand binding assays. It is 520-fold more selective at the A_{2A}AR than the A_1 and has been shown to reverse the effects of agonist on AC (Jacobson et al., 1993). The non-xanthine antagonist of the A_{2A}AR, ZM 241385 ((4-(2-[7-amino-2-(2-furyl)[1,2,4]triazolo[2,3-α][1,3,5]triazin-5-yl amino]ethyl)phenol)), displays 1000- and 91-fold selectivity for the A_{2A}AR versus the A_1 and A_{2B} receptors respectively, and has absolutely no effect at A_3ARs (Poucher et al., 1995). This has been used to generate a high-affinity selective antagonist radioligand ^{125}I-ZM 241385 (Palmer et al., 1995c).

(c) A_{2B}AR Antagonists

As with A_{2B}AR agonists, there are very few compounds, either xanthines or non-xanthines, which can be classed as A_{2B}-selective antagonists. One compound, enprofylline (propyl-xanthine) used as an anti-inflammatory in asthma, has been shown to be inactive at A_1, A_{2A} and A_3ARs and may therefore be a starting point to develop a selective A_{2B} antagonist (Feoktistov and Biagionni, 1996). Recently, the first potent and selective antagonists of A_{2B}ARs have been described. These

compounds, MRS1754 in particular, are anilide derivatives of 8-phenylxanthine. The availability of $A_{2B}AR$ antagonists increases the opportunity to explore this receptor in asthma and holds promise for the treatment of inflammatory and ischaemic diseases (Kim et al., 2000; Linden, 2001).

(d) A_3AR Antagonists

Selectivity of A_3AR antagonists has been found to be very much dependent upon the species being investigated. Xanthine derivatives display a higher affinity for human and sheep A_3ARs compared to rat, rabbit and gerbil (Zhou et al., 1992; Linden et al., 1993; Salvatore et al., 1993; Ji et al., 1994), varying from nanomolar to micromolar, respectively. Five chemical classes and three flavanoid classes of A_3-selective antagonists have also been described (Jacobson et al., 1996). The chemical class includes the compound L-268605 (3-(4-methoxyphenyl)-5-amino-7-oxo-thiazolo [3,2] pyrimidine) which is potently selective for A_3ARs and has no appreciable effect on human A_1 or A_{2A} receptors (Jacobson et al., 1996). The flavanoid class of antagonists again, shows species selectivity. This class includes MRS1523 (9-chlor-2-(2-furyl)5-phenylacetylamino [1,2,4] triazolo [1,5-c] quinazoline) which is selective for rat A_3 versus human (Jacobson et al., 1997; Fig. 1.14).

1.6 Therapeutic roles of adenosine and the A_3AR

Despite the recent identification of the A_3AR (Zhou et al., 1992), several studies have implicated this receptor in mediating effects of adenosine which may have therapeutic potential. Since the first physiological effects of adenosine were documented (Drury andSzent-Gyorgi, 1927), investigators have demonstrated that this small molecule, acting through its A_3 receptor, is involved in cardioprotection (Fenton and Dobson, 1983; Stambaugh et al., 1997) and neuroprotection (von Lubitz et al., 1994) from ischaemia-induced damage, bronchoconstriction (Linden et al., 1993; Salvatore et al., 1993; Sajjadi and Firestein, 1993), induction of hypotension (Fozard and Carruthers, 1993) and mast cell and eosinophil degranulation (Kohno et al., 1996). These data gives strong weight to the therapeutic advantages of manipulation of adenosine regulation in disease states such as cardiac disease, stroke and asthma.

Figure 1.14 Chemical structure of an A_3AR antagonist

Shown opposite is a schematic representation of the chemical structure of an A_3AR-selective antagonist, MRS1523. This is the first relatively potent and selective A_3AR antagonist for non-primate species, notably rat. In radioligand binding studies, MRS 1523 displayed a K_i value of 130nM (Li et al., 1998).

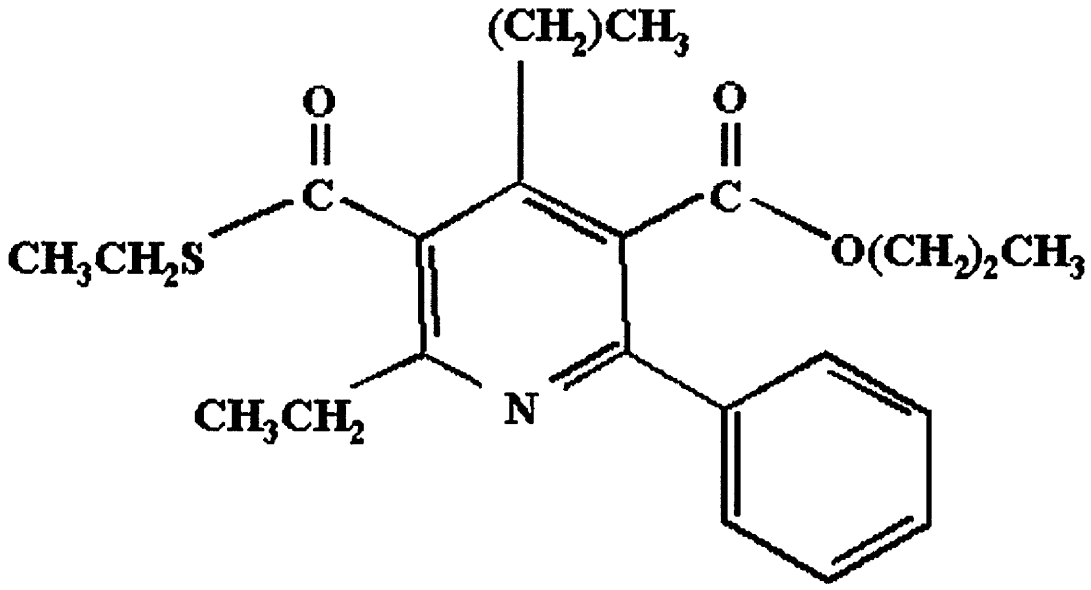
(CH2)CH3
O
C
O
C
CH3CH2S
O(CH2)2CH3
CH3CH2
N

1.6.1 Cardioprotection

Upon binding to A_3ARs, adenosine leads to interaction of the receptors with the G_i family of G-proteins (Palmer et al., 1995b). This inhibits AC, and activates PLC to elevate IP_3 concentration and mobilise intracellular Ca^{2+} (Abbracchio et al., 1995).

The phenomenon of ischaemic preconditioning was first reported by Murray et al. in 1986, who discovered that brief ischaemic periods that were too brief to cause necrosis themselves, greatly reduced the amount of infarction from a subsequent, sustained occlusion. Pre-conditioning, a brief period of reduced blood flow leading to a decrease of oxygen to the tissues, can thus protect the heart from a subsequent prolonged ischaemic episode (Tracey et al., 1997). This loss of blood flow to the myocardium causes breakdown of ATP, resulting in an increase in levels of adenosine in the interstitial fluid. The involvement of adenosine and the ARs in this process was not discovered until 1991 when Lui et al. administered AR antagonists to preconditioned hearts and found that the protective effect was blocked. The adenosine released binds A_1ARs and A_3ARs present on cardiac myocytes and limits the damage sustained by the myocardium during the ischaemic episode (Lui et al., 1994; Auchampach et al., 1997). As infarcted tissue is no longer able to contract, the global functioning of the heart can become progressively impaired, ultimately leading to heart failure. Since the discovery of preconditioning, it has been suggested that manipulation of the signalling pathway used in this phenomenon can be manipulated to develop an effective strategy to block infarction.

One possible way of increasing the adenosine concentration in the heart is to administer precursors or inhibitors of adenosine metabolism, providing the highest concentration of adenosine at the target sites i.e. the cardiac cells (Smolenski et al., 1998). An alternative approach increases the concentration of endogenous adenosine by inhibiting its transport across the cell membrane (Van Belle, 1993). This protects adenosine released from the cell during ischaemia from degradation by uptake and metabolism into the vascular endothelium, prolonging the presence of adenosine in the interstitial space. Several benefits of this approach in recovering cardiac function following ischaemia have already been documented (Masuda et al., Van Belle et al., 1993). Adenosine concentration has been increased in the ischaemic heart by the administration of the ADA inhibitor EHNA (erythro-9(2-hydroxy-3-nonyl)adenine). This prevents the degradation of endogenously formed adenosine, providing

significant improvement of myocardial infarction following ischaemia (Bolling et al., 1990).

Coronary vasodilation has long been recognised as a physiological effect of adenosine (Berne, 1980). The heart, under normal conditions, extracts most of the oxygen from the coronary blood. Unlike skeletal muscle, cardiac muscle must maintain a balance between energy supply and utilisation. This involves cross-talk between cardiac cells and the coronary blood vessels. As oxygen pressure rises, the rate of formation of potentially harmful oxidants increases and may result in myocyte damage (Winegrad et al., 1999). Cardiac myocytes in the intact organism are exposed to oxygen levels in the range of 6 to 7%. With increasing oxygen concentrations, cardiac myocytes produce angiotensin I (Ang I), which is converted into Ang II by angiotensin converting enzyme (ACE) in the blood vessel, and thus increases vascular tone (Brutseart et al., 1988). Below normal physiological oxygen levels, adenosine is released from the myocytes and acts directly on the vascular smooth muscle cells to counteract the rise in tension. This effect is normally produced by α-adrenergic receptor (αAdR)stimulation, suggesting that adenosine acts by either altering the α-adrenergic receptor directly or some factor downstream from it (Winegrad et al., 1999).

1.6.2 Neuroprotection

Although presence of the A_3AR in brain is 10-30 times lower then A_1 (cortex) or A_2ARs (striatum; Jacobson et al., 1995), it can elicit a wide range of neuronal and astrocytic responses that, dependent upon the pattern of activation, can be exceedingly lethal or highly protective. The pathophysiology of brain ischaemia can be summarised by a complex cascade of biochemical and electrophysiological processes. A decrease in cerebral blood flow leads to energy failure and disrupted ion homeostasis due to an enhanced efflux of cellular K^+ and influx of Ca^{2+} and Na^+. This leads to membrane depolarisation and cytotoxic oedema. Release of excitatory neurotransmitters triggers further membrane depolarisation and the additional accumulation of cytosolic Ca^{2+} by cellular influx (Simon et al., 1984). This Ca^{2+} accumulation plays a key role in circulation of irreversible neuronal damage leading to free radical generation, activation of proteolytic enzymes and activation of apoptotic genes (Siesjö et al., 1989).

Adenosine levels in the brain are elevated during seizures, producing two distinct effects. Short-term activation of the A_3 receptors appears to increase the amount of damage seen after cerebral ischaemia whereas a prolonged exposure to the agonist has a neuroprotective effect. It is thought that adenosine can dampen the inflammatory response and induce dilation of cerebral vessels (Ongini et al.,1997, von Lubitz, 1997) resulting in increased blood flow to the brain. Adenosine receptor activation initiates numerous cellular responses, decreasing neuronal activity and increasing nutrient supply. These responses include: 1) presynaptic attenuation of neurotransmitter release (Dolphin and Archer, 1983); 2) postsynaptic inhibition of sustained membrane depolarisation (Schubert et al., 1985) and 3) hyperpolarisation of astrocyte membranes to improve uptake of extracellular K^+ and glutamate (Drejer et al., 1985). It has been shown that an increase in extracellular adenosine levels can lead to the stimulation of A_2AR present in the brain vasculature causing: 1) smooth muscle relaxation leading to vasodilation and an increase in blood flow and nutrient supply (Collis, 1989) and 2) inhibition of the inflammatory response which would otherwise lead to capillary blockage (Grisham et al., 1989; Cronstein et al., 1986).

Adenosine itself has a very short biological half-life, somewhere in the range of 3-6 seconds (Rudolphi et al., 1992), probably penetrating the blood-brain barrier poorly. Therefore, in order to attenuate the effects of the endogenous adenosine released during cerebral ischaemia, compounds that would interfere with its inactivation and/or increase adenosine release or inhibit AR transport would be of great therapeutic potential. Administration of inhibitors of the enzymes ADA and adenosine kinase would increase the chance of endogenously formed adenosine to interact with its receptors at the exterior surface of the cell membrane. The actions of these inhibitors would be more or less specific, restricted to areas where adenosine levels are increased, thereby limiting the risks of problematic side effects. Few studies on the effects of these compounds have been published and those that have display conflicting results. Despite these data, there is a large body of evidence to suggest that adenosine does have a neuroprotective effect in ischaemic brain.

1.6.3 Mast cell and eosinophil activation

Allergic inflammation involves a complex interaction of many different inflammatory cells that release a spectrum of chemical mediators. Allergic reactions consist of an early phase response that primarily involves the degranulation of mast cells. Mast cells are found in most organs in the body including heart, brain, lungs and kidneys. Degranulation is accompanied by a release of histamine and leukotrienes leading to the migration of inflammatory cells from the circulation, and it has been shown that adenosine under stress conditions can induce degranulation without the aid of antigens (Linden, 1994). In the bronchi, degranulation causes the release of mediators that bring about constriction of the bronchiolar smooth muscle (Jin et al., 1997), while reperfusion after ischaemia in the heart leads to neutrophil accumulation and inflammatory tissue damage (Zimmerman and Granger, 1992). Both systems suggest the possible involvement of adenosine in the pathophysiology of asthma and inflammatory disease.

The indication that A_3ARs were involved in mast cell degranulation was first proposed by Ramkumar et al., (1993) when they identified A_3ARs on the surface of RBL-2H3 cells, a tumour cell line derived from rat mast cells. Further studies using hamster cheek pouch arterioles and A_3AR-selective agonists and antagonist correlated these initial findings, although the presence of other AR subtypes could not be completely ruled out (Doyle et al., 1994).

1.7 Project Aims

In order to manipulate the A_3AR in disease states, we must first understand how it is regulated in response to agonist exposure. The aims of this project were therefore three-fold: (1) to determine if there is a link between A_3AR phosphorylation and internalisation; (2) to identify the specific residues involved in the phosphorylation and desensitisation of A_3AR function and (3) to determine the cellular distribution of A_3ARs following agonist binding. Molecular biological techniques were used to create GFP-tagged forms of WT and mutant rat A_3ARs that allowed further investigation of these receptors by confocal microscopy. Coupled with previous data and computational analysis, these procedures individually and collectively led to characterisation of the rat A_3AR.

Chapter 2

Materials and Methods

2.1 Materials

All reagents used were of the highest grade commercially available and obtained by the following suppliers:

Alexis Corporation, San Diego, CA, USA

DTT

Amersham

Iodine-125

BDH Chemicals Ltd., Poole, UK

Acrylamide, coverslips

Calbiochem-Novabiochem (UK) Ltd., Nottingham, UK

Forskolin, PMA

Costar, Cambridge, MA, USA

75cm^2 tissue culture flasks, 60mm and 100mm tissue culture dishes, 6,12 and 24 well tissue culture plates, cryovials

Cruachem, Glasgow, UK

Oligonucleotides

Fisher Scientific, Loughborough, Leicestershire, UK

HEPES, sodium dodecyl sulphate, EDTA, DMSO, ethidium bromide solution, glacial acetic acid, methanol, ethanol, concentrated HCl, sodium fluoride, sodium phosphate

GIBCO BRL Life Technologies, Paisley, UK

Phenol:chloroform, LipofectAMINE, new born calf serum, OptiMEM, phosphate free DMEM

Melford, Chelsworth, Ipswich, Suffolk, UK

Kanamycin

Merck, Darmstadt, Germany

Bactotryptone, agar

Molecular Probes

Transferrin-Alexa™594 conjugate, Alexa™594 Goat-anti-mouse IgG conjugate, Alexa™594 Goat-anti-rabbit IgG conjugate, LysoTracker® Red DND-99, Concanavalin A Alexa Fluor™594 conjugate

New England Biolabs Inc., Beverley

Protein molecular weight marker, restriction enzymes

NEN Life Science Products Inc., Boston

ECL reagents, ^{32}P-orthophosphate, X-ray film

Pierce, Rockford, IL 61105, USA

EZ-Link™ Biotin-LC-hydrazide, HRP-streptavidin

Promega, Southampton, UK

T4 DNA ligase, SV mini-prep kit, G-418 sulphate, restriction enzymes

Qiagen, Crawley, West Sussex

Gel purification kit, plasmid maxi kit

Research Biochemicals International, Natick, MA, USA

(R)-PIA, NECA

Roche Molecular Biochemicals/Boehringer-Mannheim, Mannheim, Germany

Tris, DNA molecular weight marker, restriction enzymes, anti-HA mouse monoclonal IgG (clone 12CA5), adenosine deaminase

Santa Cruz Biotechnology Inc., Santa Cruz, CA, USA

β-arrestin2 (N-16) goat polyclonal IgG, dynamin I/II (N-19) goat polclonal IgG, $cPLA_2$ (N-216) rabbit polyclonal IgG, GFP (FL) rabbit polyclonal IgG

Sigma-Aldrich Company Ltd., Poole, Dorset, UK

Triton X-100, soybean, benzamidine, pepstatin A, bovine serum albumin, protein A sepharose, sodium periodate, bisacrylamide, HRP anti-mouse IgG, HRP goat anti-rabbit IgG, HRP rabbit anti-goat IgG, HRP-streptavidin, thimerosal, bromophenol blue, bichinchonic acid, sodium azide, CHAPS, DEAE-Dextran, FITC-Dextran, agarose, deoxycholic acid, polyethylenimine, ampicillin, adenosine deaminase, paraformaldehyde, TEMED, PMSF, chlorpromazine, 8-bromo-cGMP, Ham's F-12, DMEM, PBS (sterile), foetal bovine serum, trypsin, penicillin/streptomycin, L-glutamine

Stratagene

Pfu Turbo DNA polymerase

Tocris/Semat Technical (UK) Ltd., St. Albans, Herts., UK

A23187

Whatman International Ltd., Maidstone, UK

GF/C glass fibre filters

IB-MECA and the A_3-selective antagonist MRS1523 were the generous gifts of Dr Ken Jacobson, National Institutes of Health, Bethesda, MD.

A mutant human A_1AR cDNA in which the Cys 309 was changed to Ala was a gift from Dr Mark Olah, University of Cincinnati College of Medicine, Cincinnati, OH.

^{125}I-AB-MECA was synthesised and purified by high performance liquid chromatography as described previously (Olah et al. 1994).

9E10 monoclonal antibody specific to myc-epitope, was prepared in-house at Duke University, Durham, NC by Dr Tim Palmer.

2.2 Cell Culture and Transfections

2.2.1 Cell Maintenance

CHO cells were maintained in Ham's F-12 medium and Human embryonic kidney 293 (HEK293) and COS-P cells maintained in DMEM, supplemented with 10%(v/v) FBS, penicillin (100units/ml), streptomycin (100μg/ml) and 1% L-glutamine in a 37°C humidified atmosphere containing 5% CO_2. Cells stably expressing adenosine receptors were maintained in the appropriate medium supplemented with G-418. Cells were routinely passaged 1:8. When confluent, cell monolayers were washed with PBS without $CaCl_2$ and $MgCl_2$, 1ml of trypsin added and the flasks returned to the incubator to allow cells to detach. 7mls of medium were then added to the flasks and the cells pipetted gently to allow resuspension. Cells were either passaged into flasks to maintain the cell line or seeded into dishes for experimental analysis.

2.2.2 Transient Transfections using LipofectAMINE

On the day prior to transfection, 75cm^2 flasks of CHO or HEK293 cells were passaged 1:8 into 6 well plates and cells left overnight to plate down. For each well to be transfected, 2μg DNA and 4μl of LipofectAMINE reagent were mixed with 0.24ml OptiMEM and incubated at room temperature for 15 - 45 minutes in the dark. During the incubation, cell monolayers were washed with OptiMEM and the medium replaced with 0.76ml / well OptiMEM. The DNA-LipofectAMINE mix was added dropwise to the cells and the plates returned to the incubator for 3 hours. Following incubation, the DNA-OptiMEM was removed and replaced with fresh medium minus G-418. Cells were analysed 24 - 48 hours post- transfection.

2.2.3 Transient Transfections using DEAE-Dextran

On day 1, a confluent 75cm^2 flask of COS-P cells was passaged 1:4 into 100mm dishes and left to plate down overnight. On reaching 70-80% confluency, the cells were transfected. For each plate to be transfected, 4.75ml PBS-CM, (136mM NaCl, 2.7mM KCl, 8mM disodium hydrogenphosphate, 1.47mM potassium dihydrogenorthophosphate (pH 7.2 – 7.5), supplemented with 1mM $MgCl_2$, 0.1mM $CaCl_2$), 2.5-25μg of maxiprep purified DNA and 0.25ml of DEAE-Dextran

(10mg/ml solution made up in PBS-CM) were added to a sterile centrifuge tube and vortexed briefly before and after the addition of the dextran. Equal volumes of solution were added to the cell monolayers and incubated for 35-45 mins at 37°C in the incubator. 4.5mls of the transfection mix was removed, replaced with 10mls of medium supplemented with chloroquine (100μM) and the dishes returned to the incubator for a further 2.5-3 hours. The medium/chloroquine mix was removed and replaced with 2mls/dish of medium supplemented with 10% (v/v) dimethyl sulfoxide (DMSO) for 2-3 minutes at room temperature. Medium/DMSO was aspirated off, cells washed twice with PBS-CM and replaced with 10mls of regular medium. Fresh media was added to the cells 24 hours post-transfection and cells harvested for analysis between 48 and 72 hours post-transfection

2.2.4 Stable Transfection of CHO cells

Cell lines stably expressing AR's were generated using a modified calcium phosphate precipitation / glycerol shock procedure (Olah et al. 1992). Confluent CHO cells in 75cm^2 flasks were split 1:5 into 100mm dishes and the medium changed the following morning. The transfection mixture of 1.5μg DNA, 1M $CaCl_2$ (125μl) and water to a final volume of 375μl was prepared, to which 0.5mls of 2 x HEPES buffered saline stock (HBSS, 280mM NaCl, 50mM HEPES, 1.5mM Na_2HPO_4 pH 7.13) was added and gently bubbled through. Once the mix appeared milky, it was left at room temperature for 40 minutes, after which, it was added dropwise onto the cell monolayer and returned to the incubator for 4-5 hours. Following incubation, the media was apirated off, the cells washed once with PBS, 2mls of 15% (v/v) glycerol added and the cells allowed to incubate at 37°C for 2 minutes. On removal of the glycerol, the cells were washed three times with PBS, 10mls medium (minus G-418) replaced and the cells incubated overnight. Medium was changed the following day.

48 hours after transfection, the monolayer was washed with PBS, cells split 1:8 as normal and titrated into 100mm dishes in volumes ranging from 0.25 – 4mls of cell suspension. Ham's F-12 medium supplemented with G-418 was added to a final volume of 10 mls. Medium was changed every 2 days until single colonies could be observed. Colonies were picked and expanded. Those colonies containing GFP-tagged clones were screened using fluorescence microscopy.

2.3 Molecular Biology

2.3.1 Preparation of antibiotic agar plates

LB agar (1% (w/v) bactotryptone, 0.5% (w/v) yeast extract, 1% (w/v) NaCl, with 1.5% (w/v) agar) was prepared, autoclaved and allowed to cool before the addition of the appropraite antibiotic (ampicillin 50μg/ml, kanamycin 30μg/ml). The liquid LB agar was poured into 90mm diameter Petri dishes and allowed to solidify and sweat overnight at room temperature. Plates were then stored at 4°C until required.

2.3.2 Preparation of competent XL1 Blue E.coli

An overnight culture of XL1 Blue E.coli was grown in 3ml of LB broth containing tetracycline (50μg/ml). The next day, the culture was used to inoculate 250ml of LB broth, which was grown with aeration until the cells reached log phase, following which they were transferred into 2 x 250ml centrifuge tubes on ice and left for 1hour.

Log phase was determined when the optical density (OD_{600}) reached approximately 0.35-0.375. Cells were spun at 6K at 4°C for 20 minutes, the supernatant decanted and the cells resuspended and washed in ¼ starting volume of ice-cold 0.1M (w/v) $MgCl_2$. Following a second 20 minute spin, the cells were resuspended in ¼ starting volume of ice-cold 0.1M (w/v) $CaCl_2$ and placed on ice for 20 minutes. Cells were spun again for 20 minutes, the supernatant discarded and cells resuspended in 15ml of ice-cold 15% (v/v) glycerol with 0.1M (w/v) $CaCl_2$. 250μl of cells were aliquoted into sterile microfuge tubes on dry ice/methanol to obtain rapid freezing, and stored at –80°C until required.

2.3.3 Transformation of competent XL1 Blue E.coli with plasmid DNA

30-50ng of DNA was incubated with 50μl of competent XL1-blue cells on ice for 10 minutes. The cells were then placed for 5 minutes in a 37°C shaking waterbath before the addition of 0.5mls LB broth. The mix was then returned to the waterbath and incubated for 45 minutes. 200μl from each transformation was spread onto agar plates containing the appropriate antibiotic. Plates were incubated overnight at 37°C and transformed colonies selected the next day.

2.3.4 Preparaton of plasmid DNA

Transformed colonies were picked from agar plates and grown overnight in 5-10 mls of LB broth containing the appropriate antibiotic (Amp 50μg/ml, Kan 30μg/ml). Plasmid DNA was prepared using the Promega™ Wizard Plus SV miniprep purification system as per the manufacturers instructions. For larger quantities of DNA, the initial overnight culture was transferred to 500mls of LB broth containing antibiotic and again grown overnight. DNA purification was by the Qiagen plasmid maxi kit system. The concentration of DNA obtained was determined by measuring the absorbance at 260nm (A_{260}) of a 1:50 dilution in sterile H_2O, assuming that 1 absorbance unit was equivalent to 50μg/ml of double stranded DNA.

2.3.5 Digestion of plasmid DNA

1-2 μg of plasmid DNA was digested in a volume of 10μl using the buffer conditions recommended by the manufacturer with 2-4 units of the appropriate restriction enzyme. Digested DNA was analysed by agarose gel electrophoresis in which samples were prepared by the addition of a 1:3 dilution of loading buffer. Electrophoresis took place on a 1% (w/v) gel containing 2.5mg/ml ethidium bromide at 75 volts for 20-30 minutes in 1 x TAE buffer (40mM Tris-acetate, 1mM EDTA, glacial acetic acid). Purification of DNA from agarose gels was by Quiagen QIAquick gel purification kit, as per the manufacturers instructions.

2.3.6 Ligation of DNA fragments

Ligation of vector DNA was carried out overnight at 4°C in a reaction volume of 10μl containing 1 x ligation buffer (30mM Tris-HCl, pH 7.8, 10mM MgCl2, 10mM DDT, 1mM ATP), vector and insert DNAs and T4 DNA ligase. Reactions were performed with the ratio of vector:insert of 1:4. Ligated DNA was transformed as described in Section 2.3.3.

2.3.7 Construction of Adenosine Receptor-GFP fusion constructs

Modification of the pEGFP-N1 vector

A region of the enhanced green fluorescent protein vector, pEGFP-N1 (Clontech), multiple cloning site was modified by polymerase chain reaction (PCR) to convert the initiating methionine of GFP to alanine. A typical PCR contained 100ng template DNA, 100μM dNTP's, 50pmol sense / antisense primers, 0.002 units *Pfu* turbo, 10% (v/v) amplification buffer and 5% (v/v) DMSO in a final volume of 100μl. The reaction was initiated by a denaturation cycle of 95°C for 5 mins, followed by 25-30 annealing and extension cycles of 95°C (1min), 55°C (1min) and 72°C (1.5mins). A final cycle of 95°C (1min), 55°C (1min) and 72°C (10mins) was used before reactions were placed at 4°C until required.

Oligonucleotide primers, 5'-ATTACCGGTCGCCACC**GCA**GTGAGCAAG-3'(sense) and 5'-CAAATGTGGTATGGCTGATTAT-3' (antisense) were used. The bases defining the methionine (Met) to Ala mutation are shown in bold. The sense primer also included an AgeI restriction site (underlined). The antisense primer was constructed to read through a unique NotI site in the pEGFP-N1 cDNA. The AgeI / NotI digested PCR product was subcloned into similarly digested pEGFP-N1 to give a pEGFP vector with the desired Met to Ala mutation (termed pEGFPAla1). Restriction sites were confirmed by overnight digestion of the constructs with one enzyme followed by phenol:chloroform extraction of the DNA and digestion with the second enzyme of interest. Completed digests were run out on 1% agarose gels at 75v in 1x Tris-Acetate-EDTA buffer. The Met to Ala mutation was confirmed by the use of dideoxynucleotide sequencing.

Generation of Rat A_3AR-GFP cDNA Expression Constructs

These constructs were generated by PCR using previously described pCMV5 / HA epitope tagged WT, Cys (302, 305) → Ala and Thr (307, 318, 319) → Ala mutant A_3AR cDNAs as templates (Palmer and Stiles, 2000). In each case, the following primers were used:

5'-TGATT**AAGCTT**CCACC*ATG*AAAGCCAACAATACCACGAC-3' (sense) and 5'-TGATTCCCGGGCAGCGTAGTCTGGGACGTC-3' (antisense). The sense primer was designed to remove the N-terminal HA epitope tag sequence and add a HindIII site (bold) upstream of a consensus Kozak sequence (underlined) and the A_3AR initiating methionine (italics). The antisense primer was designed to remove

the A_3AR stop codon and add a SmaI site (underlined). This was to allow in-frame ligation of the A_3AR coding region with that of GFP following subcloning of HindIII / SmaI digested PCR products into similarly digested pEGFPAla1. PCR was carried out as previously described.

An A_1-A_3AR chimeric receptor was also generated with a GFP tag. The template employed was an HA epitope tagged A_1CT3AR previously described by Palmer et al. (1996). The primers:
5'-ATTTGGAATTCCCACCATGCCGCCCTCCATCTCAGC-3' (sense) and 5'-ATTTCGGTACCGCAGCTAGTCTGGGAC-3' (antisense) removed the HA tag as before and inserted an EcoRI site at the N-terminus. A KpnI site was inserted at the C-terminal tail. Restriction sites are underlined. pEGFPAla1 and A_1CT3AR were digested with EcoRI and KpnI and ligated to give the chimeric receptor expressing GFP. The presence of all indicated mutations in each construct was verified by the use of dideoxynucleotide sequencing.

2.4 Experimental Techniques

2.4.1 SDS-PAGE Electrophoresis

Samples were separated by SDS-PAGE using a 10% acrylamide resolving gel (10% (w/v) acrylamide, 0.3% (w/v) bisacrylamide, 0.4M Tris (pH 8.8), 0.1% (w/v) SDS, 3% (v/v) glycerol, 0.01% (w/v) ammonium persulphate and 0.001% (v/v) TEMED) and 3% acrylamide stacking gel (3% (v/v) acrylamide, 0.1% (v/v) bisacrylamide, 0.1M Tris (pH 6.8), 0.1% (w/v) SDS, 0.01% (w/v) ammonium persulphate and 0.001% (v/v) TEMED). Electrophoresis of the samples was carried out alongside prestained SDS molecular weight markers (6.5 – 175 kDa) in a running buffer (27.4mM Tris, 0.19M glycine, 0.1% (w/v) SDS) at 150 Volts until the dye front reached the end of the gel. At this point electrophoresis was stopped and the proteins transferred to nitrocellulose at 400 mA for 45 minutes in transfer buffer (24.7mM Tris 0.19M glycine, 20% (v/v) methanol).

2.4.2 Cell surface labelling with biotin-LC-hydrazide / receptor internalisation assay

Confluent CHO cells expressing adenosine receptors were passaged 1:8 from 75cm^2 flasks into 6-well dishes and cultured overnight in regular medium. The next day, the cells were washed and 0.75ml of Ham's F-12 medium applied. Time courses of receptor internalisation were initiated by the addition of 1μM (R)-PIA to the cells for the desired time period. Reversal of internalisation was brought about by the removal of agonist, washing once with pre-warmed medium and addition of the antagonist MRS1523 for the time required. Experiments were terminated by placing the cells on ice. All subsequent steps were carried out at 4°C unless otherwise stated.

Cell monolayers were washed three times with ice cold PBS-CM and sodium periodate in PBS-CM added at a concentration of 10mM for 30 minutes. After removal of the sodium periodate, the monolayers were washed twice with PBS-CM and three times with 0.1M sodium acetate-CM (0.1M sodium acetate (pH 5.5) supplemented with 1mM $MgCl_2$, 0.1mM $CaCl_2$). 0.1mM biotin – LC – hydrazide in sodium acetate-CM was added to the cells for a further 30 minutes. Termination of the labelling was brought about by removal of the biotin with subsequent washing of the monolayers three times in PBS. Cells were solubilised by the addition of 0.5ml / well immunoprecipitation buffer (RIPA buffer [49.92mM HEPES (pH 7.5), 149.76mM NaCl, 1% (v/v) Triton X-100, 0.5% (w/v) sodium deoxycholate and 0.1% (w/v) SDS] supplemented with 0.1M NaF, 5mM EDTA (pH 8), 0.01M $NaPO_4$, 0.1mM PMSF, 0.01mg/ml soybean, 10mg/ml benzamidine, 0.7μg/ml pepstatin A) and incubation at 4°C for 1 hour on a rotating wheel. Insoluble material was pelleted by centrifugation for 15 minutes at 14,000g and the supernatant removed to fresh microfuge tubes.

BSA standards ranging from 0-2mg/ml were used to obtain a best-fit straight line of A_{492} in a bichinchonic acid (BCA) based assay using the graph package "Prism". Protein concentrations of 10μl samples of each unknown extract were calculated by comparison to the BSA standards. Specific proteins were immunoprecipitated by incubating the extracts with 10μl protein-A Sepharose beads with 0.4% (w/v) IgG free BSA in the presence of 1μg 12CA5 overnight.

Immune complexes, isolated by centrifugation, were washed twice (1ml/wash) with immunoprecipitation buffer supplemented with 0.2M ammonium sulphate, once with immunoprecipitation buffer alone, and eluted from the protein A-Sepharose by a 1 hour incubation at 37°C with 50µl electrophoresis sample buffer (50mM Tris pH 6.8, 10% (v/v) glyerol, 12% SDS, few grains bromophenol blue).
20µl of each sample were separated by SDS-PAGE and transferred to nitrocellulose (2.4.1). Membranes were washed twice briefly in PBS and non – specific protein binding sites blocked by a 60 minute incubation in Blotto (5% (w/v) skimmed milk powder, 0.2% (v/v) Triton X-100, 0.001% (w/v) thimerosal in PBS) at room temperature.

Cell surface biotin-labelled receptors were identified by incubation of the membrane with horseradish peroxidase (HRP)-conjugated streptavidin for 60 minutes at room temperature and visualisation detected by an enhanced chemiluminescent procedure (ECL).

2.4.3 Preparation of cell extracts for immunoblotting

Confluent monolayers in 6-well dishes were washed three times with PBS and solubilised by adding 0.25 ml/well of immunoprecipitation buffer and scraping (2.4.2). Following transfer to microfuge tubes, solubilisation was achieved by a 1hour incubation on a rotating wheel at 4°C. Insoluble material was pelleted and the supernatant removed to a fresh tube. Protein concentrations were calculated as described (2.4.2), an equivalent volume of loading buffer added and the samples run directly on SDS-PAGE.

2.4.4 Immunoblotting

Samples separated by SDS-PAGE were transferred to nitrocellulose and non-specific binding sites blocked with Blotto. Membranes were then incubated with the appropriate dilution of primary antibody in fresh blocking buffer for 1 hour, washed three times with Blotto and HRP-conjugated secondary antibody added in fresh, high detergent blotto (Blotto supplemented with 1.02% Triton X-100 and 0.1% SDS). Primary antibodies giving weak signals were incubated in low detergent blotto (Blotto supplemented with 0.02% Triton X-100 and 0.1% SDS).

2.4.5 Receptor phosphorylation

Confluent receptor-expressing CHO cells in 6-well dishes were washed twice with phosphate-free DMEM and returned to the incubator for 90 minutes with medium supplemented with 0.2μCi / ml of carrier free ^{32}P-phosphate to label the intracellular ATP pool. After incubation with the indicated drug for the appropriate time period, reactions were terminated by placing the cells on ice. The monolayers were washed three times with ice-cold PBS and solubilised as previously described for the receptor internalisation assay. Receptors were then subject to immunoprecipitation with 12CA5 (2.4.2) and equal amounts of protein separated by SDS-PAGE. On completion of electrophoresis, the gel was removed, dried down and analysed by autoradiography.

2.4.6 Saturation radioligand binding assays with ^{125}I-AB-MECA in isolated membranes

A confluent 75cm^2 flask containing receptor expressing CHO cells was placed on ice and washed three times with ice-cold PBS. The cells were scraped from the bottom of the flask into 4mls of PBS and transferred to a pre-chilled, 13ml centrifuge tube on ice. Cells were pelleted by a 4K 10 minute spin at 4°C, the supernatant removed and the cell pellet resuspended in 1ml of lysis buffer (10mM Tris, 5mM EDTA [pH 7.5]). Disruption of cells on ice was by twenty up and down strokes in a glass-on-glass Dounce homogeniser. The homogenate was removed to a microfuge tube and membranes pelleted by centrifugation at 14,000g for 15 minutes.

On removal of the supernatant, the pellet was resuspended in 4mls of radioligand binding buffer (50mM Tris, 10mM $MgCl_2$, 1mM EDTA [pH 8.26]) and transferred to the homogeniser. 1μl of stock ADA was then added to give a final concentration of 0.47units/ml, and the cells disrupted by Dounce homogenisation as before. 150μl of the membranes were added immediately to duplicate assay tubes containing iodinated radioligand, ranging from 0.25-8.0nM, and incubated at 37°C for 30 - 45 minutes in a shaking water bath. Non-specific binding was defined in parallel by the inclusion of (R)-PIA to a final concentration of 10μM. A GF/B filter was pre-soaked in distilled water containing 0.03% (v/v) polyethyleneimine in preparation of harvesting using a Brandel cell harvester. The binding samples were washed through the filter three times with wash buffer (binding buffer supplemented

with 0.01% (w/v) CHAPS), filter discs removed to scintillation vials and the radioactivity counted.

To obtain the specific binding achieved by the radioligand on the receptors, non-specific counts were subtracted from the total counts and the resulting values plotted against [^{125}I-AB-MECA] nM. To determine the total number of receptors expressed (B_{max}) and the equilibrium dissociation constant (K_d), the data was fitted to a nonlinear regression equation using the graph package 'Prism'. A bichinchonic acid (BCA) protein assay, as described in 2.4.2, was used to determine the μg of protein added per tube. Combining the calculated B_{max}, final assay volume in litres and μg protein added per tube, the receptor level was expressed in pmol/mg. An example of this calculation can be found in Appendix 1.

2.4.7 Competition Radioligand Binding with ^{125}I-AB-MECA in isolated membranes

Duplicate tubes were set up containing, 50μl water, (R)-PIA (50μM) or MRS 1523 (ranging from 10^{-11}-10^{-4}M) to which was added 50μl of 0.5nM ^{125}I-AB-MECA. In all competition bindings, non-specific binding was determined as counts per minute (cpm) after addition of 10μM (R)-PIA (final concentration).

Cells were prepared as for the saturation binding assay and 150μl added per reaction tube. Specific binding was calculated by subtraction of non-specific binding from total binding and the data plotted as cpm v log [MRS 1523] M using a nonlinear regression fit ('Prism') to obtain the concentration at which 50% of specific binding was inhibited (IC_{50}). The equilibrium dissociation constant for binding of the competing unlabelled drug (K_i) was then determined using the Cheng-Prusoff equation (Cheng and Prusoff, 1973) and expressed as a μM concentration (Appendix 2).

2.4.8 Confocal Laser Scanning Microscopy

HEK 293 or CHO cells were split, transfected appropriately and analysed 24-48 hours post-transfection.

Live cells were used to visualise the internalisation and recycling of the receptor. Cells were grown on glass coverslips, mounted on the imaging chamber and maintained at 37°C in Krebs-Ringer-HEPES-BSA (KRHB) buffer (120mM NaCl,

5mM KCl, 1.2mM $MgSO_4$, 1.2mM $CaCl_2$, 20mM HEPES, 1.2mM Na_2HPO_4, 10mM glucose, 0.1% BSA). All agonists and antagonists were applied in KRHB buffer. For other studies, fixed cells were used. The cells on the coverslips were washed with PBS and fixed for 20 minutes at room temperature using 4% (w/v) paraformaldehyde in 5% (w/v) sucrose / PBS (pH 7.2). Cells were washed again with PBS and permeabilised for 3 minutes with 0.4% (v/v) Triton X-100 in PBS. Antibody dilutions were prepared in 0.1% (v/v) new born calf serum (NBCS) / 0.2% (w/v) gelatin / PBS. With the exception of the Alexa-labelled Concanavalin A antibody (1:100,000), primary and secondary antibodies were used at 1:200 and 1:400 dilutions respectively. 100µl of antibody dilution for each coverslip was placed onto nescofilm, the coverslips placed with the cells facing downwards and incubated at room temperature for 1 hour. Cells were then washed twice with PBS/NBCS/gelatin and placed onto nescofilm with secondary antibody for a further 1hour. Coverslips were then washed twice with PBS/NBCS/gelatin and once with PBS prior to mounting on microscope slides with 40% (v/v) glycerol in PBS.

Cells were observed using a Zeiss Axiovert 100 laser scanning confocal microscope (Zeiss, Oberkochen, Germany) using a Zeiss Plan-Apo 63 x 1.4 NA oil immersion objective, pinhole of 20 and electronic zoom between 1 and 4. GFP was excited using a 488 nm argon / krypton laser and detected with 515-540 nm band pass filter. The Alexa-modified antibodies were excited at 543nm and detected with a long pass band filter 590nm. The images were manipulated with Zeiss LSM or MetaMorph software (Universal Imaging Corporation, West Chester, PA).

2.4.9 Statistical Analysis

All statistical analysis was carried out using the student t-test as described in the GraphPad softwear, 'Prism 3.0'.

Chapter 3

Kinetics of Inhibitory Adenosine Receptor Internalisation

3.1 Introduction

The A_3AR is the most recently cloned of the adenosine receptors, a family of GPCRs comprising of A_1, A_{2A}, A_{2B} and A_3 (Zhou 1992). The A_I and A_3ARs have been shown to be important in cardioprotection (Auchampach & Bolli, 1999), mast cell and eosinophil activation (Kohno et al., 1996) and neuroprotection (Abbracchio et al., 1997). Due to the critical role of adenosine in these processes, it is crucial that we understand both the signalling pathways that are activated by these receptors and how signalling is regulated at the molecular level. This information may allow us to propose strategies with which to modify AR signalling in disease states.

ARs couple to the inhibitory (G_i) family of G proteins. Upon agonist binding, G_i inhibits AC (Gilman; 1987) leading to a decrease in intracellular cAMP levels, activates the MAPK signalling cascade, and elevates intracellular IP_3 concentration *via* activation of PLC-β (Ramkumar et al., 1993). Rapid termination of GPCR signalling is typically regulated *via* receptor phosphorylation by either second messenger-activated and/or GRKs (Haussdorf, 1990). The A_3AR as been shown to have 3 principal phosphorylation sites in its C-terminal tail at Thr 307, 318 and 319 which are targets for the GRK-family (Palmer et al; 1995, 1996 and 2000). Work principally performed on the β_2AdR has resulted in a model where agonist stimulated phosphorylation of GPCRs by GRKs leads to the binding of arrestin proteins (Krupnick and Benovic, 1998; Pitcher et al.; 1998) resulting in: 1) uncoupling of activated receptors from G-proteins leading to a functional desensitisation of G-protein-linked signalling; 2) clustering of activated receptors to CCVs - it is thought that receptors proceed from the CCVs to endosomes where they may either be dephosphorylated and recycled back to the plasma membrane for another round of agonist activation, or targeted to lysosomes where they are degraded and down-regulated; and 3) recruitment and activation of src family tyrosine kinases leading to activation of the ERK signalling cascade (Luttrell et al., 1997,1999a,b)

Desensitisation, the process whereby a GPCR-initiated response reaches a plateau and then diminishes despite the continual presence of agonist, can simultaneously initiate alternate signalling pathways after receptor clustering and internalisation (Lefkowitz; 1998). However, not all GPCRs follow this paradigm. For example, activation of the ERK pathway by the A_1AR precedes the onset of receptor internalisation. (Dickenson et al.; 1998). We must therefore understand the unique roles played by receptor phosphorylation and/or internalisation in controlling

A_3AR-activated intracellular signalling cascades.

In the case of the A_3AR, although it has been shown to be rapidly phosphorylated in response to agonist exposure (Palmer et al., 1995c), it is not known if the receptor is internalised. By employing a panel of wild type and mutant A_3 and A_1ARs, the sensitivity of these receptors to agonist stimulated phosphorylation and internalisation was examined.

3.2 Results

The role of A_3AR-activated signalling cascades on receptor internalisation was investigated by treating A_3AR-expressing CHO cells with an AR agonist and activators of various second messenger regulated kinases. As described in the Methods, the presence of a HA - epitope tag at the N and C-termini of the A_3AR facilitated identification of cell surface A_3AR glycoproteins. This was utilised as an assay for detecting reductions in cell-surface A_3ARs. Following treatment as shown in the Figure Legend, cell surface glycoproteins were labelled with biotin and the cells solubilised with immunoprecipitation buffer (see Methods, section 2.4.2). As biotin hydrazide does not cross the cell membrane, only receptors present at the cell surface are labelled. Receptor proteins were immunoprecipitated with the HA-specific antibody 12CA5, fractionated by SDS-PAGE and transferred to a nitrocellulose membrane. The cell surface biotin-labelled receptors were identified by incubation of the membrane with horseradish peroxidase-conjugated (HRP) streptavidin and enhanced chemiluminescence (ECL). Figure 3.1 shows the results of this assay.

The AR agonist NECA induced a 56 ± 18% ($p<0.05$) loss of receptor from the cell surface. Several activators of second messenger-regulated kinases such as the phorbol ester phorbol-12-myristate-13-acetate (a direct stimulator of conventional and novel PKC enzymes), the calcium ionophore A23187, and 8-bromo-cyclic guanosine monophosphate (cGMP), which activates cGMP-dependent protein kinases, could not mimic the action of NECA. However, elevation of intracellular cAMP levels by forskolin resulted in a smaller reduction in cell-surface receptor levels than NECA and induced a reduced mobility of the A_3AR protein on SDS-PAGE. Phosphorylation is known to reduce the electrophoretic mobility of a variety of GPCRs (Ali et al., 1993) but an increase in phosphorylation was undetectable in response to forskolin treatment, consistent with previous observations (Palmer et al., 1995c, Fig. 3.2). The elevation of cAMP levels is unlikely to be responsible for the effects of agonist on A_3AR internalisation for three reasons. Firstly, studies on the A_3AR have shown it to be linked to G_i, leading to a decrease in cAMP levels (Linden et al., 1993; Palmer et al., 1995b). Secondly, unlike the effect of forskolin treatment, exposure to agonist does not alter the mobility of the A_3AR protein on SDS-PAGE. Thirdly, agonist treatment induces a much greater level of internalisation of cell-surface A_3ARs than that observed after

forskolin treatment. Taken together these data suggest that agonist and forskolin are causing loss of receptor *via* distinct mechanisms.

To further characterise the effect of agonist on loss of cell surface receptors, the relationship between agonist concentration and the extent of receptor internalisation was assessed (Fig. 3.3). The response appeared to be biphasic, with low nanomolar concentrations of (R)-PIA (5-50nM) consistently producing a small, albeit statistically insignificant ($p>0.05$, N/S) increase in the levels of cell-surface A_3ARs, with higher concentrations giving an effective concentration 50% (EC_{50}) value for loss of cell surface A_3ARs of approximately 0.2μM.

To determine if A_3AR internalisation was agonist-specific, the effect of pre-incubating transfected cells with MRS 1523, a selective A_3AR antagonist, was assessed (Li et al., 1998). CHO cells stably transfected with the WT A_3AR were pre-incubated for 30 minutes with increasing concentrations of MRS 1523 (2.5nM–2.5μM). Cells were then washed and stimulated with 1μM (R)-PIA, an agonist concentration sufficient to produce maximal receptor internalisation (Fig. 3.3). MRS 1523 alone had no observed effect on cell surface receptor levels, but after agonist stimulation, it was found to inhibit (R)-PIA-induced internalisation in a concentration-dependent manner. Quantitation of the blots revealed that half-maximal internalisation occurred between 2.5 and 25nM MRS 1523 (Fig. 3.4). Having shown concentration-dependent antagonism of agonist-mediated receptor internalisation by MRS 1523, the effect of this A_3AR-selective antagonist on receptor phosphorylation was assessed. A_3AR-expressing CHO cells were pre-labelled with ^{32}P-orthophosphate and incubated with the indicated concentrations of MRS1523 for 30 minutes prior to treatment with (R)-PIA at a final concentration of 1μM for 10 minutes (Fig. 3.5). As was seen with internalisation, increasing MRS 1523 concentration led to inhibition of receptor phosphorylation with an IC_{50} value between 0.5 and 5μM. These data demonstrate that both phosphorylation and internalisation of the A_3AR are agonist-mediated processes that can be blocked by the A_3AR-selective antagonist MRS 1523. Competition binding studies carried out in membranes isolated from the same transfected cells using MRS 1523 *versus* ^{125}I-AB-MECA produced a K_i value of 130 ± 0.3nM corresponding to a previously reported K_i value of 130nM for this antagonist at the rat A_3AR (Li et al., 1998) (Fig. 3.6).

To further characterise any relationship between A_3AR phosphorylation and internalisation, we compared the time-courses for (R)-PIA-mediated phosphorylation and internalisation of WT A_3ARs. CHO cells expressing the WT A_3AR were labelled with ^{32}P-orthophosphate and stimulated with 10μM (R)-PIA at the time points indicated (Fig. 3.7). Following immunoprecipitation with 12CA5 and SDS-PAGE, phosphorylated A_3ARs were visualised by autoradiography. The $t_{½}$ for phosphorylation was determined to be approximately 1 minute (Fig. 3.7, n = 3). Cell surface labelling experiments demonstrated that over a 60 minute time-course, the number of cell surface receptors decreased by 78 ± 6% ($p<0.05$), with a $t_{½}$ of approximately 10 minutes (Fig. 3.8). Together, these data show internalisation of the A_3AR is temporally preceded by receptor phosphorylation ($t_{½}$ = 1 & 10 minutes for phosphorylation and internalisation respectively). This suggests that the A_3AR may require phosphorylation to enable it to undergo internalisation.

In contrast to the A_3AR, the A_1AR has no defined phosphorylation sites in its C-terminal tail (Fig. 3.9). Despite coupling to the same inhibitory G protein, it is hypothesised that the A_1AR may show differences in its ability to undergo agonist-mediated phosphorylation and internalisation. Time-courses of phosphorylation and internalisation of HA-tagged A_1ARs expressed in CHO cells were carried out as previously described. Treatment with 5μM (R)-PIA induced no visible phosphorylation of A_1ARs compared to WT A_3ARs after 10 minutes (Fig. 3.10). Agonist stimulation of A_1AR-expressing CHO cells with 1 μM (R)-PIA induced a 55 ± 4% ($p<0.05$) reduction of A_1AR from the cell membrane with a $t_{½}$ of 90 minutes (Fig. 3.11). This contrasts dramatically with $t_{½}$ of internalisation of 10 minutes displayed by the A_3AR.

Experimental work on other receptors has shown the C-terminal domain to be important in controlling receptor regulation (Cyr et al.; 1993, Koshimizu et al.; 1995, Shibasaki et al.; 1999 and Trejo et al.; 1999). In contrast to the A_1AR, the A_3AR is a good substrate for agonist-mediated phosphorylation by GRKs on Thr residues present in its C-terminal tail (Palmer et al.; 1996). To ascertain if the rapid internalisation of the A_3AR was initiated by phosphorylation of the receptor by GRKs, an A_3AR in which the GRK phosphorylation sites at Thr 307, 318 and 319 were mutated to non-phosphorylatable Ala residues was constructed and termed (T-A)A_3AR. This mutant receptor was subjected to treatment with (R)-PIA as before. In

contrast to WT A_3AR, after 10 minutes of 5μM (R)-PIA stimulation, no phosphorylation of the (T-A)A_3AR was detectable (Fig. 3.12) and only following a 60 minute treatment was a small reduction in cell surface receptor observed (8.2 ± 9.5%, $p>0.05$ N/S, Fig. 3.13). These data suggest that disruption of the GRK phosphorylation sites lead to a dramatic impairment in the ability of the A_3AR to undergo agonist-mediated internalisation. In addition, it supports the hypothesis that phosphorylation is required for rapid A_3AR internalisation.

By employing a second mutant A_3 receptor, the (C-A)A_3AR, in which the predicted palmitoylation sites at Cys 302 and 305 were mutated to non-palmitoylatable Ala, the effect of loss of palmitoylation on receptor phopshorylation and internalisation was investigated. On comparison to WT A_3AR, the Cys to Ala mutant was found to display substantial basal phosphorylation (Fig. 3.14). However following agonist stimulation, the overall phosphorylation level reached was equivalent to WT A_3AR. Following agonist stimulation, (C-A)A_3AR internalised at a faster rate than WT with a $t_{½}$ of approximately 3-4 minutes (Fig. 3.15). As this mutation increased the rate of receptor internalisation, potential effects on receptor recycling following agonist removal were examined. CHO cells transfected with WT A_3 or (C-A)A_3ARs were stimulated with 1μM (R)-PIA for 30 minutes, a time sufficient to allow maximal internalisation of both receptors. Following agonist removal, monolayers were washed and MRS 1523 added to a final concentration of 5μM for a further 30 minutes. Cell surface receptors were then labelled with biotin hydrazide and immunoprecipitated as described previously. These experiments revealed that the (C-A)A_3AR recycled back to the membrane at a greater rate (Fig. 3.16, $t_{½}$ = 6 mins) than WT and a visibly, statistically significantly higher percentage was recovered (94 ± 5% compared with 49 ± 11% for WT, $p<0.05$). Having shown the C-terminal tail to be important in regulating A_3AR phosphorylation and internalisation, these data suggest that this region of the A_3AR controls the internalisation kinetics of this receptor.

With the main differences between the A_1 and A_3ARs being their ability to undergo phosphorylation and subsequent internalisation upon agonist stimulation, the possibility that the A_3AR could confer regulatory kinetics to the A_1AR by exchange of the C-terminal tails was investigated using a chimeric receptor termed A_1CT3AR. Constructed by Palmer et al.(1996), this receptor comprises the main body of the

human A_1AR (aa's 1 - 310), up to and including its predicted palmitoylation site (Cys 309), fused to the 14 C-terminal amino acids of the rat A_3AR (Fig. 3.17) containing the GRK phosphorylation sites at Thr 307, 318 and 319. This chimera had been shown to be pharmacologically similar to the A_1AR with respect to its ability to bind A_1AR-selective ligands (Palmer et al., 1996). Time-course experiments revealed that A_1CT3AR phosphorylation occurred with a $t_{½}$ of approximately 1 minute (Fig. 3.18). Analysis of loss of receptor from the cell surface revealed that the chimeric receptor internalised in a time-frame that both followed that of receptor phosphorylation, and was similar to that of WT A_3AR ($t_{½}$ = 15 minutes, Fig. 3.19). It can therefore be suggested that the rapid agonist induced internalisation of the A_3AR, is regulated entirely by phosphorylation in its C-terminal region by GRKs.

A substantial body of biochemical and functional data revealed that A_1 and A_3ARs were subject to distinct regulation. We were interested in visualising the dynamics of this in real time in single cells. The use of chimeric proteins containing modified forms of the GFP from *Aequorea victoria* has provided the means to visualise the expression, distribution and trafficking of proteins in response to stimulation in intact cells in real-time (Barak et al.; 1997, Kallal et al.; 1998, Drmota et al.; 1998 and Groarke et al.; 1999). Visualisation of a panel of ARs was by the fusion of an enhanced form of GFP at the C-terminus of each receptor (see Methods, section 2.3.7 & Figs. 3.20, 3.21). The enhanced form of GFP, approximately 27kDa in size, has a mutation at Ser65 (S65T). This single mutation causes a shift in the excitation spectrum of the protein leading to an enhanced fluorescence compared to WT GFP (Barak et al., 1997). One issue in any approach of this nature must be to demonstrate that the chimeric receptor-GFP maintains the pharmacological and signal transduction properties of the native receptor. To investigate this, CHO cells were transfected with WT A_3 or A_3AR-GFP, labelled with biotin and immunoprecipitated using 12CA5, which binds the HA-epitope tag present on both receptors. Both WT and GFP-tagged receptors were detected by biotin labelling, suggesting that the receptor-GFP construct could be processed correctly and targeted to the membrane (Fig. 3.22). To determine if the addition of GFP altered agonist binding to the receptors, COS cells were transiently transfected with either WT or A_3AR-GFP receptors and membranes prepared for ^{125}I-AB-MECA radioligand binding assays (see Methods, section 2.4.6). Saturation isotherm analysis of ^{125}I-AB-

MECA binding produced a K_d of 2.175 ± 0.31 nM and 2.03 ± 0.18nM ($p>0.05$, N/S) and B_{max} of 1.2 ± 0.3pmol/mg and 1.4 ± 0.2pmol/mg ($p>0.05$, N/S) for the WT and GFP-tagged ARs respectively (Fig. 3.23), indicating that the presence of the GFP tag had no effect on agonist binding affinity. These values for transfected A_3ARs correlate with binding data obtained from RBL-2H3 cells that express the A_3AR endogenously (K_d = 3.61 ± 0.3nM; Olah et al., 1994). To determine if agonist-mediated GRK phosphorylation of the receptors was affected by the presence of the GFP tag at the C-terminus of the ARs, CHO cells were transfected without or with WT A_3 or A_3AR-GFP and labelled with ^{32}P-orthophosphate prior to agonist stimulation as previously described. Following a 5 minute agonist exposure, phosphorylation was detected for both the WT A_3 and A_3AR-GFP (Fig. 3.24). This suggested that accessibility of the phosphorylation sites in the C-terminal tail to GRK was not being blocked by the presence of GFP. Finally, although the A_3AR-GFP construct had been shown to bind ligand and become phosphorylated after agonist exposure, to use these GFP-tagged receptors for visualisation of receptor trafficking, we had to ensure that the A_3AR-GFP construct did in fact undergo internalisation following agonist stimulation. A time course of agonist-mediated internalisation was carried out for A_3AR-GFP as previously described. As Fig. 3.25 shows, agonist stimulated loss of cell surface receptors was detectable despite the addition of the GFP tag.

Having constructed GFP-tagged receptors demonstrating pharmacological and signal transduction properties similar to the WT receptor, the next step was to gain a visual perspective on the biochemical data obtained. GFP-tagged receptors were transiently transfected into CHO cells and seeded onto coverslips prior to visualisation of receptor distribution by confocal laser scanning microscopy (see Methods, section 2.4.8). AR-GFP constructs were subjected to treatment with 1μM (R)-PIA and images collected between 0 – 30 minutes following agonist addition.

In the basal state, the expressed receptors had a predominantly plasma membrane localisation with only low levels of receptor visible intracellularly. Following agonist stimulation, WT A_3 AR-GFP was seen initially to cluster into distinct punctate spots on the cell surface. Over a 30 minute time period, cells underwent structural changes and ruffling of the cell membrane became apparent. This was associated with the formation of small extensions of the cell, which could be identified as lamellipodia. Receptors internalised to cluster in a peri-nuclear

location by approximately 15 minutes (Fig. 3.26). Images obtained for the (C-A)A_3AR-GFP displayed the enhanced internalisation rate ($t_{½}$ = 4 minutes) observed in immunoprecipitation assays (Fig. 3.27) although changes in cell structure were not as apparent. In contrast, the phosphorylation-deficient (T-A)A_3AR-GFP receptor remained at the cell membrane over the 30 minute time-course (Fig.3.28), providing further visual evidence for the requirement of phosphorylation to induce A_3AR internalisation. While the (T-A)A_3AR-GFP transfected cells displayed the cellular protrusions observed with the WT A_3AR-GFP stimulation, this appeared to be a transient phenomenon, with the cells returning to basal morphology approximately 20-30 minutes after agonist treatment.

As with the WT A_3AR-GFP, the WT A_1AR-GFP clustered at the cell membrane, but over a 30 minute time period, no significant internalisation was evident (Fig. 3.29). Structural changes were minor, could not be defined, and were seen to be transient as for (T-A)A_3AR-GFP. This was in dramatic contrast to the chimeric A_1CT3AR-GFP which again showed receptor clustering, but was followed by rapid internalisation ($t_{½}$ = 15 min, Fig. 3.30). The membranes of the cells became ruffled and extensions were observed as seen for the WT A_3ARs, which were sustained for at least 30 minutes. Internalised A_1CT3AR-GFP appeared not to cluster so much to a peri-nuclear location as that observed for WT A_3AR-GFP, but was seen to distribute in small punctate spots throughout the cytoplasm.

Figure 3.1 **Effect of short-term agonist exposure and activators of second messenger regulated kinases on cell-surface A_3AR levels**

CHO cells stably expressing an HA-tagged WT A_3AR were subjected to a 30 minute exposure at 37°C to either vehicle, AR agonist (NECA), phorbol-12-myristate-13-acetate (PMA), calcium ionophore A23187, forskolin or 8-bromo-cGMP at the concentrations shown. The cell surface glycoproteins were then labelled with biotin hydrazide followed by receptor immunoprecipitation with 12CA5.

Immunoprecipitates were separated by SDS-PAGE and biotin-labelled cell-surface receptors visualised by transfer to nitrocellulose and blotting with straptavidin-conjugated HRP as described in the Methods. Typical data is shown from one of three experiments.

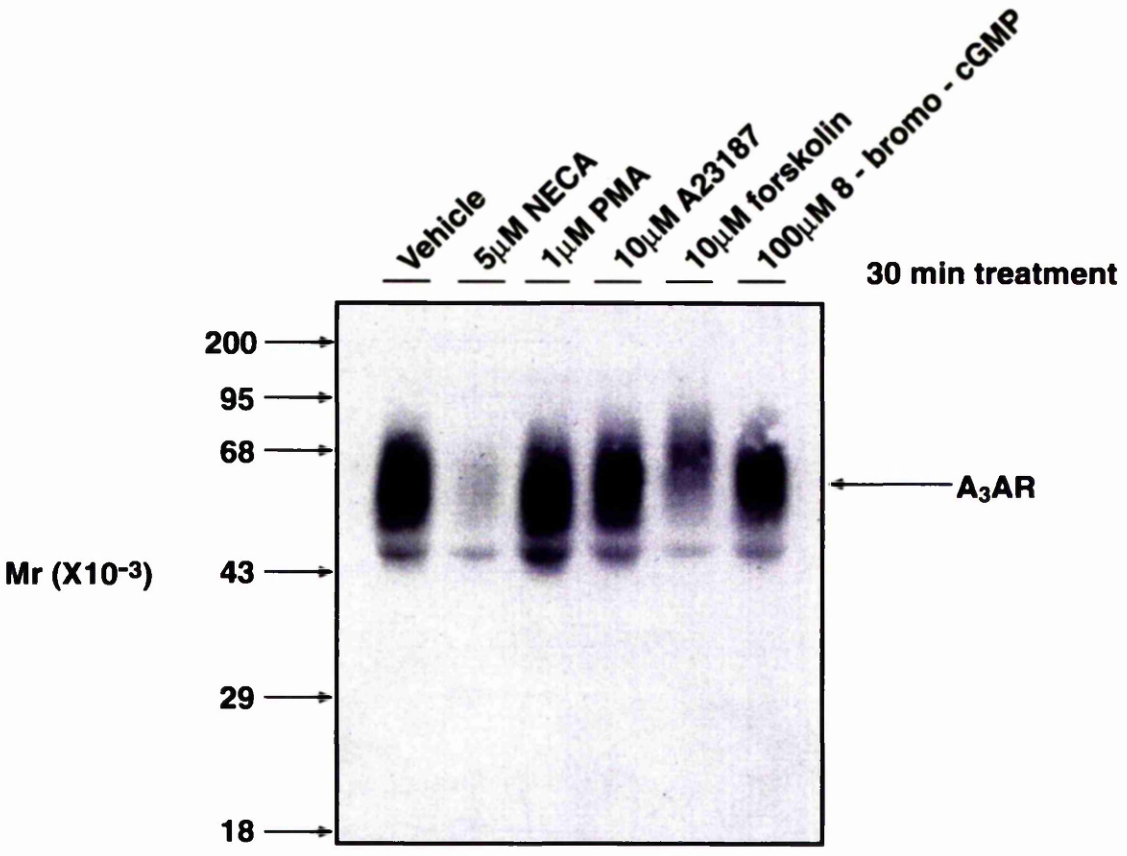
Vehicle
5μM NECA
1μM PMA
10μM A23187
10μM forskolin
100μM 8 - bromo - cGMP
30 min treatment
200
95
68
43
29
18
Mr (X10-3)
A3AR

Figure 3.2 Effect of forskolin treatment on A_3AR phosphorylation

^{32}P-labelled CHO cells expressing the WT A_3AR were incubated with or without 10μM NECA for 5 minutes or with foskolin for 1 or 2 hours at 37°C. Reactions were terminated and receptors immunoprecipitated with 12CA5 as previously described. Immunoprecipitated proteins were fractionated by SDS-PAGE, the gel dried and visualised by autoradiography. Typical data is shown from one of three experiments.

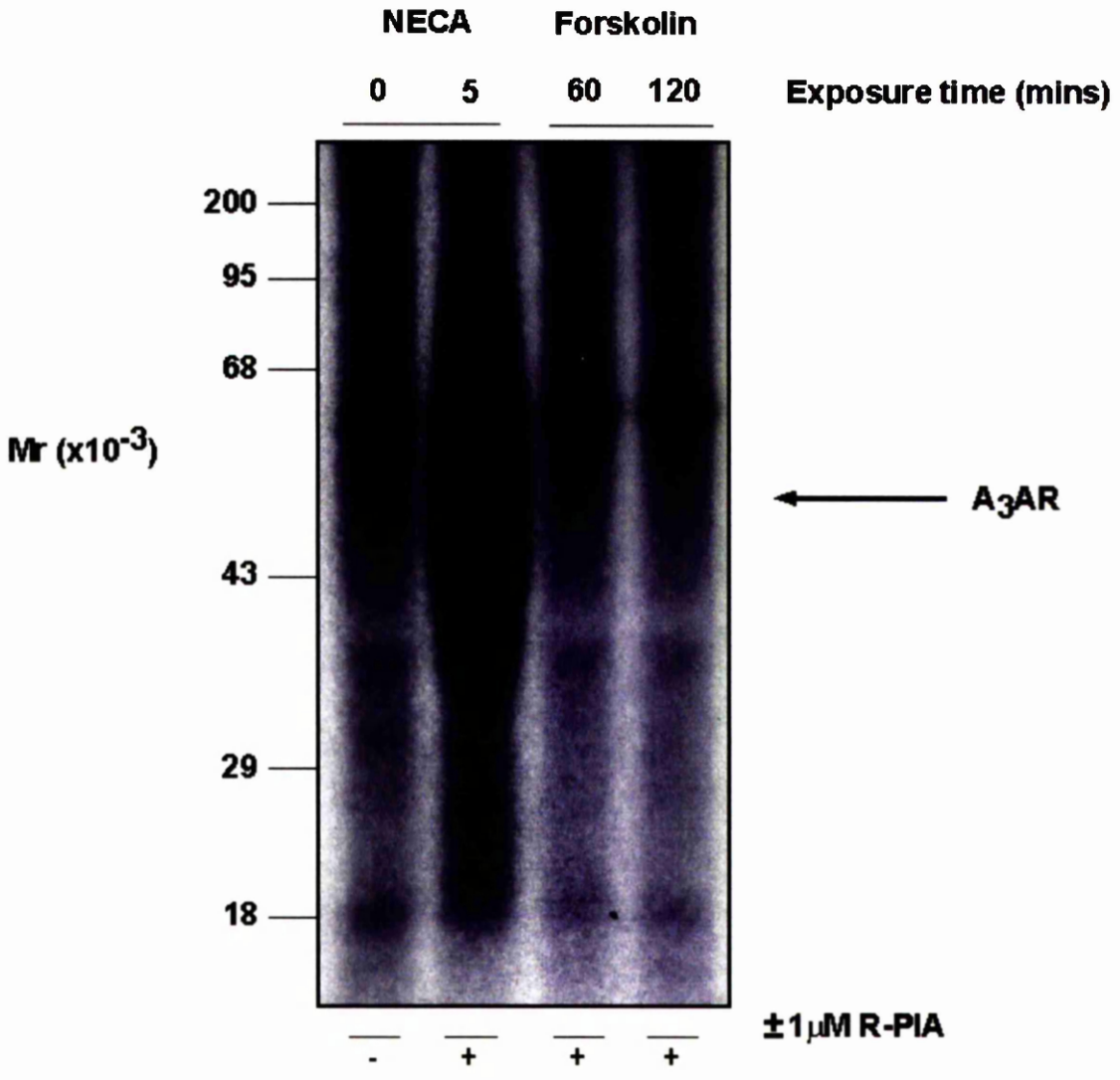
NECA
Forskolin
0
5
60
120
Exposure time (mins)
200
95
68
43
29
18
Mr (x10-3)
A3AR
±1μM R-PIA
-
+
+
+

Figure 3.3 Effect of increasing agonist concentration on A_3AR receptor internalisation

WT A_3AR expressing CHO cells were incubated with (R)-PIA at the concentrations indicated for 30 minutes at 37°C. Cell surface glycoproteins were then labelled with biotin before receptor immunoprecipitation with 12CA5 and visualisation as described in the Methods (section 2.4.2). Blots were quantified by densitometric scanning and values represent mean ± S.E. for three experiments. The level of cell surface receptor in the absence of agonist is set at 100%.

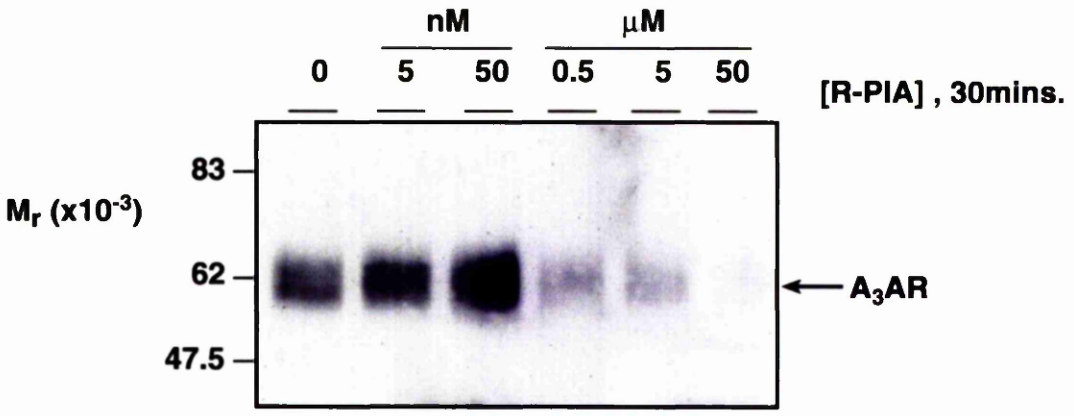
nM
μM
0
5
50
0.5
5
50
[R-PIA] , 30mins.
M_r (x10^{-3})
83
62
47.5
A_3AR

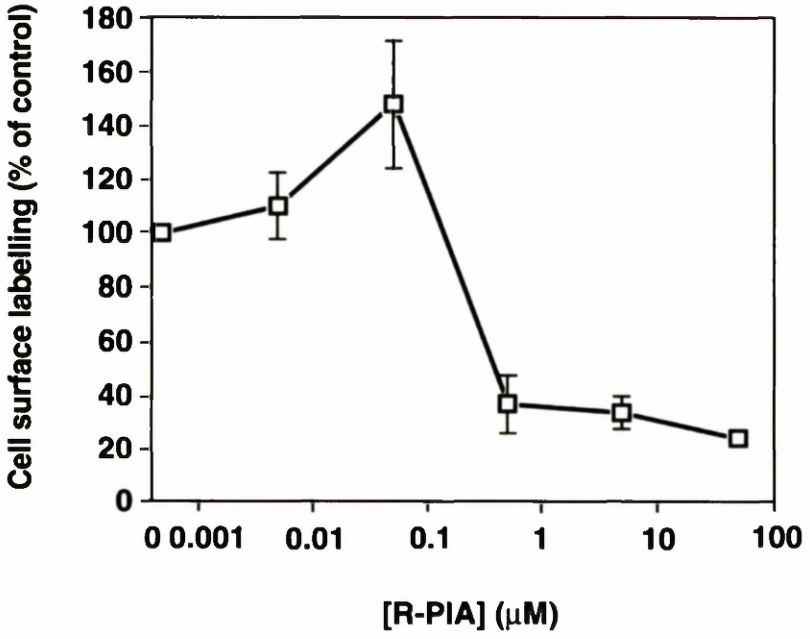
Cell surface labelling (% of control)
180
160
140
120
100
80
60
40
20
0
0 0.001
0.01
0.1
1
10
100
[R-PIA] (μM)

Figure 3.4 Effect of increasing antagonist concentration on rat A_3AR internalisation

CHO cells stably expressing HA-tagged A_3ARs were subjected to pre-treatment with increasing concentrations of the A_3-selective antagonist MRS 1523 for 30 minutes at 37°C. Vehicle or (R)-PIA to a final concentration of 1μM was then added for a further 30 minutes. Placing the cells on ice terminated the reaction. The loss of cell-surface receptors was detected by labelling the cell-surface glycoproteins with biotin prior to receptor immunoprecipitation with 12CA5. Immunoprecipitates were resolved by SDS-PAGE and cell-surface A_3ARs visualised by enhanced chemiluminescence as described in the Methods.

Blots obtained from three experiments were quantitated by densitometric scanning. The levels of cell-surface receptors in untreated cells were set at 100% and those treated only with agonist at 0%. The levels of cell-surface receptors in the agonist treated samples were normalised with respect to these limits. The figures opposite are a representative example of three experiments that produced similar results.

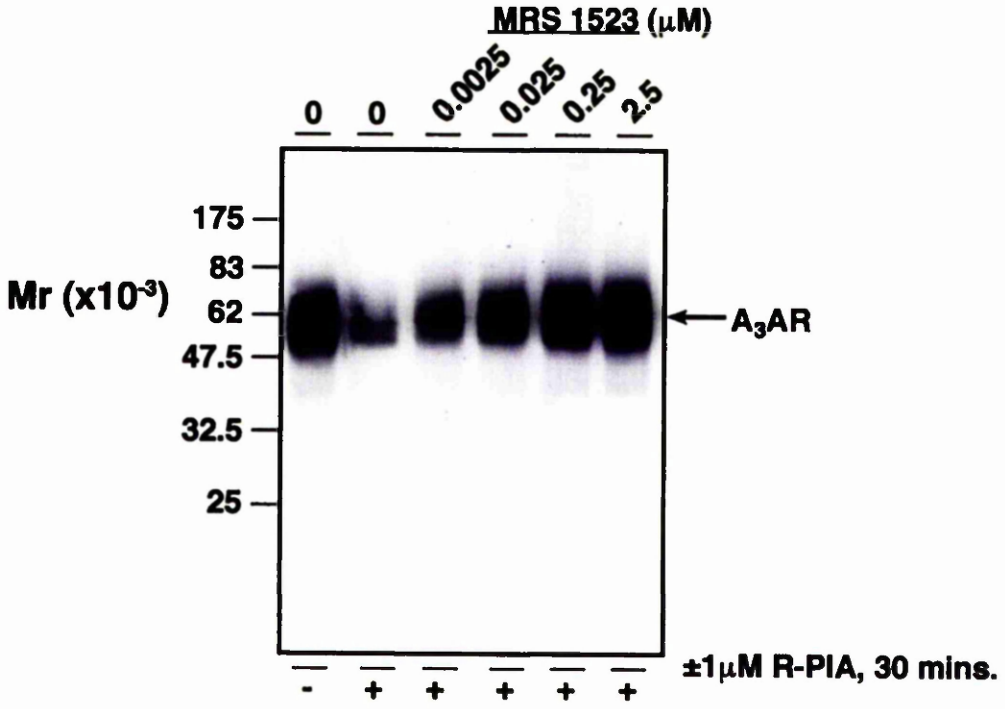
MRS 1523 (μM)
0
0
0.0025
0.025
0.25
2.5
175
83
62
47.5
32.5
25
Mr (x10-3)
A3AR
- + + + + +
±1μM R-PIA, 30 mins.

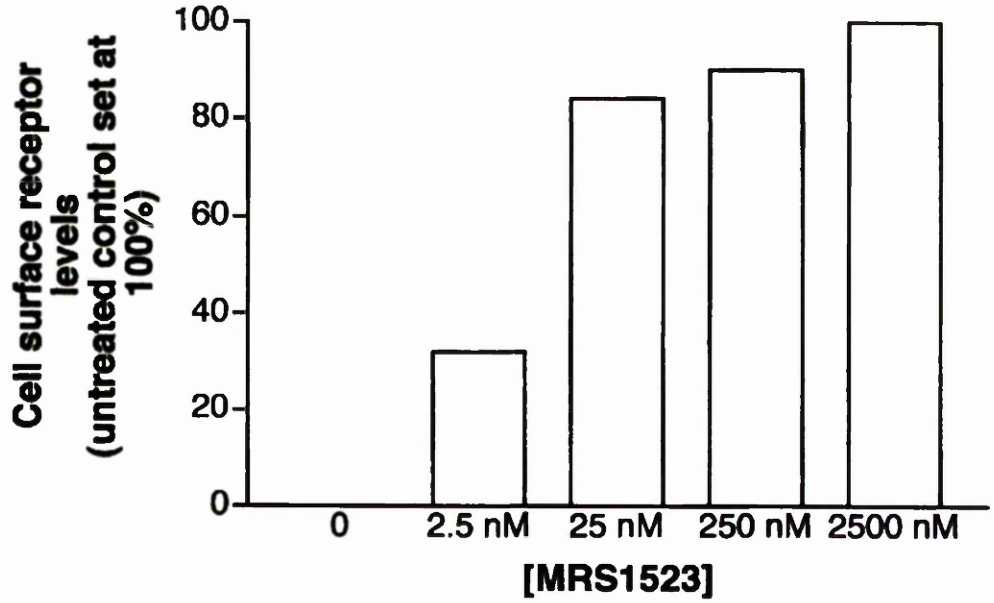
Cell surface receptor levels (untreated control set at 100%)
100
80
60
40
20
0
0
2.5 nM
25 nM
250 nM
2500 nM
[MRS1523]

Figure 3.5 **Effect of increasing concentrations of the A_3-selective antagonist MRS 1523 on agonist-stimulated A_3AR phosphorylation**

^{32}P-labelled CHO cells stably expressing the A_3AR were incubated for 30 minutes with increasing concentrations of MRS 1523 at 37°C as described in the Methods. Vehicle or (R)-PIA (final concentration of 1μM) was then added for 10 minutes. Reactions were terminated and receptors immunoprecipitated with 12CA5 as previously described. Immunoprecipitated proteins were fractionated by SDS-PAGE, the gel dried and visualised by autoradiography (top). The graph shown opposite was calculated from three autoradiographs and plotted as mean ± S.E. Receptor stimulation with agonist alone was set at 100%.

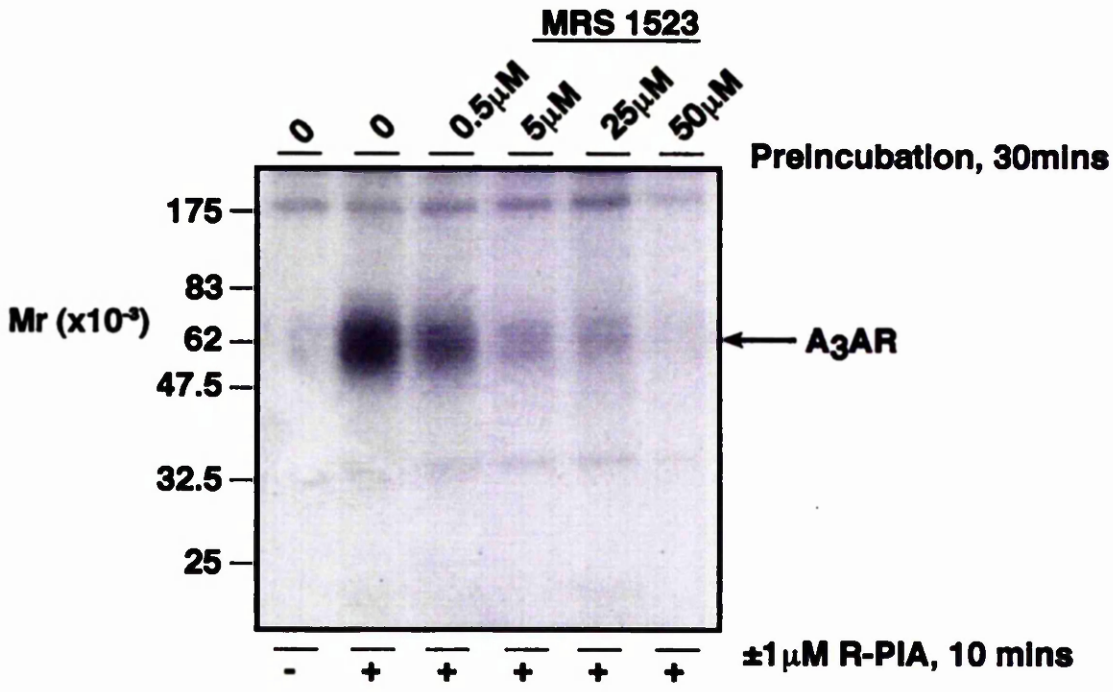
MRS 1523
0
0
0.5μM
5μM
25μM
50μM
Preincubation, 30mins
175
83
62
47.5
32.5
25
Mr (x10-3)
A3AR
-
+
+
+
+
+
±1μM R-PIA, 10 mins

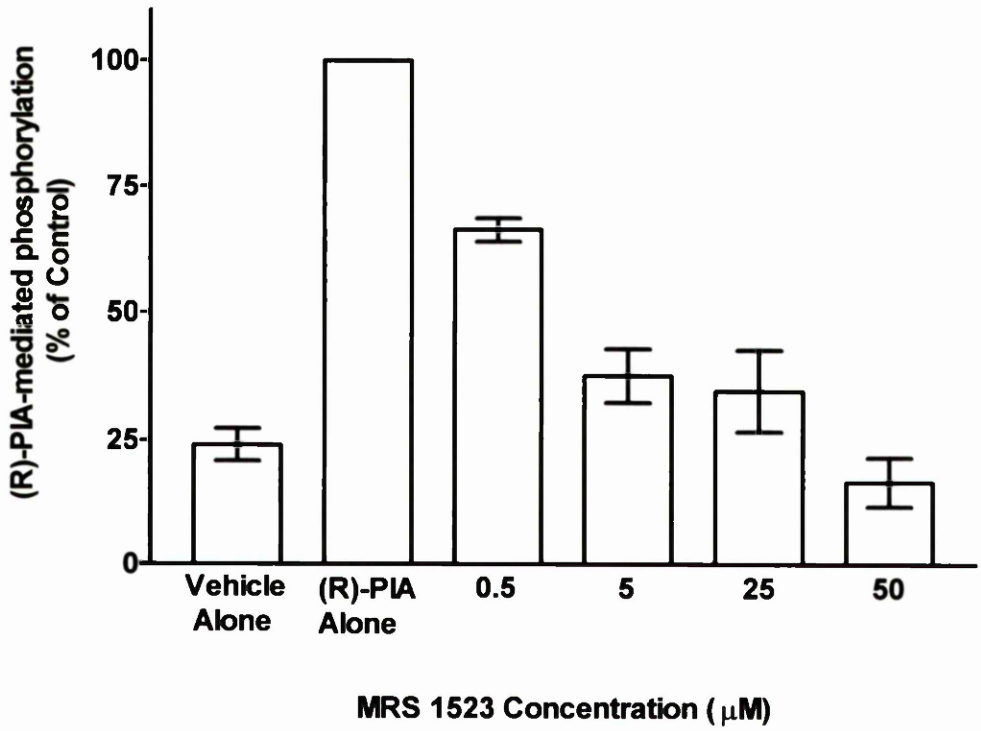
(R)-PIA-mediated phosphorylation (% of Control)
100
75
50
25
0
Vehicle Alone
(R)-PIA Alone
0.5
5
25
50
MRS 1523 Concentration (μM)

Figure 3.6 **MRS 1523 competition curves versus ^{125}I-AB-MECA binding in CHO cells stably expressing HA-tagged A_3AR**

Competition binding studies were carried out between ^{125}I-AB-MECA (0.5nM) and increasing concentrations of the A_3-selective antagonist MRS 1523 (10^{-11}-10^{-4}M) in membranes isolated from cells expressing HA-tagged WT A_3ARs. Data was plotted as ^{125}I-AB-MECA (cpm) v log [MRS 1523] M using a non-linear regression curve-fitting programme. Result shown is a representative example from one of three experiments.

Average K_i values of 0.13 ± 0.03μM were calculated from 3 experiments.

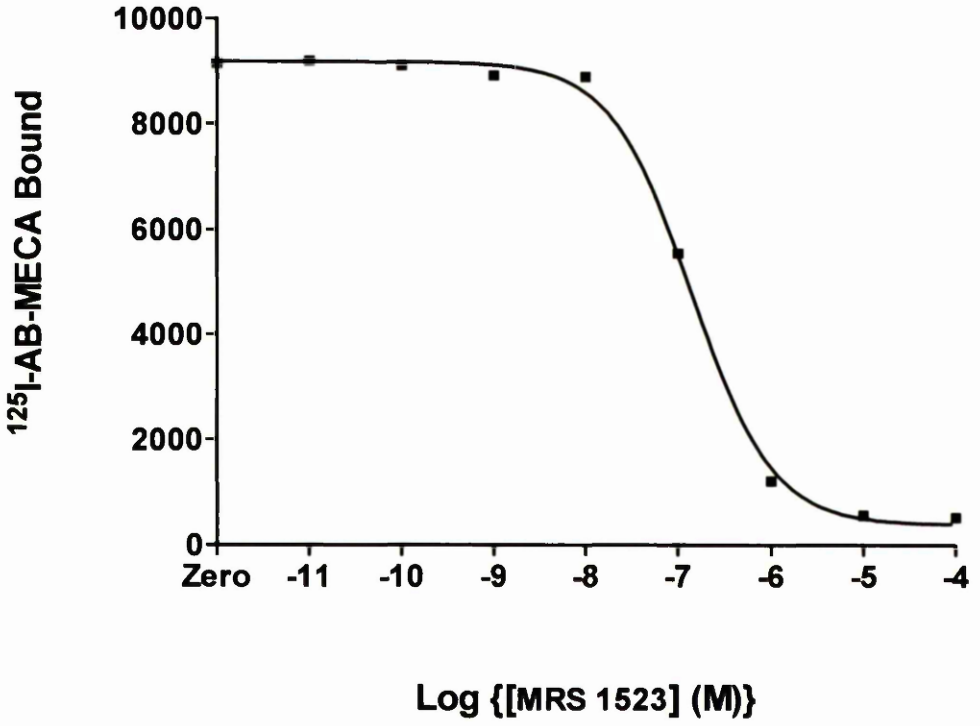
10000
8000
6000
4000
2000
0
^{125}I-AB-MECA Bound
Zero
-11
-10
-9
-8
-7
-6
-5
-4
Log {[MRS 1523] (M)}

Figure 3.7 Time course of phosphorylation of WT A_3AR

^{32}P pre-treated CHO cells expressing the WT A_3AR were incubated with 10μM (R)-PIA for the indicated times at 37°C. The reaction was then terminated and receptors immunoprecipitated with 12CA5 as described in the Methods. Proteins were separated by SDS-PAGE, the gel dried and phosphorylated A_3ARs visualised by autoradiography. Quantitative analysis is from data pooled from three such experiments.

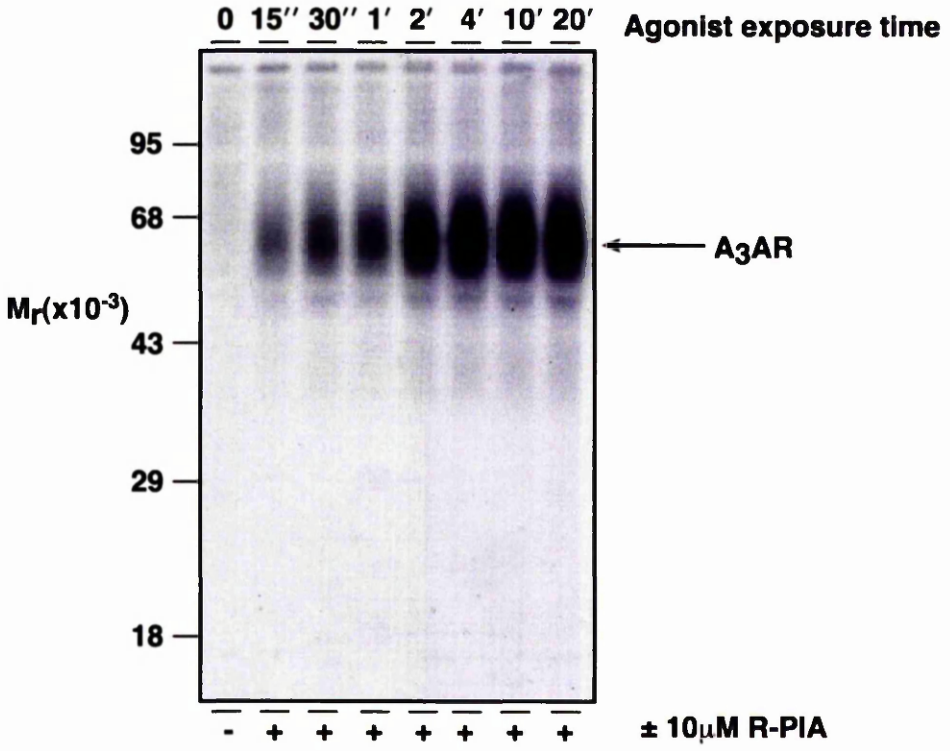
0 15'' 30'' 1' 2' 4' 10' 20'
Agonist exposure time
95
68
43
29
18
$M_r(x10^{-3})$
A_3AR
- + + + + + + +
± 10μM R-PIA

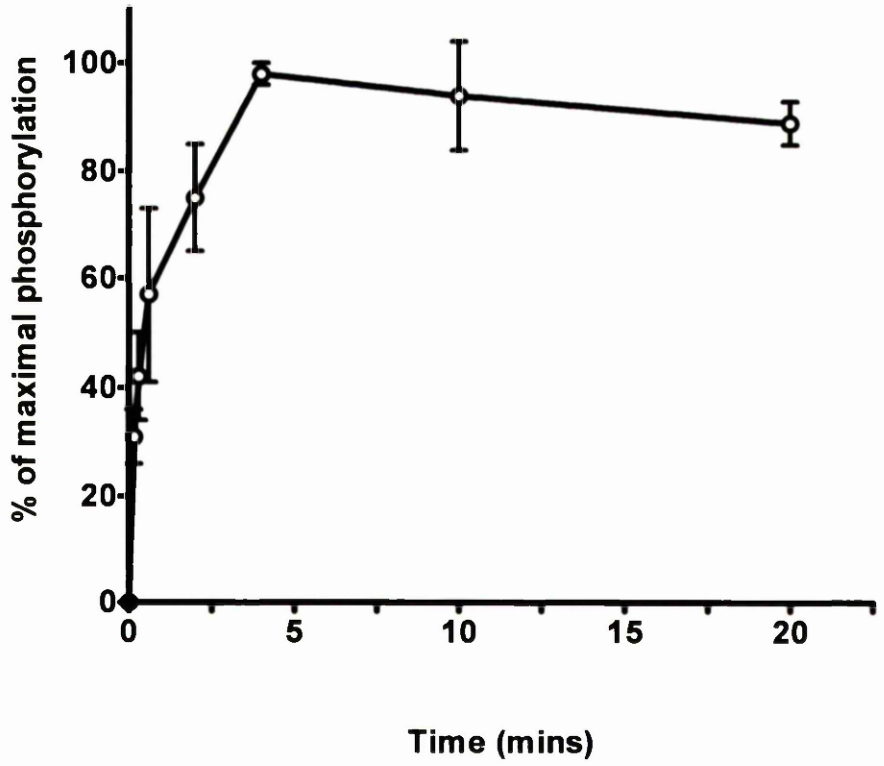
% of maximal phosphorylation
100
80
60
40
20
0
0
5
10
15
20
Time (mins)

Figure 3.8 Time course of agonist-mediated internalisation of WT A_3AR

A_3 expressing CHO cells were incubated with 1μM (R)-PIA for the indicated times at 37°C. Cell surface glycoproteins were then labelled with biotin hydrazide before receptor immunoprecipitation with 12CA5 and visualisation as described in the Methods. Blots were quantified by densitometric scanning and the values shown represent mean ± S.E. for three experiments. The levels of cell-surface receptors observed in the absence of agonist were set at 100%.

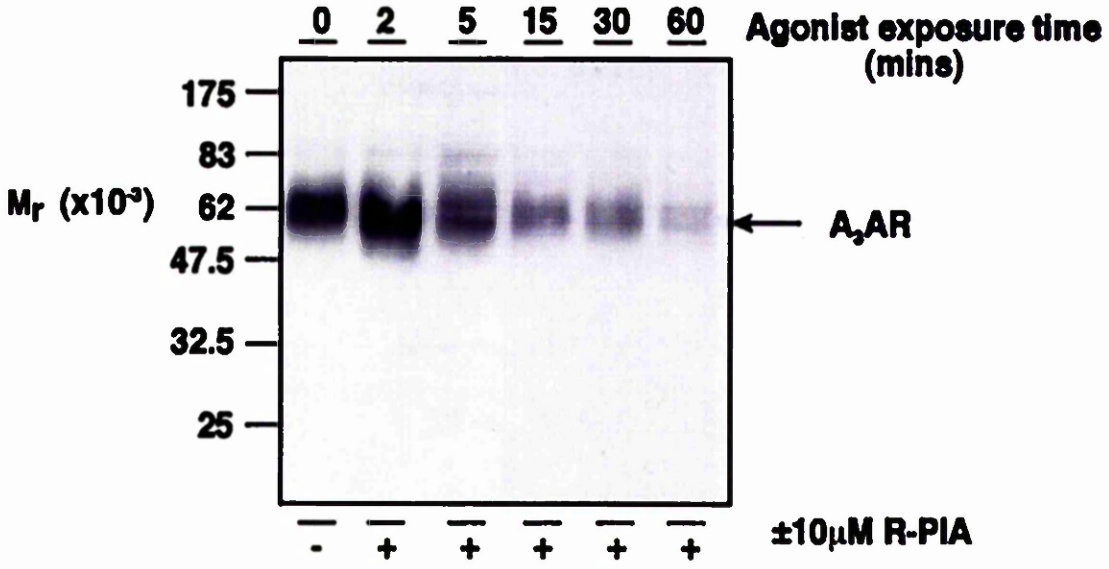
0
2
5
15
30
60
Agonist exposure time (mins)
175
83
62
47.5
32.5
25
M_r (x10^{-3})
A_2AR
-
+
+
+
+
+
±10μM R-PIA

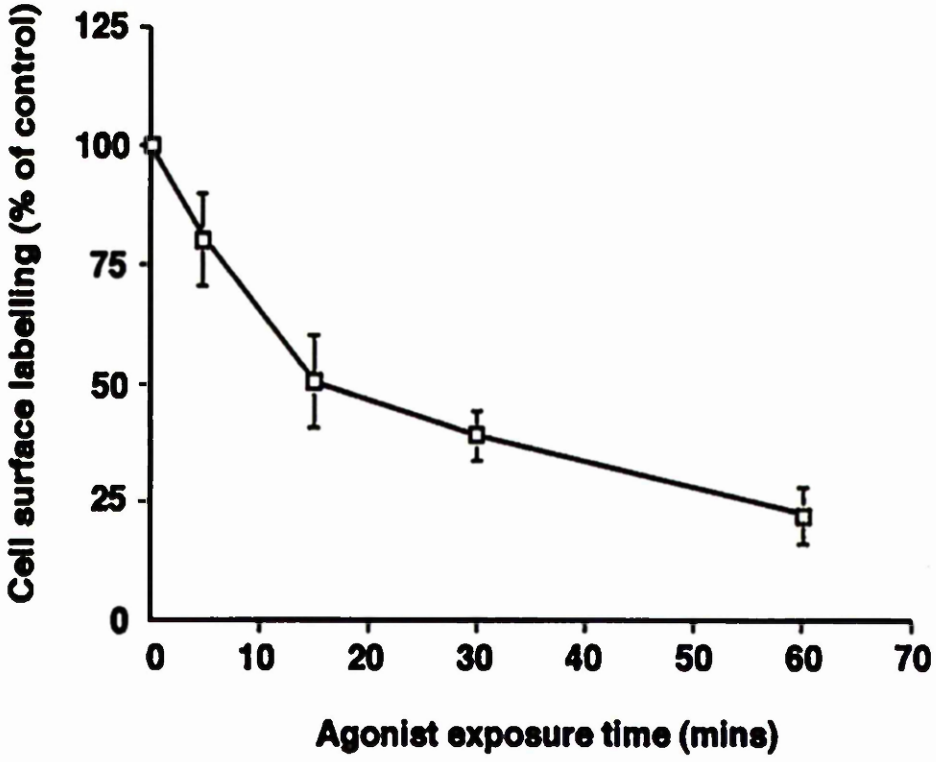
Cell surface labelling (% of control)
125
100
75
50
25
0
0
10
20
30
40
50
60
70
Agonist exposure time (mins)

Figure 3.9 Alignment of A_1AR and A_3AR C-terminal domains

The primary sequences of the C-terminal domains of the human A_1AR and rat A_3AR are shown. Phosphorylation sites at Thr 307, 318 and 319 of the A_3AR are shown in blue.

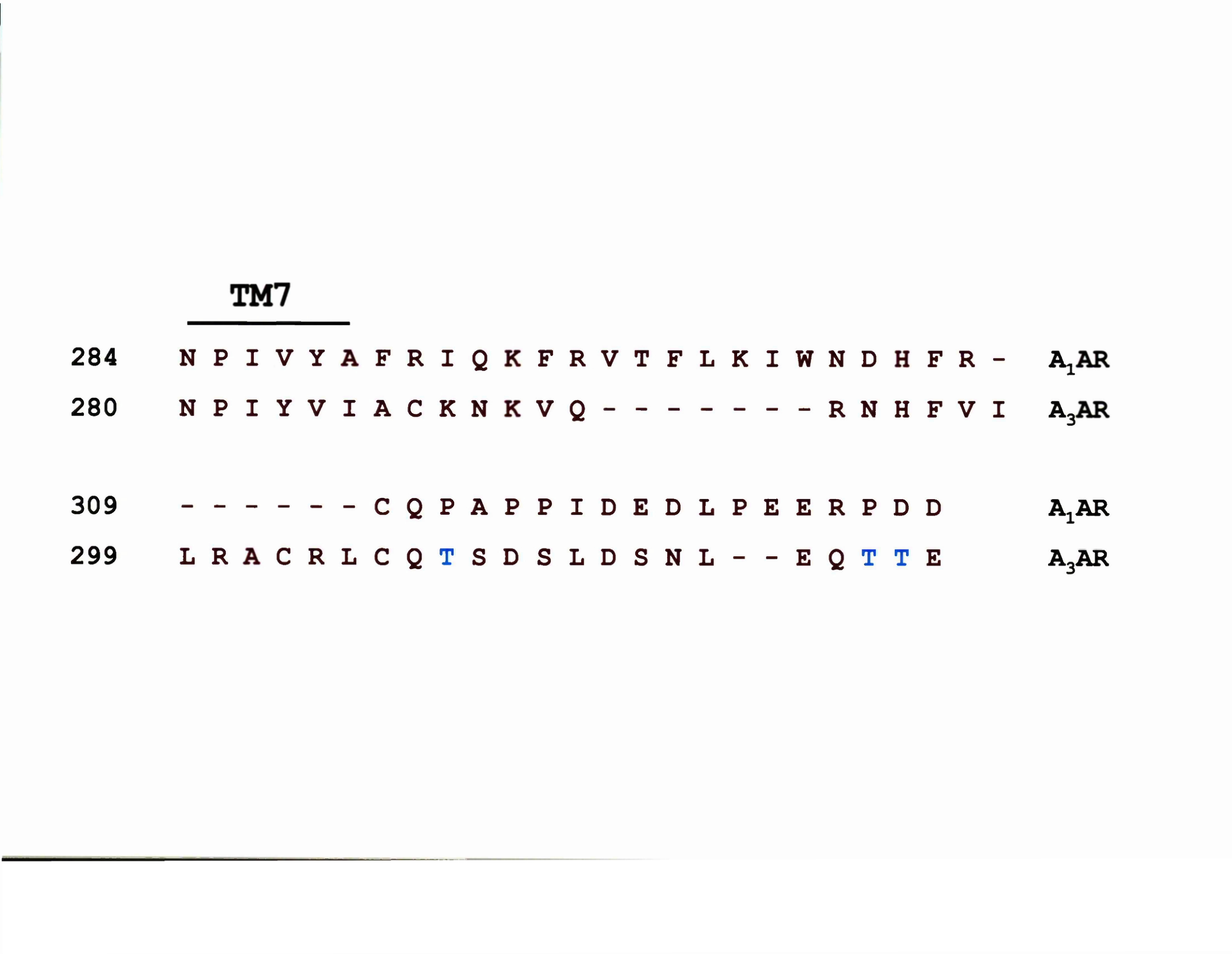
TM7
284 N P I V Y A F R I Q K F R V T F L K I W N D H F R - A1AR
280 N P I Y V I A C K N K V Q - - - - - - - - R N H F V I A3AR
309 - - - - - - - C Q P A P P I D E D L P E E R P D D A1AR
299 L R A C R L C Q T S D S L D S N L - - E Q T T E A3AR

Figure 3.10 Comparison of agonist-mediated phosphorylation of WT A_3 and A_1ARs

^{32}P-labelled CHO cells expressing the WT A_1AR and WT A_3ARs were incubated for 10 minutes with or without 5μM (R)-PIA at 37°C. The reaction was terminated and receptors immunoprecipitated with 12CA5 as described in the Methods. Proteins were separated by SDS-PAGE. Panel (A) shows a Western blot of the immunoprecipitated samples, demonstrating equal loading of each receptor construct. This process was carried out for all subsequent experiments. Phosphorylated A_3ARs were visualised by autoradiography (B) following drying of the gel. This is a representative of multiple experiments giving the same results.

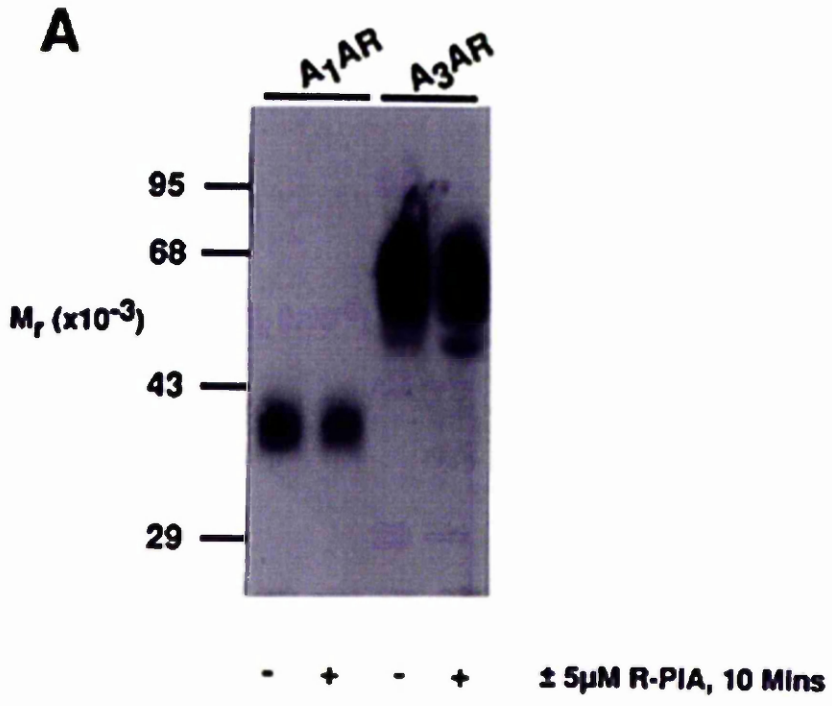
A
A1AR
A3AR
95
68
Mr (x10-3)
43
29
- + - +
± 5μM R-PIA, 10 Mins

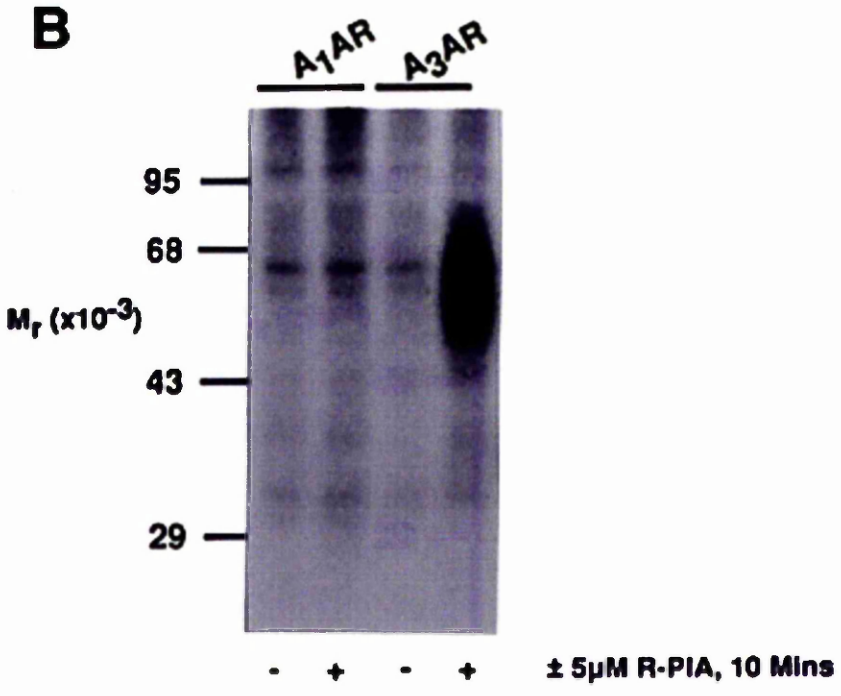
B
A1AR
A3AR
95
68
Mr (x10-3)
43
29
- + - +
± 5μM R-PIA, 10 Mins

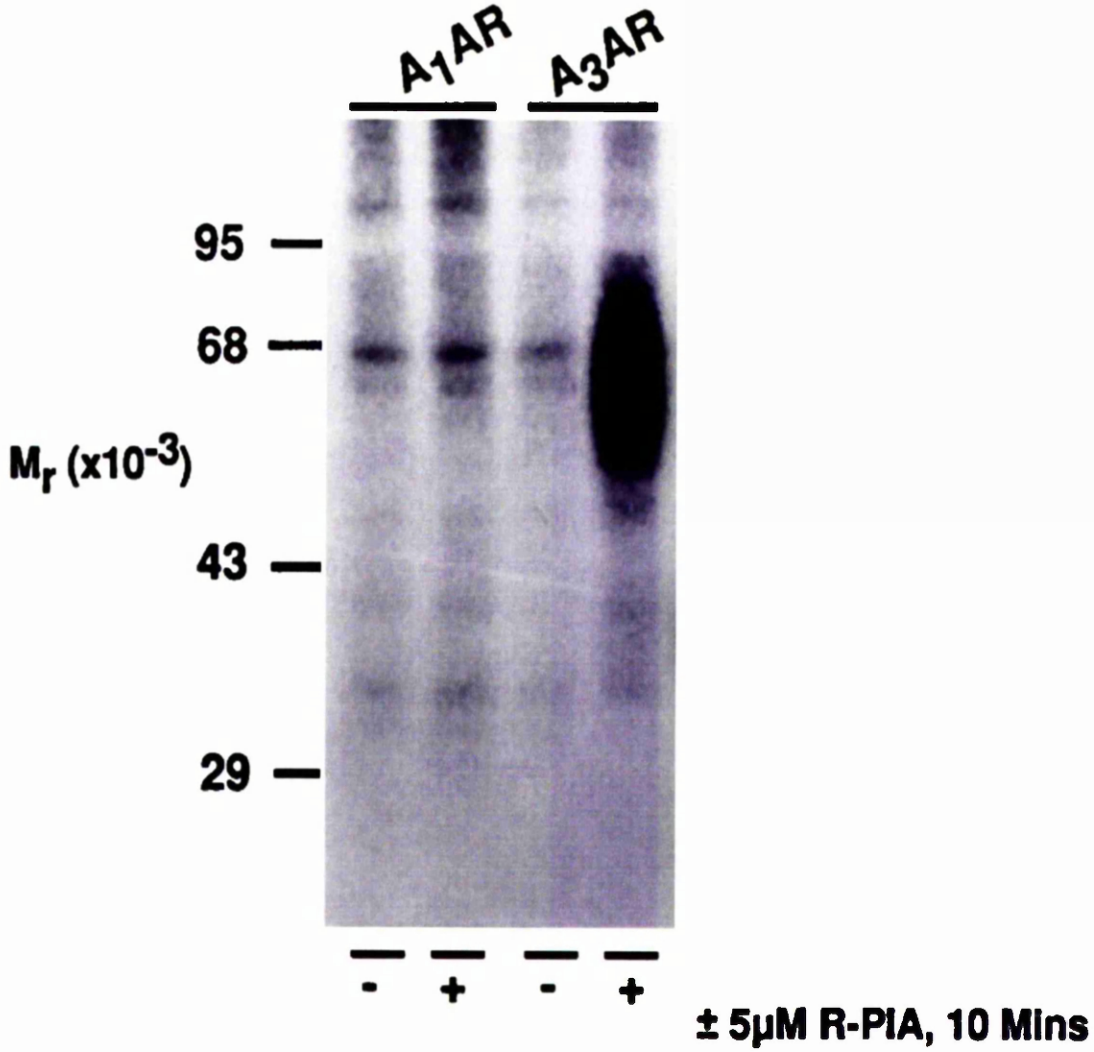
A1AR
A3AR
95
68
Mr (x10-3)
43
29
-
+
-
+
± 5μM R-PIA, 10 Mins

Figure 3.11 Time course of agonist-mediated internalisation of WT A_1AR

A_1 expressing CHO cells were incubated with 5μM (R)-PIA over a 20 hour period, as shown opposite, at 37°C. Cell surface glycoproteins were then labelled with biotin before receptor immunoprecipitation with 12CA5 and visualisation as described in the Methods. Blots were quantified by densitometric scanning and the values shown represent mean ± S.E. for three experiments. The levels of cell-surface receptors observed in the absence of agonist were set at 100%.

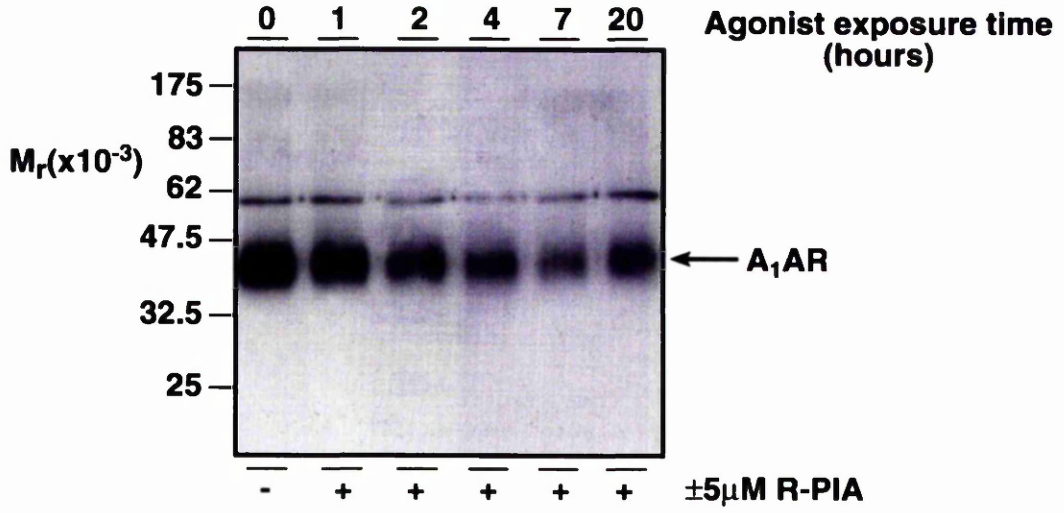
0
1
2
4
7
20
Agonist exposure time (hours)
175
83
62
47.5
32.5
25
$M_r(x10^{-3})$
A_1AR
-
+
+
+
+
+
±5μM R-PIA

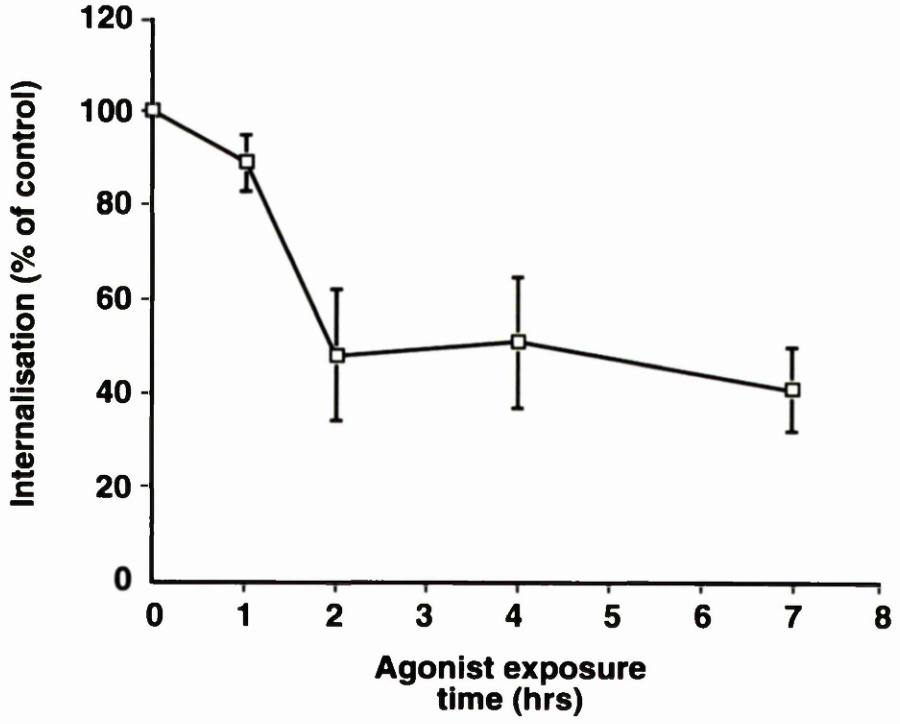
120
100
80
60
40
20
0
Internalisation (% of control)
0
1
2
3
4
5
6
7
8
Agonist exposure time (hrs)

Figure 3.12 Comparison of agonist-mediated phosphorylation of WT and (T-A)A_3ARs

^{32}P-labelled CHO cells expressing the mutant (T-A)A_3AR were incubated for 10 minutes with or without 5μM (R)-PIA at 37°C. The reaction was then terminated and receptors immunoprecipitated with 12CA5 as described in the Methods. Proteins were separated by SDS-PAGE, the gel dried and phosphorylated A_3ARs visualised by autoradiography. This is a representative example of three experiments showing the same results.

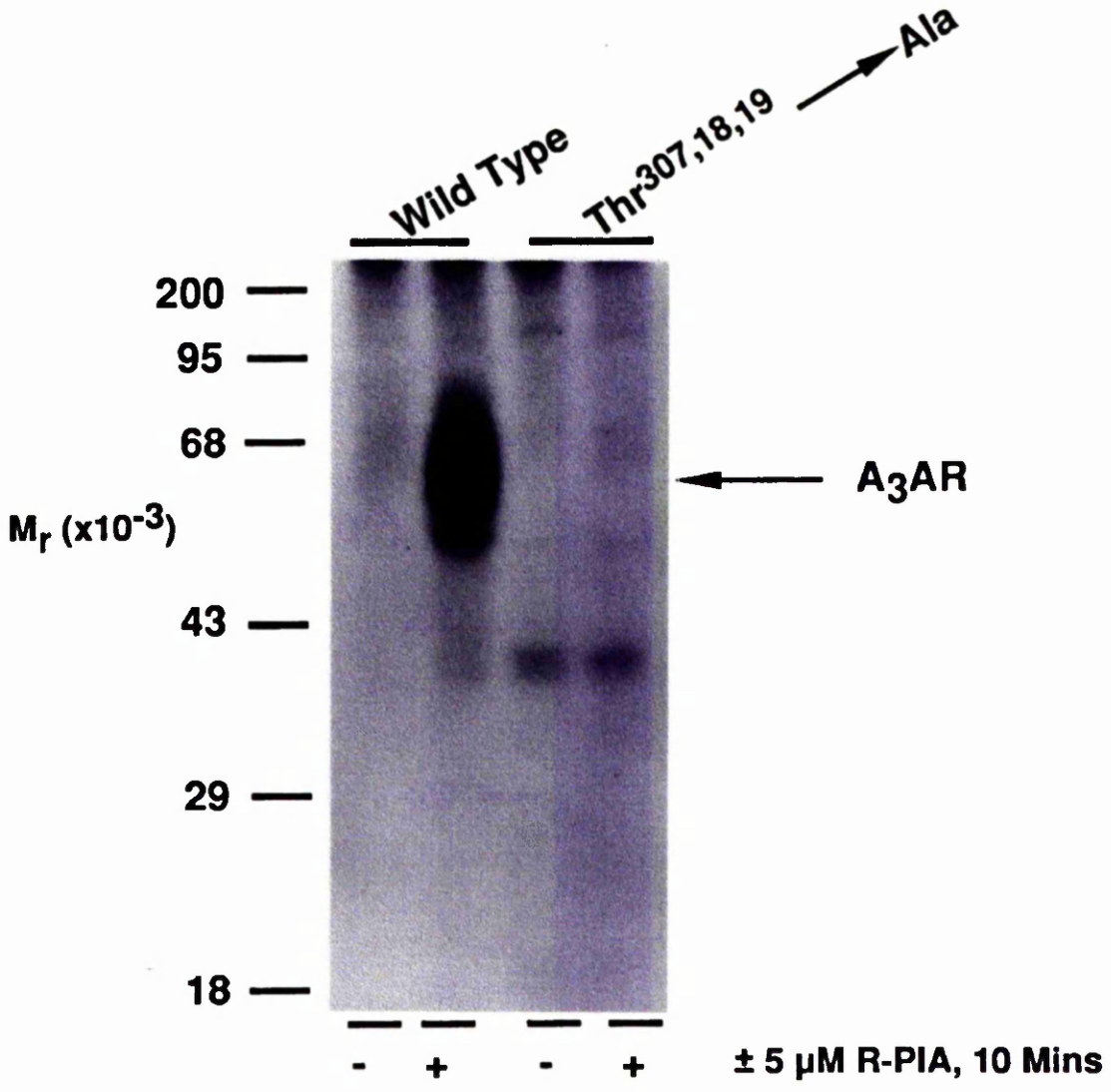
Wild Type
Thr307,18,19 → Ala
200
95
68
43
29
18
Mr (x10-3)
A3AR
- + - +
± 5 μM R-PIA, 10 Mins

Figure 3.13 Comparison of the effects of agonist treatment on cell surface levels of WT and (T-A)A_3ARs

CHO cells stably expressing the WT A_3AR (top) or the phosphorylation deficient mutant (T-A)A_3AR (bottom) were incubated with 5μM (R)-PIA for the indicated times at 37°C. Cell surface glycoproteins were labelled with biotin before immunoprecipitation of receptors with 12CA5. Visualisation was as described in the Methods. This is a representative example of one of three experiments showing essentially identical results.

The graph shown represents quantitation of the results obtained from the blots and shows a statistically significant difference ($p < 0.05$) in the internalisation of the two receptors at 60 minutes.

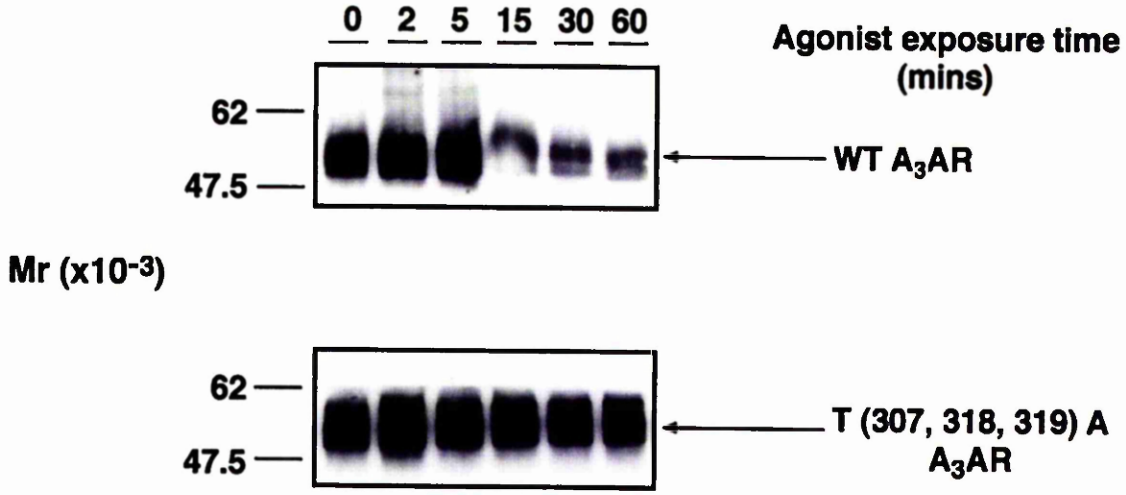
0 2 5 15 30 60
Agonist exposure time (mins)
62
47.5
WT A_3AR
Mr (x10-3)
62
47.5
T (307, 318, 319) A A_3AR

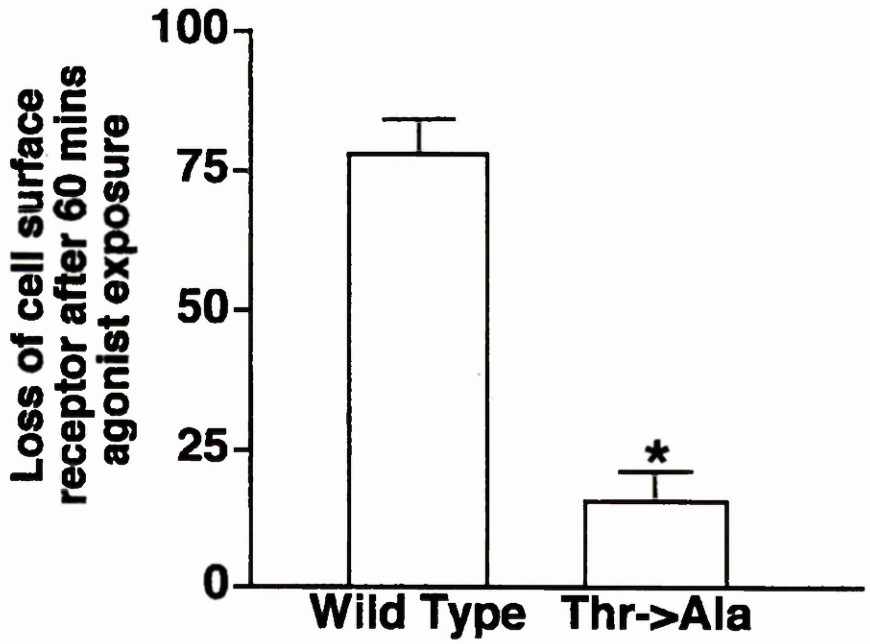
Loss of cell surface receptor after 60 mins agonist exposure
100
75
50
25
0
*
Wild Type
Thr->Ala

Figure 3.14 Comparison of agonist-mediated phosphorylation of WT and (C-A)A_3AR

^{32}P pre-treated CHO cells expressing the mutant (C-A)A_3AR were incubated for 10 minutes with or without 5μM (R)-PIA for the 10 minutes at 37°C. The reaction was then terminated and receptors immunoprecipitated with 12CA5 as described in the Methods. Proteins were separated by SDS-PAGE, the gel dried and phosphorylated A_3ARs visualised by autoradiography. This is a representative of three experiments giving the same results.

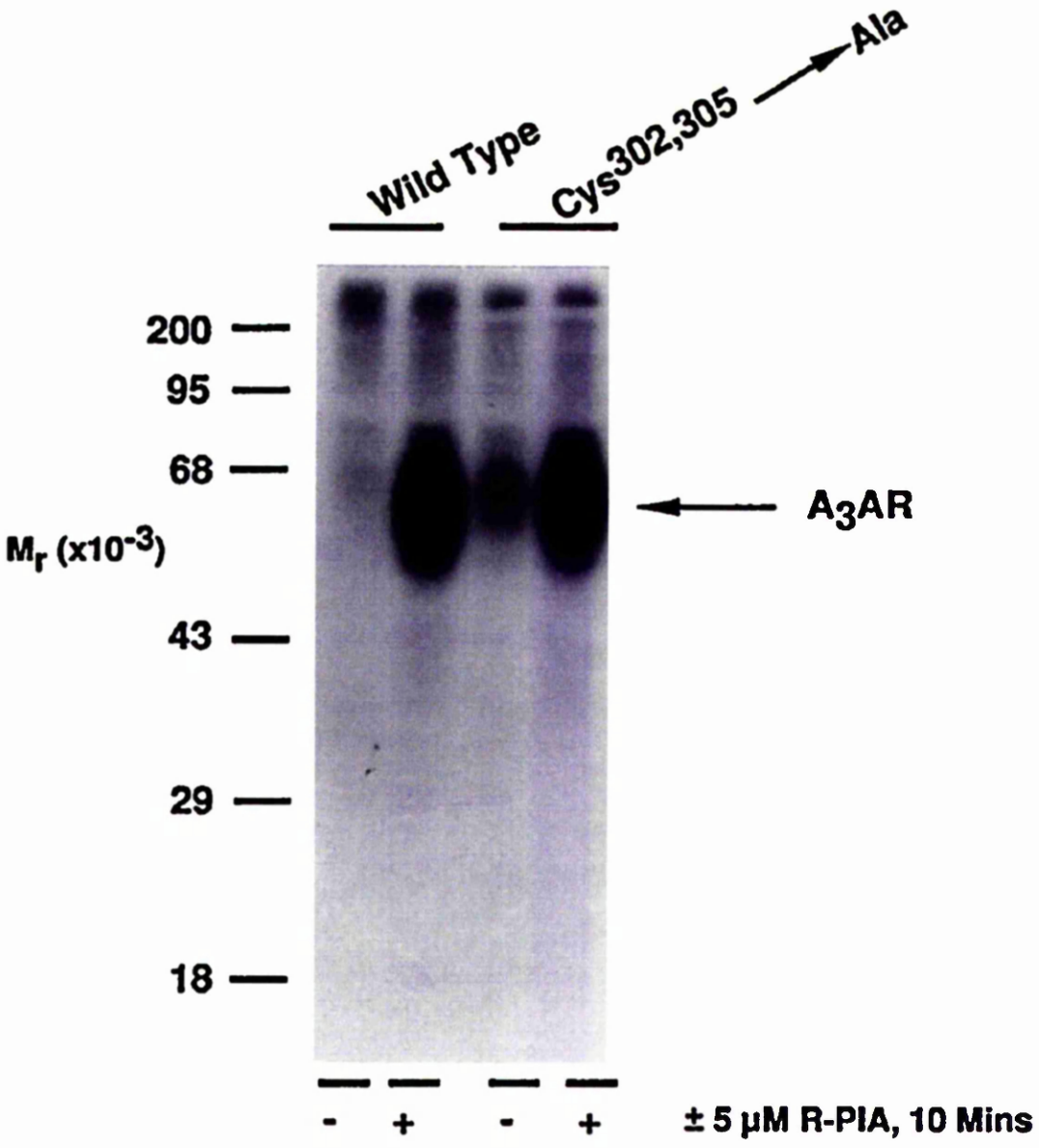
Wild Type
Cys302,305 → Ala
200
95
68
M_r (x10^{-3})
43
29
18
A_3AR
- + - +
± 5 μM R-PIA, 10 Mins

Figure 3.15 Time course of agonist-mediated internalisation of the mutant (C-A)A_3AR

(C-A)A_3AR expressing CHO cells were incubated with 1μM (R)-PIA over a 20 minute period at 37°C. Cell-surface glycoproteins were then labelled with biotin hydrazide before receptor immunoprecipitation with 12CA5 and visualisation as described in the Methods. Blots were quantified by densitometric scanning and the values shown represent mean ± S.E. for three experiments. The levels of cell-surface receptors observed in the absence of agonist were set at 100%.

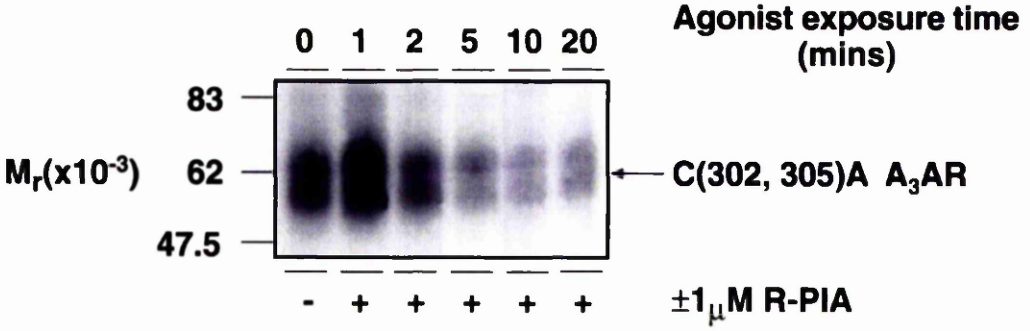
Agonist exposure time (mins)
0 1 2 5 10 20
83
62
47.5
$M_r(x10^{-3})$
C(302, 305)A A_3AR
- + + + + +
±1μM R-PIA

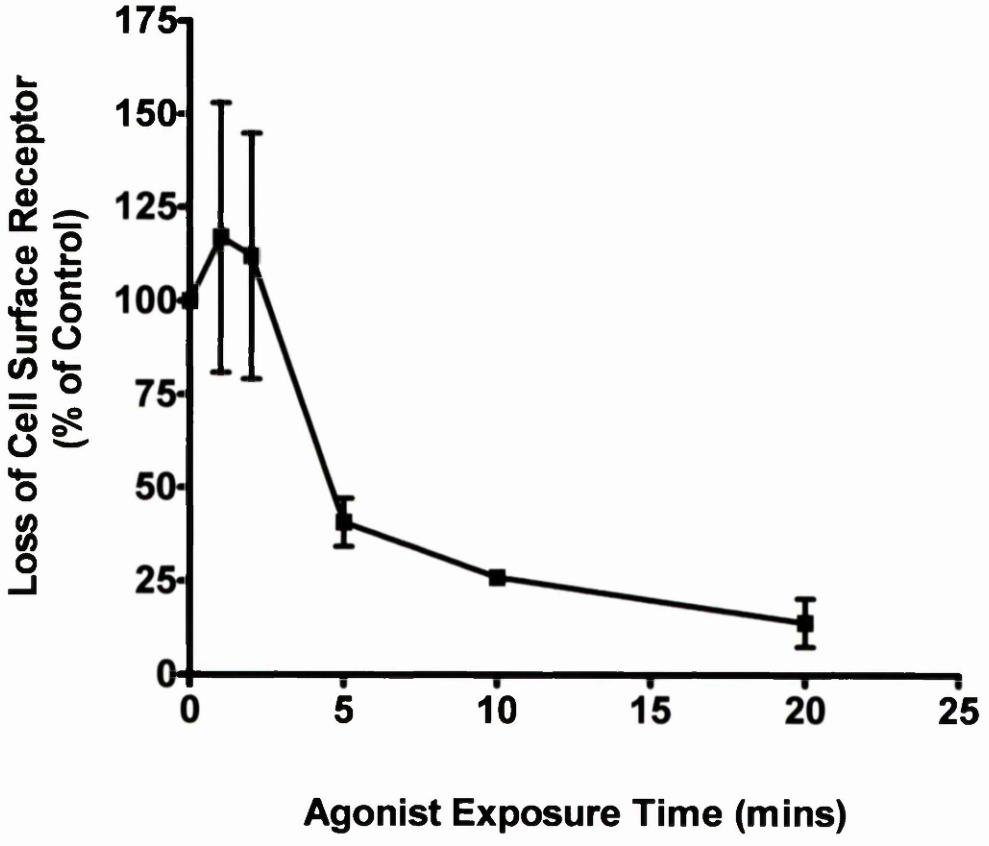
Loss of Cell Surface Receptor (% of Control)
175
150
125
100
75
50
25
0
0 5 10 15 20 25
Agonist Exposure Time (mins)

Figure 3.16 **Effect of MRS 1523 on (R)-PIA-induced internalisation and recycling of WT A_3 and (C-A)A_3ARs**

CHO cells transiently transfected with WT A_3AR or (C-A)A_3AR cDNAs were incubated with 1μM (R)-PIA for 30 minutes at 37°C. Membranes were then washed once with fresh medium and incubated with MRS 1523 to a final concentration of 5μM for the indicated times. Cell surface glycoproteins were labelled with biotin hydrazide before receptor immunoprecipitation with 12CA5 and visualisation as described in the Methods. Blots were quantified by densitometric scanning and the values shown represent mean ± S.E. for three experiments. The levels of cell-surface receptors observed in the absence of agonist were set at 100%.

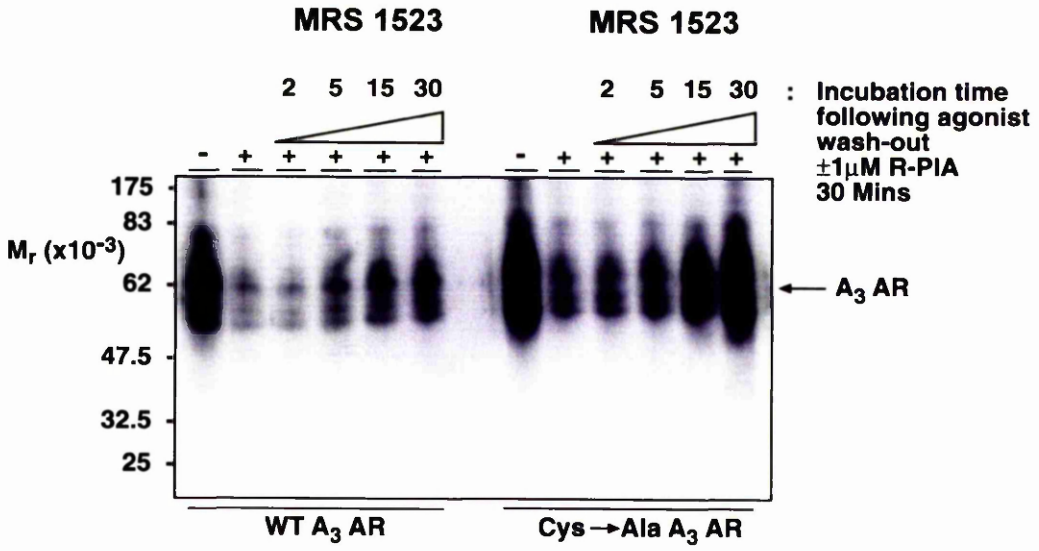
MRS 1523
MRS 1523
2 5 15 30
2 5 15 30
: Incubation time following agonist wash-out ±1μM R-PIA 30 Mins
- + + + + +
- + + + + +
175
83
M_r (x10^{-3})
62
47.5
32.5
25
A_3 AR
WT A_3 AR
Cys→Ala A_3 AR

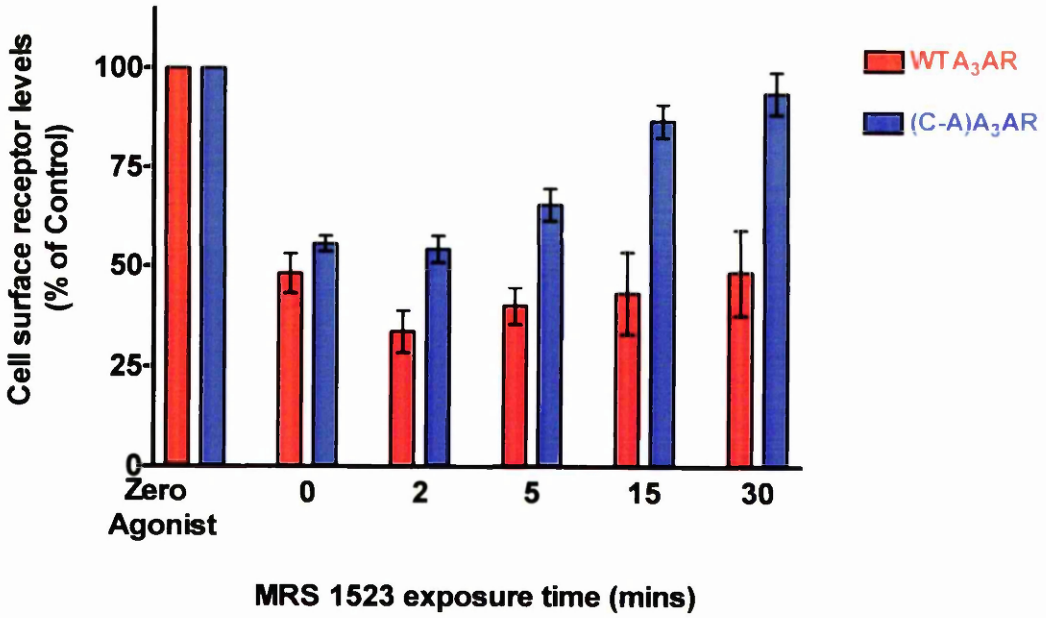
Cell surface receptor levels (% of Control)
100
75
50
25
0
WT A_3AR
(C-A)A_3AR
Zero Agonist
0
2
5
15
30
MRS 1523 exposure time (mins)

Figure 3.17 2D snake diagram of A_1CT3AR

Schematic representation of the chimeric A_1-A_3AR constructed by Palmer et al.,(1996). The C-terminal tail of the A_3AR was exchanged with that of the non-phosphorylatable A_1AR. The main body of the A_1AR was left intact up to and including its predicted palmitoylation site at Cys 309. HA-epitope tags were present at both the N and C-termini.

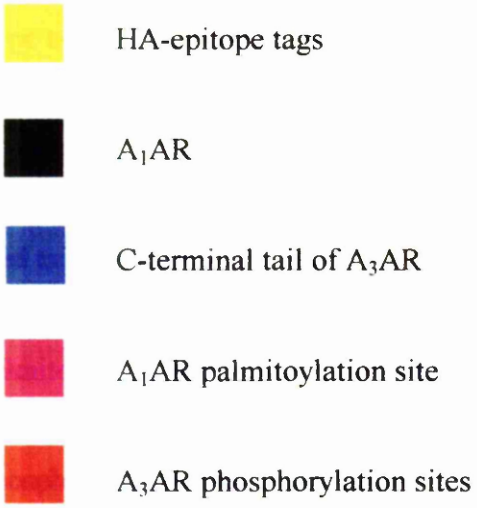

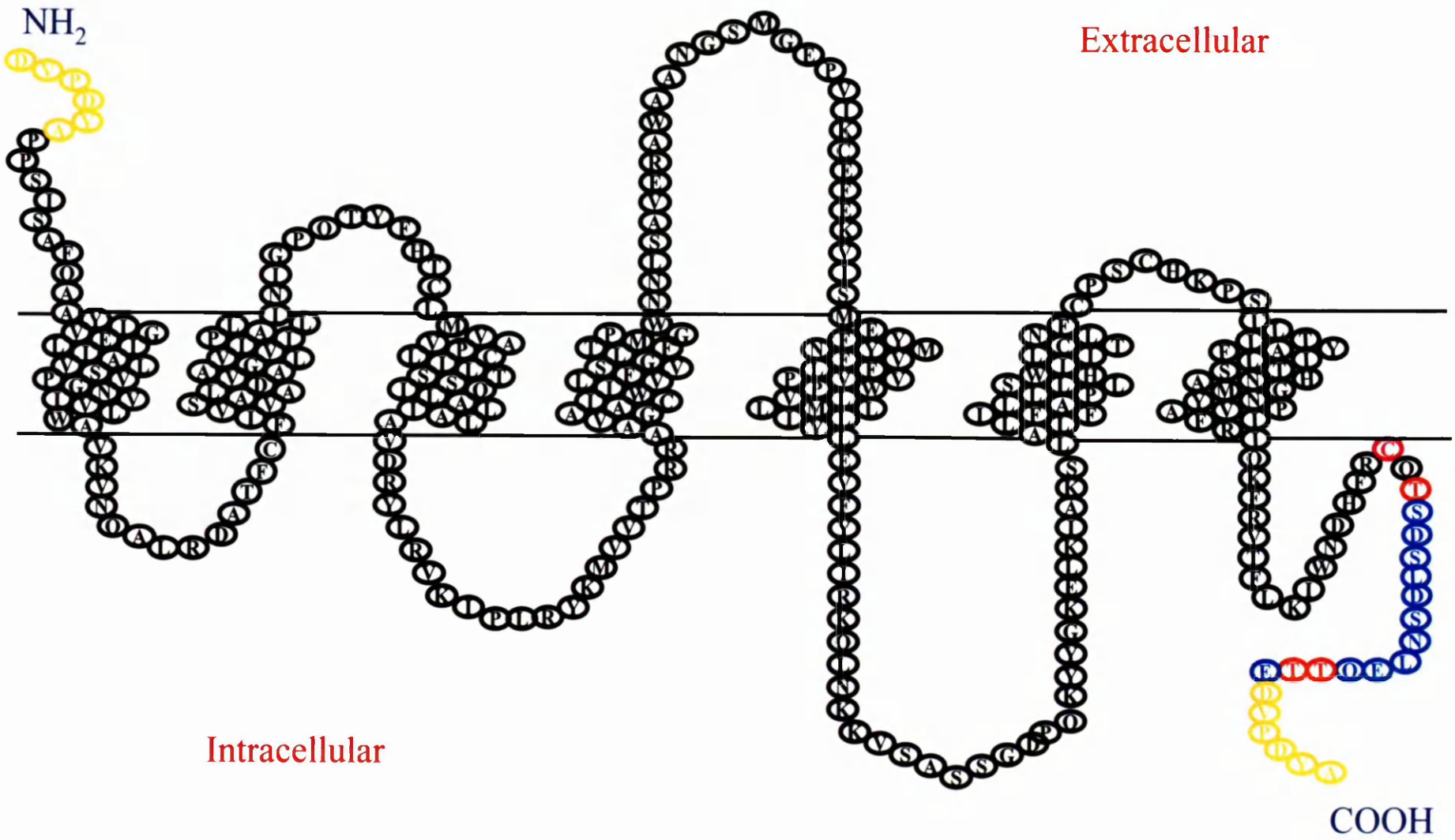
NH2
Extracellular
Intracellular
COOH

Figure 3.18 Time course of agonist-stimulated phosphorylation of the chimeric A_1CT3AR

^{32}P-labelled CHO cells stably expressing A_1CT3AR were treated ± 1μM (R)-PIA at 37°C for the indicated times before termination of the reaction and receptor immunoprecipitation with 12CA5 as described in the Methods. Proteins were separated by SDS-PAGE and gels visualised by autoradiography. Quantitative analysis is from data pooled from three such experiments.

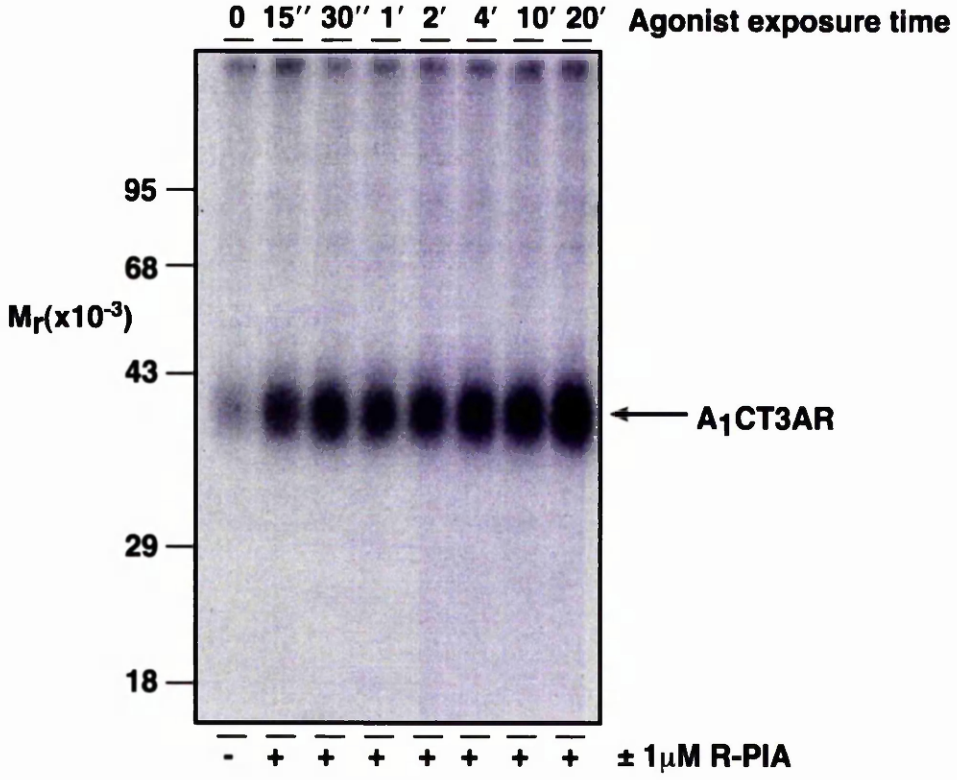
0 15'' 30'' 1' 2' 4' 10' 20' Agonist exposure time
95
68
$M_r(x10^{-3})$
43
29
18
A_1CT3AR
- + + + + + + + ± 1μM R-PIA

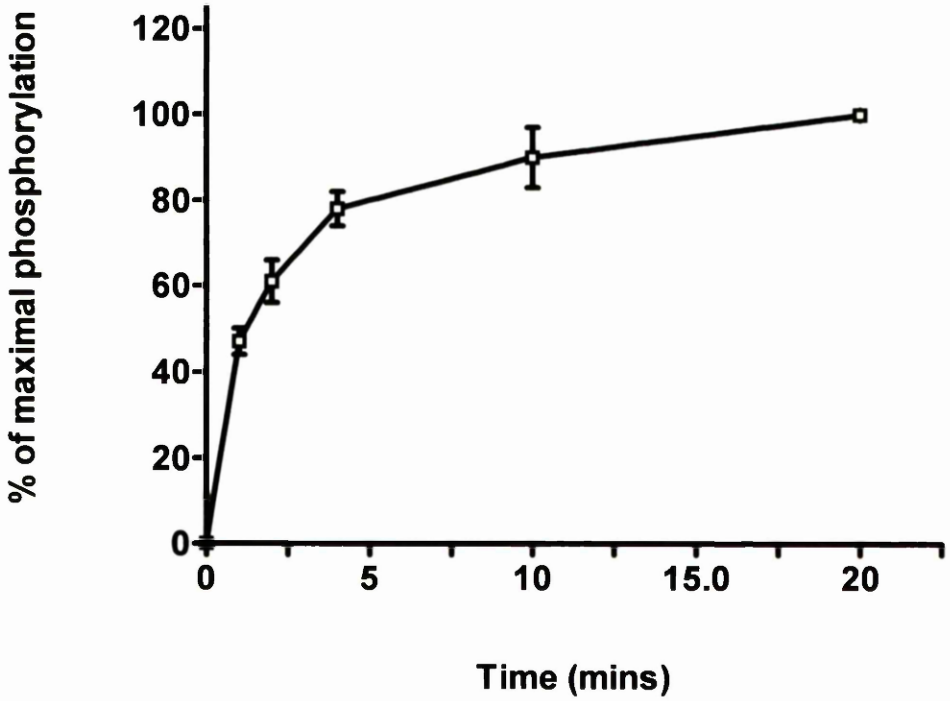
% of maximal phosphorylation
120
100
80
60
40
20
0
0
5
10
15.0
20
Time (mins)

Figure 3.19 Time course of agonist-mediated internalisation of the A_1CT3AR

CHO cells expressing the A_1CT3AR were incubated with 1μM (R)-PIA for the indicated times at 37°C. Cell-surface glycoproteins were labelled with biotin and immunoprecipitation carried out using 12CA5 prior to visualisation as previously described. Blots were quantified by densitometric scanning. Values represent mean ± S.E. for three experiments, with the levels of cell-surface receptor in the absence of agonist set at 100%.

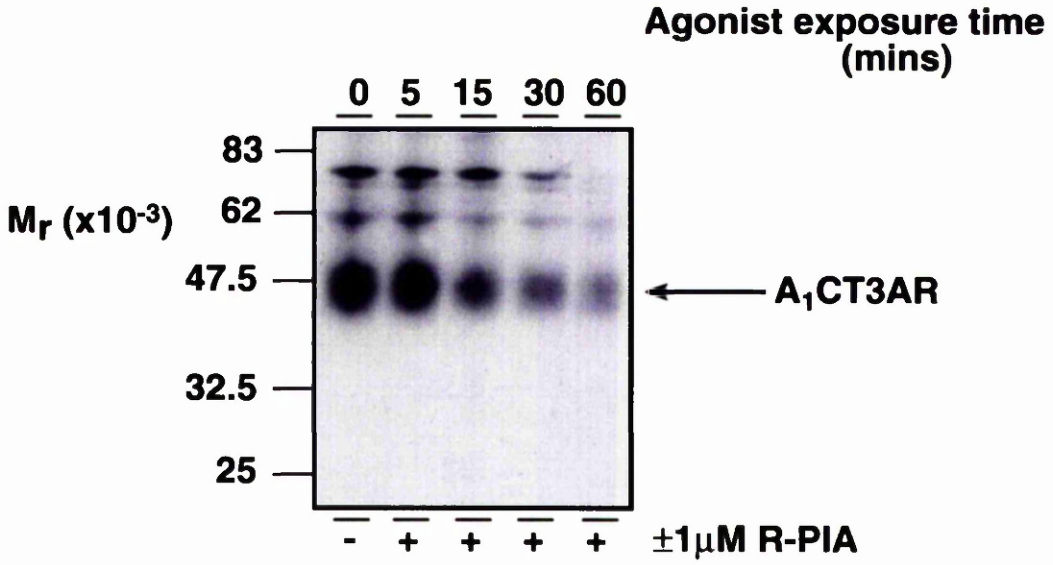
Agonist exposure time (mins)
0 5 15 30 60
83
62
47.5
32.5
25
M_r (x10^{-3})
A_1CT3AR
- + + + +
±1μM R-PIA

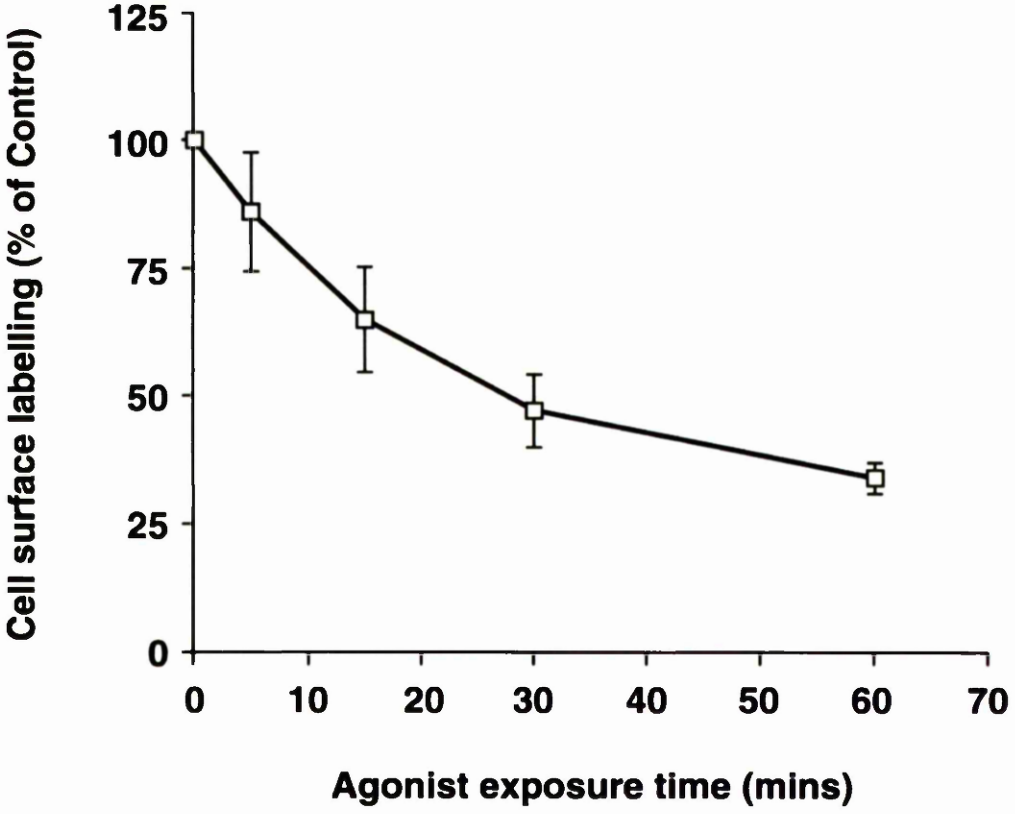
Cell surface labelling (% of Control)
125
100
75
50
25
0
0 10 20 30 40 50 60 70
Agonist exposure time (mins)

Figure 3.20 Schematic representation of GFP-tagged A_3ARs

The C-terminal HA-tag present on the A_3AR was removed by PCR and the mutated receptor ligated into the multiple cloning site of pEGFP-N1 at HindIII / SmaI. The N-terminal HA-tag was left intact. The ATG start codon of GFP was mutated to Ala so that the ATG start codon of the A_3AR was the only consensus initiator of translation for the whole construct. The Thr and Cys residues mutated to give the (T-A) and (C-A) mutant A_3 receptors are also shown.

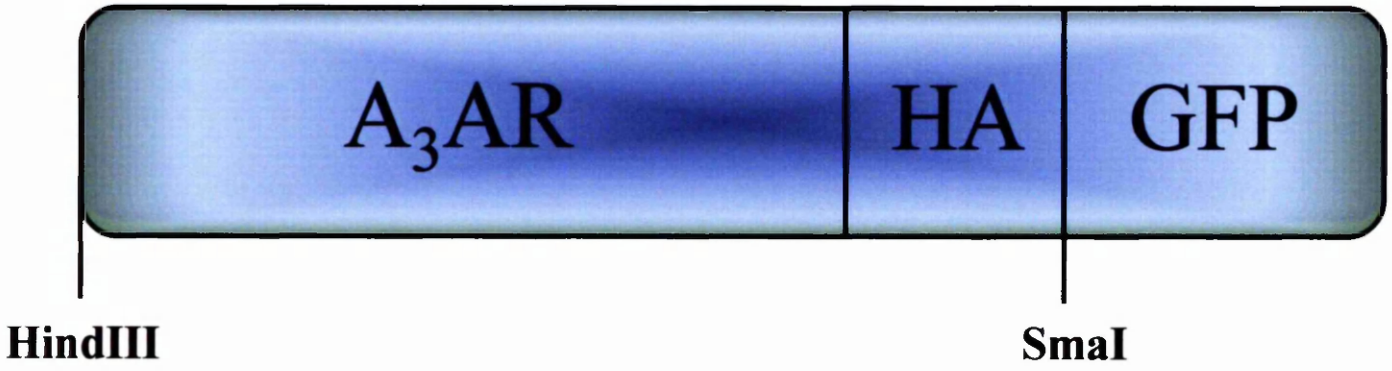
A3AR
HA
GFP
HindIII
SmaI

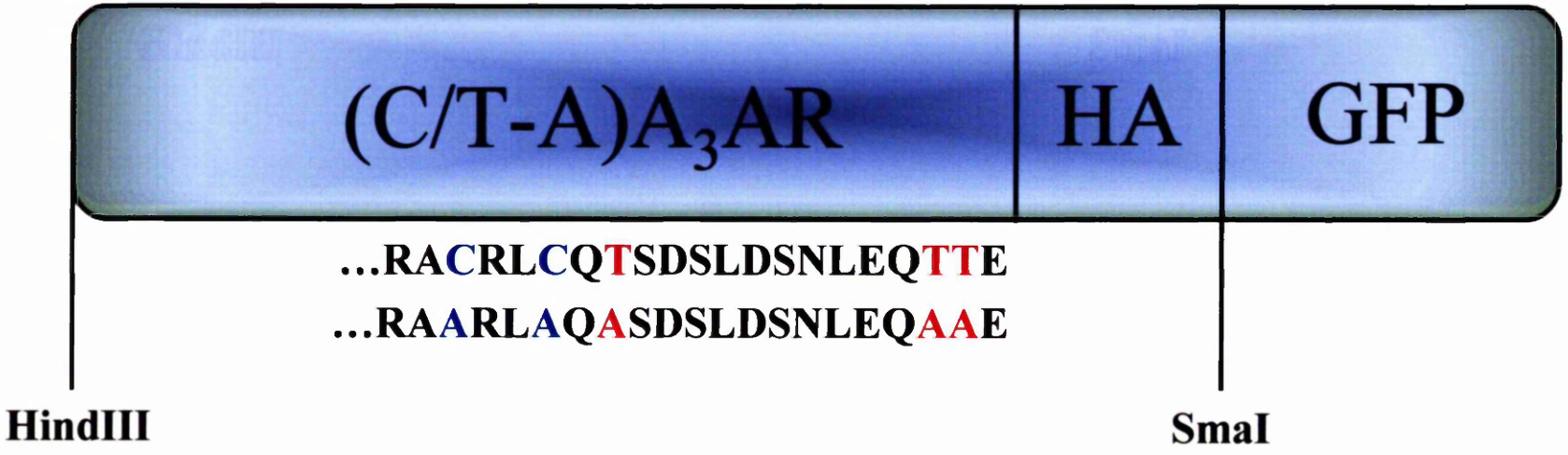
(C/T-A)A3AR
HA
GFP
…RACRLCQTSDSLDSNLEQTTE
…RAARLAQASDSLDSNLEQAAE
HindIII
SmaI

Figure 3.21 Schematic representation of GFP-tagged WT A_1AR AND A_1CT3AR

The C-terminal HA-tag present on the A_1AR was again removed by PCR and the mutated receptor ligated into the multiple cloning site of pEGFP-N1 at HindIII / KpnI. The N-terminal HA-tag was left intact. The ATG start codon of GFP was mutated to Ala so that the ATG start codon of the A_1AR was the only consensus initiator of translation for the whole construct. The C-terminal tail insertion, present in the A_1CT3AR, is also shown.

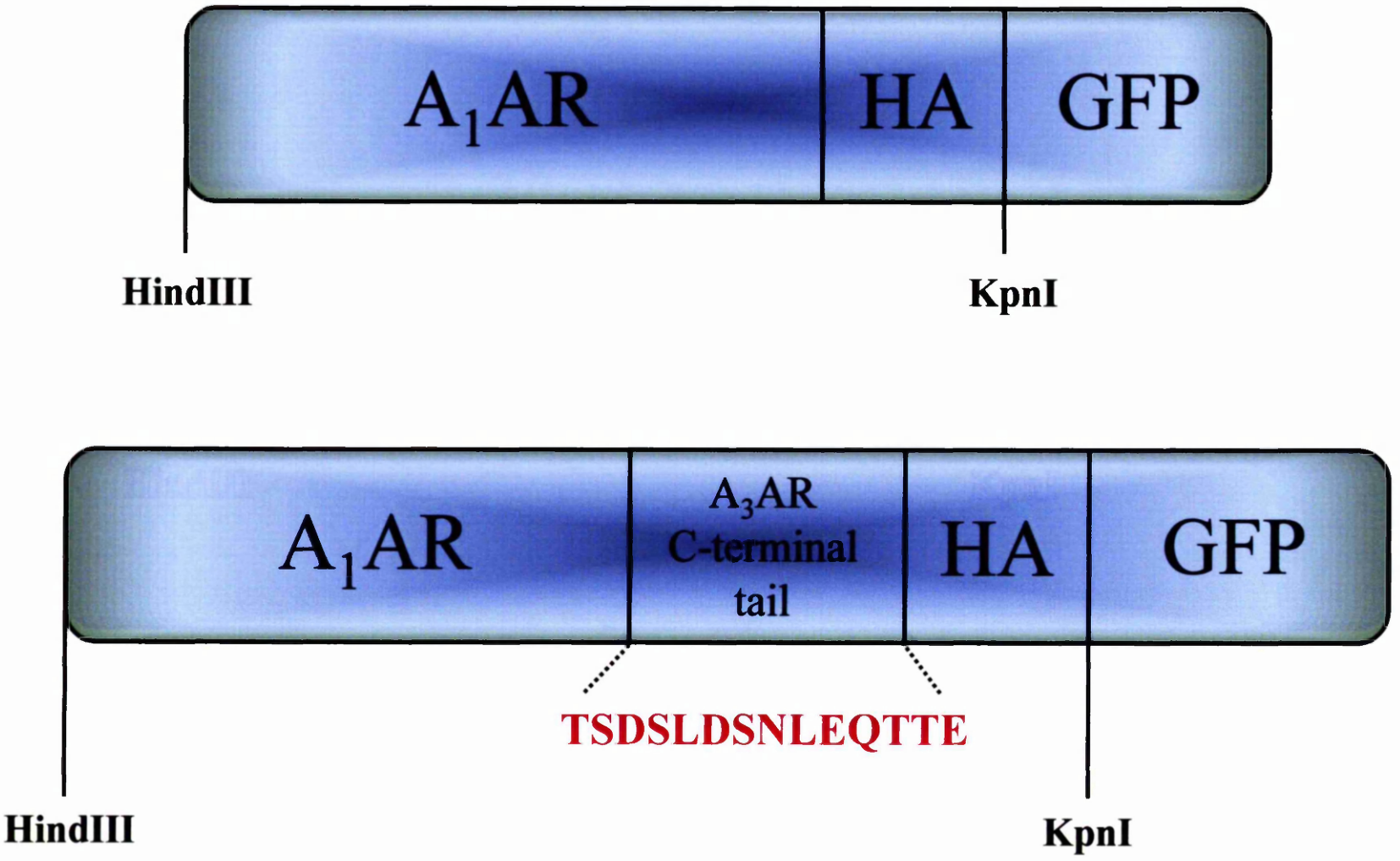
A1AR
HA
GFP
HindIII
KpnI
A1AR
A3AR
C-terminal
tail
HA
GFP
TSDSLDSNLEQTTE
HindIII
KpnI

Figure 3.22 Cell-surface labelling of A_3AR and A_3AR-GFP

CHO cells expressing either WT or GFP-tagged A_3ARs were labelled with biotin and cell surface receptors immunoprecipitated with 12CA5 as previously described. Immunoprecipitates were resolved by SDS-PAGE and biotin-labelled cell-surface receptors visualised by transfer to nitrocellulose and blotting with straptavidin-conjugated HRP as described in the Methods (section 2.4.2). This is a representative example of one of three experiments giving the same results.

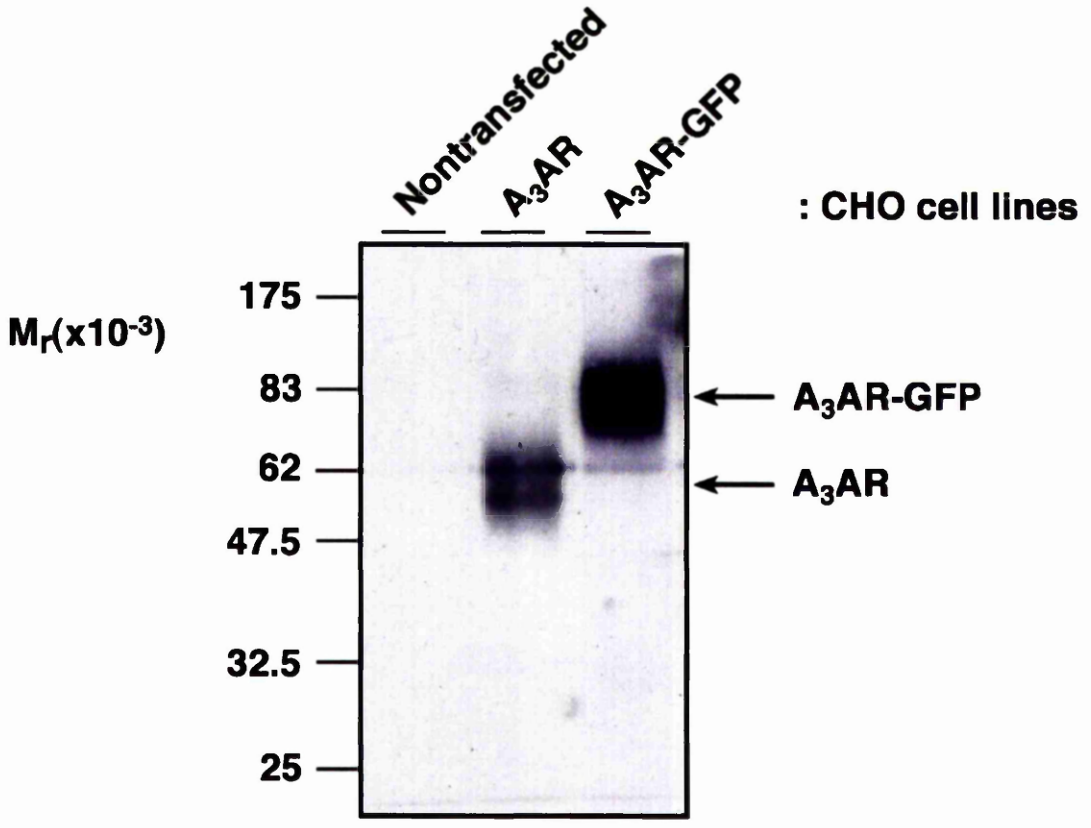
Nontransfected
A3AR
A3AR-GFP
: CHO cell lines
Mr(x10-3)
175
83
62
47.5
32.5
25
A3AR-GFP
A3AR

Figure 3.23 **Saturation analysis of ^{125}I-AB-MECA binding to WT and GFP-tagged rat A_3ARs**

Membranes prepared from COS cells transiently transfected with WT (blue) and GFP-tagged (red) forms of the rat A_3AR were used in saturation binding studies with ^{125}I-AB-MECA. Membrane preparation and radioligand binding procedures are as described in the Methods (Section 2.4.6).

To obtain the specific binding achieved by the radioligand on the receptors, non-specific counts were subtracted from the total counts and the resulting values plotted against [^{125}I-AB-MECA] nM. To determine the total number of agonist binding sites (B_{max}) and the equilibrium dissociation constant (K_d), the data was fitted by nonlinear regression analysis (Graphpad Prism). Average K_d and B_{max} values of three experiments are shown in Table 3.1.

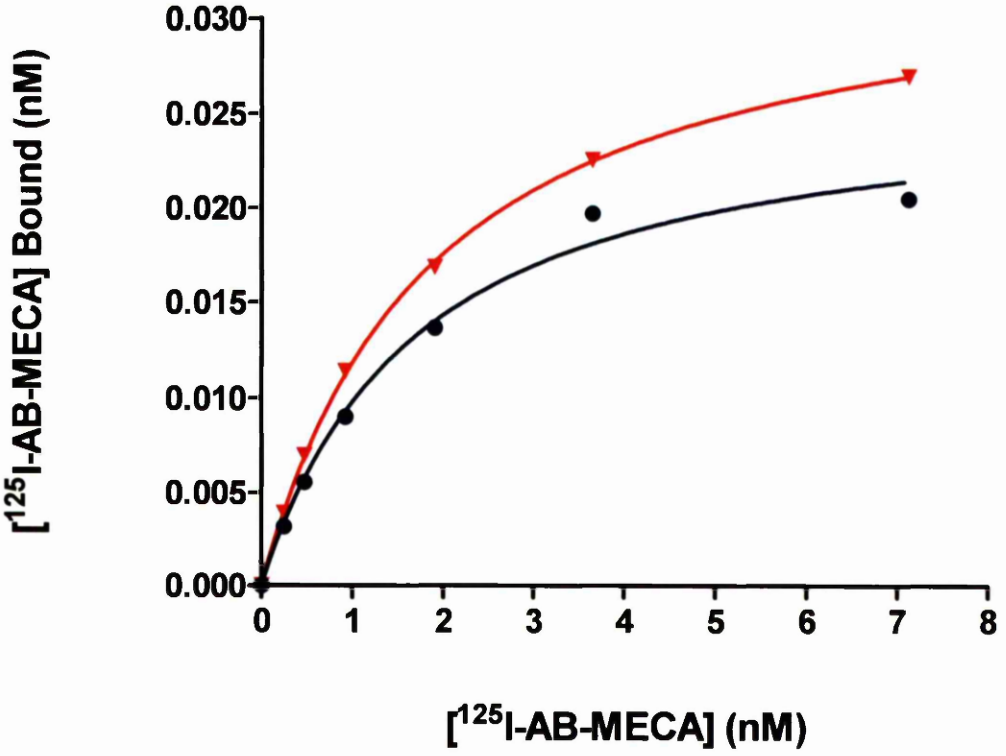
0.030
0.025
0.020
0.015
0.010
0.005
0.000
0
1
2
3
4
5
6
7
8
[125I-AB-MECA] Bound (nM)
[125I-AB-MECA] (nM)

Table 3.1 **Table of ligand affinities and expression levels of WT A_3AR and A_3AR-GFP**

Receptor	K_d (nM)	B_{max} (pmol/mg)	Significance
WT A_3AR	2.175 ± 0.31	1.2 ± 0.3	$p>0.05$
A_3AR-GFP	2.03 ± 0.18	1.4 ± 0.2	$p>0.05$

Figure 3.24 **Agonist-stimulated phosphorylation of WTA_3 and A_3GFP-tagged receptors**

^{32}P-labelled CHO cells stably expressing WT A_3AR and A_3AR-GFP were treated with or without 1μM (R)-PIA at 37°C for 5 minutes before termination of the reaction and receptor immunoprecipitation with 12CA5 as described in the Methods. Proteins were separated by SDS-PAGE and gels visualised by autoradiography. Shown opposite is a representative example of three experiments showing essentially identical results.

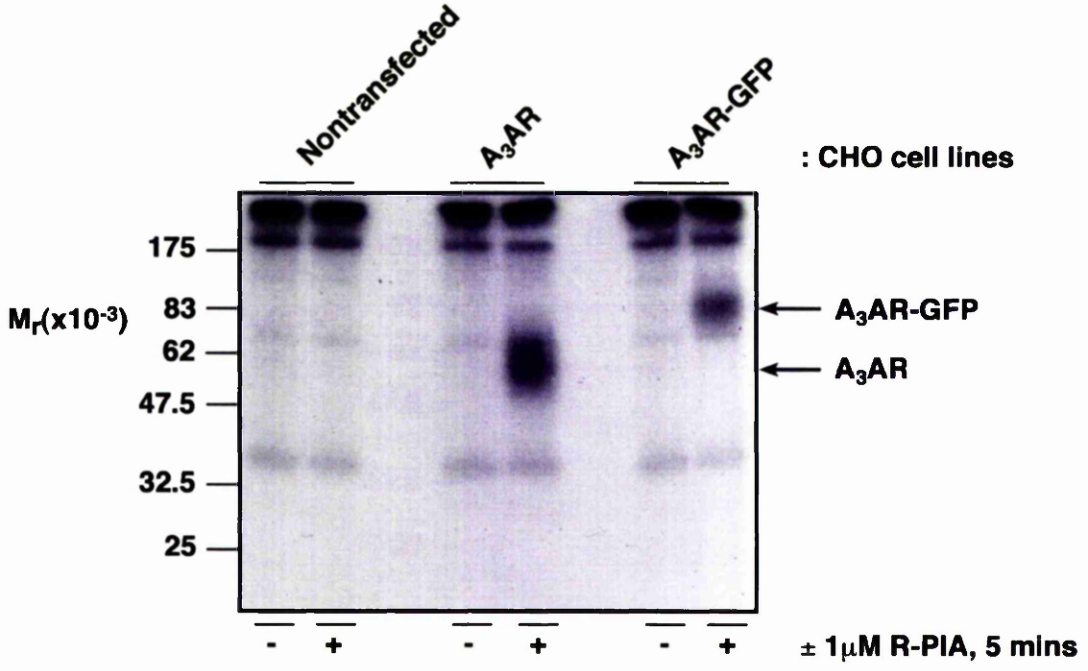
Nontransfected
A3AR
A3AR-GFP
: CHO cell lines
175
83
62
47.5
32.5
25
Mr(x10-3)
A3AR-GFP
A3AR
- + - + - +
± 1μM R-PIA, 5 mins

Figure 3.25 Time course of agonist-mediated internalisation of A_3AR-GFP

A_3AR-GFP expressing CHO cells were incubated with 1μM (R)-PIA over a 60 minute period at 37°C. Cell-surface glycoproteins were then labelled with biotin hydrazide before receptor immunoprecipitation with 12CA5 and visualisation as described in the Methods. Shown opposite is a representative example of three experiments showing essentially identical results.

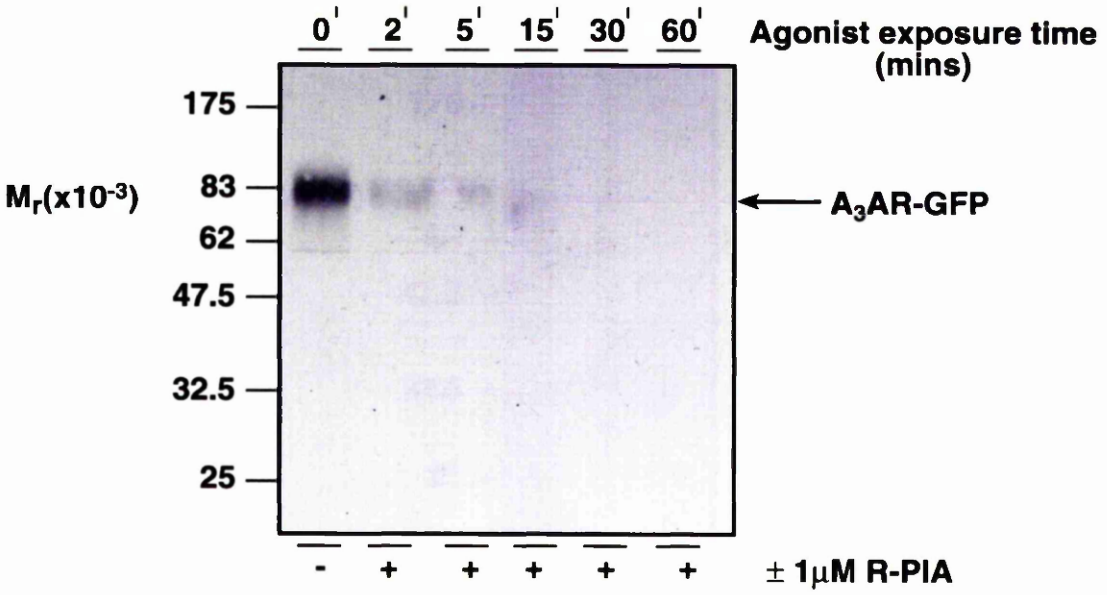
0'
2'
5'
15'
30'
60'
Agonist exposure time (mins)
175
83
62
47.5
32.5
25
Mr(x10-3)
A3AR-GFP
-
+
+
+
+
+
± 1μM R-PIA

Figure 3.26 **Real time visualisation of WT A_3AR-GFP Internalisation**

CHO cells transiently transfected with WT A_3AR-GFP cDNA were examined in live cell confocal microscopy experiments. Cells were maintained in KRHB buffer and treated with 1μM (R)-PIA over a 30 minute period. Images were recorded at 1 minute intervals. Shown opposite is a representative example of multiple experiments that gave essentially identical results.

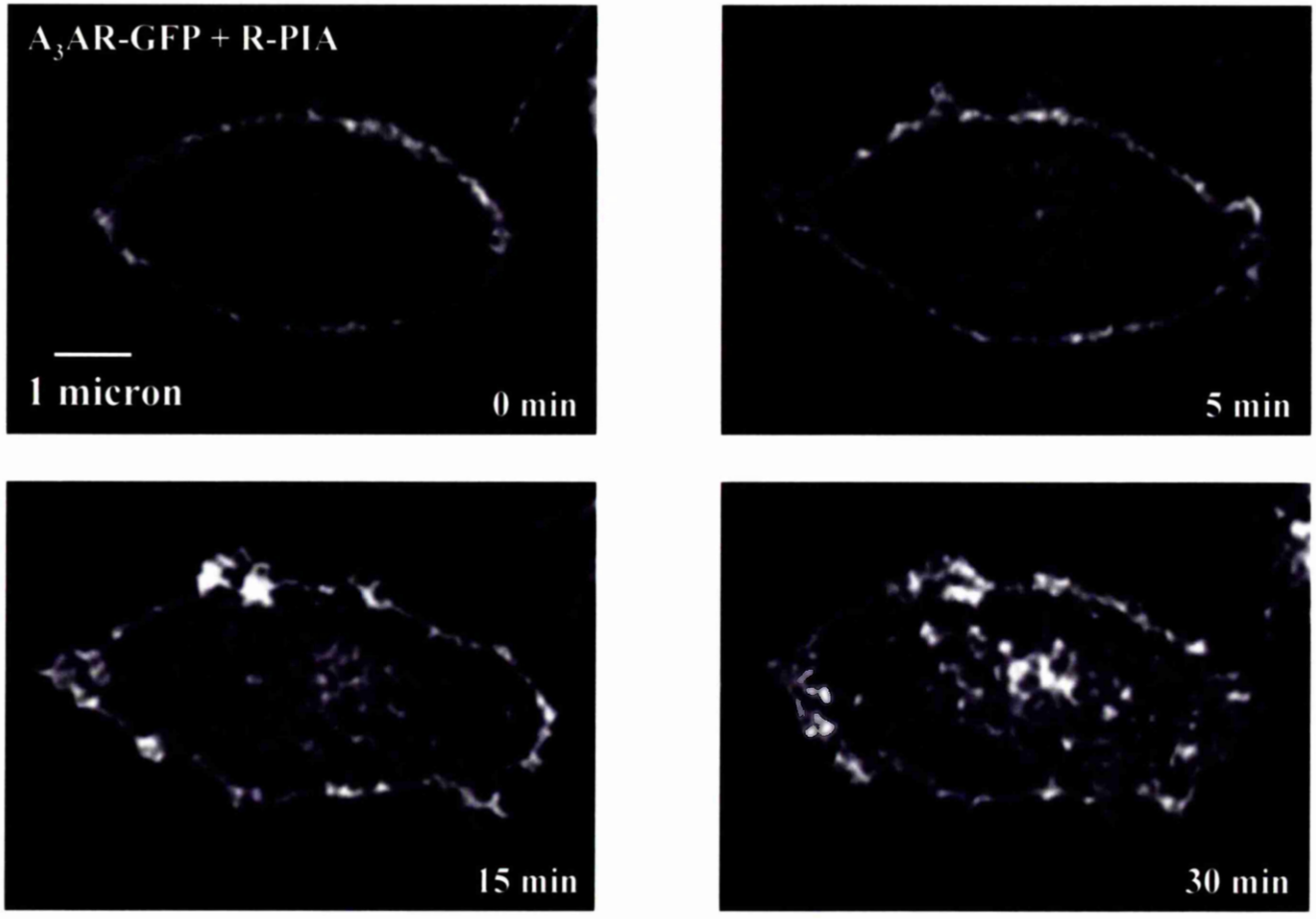
A_3AR-GFP + R-PIA
1 micron
0 min
5 min
15 min
30 min

Figure 3.27 Real time visualisation of (C-A)A_3AR-GFP internalisation

CHO cells transiently transfected with (C-A)A_3AR-GFP cDNA were examined in live cell confocal microscopy experiments. Cells were sustained in KRHB buffer and treated with 1μM (R)-PIA over a 30 minute period. Images were recorded at 1 minute intervals. Shown opposite is a representative example of three experiments showing essentially identical results.

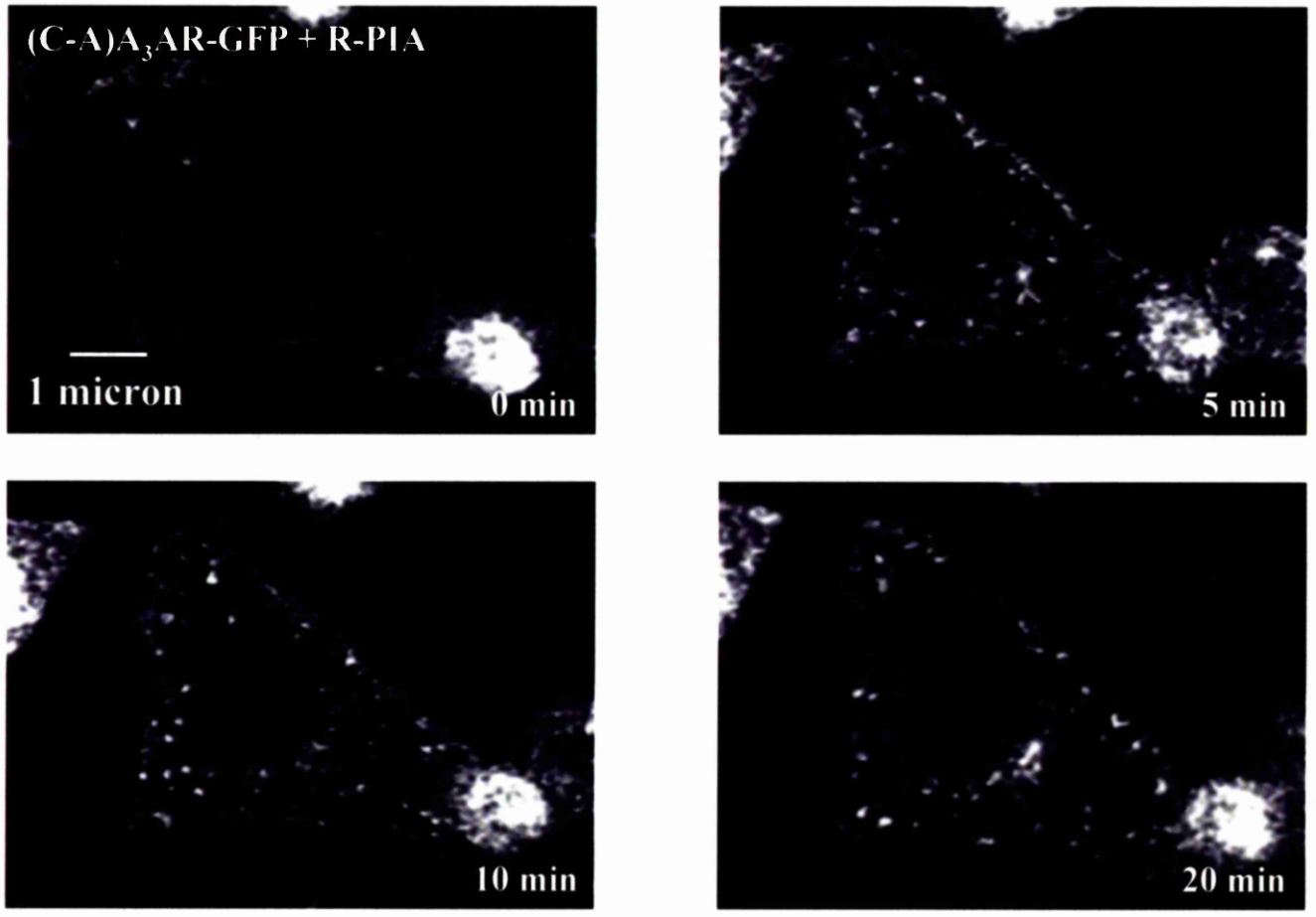
(C-A)A3AR-GFP + R-PIA
1 micron
0 min
5 min
10 min
20 min

Figure 3.28 Real time visualisation of (T-A)A_3AR-GFP internalisation

CHO cells transiently transfected with (T-A)A_3AR-GFP cDNA were examined in live cell confocal microscopy experiments. Cells were sustained in KRHB buffer and treated with 1μM (R)-PIA over a 30 minute period. Images were recorded at 1 minute intervals. Shown opposite is a representative example of three experiments showing essentially identical results.

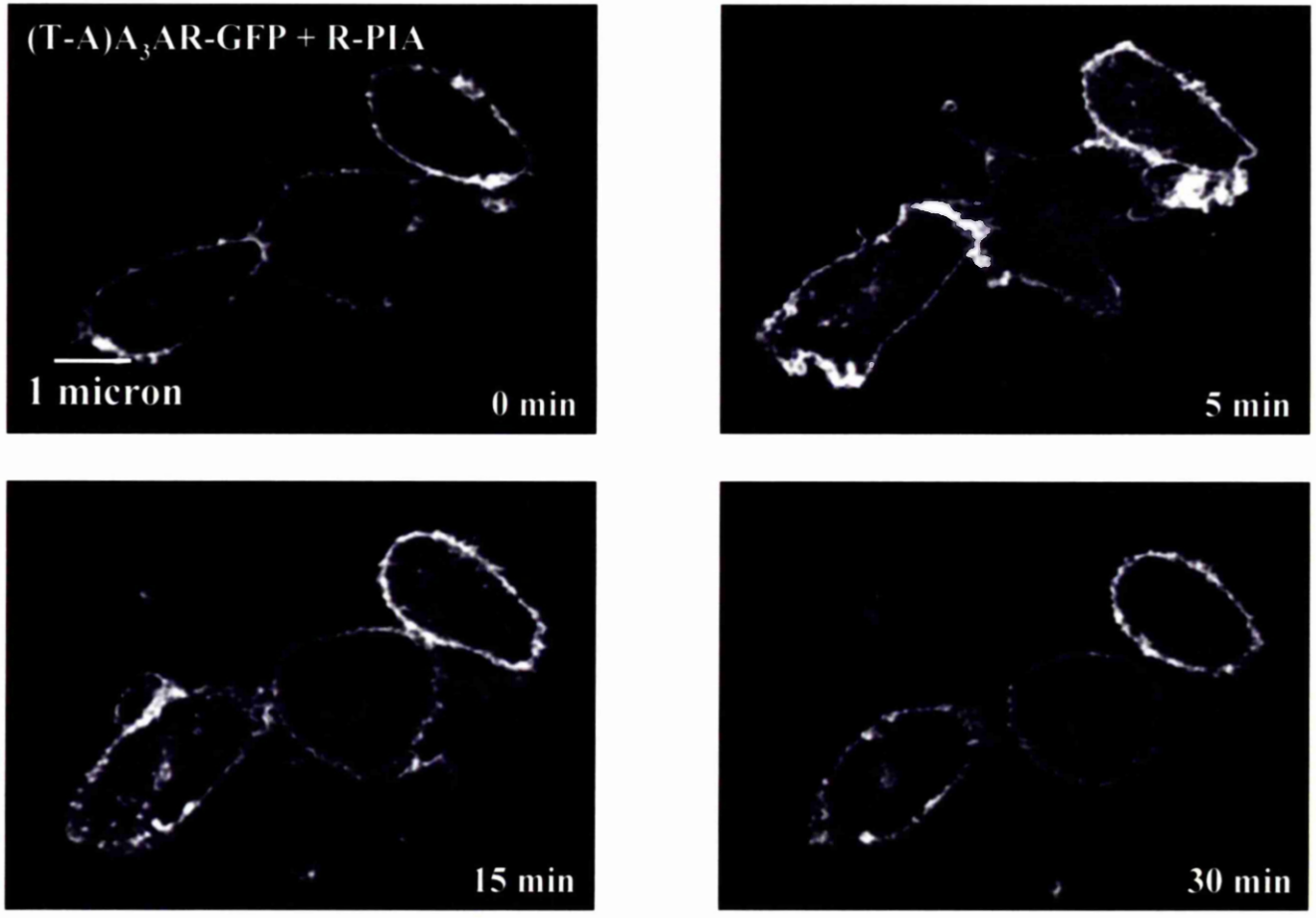
(T-A)A3AR-GFP + R-PIA
1 micron
0 min
5 min
15 min
30 min

Figure 3.29 **Real time visualisation of WT A_1AR-GFP internalisation**

CHO cells transiently transfected with WT A_1AR-GFP cDNA were examined in live cell confocal microscopy experiments. Cells were sustained in KRHB buffer and treated with 1μM (R)-PIA over a 30 minute period. Images were recorded at 1 minute intervals. Shown opposite is a representative example of three experiments showing essentially identical results.

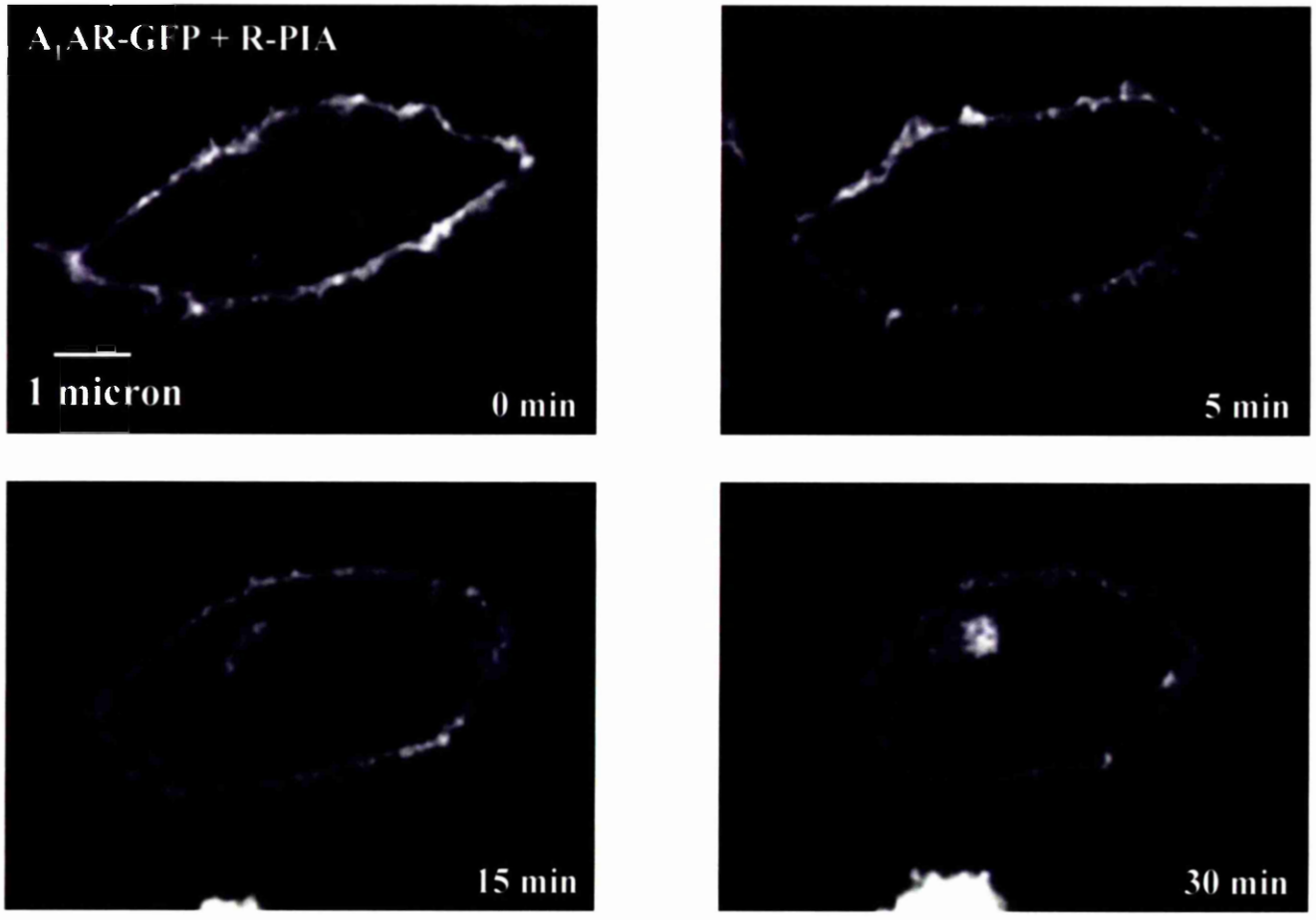
A_1AR-GFP + R-PIA
1 micron
0 min
5 min
15 min
30 min

Figure 3.30 **Real time visualisation of A_1CT3AR-GFP internalisation**

CHO cells transiently transfected with A_1CT3AR-GFP cDNA were examined in live cell confocal microscopy experiments. Cells were sustained in KRHB buffer and treated with 1μM (R)-PIA over a 30 minute period. Images were recorded at 1 minute intervals. Shown opposite is a representative example of three experiments showing essentially identical results.

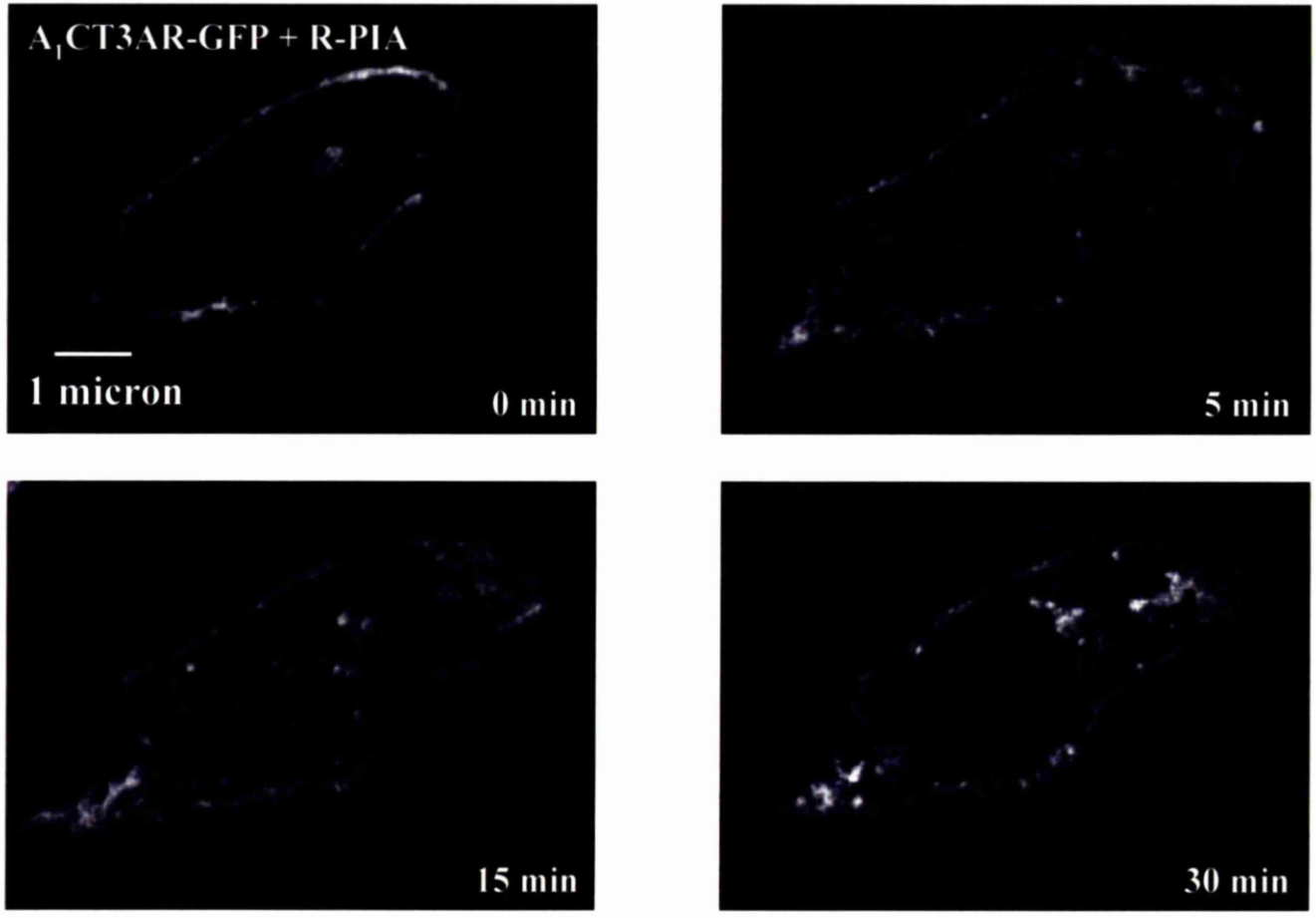
A1CT3AR-GFP + R-PIA
1 micron
0 min
5 min
15 min
30 min

3.3 Discussion

Each AR subtype has unique ligand-binding properties and distinct patterns of tissue expression. The purpose of this work was to examine the inhibitory A_3AR and to characterise its regulation. As stated previously, A_3ARs have been shown to be important in mediating the effect of adenosine in cardioprotection (Tracey et al., 1996, 1998; Liang et al., 1998 (a), (b); Dougherty et al., 1998 and Thourani et al., 1999), neuroprotection (von Lubitz et al., 1994,1999 and Dunwiddie et al., 1997) and mast cell and eosinophil activation (Ramkumar et al., 1993; Shepherd et al., 1996; Ezeamuzie et al., 1999 and Salvatore et al., 2000). If the regulation of these receptors could be characterised, it would represent a significant step towards deriving ways to manipulate AR signalling for treatment of cardiac disease, stroke and asthma.

The internalisation and regulatory properties of the β_2AdR were used as starting points for our initial experiments. Agonist occupancy of the β_2AdR leads to phosphorylation of the receptor protein by GRKs 2 & 5 and cAMP-dependent protein kinase (PKA) (Haussdorf et al., 1990, Pitcher et al., 1998). It was shown by Palmer et al. (1995c, 1996) that the A_3AR is phosphorylated by GRKs, a process occurring within seconds of agonist exposure (Ferguson et al., 2000; Fig. 3.7). Sibley and co-workers (1987) demonstrated that GRK phosphorylates only agonist-occupied or activated GPCRs. This initiates the binding of additional cytosolic factors such as arrestins (Lohse et al., 1992). Arrestins are a class of soluble proteins that function in partnership with GRKs to stop or 'arrest' intracellular signalling by disrupting receptor-G-protein interaction, and targeting cytosolic proteins required for CCV formation to the membrane, initiating receptor sequestration. From work on the β_2AdR it was proposed that receptor phosphorylation and subsequent binding of arrestin impairs interaction with the G-protein (Bouvier et al., 1988; Hausdorff et al., 1990). To determine if agonist activation was required in order for A_3AR internalisation to occur, receptors were stimulated with agonist and several activators of second messenger regulated kinases (Fig. 3.1). The data obtained supported the theory that agonist activation was required to produce a decrease in the number of cell-surface receptors. However, a loss could also be detected following treatment with forskolin. Forskolin binds directly to AC leading to an increase in cAMP levels, which is opposite to the effect shown by the A_3AR. Also, forskolin affected

receptors were shown to have an impaired mobility on SDS-PAGE not accountable to receptor phosphorylation (Palmer et al., 1995c, Fig 3.2) and induced a lower level of receptor internalisation. Therefore it could be concluded that the action of agonist and forskolin are *via* separate, distinct pathways with agonist treatment being predominant. The requirement of agonist binding and not just the presence of a ligand were supported by the treatment of A_3ARs with an A_3 specific antagonist MRS 1523. This antagonist inhibited both the loss of cell surface receptors and agonist-stimulated phosphorylation in a concentration-dependent manner (Figs. 3.4 and 3.5).

A more detailed investigation of agonist stimulation on A_3AR internalisation revealed a biphasic response to increasing agonist concentration. It appeared that low-level agonist stimulation (nM) led to a noticeable albeit not significant ($p>0.05$), increase in the number of cell-surface receptors detected. It is possible that at low nM concentrations, signalling pathways regulating membrane trafficking are initiated, mobilising intracellular pools of receptor to the PM and producing the observed increase in receptor number at the cell surface. Increasing agonist concentration leads to an increase in receptor occupancy, thereby initiating receptor internalisation and causing the subsequent reduction in cell-surface receptor number (Fig. 3.3). In support of this theory, internal pools of receptor can be observed in the confocal images at the zero time points (Figs. 3.26-3.30).

Work by Palmer and Stiles (2000) localised the GRK phosphorylation sites of the A_3AR to 3 specific threonine residues (Thr 307, 318 & 319) in the C-terminal tail. The A_1AR lacks equivalent residues and has been shown not to be a substrate for phosphorylation by GRKs (Palmer et al., 1996; Gao et al., 1999; Figs. 3.7 & 3.13). Time courses of agonist-mediated A_3 and A_1AR internalisation showed dramatic differences in the rates at which the receptors were removed from the cell surface ($t_{½}$ = 10 minutes and 90 minutes respectively; Figs 3.8 & 3.11). Further studies into the role of phosphorylation acting as a regulator of rapid inhibitory AR internalisation employed the use of a mutated receptor, (T-A)A_3AR. Mutating Thr residues 307, 318 and 319 to Ala produced a receptor that was deficient in agonist-mediated phosphorylation and showed no significant internalisation over the time course investigated compared to WT (Palmer and Stiles, 2000; Figs. 3.12 & 3.13). Either loss of native phosphorylation sites (A_1AR) or mutation of GRK phosphorylation sites in A_3AR produce receptors that fail to internalise after 60 minutes agonist

exposure. This suggests that phosphorylation is important in the process of agonist-mediated internalisation.

So why have two distinctly regulated inhibitory receptors activated by the same endogenous ligand that both amplify the same signalling pathway? Stimulation of a wide variety of GPCRs leads to activation of many tyrosine kinases and proteins activating the MAPK signalling pathway, affecting the mitogenic response (van Biesen et al., 1996; Gutkind, 1998). It has been suggested that activation of the MAPK pathway requires endocytosis of these receptors (Luttrell et al., 1997; Daaka et al., 1998). However, agonist activation of A_1ARs in DDT1MF-2 cells has been shown to produce a rapid (5 minute) clustering of the receptors on the cell surface (Ciruela et al. 1997), with a considerable delay between receptor aggregation and internalisation ($t_{½}$ = 5hrs). As maximal MAPK activation was seen within 5 minutes of agonist exposure (Dickenson et al. 1998), this demonstrated that internalisation was not required to activate downstream signalling pathways. Lefkowitz (1998) suggested that agonist-occupied receptors may organise the assembly of multi-protein signalling complexes at the PM including some or all of the components in the MAPK pathway, hence the appearance of receptor clustering (Lefkowitz, 1998). Further activation of the pathway in certain cases may require receptor internalisation which is in contrast to established paradigms for classical second messenger-activated signalling pathways such as those involving AC and PLC, pathways which do not require endocytosis and are unaffected by inhibition of CCV formation (Daaka et al., 1998). This could be of great significance in explaining why even though the A_1 and A_3ARs couple to G_i, both display distinct patterns of sequestration in response to agonist stimulation, potentially controlling subtype-specific activation of various downstream signalling cascades.

A second important regulatory region of the A_3AR C-terminal tail is the area encompassing the putative sites of palmitoylation at Cys 302 and 305. The role of palmitoylation in internalisation was first demonstrated for the Tfn receptor (Alvarez et al., 1990). Palmitoylation sites are typically found close to hydrophobic stretches of amino acids and the attached palmitate, a 16 carbon saturated fatty acid, may either be embedded in the lipid bilayer, or influence protein-protein interactions (Mumby et al., 1997). Palmitoylation sites are found in almost all GPCRs, as well as G-protein α-subunits and AC (Milligan et al., 1995). All of the AR subtypes, except the A_{2A}, have one or more consensus sites for palmitoylation (Linden et al., 1994).

One important aspect of palmitoylation, also found in the A_1AR (Cao et al., 2000) is that in the presence of agonist, turnover of palmitate can be rapidly accelerated (Wedegaertner et al., 1995; Loisel et al, 1996). Data have shown that β_2AdR receptor has a palmitoylation site at Cys 341 that regulates the accessibility of a PKA phosphorylation site at Ser 345 & 346 (O'Dowd et al., 1989; Moffet et al., 1993). Mutation of this Cys to Gly ($C^{341}G$) prevents palmitoylation and causes a reduction in the receptors ability to stimulate AC, associated with an increase in the basal phosphorylation state of the receptor. Cys residues located at similar positions to this Cys 341 have been found in most GPCRs. The occurrence of palmitoylation on these residues has been shown for the α_{2A}adrenergic (Kennedy et al., 1993), dopamine D_1 (Ng et al., 1994), 5-HT_{1A} / 5-HT_{1B} (Butkeirat et al., 1995; Ng et al., 1993) and luteinising hormone (LH) receptors (Kawate et al., 1994). The predicted palmitoylation sites in the A_3AR are located 2 aa's N-terminally from the first site of phosphorylation at Thr 307. These Cys residues at positions 302 and 305 may serve to anchor the C-terminal tail to the membrane forming a fourth intracellular loop. Mutation of these residues to non-palmitoylatable Ala ($C^{302, 305}A$) in the A_3AR was used to examine effects on receptor phosphorylation and internalisation. Prior to agonist stimulation of the (C-A)A_3AR, basal phosphorylation was observed (Palmer and Stiles, 2000; Fig. 3.14). However, equivalent phosphorylation levels were observed in the WT A_3AR and (C-A)A_3AR mutant after a 10 minute agonist treatment suggesting that a loss of predicted palmitoylation sites does not prevent agonist-mediated receptor phosphorylation. A time course of agonist-stimulated receptor internalisation revealed an increased internalisation rate ($t_{½}$ = 4-5 minutes; Fig. 3.15) for the (C-A)A_3AR compared to WT. A possible explanation is that mutation of the Cys residues could result in the loss of palmitate anchorage of the C-terminal tail to the membrane. The tail may then move more freely in the cytoplasm allowing the phosphorylation sites at Thr 307, 318 and 319 to become more accessible to GRKs allowing basal phosphorylation. As the (C-A)A_3AR mutant does not require depalmitoylation and is basally phosphorylated, the time required to bring about full agonist-mediated phosphorylation is reduced and the receptor undergoes an increased rate of internalisation. These data strongly suggest that Cys residues 302 and 305 play an important role in A_3AR phosphorylation and internalisation by controlling the accessibility of activated GRKs to the C-terminal regulatory domain. However, work by Eason et al. (1994) has shown that palmitoylated cysteine

residues do not have a universal role as deletion of the Cys in the α_{2A}AR had no effect on desensitisation. This could be associated with the fact that the phosphorylation sites of the α_{2A}AR are present in the third intracellular loop and not in the C-terminal tail. Therefore, any disruption to the C-terminal domain proximal to these phosphorylation sites will exert no effect on receptor activation and subsequent desensitisation. Nevertheless, in the case of the A_3AR, it appears that the absence of the predicted palmitoylated Cys residues may allow exposure of the C-terminal tail, influencing its interaction with various regulatory proteins. Previous studies on the β_2AdR suggested that before resensitisation and recycling to the plasma membrane could take place, the sequestered receptors must be dephosphorylated (Yu et al., 1993; Pitcher et al., 1995). The (C-A)A_3AR appears to contradict this model as it showed a basal level of phosphorylation with its internalisation and recycling upon agonist removal increased compared to WT A_3AR, suggesting that in the case of this AR, complete dephosphorylation is not a requirement to bring about receptor resensitisation.

Having shown that the mechanism of termination of A_3AR signalling is by phosphorylation on Thr residues present in its C-terminal tail by GRKs, the possibility that this regulation could be transferred to the non-phosphorylated A_1AR was investigated. In recent years, the use of chimeric receptors has become a predominant tool with which to study the role of the C-terminal region of GPCRs. Whistler et al. (1999), constructed a chimeric receptor comprising the body of the μ opioid receptor fused to the tail of the δ opioid receptor. Analysis showed that this mutation enhanced the endocytosis of the μ receptor and uncoupling from G-proteins, but had no effect on the receptors function compared to WT (Afify et al. 1998). Similarly, exchange of the ET_A and ET_B receptor tails (Abe et al.; 2000) resulted in re-localisation of the receptors. The ET_A receptor C-terminal tail contains a sequence that anchors the receptor to the plasma membrane. Mutation of the tail to that of the ET_B receptor promoted sorting of the chimera to lysosomes resulting in proteolytic degradation. The reciprocal is true for the ET_B-ET_A tail chimera. In the same way, using a chimeric receptor constructed by Palmer et al. (1996), A_3AR internalisation kinetics were conferred onto a predominantly A_1AR. Comprising of the main body of the A_1AR fused to the C-terminal region of the A_3AR, A_1CT3 (Fig. 3.17) was shown to be pharmacologically similar to the A_1AR (Palmer et al., 1996).

However, unlike the A_1AR, the chimera was phosphorylated and internalised similar to the A_3AR ($t_{½}$ = 1 & 15 minutes respectively, Figs. 3.18 & 3.19). Thus the GRK phosphorylated C-terminal domain of the A_3AR is able to confer the property of rapid agonist-induced internalisation on a predominantly A_1AR-containing chimeric AR.

GFP, discovered by Shimomura and Johnson (1969), has been used extensively to enable visualisation of GPCRs and other proteins within individual cells (Tsien, 1998). It has been targeted successfully to almost every major cell organelle including the plasma membrane (Barak et al., 1997a), nucleus (Chatterjee and Stochaj, 1996), endoplasmic reticulum (ER), Golgi apparatus (Presley et al., 1997) and mitochondria (Yano et al., 1997). GFP has commonly and most successfully been applied as a fusion to the protein of interest. The gene encoding GFP is fused in-frame with the gene encoding the protein under investigation and the resulting chimera expressed in the system of interest. Ideally, the activity and localisation of the protein would be unaffected by the GFP tag. With the C-terminal tail of GPCRs being shown to be important in receptor regulation, it could be expected that the addition of a 27kDa molecule to the end of this tail would disrupt regulation. It had been shown previously that the addition of a GFP tag had no adverse effects on the pharmacological or signal transduction properties of receptors such as cholecystokinin A (Tarasova et al., 1997), β_2AdR (Barak et al., 1997a; Kallal et al., 1998; McLean et al., 1999) and the thyrotropin releasing hormone (TRH) receptor (Drmota et al., 1998). As discussed in this chapter, immunoblotting, phosphorylation and radioligand binding studies investigated any consequence of GFP-tagging the WT and mutant ARs. Biotin labelling experiments confirmed the presence of GFP-tagged receptors at the cell surface compared to WT A_3ARs verifying that the GFP tag was not interfering with receptor assembly or targeting to the membrane (Fig. 3.22). Radioligand binding using ^{125}I-AB-MECA demonstrated the ability of the GFP-tagged receptor to bind agonist (Fig. 3.23) resulting in receptor phosphorylation (Fig. 3.24) and subsequent internalisation (Fig. 3.25) as was seen for WT A_3AR. These data suggested that the AR-GFP construct could be used in live cell systems to visualise receptor trafficking following agonist stimulation, as it appeared to be functionally indistinguishable from WT receptors.

In unstimulated cells, A_3AR-GFP was found predominantly at the cell surface with a small amount of receptor present intracellularly. Upon agonist stimulation,

WT A_3, chimeric A_1CT3 and mutant (C-A)A_3ARs all containing phosphorylatable residues in the C-terminal tail, were seen to redistribute to intracellular pools (Figs. 3.26, 3.27 & 3.30). Membrane localised fluorescence of the WT A_1 and mutant (T-A)A_3ARs were not seen to alter over the time-courses investigated (Fig. 3.28 & 3.29). A noticeable consequence of agonist stimulation was the structural changes in cell shape over time. Dependent upon receptor type, these changes were either sustained to the end of the experiment (WT A_3 & A_1CT3AR-GFP) or transient, with small shape changes being observed within the first 10 minutes and the cells returning to the unstimulated morphology within the time-course investigated (WT A_1 & (T-A)A_3AR-GFP). The actin cytoskeleton is a dynamic structure responding to multiple extracellular stimuli contributing to cell-cell and cell-substrate interactions by providing a structural framework and modulating signal transduction cascades (Yin & Stull, 1999). Low molecular weight G-proteins of the Rho subfamily (Rho GTPases comprising of Rho, Rac and Cdc42) are responsible for the organisation of the actin cytoskeleton (Tapon and Hall, 1997; Van Aelst and D'Souza-Schorey, 1997). Functioning of Rho has also been implicated in regulation of endocytosis, exocytosis and glucose transport (Sah et al., 2000). The phenomenon of endocytosis can be broken down into distinct steps, from membrane invagination, to removal of the new endocytic compartment from the plasma membrane to the cytosol (Qualmann et al., 2000), with each step possibly involving the actin cytoskeleton. It is possible that alterations in membrane lipids may trigger the recruitment of components required to initiate vesicle budding e.g. clathrin and dynamin, to the plasma membrane where they are organised or anchored by cytoskeletal components in preparation for internalisation (Lamaze et al., 1996). Actin may also be required to drive the detached endocytic vesicles through the cytoplasm to their final destination (Frischknecht et al., 1999; Merrifield et al., 1999 and Rozelle et al., 2000).

As agonist stimulation of A_3AR expressing cells results in changes in cell shape, further studies are required to determine any involvement of the actin cytoskeleton and small G-proteins in this process. It would also be of interest to determine which internalisation pathway is used by the A_3AR upon its stimulation and the down-stream signalling pathways it activates.

Chapter 4

Characterisation of A_3AR Internalisation *via* an Endosomal Pathway

4.1 Introduction

Having shown the A_3AR to be phosphorylated by GRK and internalised in response to agonist, it was of importance to determine which endocytic pathway the receptor used. Receptor endocytosis has been best characterised for receptors such as low-density lipoprotein (LDL) and Tfn, receptors that cycle continuously between the cell surface and endosomes *via* the CCV pathway (Koenig and Edwardson, 1997). In contrast to this 'conveyor belt' mode of operation, GPCRs reside predominantly at the plasma membrane and are endocytosed in response to agonist stimulation. The most well defined model for GPCR sequestration has been documented for receptors such as the β_2AdR and M_1 muscarinic receptor, where upon agonist stimulation, the receptor becomes phosphorylated and leads to the attraction of arrestin molecules to the cell surface. Arrestins have a two-fold role in that they uncouple the receptor from the G-protein leading to an inhibition of signal and target phosphorylated receptors for endocytosis *via* CCVs. The binding of arrestin also serves to activate clathrin associated protein components such as amphiphysin and dynamin that are involved in the pinching off of the vesicles from the plasma membrane.

4.2 Results

To determine if the internalisation pathway utilised by the A_3AR involved CCVs, we examined the interaction of GFP-tagged VSV-TRHR and A_3AR with Alexa-labelled Tfn (red). TRHR has been shown to internalise *via* a clathrin-mediated pathway therefore this receptor was used as a control for comparison of subsequent data. HEK293 cells were plated onto coverslips and transiently transfected with either VSV-TRH-GFP or WT A_3AR-GFP as described in the Methods. Prior to agonist stimulation, cells were treated with Alexa-tagged Tfn (5units/ml) for 30 minutes. Cell monolayers were then washed once to remove any unbound Alexa-Tfn and internalisation initiated by the addition of 10μM TRH or 1μM (R)-PIA over a 30 minute time-course. Cells were then fixed and visualised by confocal microscopy as described in the Methods. With no agonist treatment, images obtained for the control VSV-TRH-GFP revealed this receptor to be present predominately at the cell surface (green) with the Alexa-Tfn (red) visible in distinct punctate spots throughout the cell (Fig. 4.1). Agonist stimulation caused internalisation of VSV-TRH-GFP resulting in overlapping of the internal vesicles with Alexa-Tfn producing a distinct yellow staining (Fig. 4.1, merge 30 minutes). Similar distributions were observed for WT A_3AR-GFP and Alexa-Tfn before (Fig. 4.2, 0 minutes) and after (Fig. 4.2, 15minutes) agonist stimulation. This overlapping or co-localisation (yellow) of the GFP-tagged receptors with Alexa-Tfn suggested that A_3AR-GFP is internalising *via* an endosomal pathway similar to that used by TRHR and TfnR. Co-expression of the inhibitory A_1AR-GFP with Tfn failed to promote colocalisation following agonist stimulation (Fig. 4.3)

Having previously shown the C-terminal tail to be important in the regulation of receptor internalisation, one hypothesis is that alterations to this regulatory region could lead to a variation or complete deviation in the internalisation pathway being used. To determine this, the mutants (C-A)A_3AR-GFP and A_1CT3AR-GFP were transiently transfected into HEK 293 cells and treated with Alexa-Tfn prior to agonist stimulation as previously described. The confocal images obtained revealed that both (C-A)A_3AR-GFP (Fig. 4.4) and A_1CT3AR-GFP (Fig. 4.5) co-localised (yellow) with the Alexa-Tfn (red) an interaction which persisted for the duration of the time-course investigated. In both receptors, even though the C-terminal domain has been altered in some way, the receptor continues to internalise similar to WT

A_3AR-GFP. These data show that mutation of the regulatory region of the A_3AR does not inhibit agonist-mediated internalisation *via* an endosomal pathway.

Having determined that A_3AR internalisation follows an endosomal pathway possibly involving CCVs, a more detailed study of the mechanisms of this pathway was explored. Internalisation mediated *via* CCVs has been described in great detail for receptors such as the β_2Ad and TRH. Fig 4.6 shows a schematic representation of this. Upon agonist stimulation, GPCRs interact with their G-proteins to initiate signalling through α and $\beta\gamma$ subunits. This signalling is primarily 'turned off' by phosphorylation on Ser / Thr residues by GRKs. A chain of events is then initiated, beginning with the activation of arrestin molecules which uncouple the receptor from the G-protein and lead to the mobilisation of clathrin and other cytosolic factors involved in receptor internalisation. The C-terminal tail of non-visual arrestins interacts with clathrin through its N-terminal region leading to translocation of clathrin to the membrane. Clathrin triskelions interact to form a pit at the plasma membrane into which the receptor internalises. Clathrin simultaneously interacts with amphiphysin, recruiting dynamin to the collar of the clathrin vesicles through its SH3 domain. Dynamin, a GTPase, then hydrolyses GTP to GDP causing the clathrin to be displaced from the complex and the vesicle is pinched off from the membrane. Internalised receptor can then either be targeted for degradation or dephosphorylated and returned to the membrane for another round of agonist activation.

The role of arrestins in these events has been characterised for a number of receptors. Four isoforms of arrestin have been detailed: visual arrestin (arrestin1), β-arrestin1 (arrestin2), β-arrestin2 (arrestin3) and cone arrestin (arrestin4). Arrestins 1 and 4 are localised in the eye and are involved in the regulation of rhodopsin following light activation. Arrestins 2 and 3 are expressed ubiquitously therefore their role in clathrin-mediated endocytosis has been studied extensively. To establish if AR internalisation was mediated by arrestin activation, GFP-tagged forms of arrestin2 and arrestin3 (Groarke et al. 1999) were transiently co-expressed in HEK 293 cells on coverslips with VSV-TRHR or HA-tagged WT or mutant A_3ARs. Cells were agonist treated over a 30 minute time course, fixed and permeabilised as described in the Methods. TRHR and A_3ARs were visualised by treatment with anti-VSV or 12CA5 antibody respectively followed by secondary antibody incubation with Alexa-tagged anti-mouse antibody (red).

Confocal analysis of VSV-TRHR with arr2-GFP or arr3-GFP showed VSV-TRHR (red) to be present predominately on the cell membrane with the arrestin (green) diffusely in the cytoplasm (Figs. 4.7 and 4.8). No co-localisation of receptor was observed with either arrestin isoform prior to agonist treatment (Figs. 4.7 and 4.8, 0 minutes). Upon agonist exposure (10μM TRH) the VSV-TRHR was seen to internalise to distinct spots within the cytoplasm. Over the time course, yellow spots were observed within cells expressing both the receptor (red) and either form of arrestin (green), indicating co-localisation of the two proteins (Figs. 4.7 and 4.8, 30 minutes). This co-localisation persisted over the 30 minute time course investigated, providing data consistent with previous studies showing interactions of TRHR with both arrestin2 and arrestin3.

HEK 293 cells co-transfected with WT HA-A_3AR and arr2-GFP revealed expression of WT A_3AR at the membrane with arr2-GFP located in the cytoplasm (Fig. 4.9, 0 minutes). 1μM (R)-PIA exposure induced receptor internalisation but no co-localisation (yellow) of HA-tagged receptor (red) with arr2-GFP (green) was apparent over the 30 minute time course investigated (Fig. 4.9, 30 minutes). Co-expression of WT HA-A_3AR with arr3-GFP showed receptor and arrestin expression as seen previously (Fig. 4.10) at 0 minutes. However, a transient co-localisation of HA-A_3AR and arr3-GFP was observed between 10 and 15 minutes following agonist treatment (Fig. 4.10, 10 minutes). This was not however, a consistent interaction as confocal images obtained at a later date were not seen to exhibit this phenomenon (Fig. 4.11), although arr3-GFP was seen to cluster into distinct spots within the cytoplasm.

The effect of mutating the A_3ARs predicted palmitoylation sites on the interaction with arrestin was investigated using the HA-(C-A)A_3AR mutant. HA-(C-A)A_3AR co-expressed with arr2-GFP was observed on the membrane with arr2-GFP located in the cytoplasm (Fig. 4.12, 0 minutes). 1μM (R)-PIA stimulation led to a rapid internalisation of the mutant AR but no co-localisation (yellow) was observed between the HA-(C-A)A_3AR (red) and arr2-GFP (green) over the time course investigated (Fig. 4.12, 4 minutes). HEK293 cells co-transfected with (C-A)A_3AR and arr3-GFP were seen to express receptor and arrestin as described previously (Fig. 4.13, 0 minutes). Agonist stimulation promoted rapid receptor internalisation and, as seen with WT A_3 and arr3-GFP, a transient co-localisation

(yellow) of (C-A)A_3AR and arr3-GFP was observed between 4 and 6 minutes. Again this was not seen to be a consistent interaction as later confocal experiments failed to produce similar results (Fig. 4.14).

With little evidence of arr2-GFP interacting with either WT A_3AR or (C-A)A_3AR it was decided to turn our attentions to arr3-GFP which appeared to be having some, if only a transient interaction with the ARs investigated so far. Having shown that exchange of the A_1AR C-terminal tail for that of the A_3AR (A_1CT3AR) promoted receptor internalisation *via* an endosomal pathway (Figs. 4.3 and 4.5), we investigated the possible role of arr3 in the internalisation of this mutant. HEK 293 cells were transiently transfected with A_1CT3AR and arr3-GFP as previously described and subjected to confocal microscopy. As was observed with the other receptors, A_1CT3AR was expressed on the membrane, arr3-GFP expressed in the cytoplasm and no co-localisation was detected at 0 minutes prior to agonist treatment (Fig. 4.15). Agonist stimulation promoted receptor internalisation but no co-localisation (yellow) of the two proteins, receptor and arrestin, was detected over the time course investigated (Fig. 4.15, 15 minutes). However, the images obtained did show the arr3-GFP clustering into spots within the cytoplasm but staying distinct from those vesicles occupied by the internalised receptor (Fig. 4.15).

With the data obtained thus far being inconclusive as to the requirement of arrestin and clathrin vesicles in AR endocytosis, we decided to investigate the effects of mutating various co-factors involved at different stages of clathrin-mediated endocytosis. It has been shown for a number of receptor types that their internalisation *via* clathrin can be inhibited or enhanced by over-expression of dominant-negative or truncated versions of proteins required for clathrin-mediated endocytosis. In this study, using three modified proteins, their effects on AR endocytosis were investigated (Fig. 4.16). The A_3AR is known to be phosphorylated by GRKs on its C-terminal tail following agonist stimulation, leading to receptor internalisation. To try to inhibit this phosphorylation, a truncated mutant of GRK2 was transfected into CHO cells stably expressing HA-tagged WT A_3AR. The mutant, βARK-CT (GRK2[BK-CT]), comprising the C-terminal tail of GRK2 interacts with free βγ subunits released following agonist binding to receptor, resulting in a decrease in receptor phosphorylation. To establish the concentration of GRK2[BK-CT] required to produce an effect in our system, WT bovine GRK2 and GRK2[BK-CT] were transiently transfected into plain CHO cells at increasing

concentrations and solubilised cell extracts transferred to nitrocellulose as described in the Methods. Nitrocellulose membranes were probed with the GRK2-specific monoclonal antibody 3A10 and then with HRP conjugated anti-mouse secondary antibody. WT GRK2 displayed an increase in band intensity with increasing concentration of transfected protein (Fig. 4.17a). However the mutant GRK2[BK-CT] appeared to reach a peak of intensity at 0.5μg and then diminish (Fig. 4.17b).

To assess the effect of this GRK2 mutant on agonist-mediated A_3AR phosphorylation, a concentration response to GRK2[BK-CT] was carried out. CHO cells expressing WT A_3AR were transiently transfected with increasing concentrations of GRK2[BK-CT] ranging from 0 to 0.5μg, labelled with ^{32}P-orthophosphate and stimulated with or without 10μM (R)-PIA for 30 minutes. Receptors were immunoprecipitated with 12CA5 as previously described and fractionation of the proteins carried out using SDS-PAGE. Phosphorylated A_3ARs were visualised by autoradiography. Resulting data showed a decrease in the level of receptor phosphorylation in the presence of increasing GRK2[BK-CT] concentration (Fig. 4.18). The effect of 0.5μg of GRK2[BK-CT] was found to be significantly different from the effect produced with cells expressing vector alone ($p<0.05$). To visualise this, CHO cells stably expressing A_3AR-GFP were transfected with 0.5μg/μl GRK2[BK-CT] and stimulated with 1μM (R)-PIA over a 30 minute time period. Cells were fixed and solubilised as described in the Methods. The presence of GRK2[BK-CT] was detected with 3A10 primary antibody followed by Alexa-tagged anti-mouse secondary antibody (red). From the phosphorylation data obtained previously, it was hoped that internalisation of the A_3AR-GFP construct would be inhibited in the presence of the mutant GRK2 molecule. Fig. 4.19 shows that in the presence of 0.5μg/μl GRK2[BK-CT] (red), a concentration sufficient to inhibit receptor phosphorylation, A_3AR-GFP (green) underwent internalisation in a manner similar to that seen in cells not expressing the mutant GRK2.

Further characterisation of the internalisation pathway utilised by the A_3AR employed a mutated form of arrestin. Consisting of the last 99 aa's of the arrestin2 molecule, arr2[319-418] has been shown to inhibit the clathrin-mediated endocytosis of many receptor types. As only the C-terminal region of arr2 is expressed, the arrestin mutant interacts only with clathrin *via* its N-terminal domain and not with the receptor (Fig. 4.16), therefore inhibiting the interaction of clathrin with

stimulated receptor and disrupting clathrin-mediated endocytosis. CHO cells were transiently transfected with increasing concentrations of arr2[319-418] (0-2μg/well) and solubilised cell extracts transferred to nitrocellulose as described in the Methods. Nitrocellulose membranes were probed with the arrestin-specific monoclonal antibody β-arrestin1 and then with HRP conjugated anti-mouse secondary antibody. From the blots obtained, (Fig. 4.20), a concentration of 0.5μg was used in subsequent experiments.

To investigate the effect of this mutant in the A_3AR system, CHO cells stably expressing A_3AR-GFP were tranfected with 0.5μg/well of arr2[319-418] which was detected by incubation with anti-arrestin primary antibody followed by Alexa-tagged anti mouse secondary antibody (red). Confocal microscopy revealed that prior to agonist treatment (Fig. 4.21, 0 minutes) A_3AR-GFP was expressed at the membrane (green) and the truncated arrestin molecule (red) was located in the cytoplasm as seen for WT arrestin expression (Fig. 4.7). arr2[319-418] was not seen to inhibit agonist-mediated internalisation over the time course investigated (Fig. 4.21). This effect was also observed with VSV-TRHR-GFP (Fig. 4.22) and (C-A)A_3AR-GFP (Fig. 4.23).

In the case of clathrin-mediated endocytosis, if vesicles cannot be released from the membrane the receptor is unable to internalise and be targeted for recycling or down-regulation. Separation of clathrin vesicles from the membrane can be inhibited by expression of a dynamin mutant, Dyn[K44E], known to be defective in GTP hydrolysis. CHO cells transiently transfected with myc-epitope tagged Dyn[K44E] at increasing concentrations were subjected to immunoblotting analysis as described in the Methods. From the blots obtained (Fig. 4.24), a concentration of 0.5μg/well was transfected into CHO cells expressing A_3AR-GFP and visualised confocally by staining the permeabilised cells with anti-myc 9E10 primary antibody and Alexa-tagged anti mouse secondary antibody (red). Confocal imaging revealed A_3AR-GFP localisation to the membrane and myc-Dyn/Dyn[K44E] in the cytoplasm prior to agonist treatment (Fig. 4.25 and 4.26, 0 minutes). Agonist stimulation over 30 minutes promoted receptor internalisation that was not seen to be inhibited by the presence of the mutant myc-Dyn[K44E] (Fig. 4.25 and 4.26). These data collected so far suggested either that the concentrations of mutants being used were

insufficient to inhibit clathrin-mediated endocytosis in the A_3AR system or that the A_3AR was internalising *via* a clathrin-independent pathway.

One other procedure known to disrupt clathrin is the treatment of cells with a sucrose solution. Sucrose has been shown to inhibit the formation of CCVs by disrupting the interaction of the clathrin triskelions therefore inhibiting clathrin-mediated endocytosis. To investigate the effects of this, plain HEK 293 cells labelled with Alexa-tagged Tfn were subject to treatment in the absence or presence of 0.4M sucrose. In the absence of sucrose, Alexa-Tfn was seen to internalise and recycle normally (Fig. 4.27a). However, when cells were treated with Alexa-Tfn and sucrose simultaneously for 30 minutes (Fig. 4.27b), the Alexa-Tfn was seen to cluster at the membrane with very little staining observed internally, suggesting that sucrose was inhibiting the clathrin-mediated pathway of internalisation for the TfnR. The effect of sucrose on A_3AR-GFP internalisation in stably transfected CHO cells was investigated in the same way. In the absence or presence of sucrose (Fig. 4.28a and 4.28b) prior to agonist treatment, A_3AR-GFP was expressed predominately at the membrane. Upon agonist stimulation, A_3AR-GFP was seen to internalise as had been observed previously (Fig. 4.28c) over a 30 minute time period. In the presence of 0.4M sucrose, agonist-mediated internalisation of A_3AR-GFP was inhibited and A_3AR-GFP remained at the membrane (Fig. 4.28d). These data suggest that internalisation of A_3AR-GFP is *via* a clathrin-mediated pathway which can be inhibited by disrupting the formation of clathrin vesicles. It must be noted however that 0.4M sucrose is a very severe treatment to use to inhibit internalisation and it therefore may not be as specific as hoped in interrupting only the clathrin pathway.

Many other mechanisms of internalisation have been documented which do not require the use of clathrin vesicles. One such pathway involves vesicles composed of lipids, proteins and chiefly caveolin, a 21-24kDa integral membrane protein. Caveolae are small vesicles 50-100nm in size that can be defined by their unique morphology as viewed by electron microscopy (Parton, 1996 and Schlegel et al., 1998). Caveolae are abundant in cell types such as endothelial cells, adipocytes, cardiac smooth and striated myocytes and have so far been shown to be involved in vesicular transport (Severs, 1988), potocytosis (Anderson, 1993) and signal transduction (Okamoto et al., 1998 and Engelmann et al., 1998). To determine if the A_3AR required association with caveolae to undergo internalisation, CHO cells stably expressing A_3AR-GFP were plated onto coverslips and treated with or without

1μM (R)-PIA over a 30 minute time period. Cells were then fixed, permeabilised as described in the Methods and stained with anti-caveolin primary antibody followed by Alexa-tagged anti mouse secondary antibody (red). Confocal microscopy revealed that prior to agonist stimulation, A_3AR-GFP (green) and caveolin (red) were both localised at the membrane (Fig. 4.29, 0 minutes) with very little co-localisation (yellow). Agonist treatment led to internalisation of A_3AR-GFP but the caveolin staining did not progress from the membrane suggesting that the endocytic mechanism employing caveolae was not involved in A_3AR internalisation.

Figure 4.1 **Co-localisation of internalised VSV-TRHR-GFP with Alexa-labelled Transferrin (Tfn)**

HEK 293 cells transiently expressing VSV-TRHR-GFP were treated with Alexa-Tfn for 30 minutes prior to stimulation with 10μM TRH over a 30 minute time period. TRH induced translocation of VSV-TRHR-GFP (green) from the membrane to distinct, punctate vesicles within the cytoplasm. These vesicles can be seen to overlap with internalised Alexa-Tfn (red) to give a distinct yellow staining when the red and green images are merged (merge, 30 minutes). The images shown opposite are representatives of multiple experiments showing similar results.

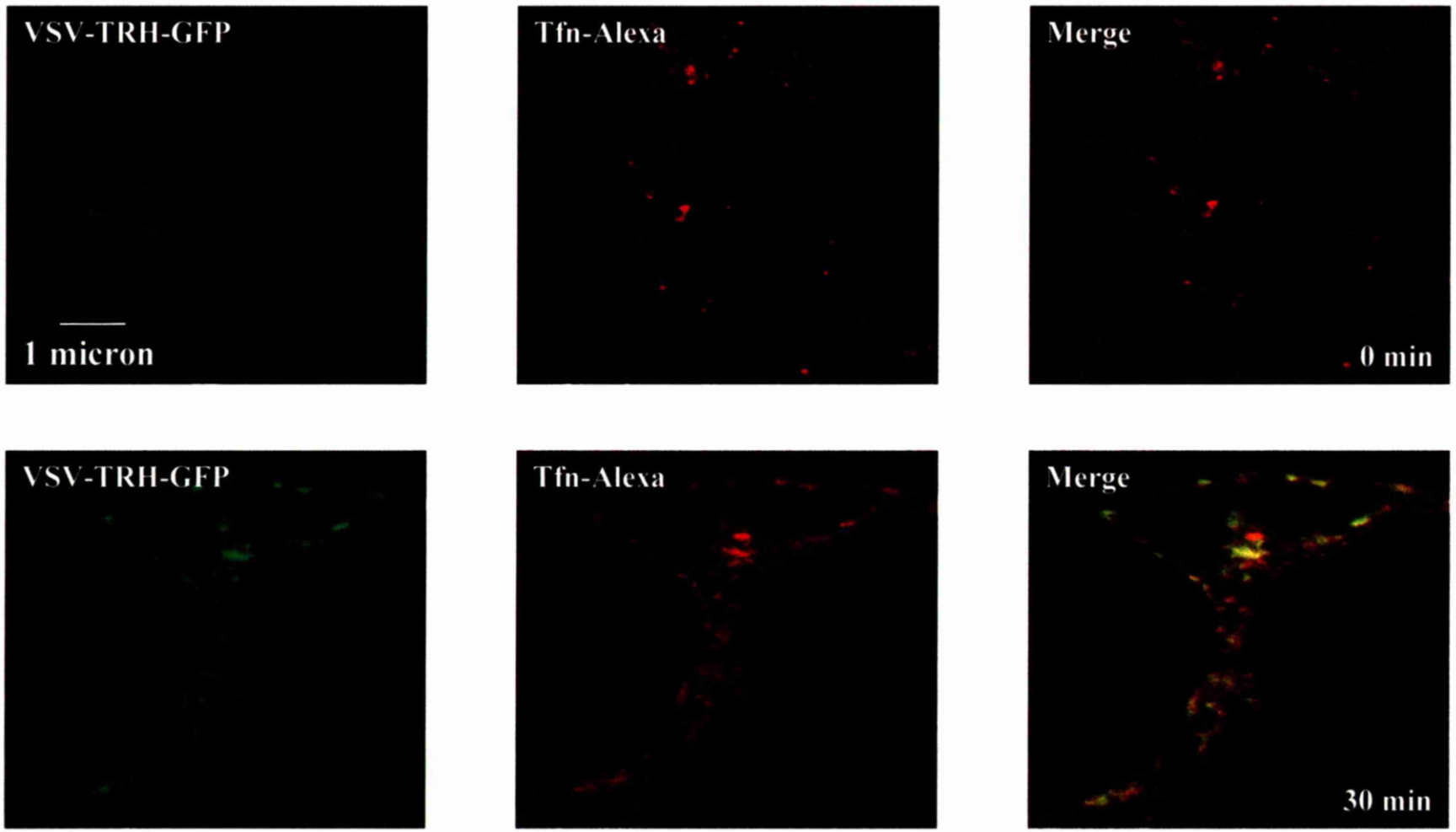
VSV-TRH-GFP
1 micron
Tfn-Alexa
Merge
0 min
VSV-TRH-GFP
Tfn-Alexa
Merge
30 min

Figure 4.2 **Co-localisation of internalised A_3AR-GFP with Alexa-labelled Transferrin (Tfn)**

HEK 293 cells transiently expressing A_3AR-GFP were treated with Alexa-Tfn for 30 minutes prior to stimulation with 1μM (R)-PIA over a 30 minute time period. Agonist induced translocation of A_3AR-GFP (green) from the membrane to distinct vesicles within the cytoplasm. These vesicles can be seen to overlap with internalised Alexa-Tfn (red) to give a distinct yellow staining upon merging of the red and green images (merge, 15 minutes). The images shown opposite are representatives of multiple experiments showing similar results.

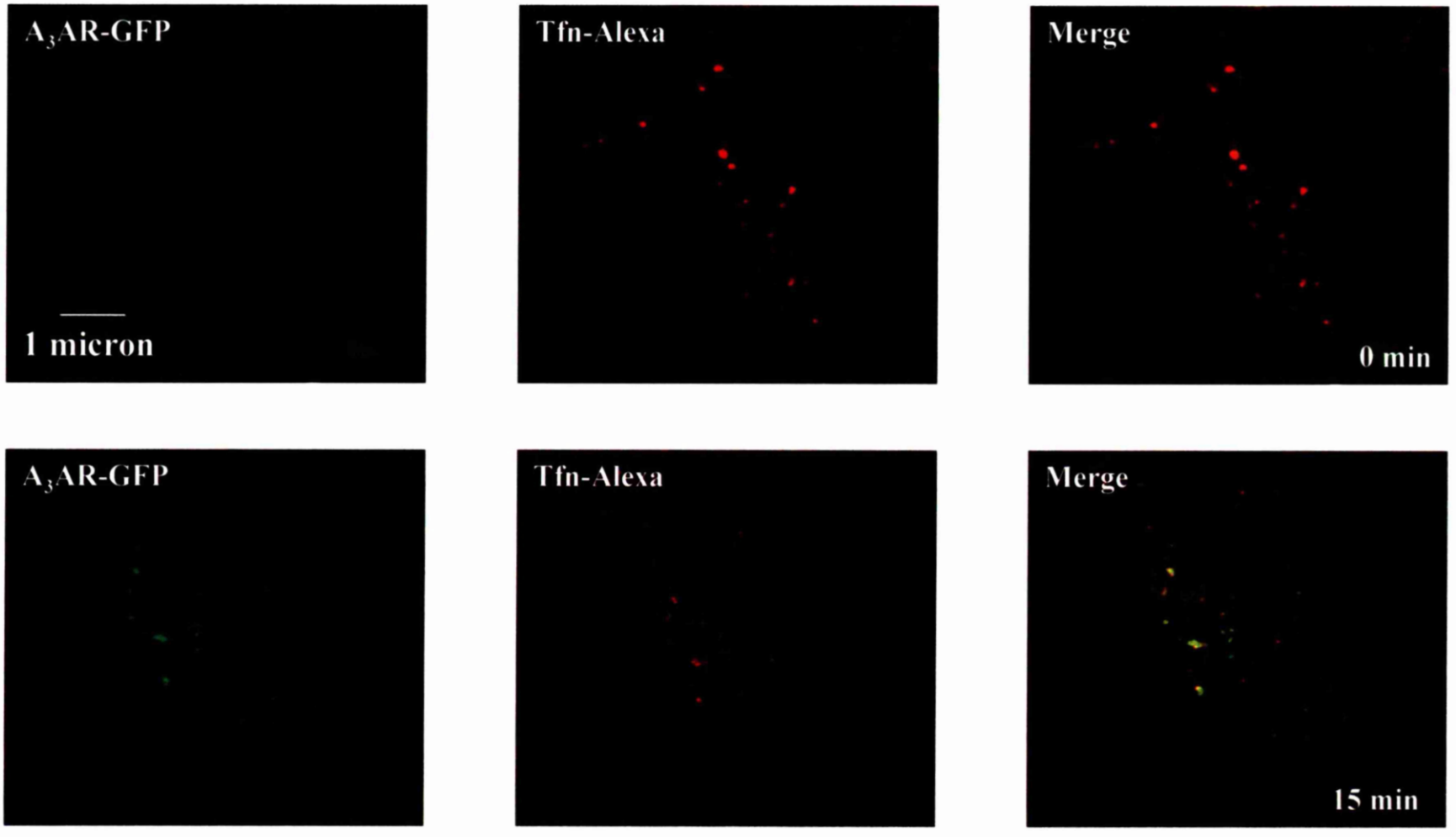
A_3AR-GFP
1 micron
Tfn-Alexa
Merge
0 min
A_3AR-GFP
Tfn-Alexa
Merge
15 min

Figure 4.3 Distribution of WT A_1AR-GFP and Alexa-labelled transferrin (Tfn)

HEK 293 cells transiently expressing WT A_1AR-GFP were treated with Alexa-Tfn for 30 minutes prior to stimulation with 1μM (R)-PIA over a 30 minute time period. Addition of agonist produced no noticeable translocation of WT A_1AR-GFP (green) from the membrane over the time course investigated. Alexa-Tfn (red) was distributed throughout the cytoplasm The images shown opposite are representatives of multiple experiments showing similar results.

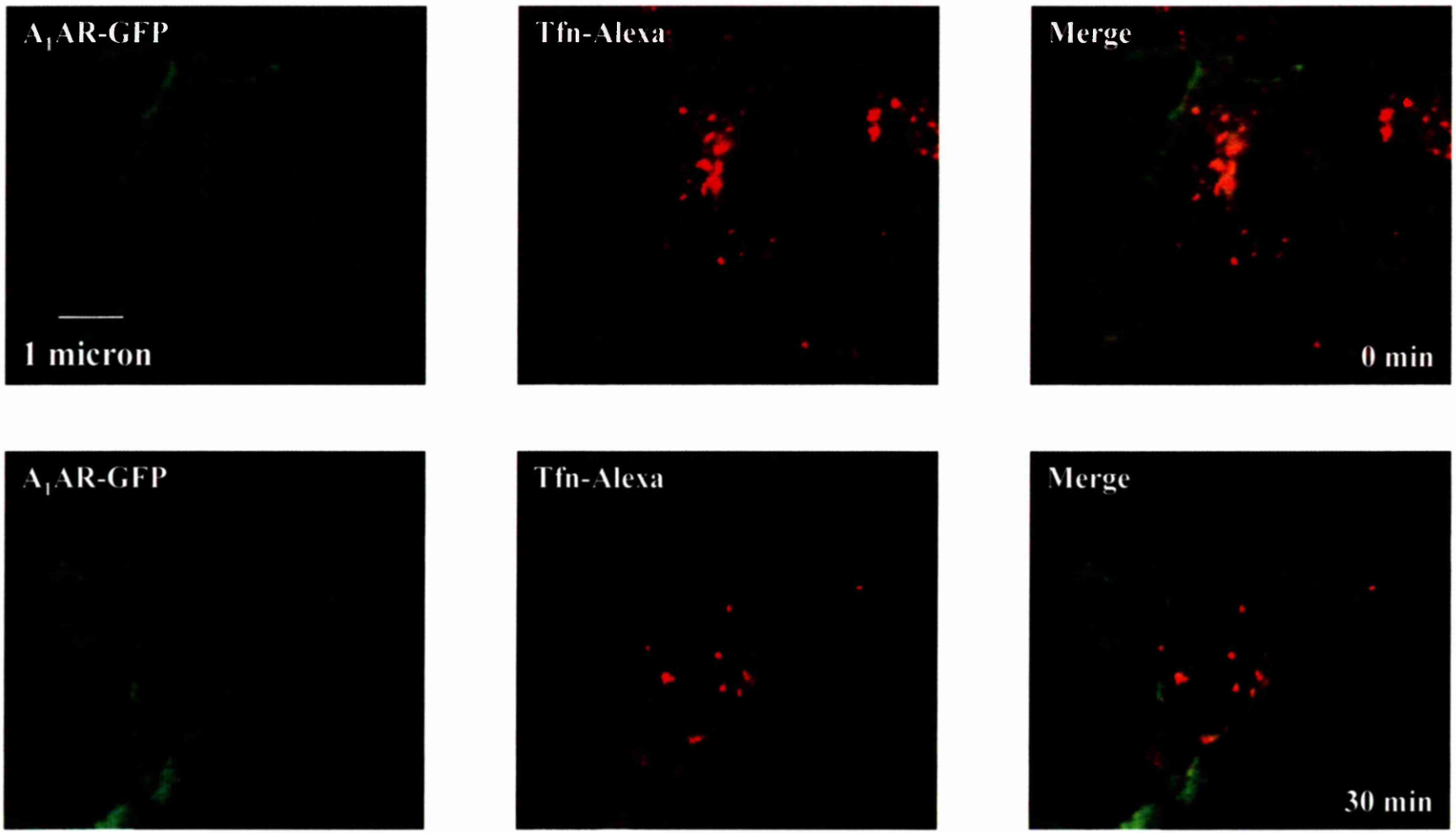
A_1AR-GFP
1 micron
Tfn-Alexa
Merge
0 min
A_1AR-GFP
Tfn-Alexa
Merge
30 min

Figure 4.4 Co-localisation of internalised (C-A)A_3AR-GFP with Alexa-labelled Transferrin (Tfn)

HEK 293 cells transiently expressing (C-A)A_3AR-GFP were treated with Alexa-Tfn for 30 minutes prior to stimulation with 1μM (R)-PIA over a 30 minute time period. Agonist induced translocation of (C-A)A_3AR-GFP (green) from the membrane to distinct vesicles within the cytoplasm. These vesicles can be seen to overlap with internalised Alexa-Tfn (red) to give a distinct yellow when the red and green images are merged (merge, 10 minutes). The images shown opposite are representatives of multiple experiments showing similar results.

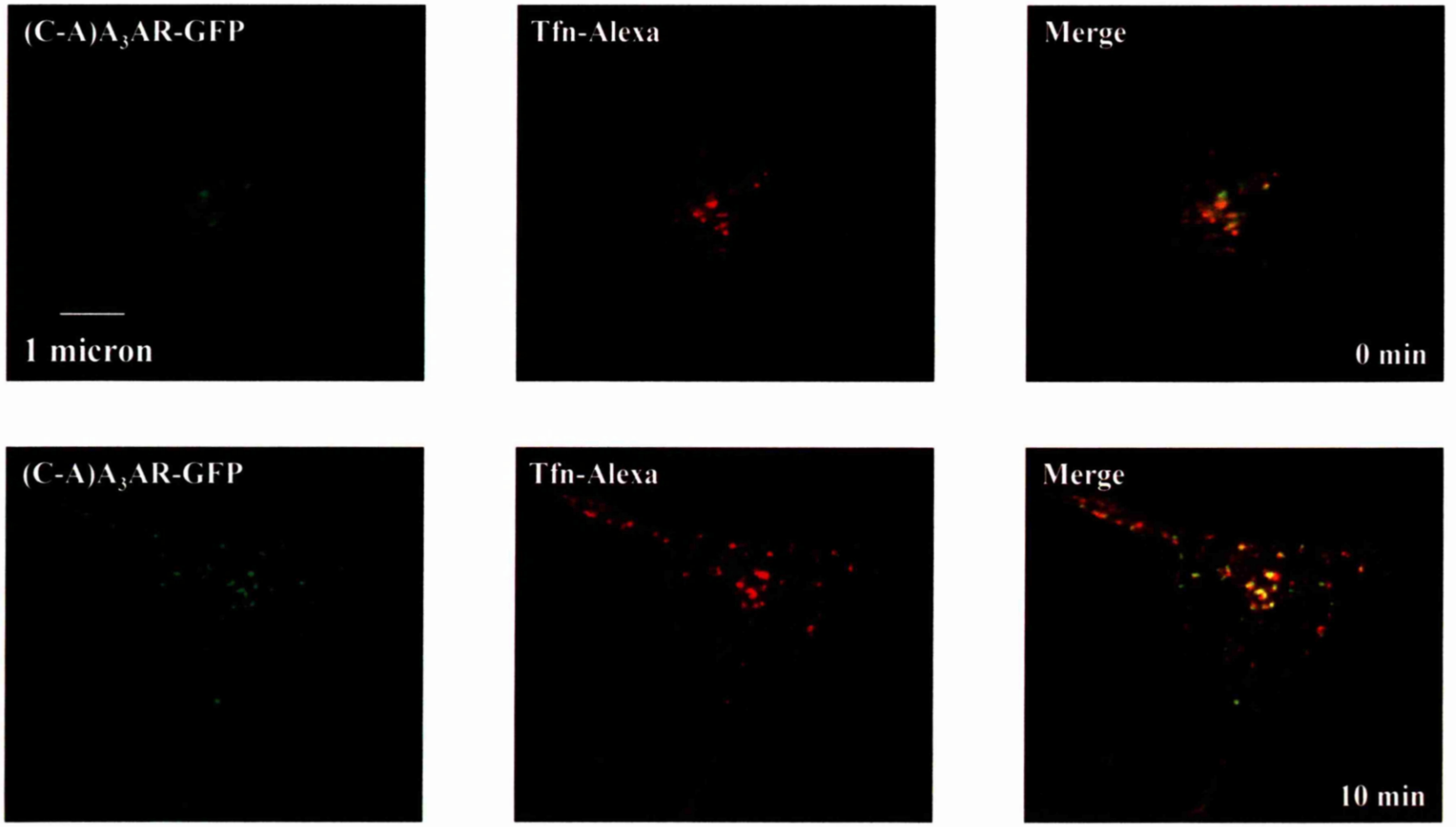
(C-A)A_3AR-GFP
1 micron
Tfn-Alexa
Merge
0 min
(C-A)A_3AR-GFP
Tfn-Alexa
Merge
10 min

Figure 4.5 Co-localisation of internalised A_1CT3AR-GFP with Alexa-labelled Transferrin (Tfn)

HEK 293 cells transiently expressing A_1CT3AR-GFP were treated with Alexa-Tfn for 30 minutes prior to stimulation with 1μM (R)-PIA over a 30 minute time period. Agonist induced translocation of A_1CT3AR-GFP (green) from the membrane to distinct vesicles within the cytoplasm. These vesicles can be seen to overlap with internalised Alexa-Tfn (red) to give a distinct yellow staining when the red and green images are merged (merge, 15 minutes). The images shown opposite are representatives of multiple experiments showing similar results.

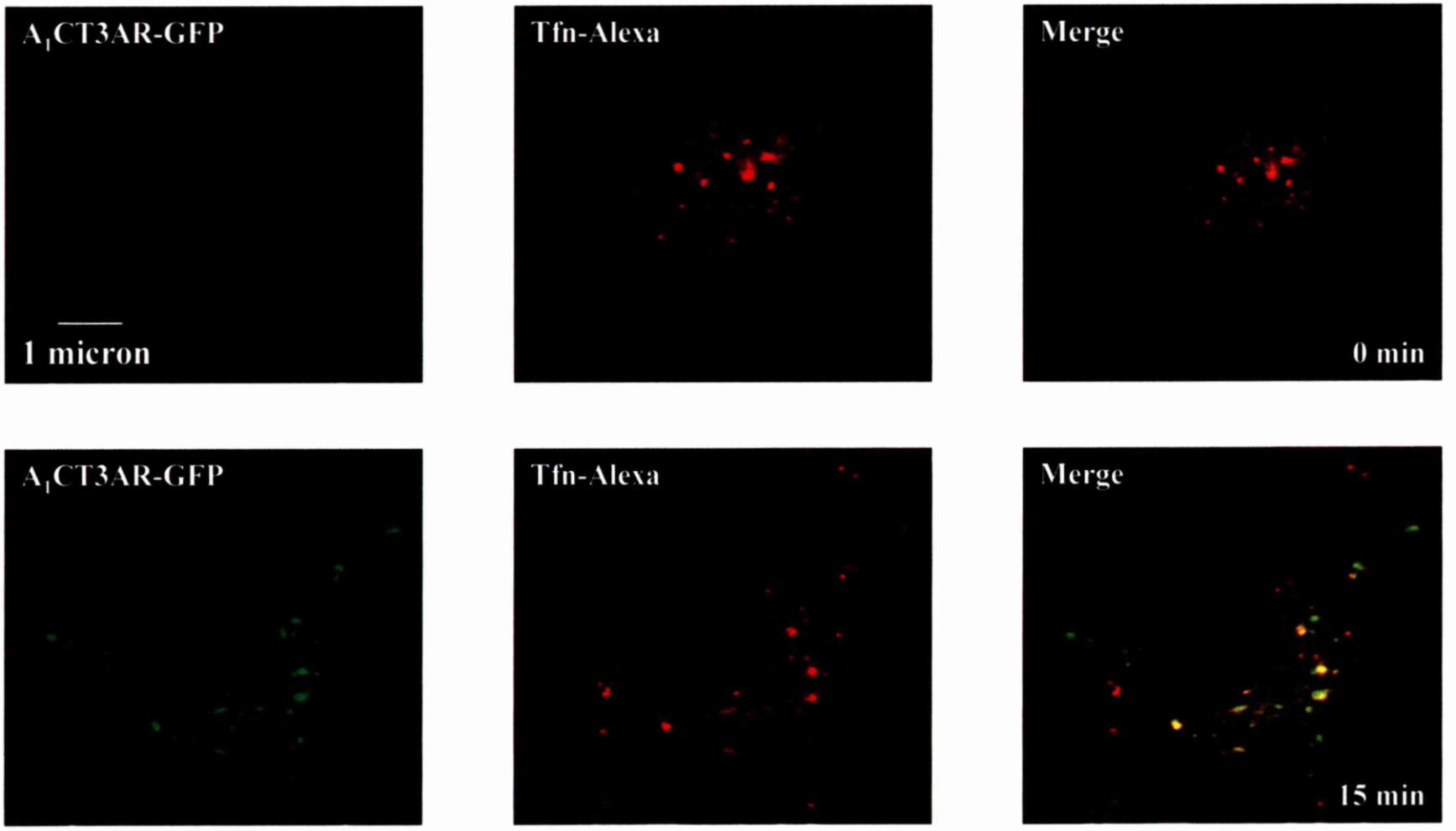
A_1CT3AR-GFP
1 micron
Tfn-Alexa
Merge
0 min
A_1CT3AR-GFP
Tfn-Alexa
Merge
15 min

Figure 4.6 **Schematic representation of GPCR agonist-mediated internalisation *via* the clathrin-coated vesicle pathway**

Agonist stimulation promotes the phosphorylation and internalisation of many GPCRs *via* clathrin-coated vesicles. Shown opposite is a simplified diagram of the major components of this internalisation pathway.

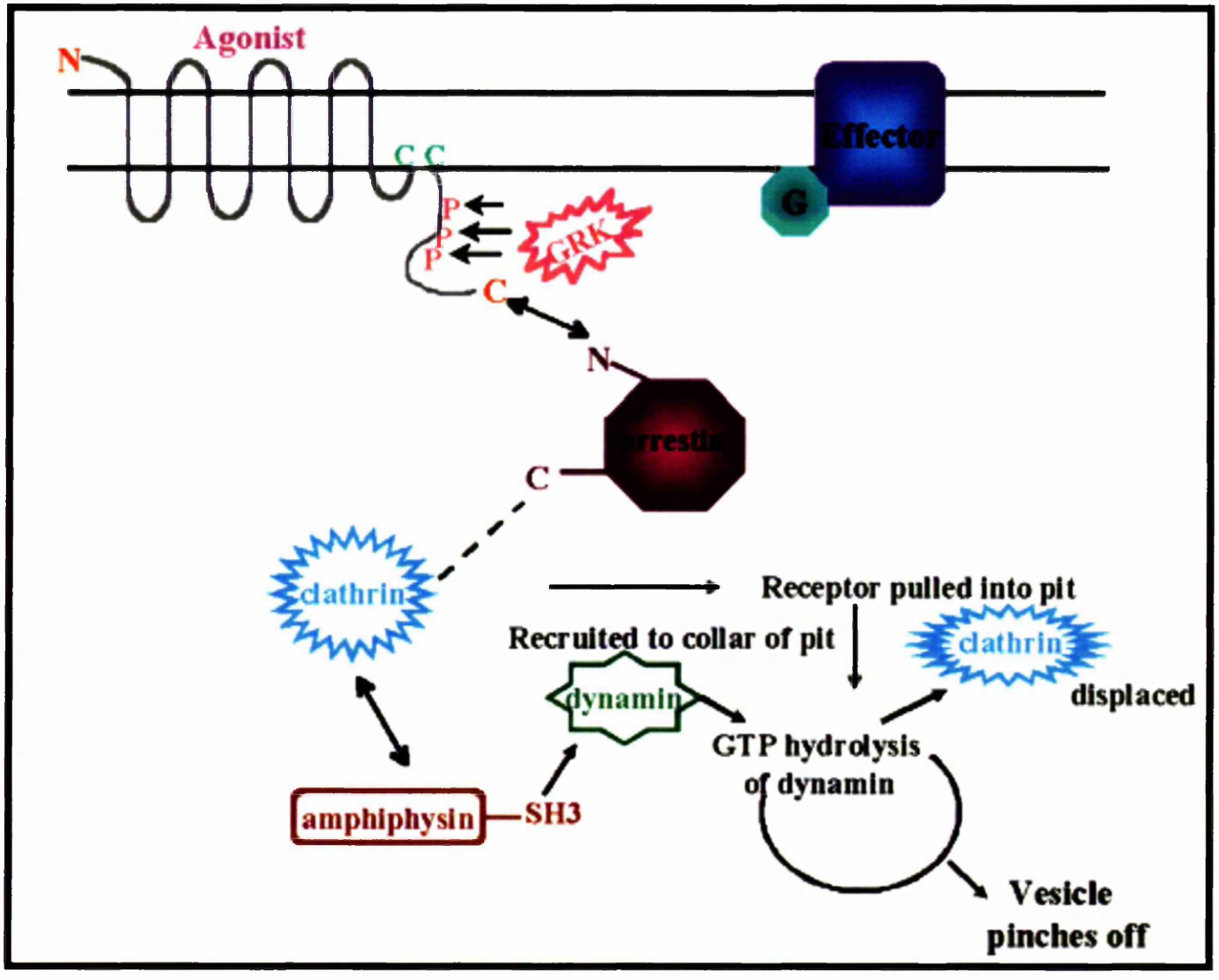
Agonist
N
Effector
G
C C
P
P
P
GRK
C
N
arrestin
C
clathrin
Receptor pulled into pit
Recruited to collar of pit
clathrin
displaced
dynamin
GTP hydrolysis
of dynamin
amphiphysin
SH3
Vesicle
pinches off

Figure 4.7 **Confocal microscopic analysis of arr2-GFP and VSV-TRHR cellular distribution in transiently transfected HEK 293 cells**

HEK 293 cells transiently co-transfected with VSV-TRHR (red) and arr2-GFP (green) cDNA were stimulated with 10μM TRH over a 30 minute time period to induce TRHR internalisation. In unstimulated cells, VSV-TRHR was observed predominately at the membrane with arr2-GFP present diffusely in the cytoplasm. Agonist activation led to re-location of arr3-GFP to distinct spots within the cytoplam and accumulation of internalised VSV-TRHR. Co-localisation (yellow) was observed upon merging of the red and green images, and sustained over the time-course investigated (yellow; merge, 30 minutes). The images shown opposite are representatives of multiple experiments showing similar results.

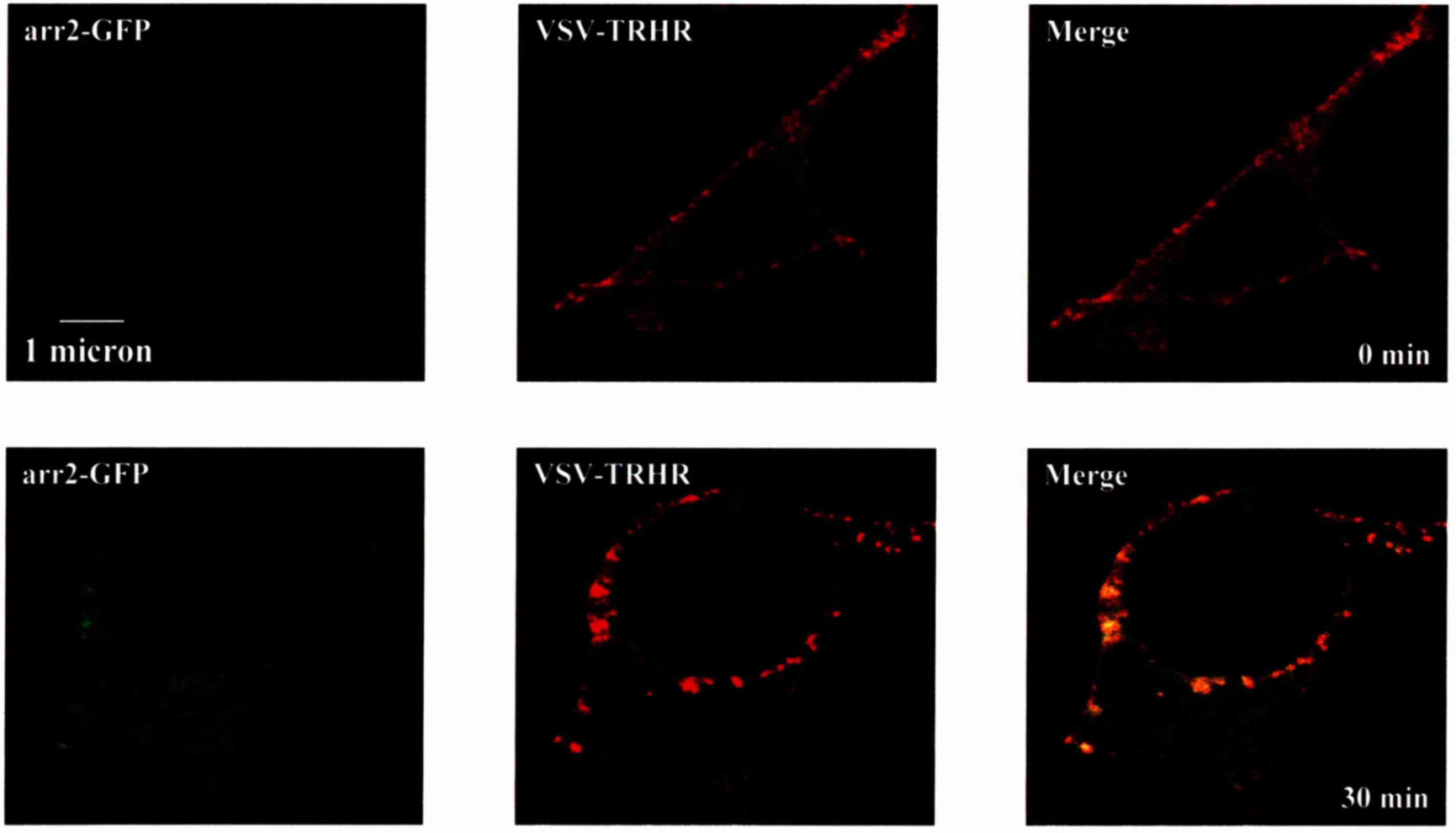
arr2-GFP
1 micron
VSV-TRHR
Merge
0 min
arr2-GFP
VSV-TRHR
Merge
30 min

Figure 4.8 **Confocal microscopic analysis of arr3-GFP and VSV-TRHR cellular distribution in transiently transfected HEK 293 cells**

HEK 293 cells transiently co-transfected with VSV-TRHR (red) and arr3-GFP (green) cDNA were stimulated with 10μM TRH over a 30 minute time period to induce TRHR internalisation. In unstimulated cells, VSV-TRHR was observed predominately at the membrane with arr3-GFP present diffusely in the cytoplasm. Agonist activation led to the accumulation of internalised VSV-TRHR to distinct spots in the cytoplasm. A small amount of co-localisation was observed between VSV-TRHR and arr2-GFP upon merging of the red and green images (yellow; merge, 30 minutes). The images shown opposite are representative examples from multiple experiments.

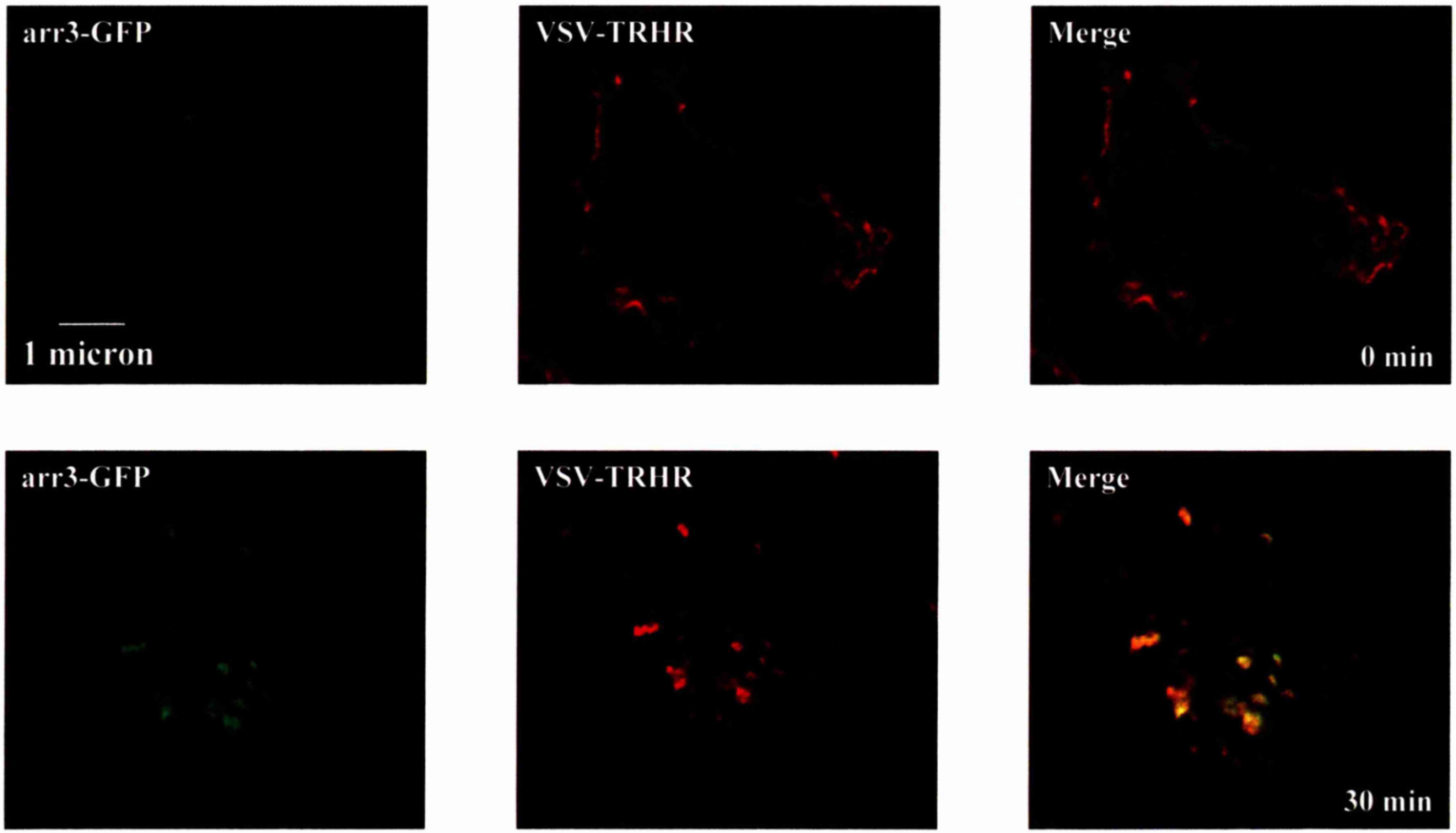
arr3-GFP
1 micron
VSV-TRHR
Merge
0 min
arr3-GFP
VSV-TRHR
Merge
30 min

Figure 4.9 **Confocal microscopic analysis of arr2-GFP and HA-A_3AR cellular distribution in transiently transfected HEK 293 cells**

HEK 293 cells transiently co-transfected with HA-A_3AR (red) and arr2-GFP (green) cDNA were stimulated with 1μM (R)-PIA over a 30 minute time period to induce A_3AR internalisation. In unstimulated cells, HA-A_3AR was observed predominately at the membrane with arr2-GFP present diffusely in the cytoplasm. Agonist activation led to the accumulation of internalised HA-A_3AR to distinct spots in the cytoplasm. No co-localisation was observed between HA-A_3AR and arr2-GFP upon merging of the red and green images (merge, 30 minutes). The images shown opposite are representatives of multiple experiments showing similar results.

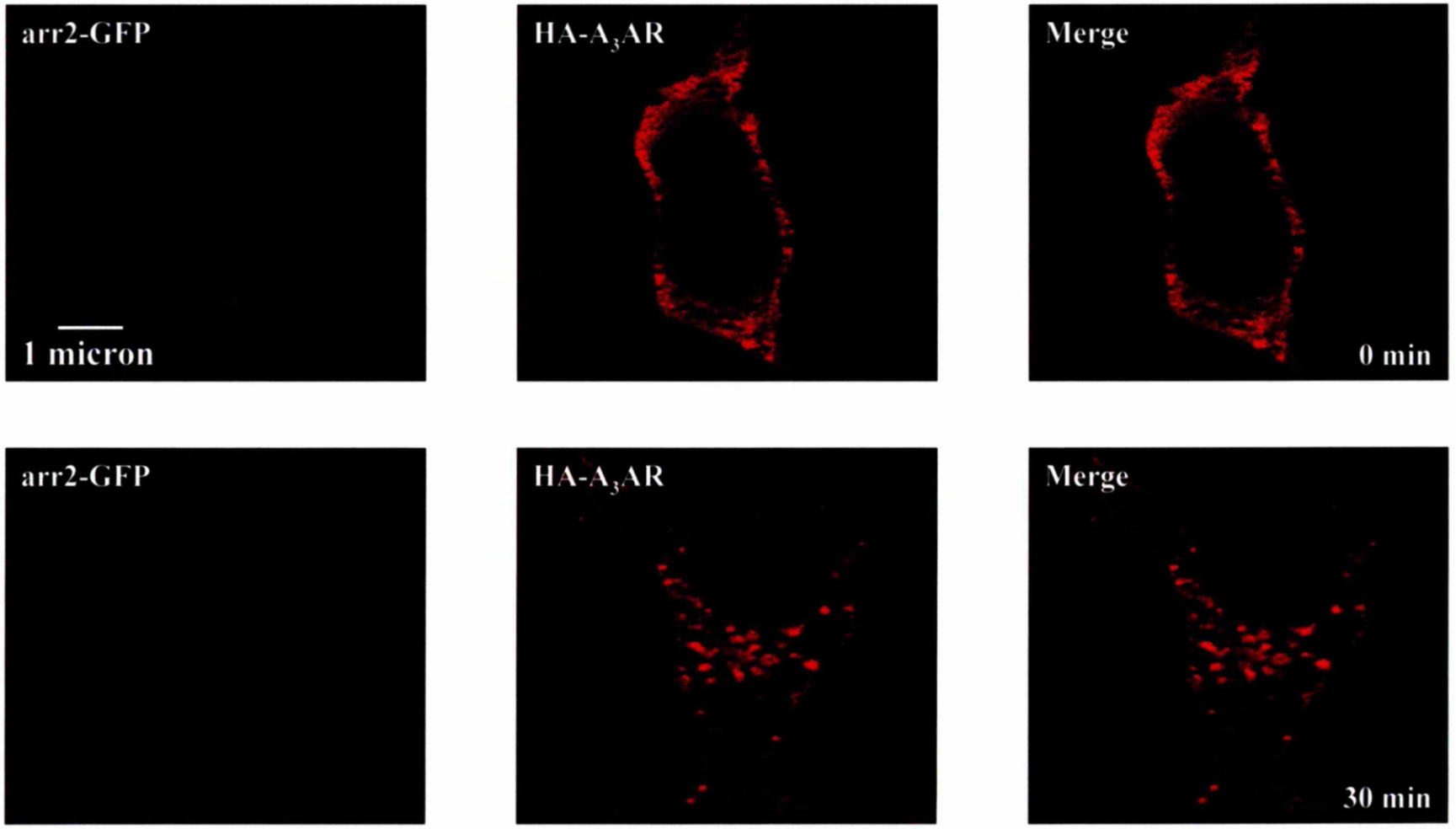
arr2-GFP
1 micron
HA-A3AR
Merge
0 min
arr2-GFP
HA-A3AR
Merge
30 min

Figure 4.10 **Confocal microscopic analysis of arr3-GFP and HA-A_3AR cellular distribution in transiently transfected HEK 293 cells**

HEK 293 cells transiently co-transfected with HA-A_3AR (red) and arr3-GFP (green) cDNA were stimulated with 1μM (R)-PIA over a 30 minute time period to induce A_3AR internalisation. In unstimulated cells, HA-A_3AR was observed predominately at the membrane with arr3-GFP present diffusely in the cytoplasm. Agonist activation led to the accumulation of arr3-GFP to distinct spots within the cytoplasm and internalised HA-A_3AR from the membrane. A transient co-localisation (yellow) of the two proteins was observed between 10 and 15 minutes when the red and green images were merged (yellow; merge, 10 minutes). The images shown opposite are representatives of multiple experiments showing similar results.

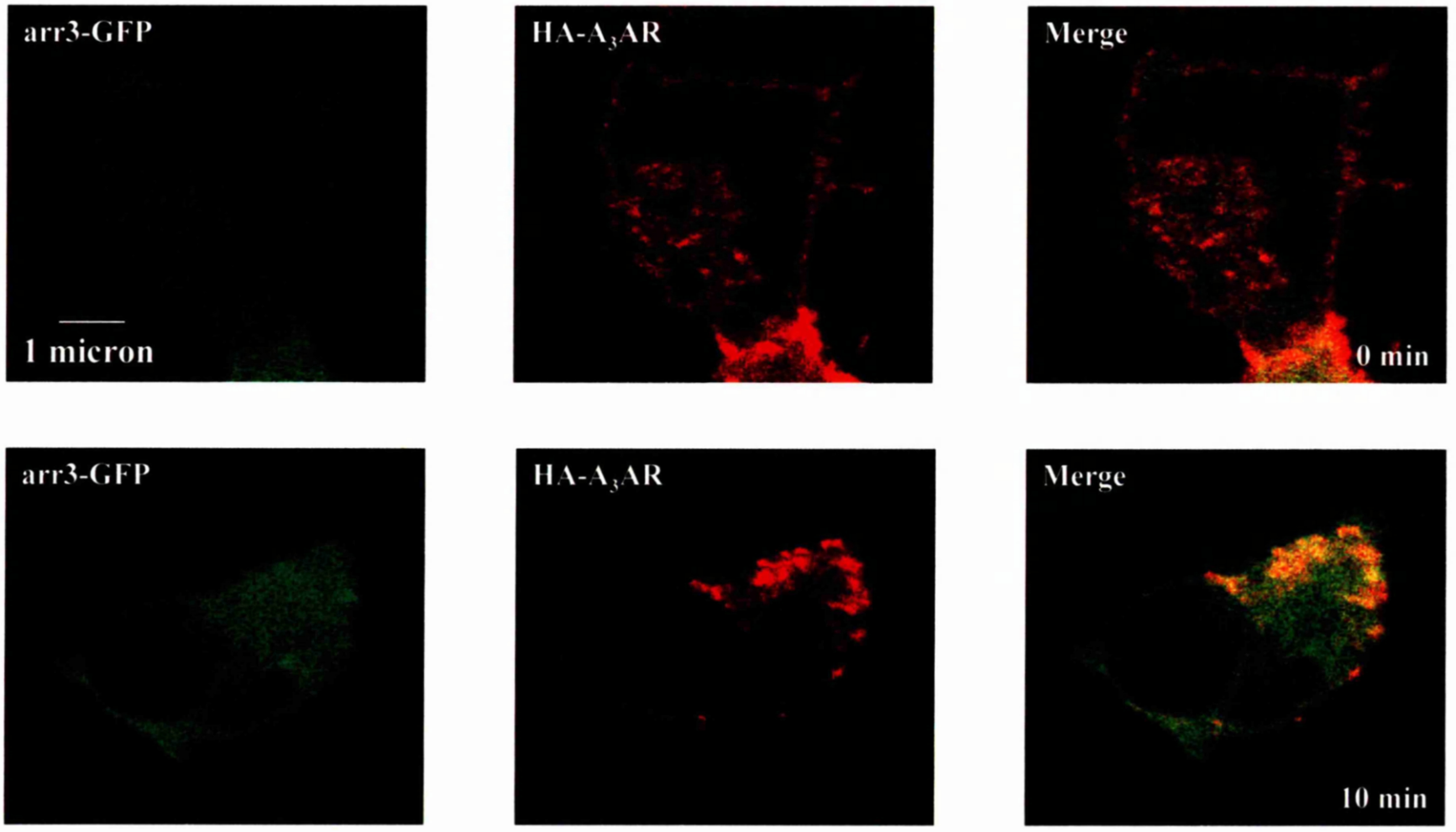
arr3-GFP
1 micron
HA-A_3AR
Merge
0 min
arr3-GFP
HA-A_3AR
Merge
10 min

Figure 4.11 **Confocal microscopic analysis of arr3-GFP and HA-A_3AR cellular distribution in transiently transfected HEK 293 cells**

HEK 293 cells transiently co-transfected with HA-A_3AR (red) and arr3-GFP (green) cDNA were stimulated with 1μM (R)-PIA over a 30 minute time period to induce A_3AR internalisation. In unstimulated cells, HA-A_3AR was observed predominately at the membrane with arr3-GFP present diffusely in the cytoplasm. Agonist activation induced internalisation of HA-A_3AR from the membrane and led to the accumulation of arr3-GFP to distinct spots within the cytoplasm and at the plasma membrane (agonist-treated, green). No co-localisation of the two tagged proteins was observed upon merging of the red and green images (merge, 15 minutes). The images shown opposite are representatives of multiple experiments showing similar results.

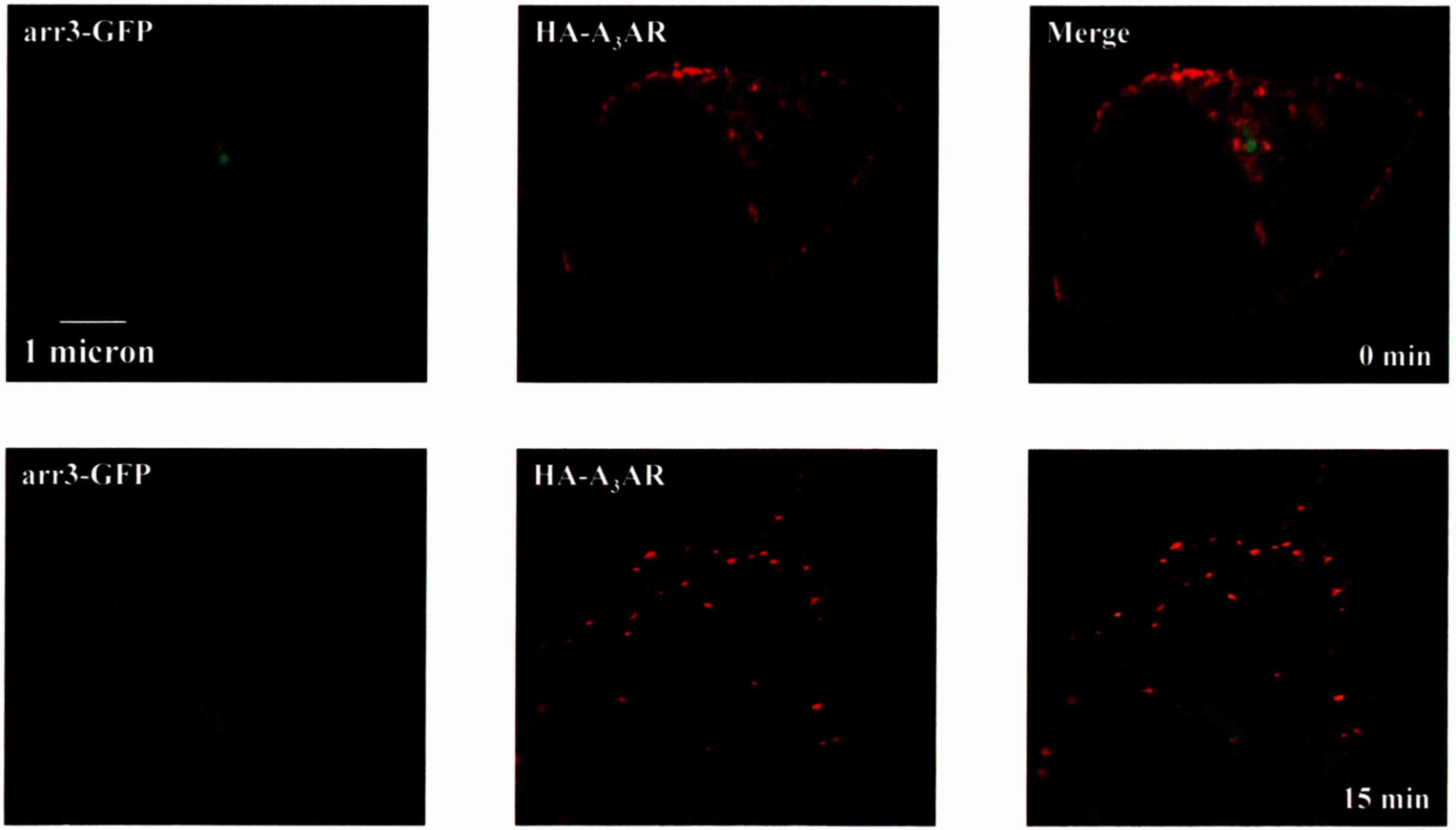
arr3-GFP
1 micron
HA-A3AR
Merge
0 min
arr3-GFP
HA-A3AR
15 min

Figure 4.12 **Confocal microscopic analysis of arr2-GFP and HA-(C-A)A_3AR cellular distribution in transiently transfected HEK 293 cells**

HEK 293 cells transiently co-transfected with HA-(C-A)A_3AR (red) and arr2-GFP (green) cDNA were stimulated with 1μM (R)-PIA over a 30 minute time period to induce (C-A)A_3AR internalisation. In unstimulated cells, HA-(C-A)A_3AR was observed predominately at the membrane with arr2-GFP present diffusely in the cytoplasm. Agonist activation induced internalisation of HA-(C-A)A_3AR to distinct spots within the cytoplasm. No co-localisation was observed between HA-(C-A)A_3AR and arr2-GFP when the red and green images were merged (merge, 4 minutes). The images shown opposite are representatives of multiple experiments showing similar results.

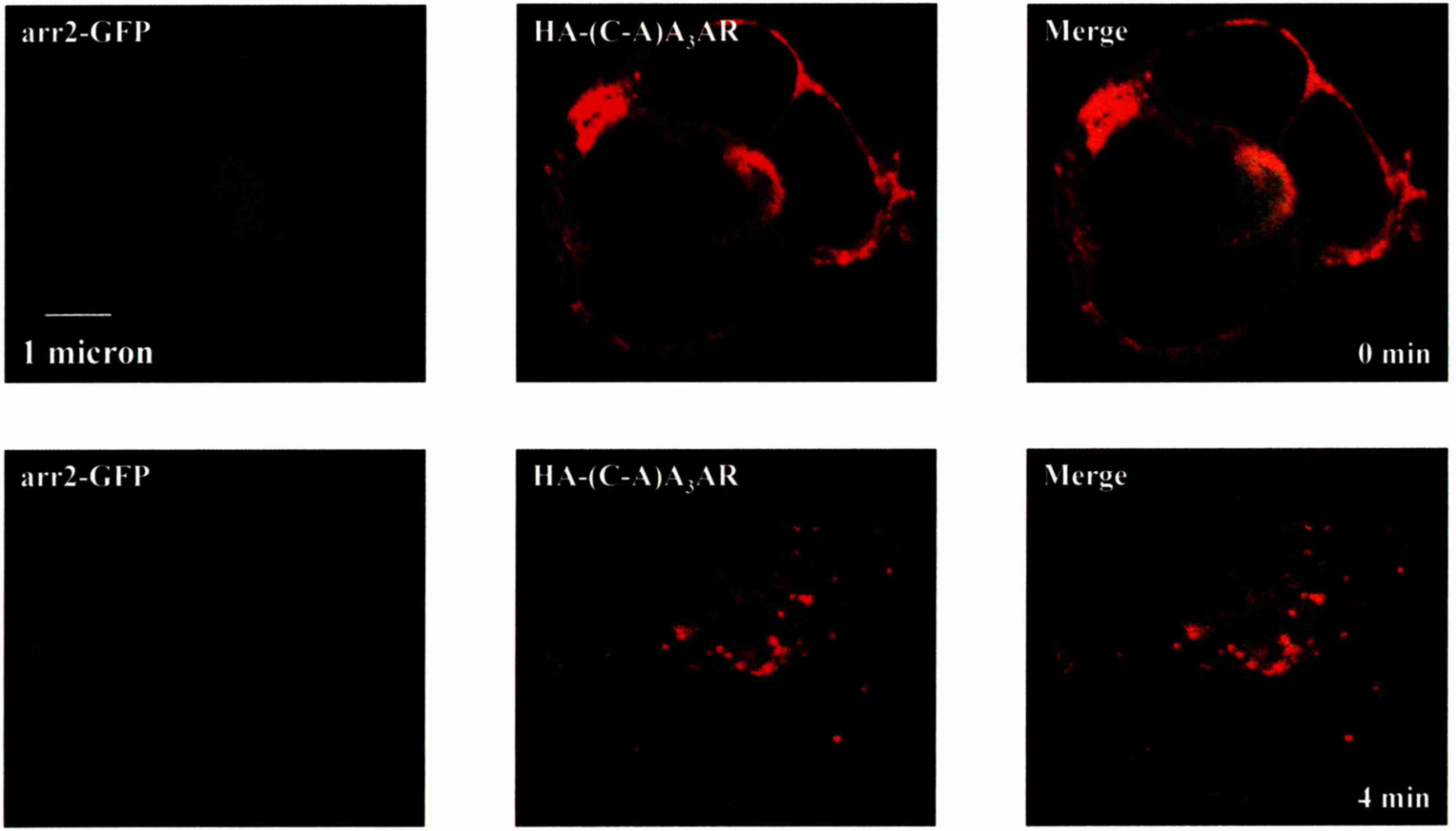
arr2-GFP
1 micron
HA-(C-A)A3AR
Merge
0 min
arr2-GFP
HA-(C-A)A3AR
Merge
4 min

Figure 4.13 **Confocal microscopic analysis of arr3-GFP and HA-(C-A)A_3AR cellular distribution in transiently transfected HEK 293 cells**

HEK 293 cells transiently co-transfected with HA-(C-A)A_3AR (red) and arr3-GFP (green) cDNA were stimulated with 1μM (R)-PIA over a 30 minute time period to induce (C-A)A_3AR internalisation. In unstimulated cells, HA-(C-A)A_3AR was observed predominately at the membrane with arr3-GFP present diffusely in the cytoplasm. Agonist activation led to the accumulation of arr3-GFP to distinct spots within the cytoplasm and induced internalisation of HA-(C-A)A_3AR from the membrane. A transient co-localisation (yellow) of the two proteins was observed between 4 and 10 minutes upon merging of the red and green images (merge, 4 minutes). The images shown opposite are representatives of multiple experiments showing similar results.

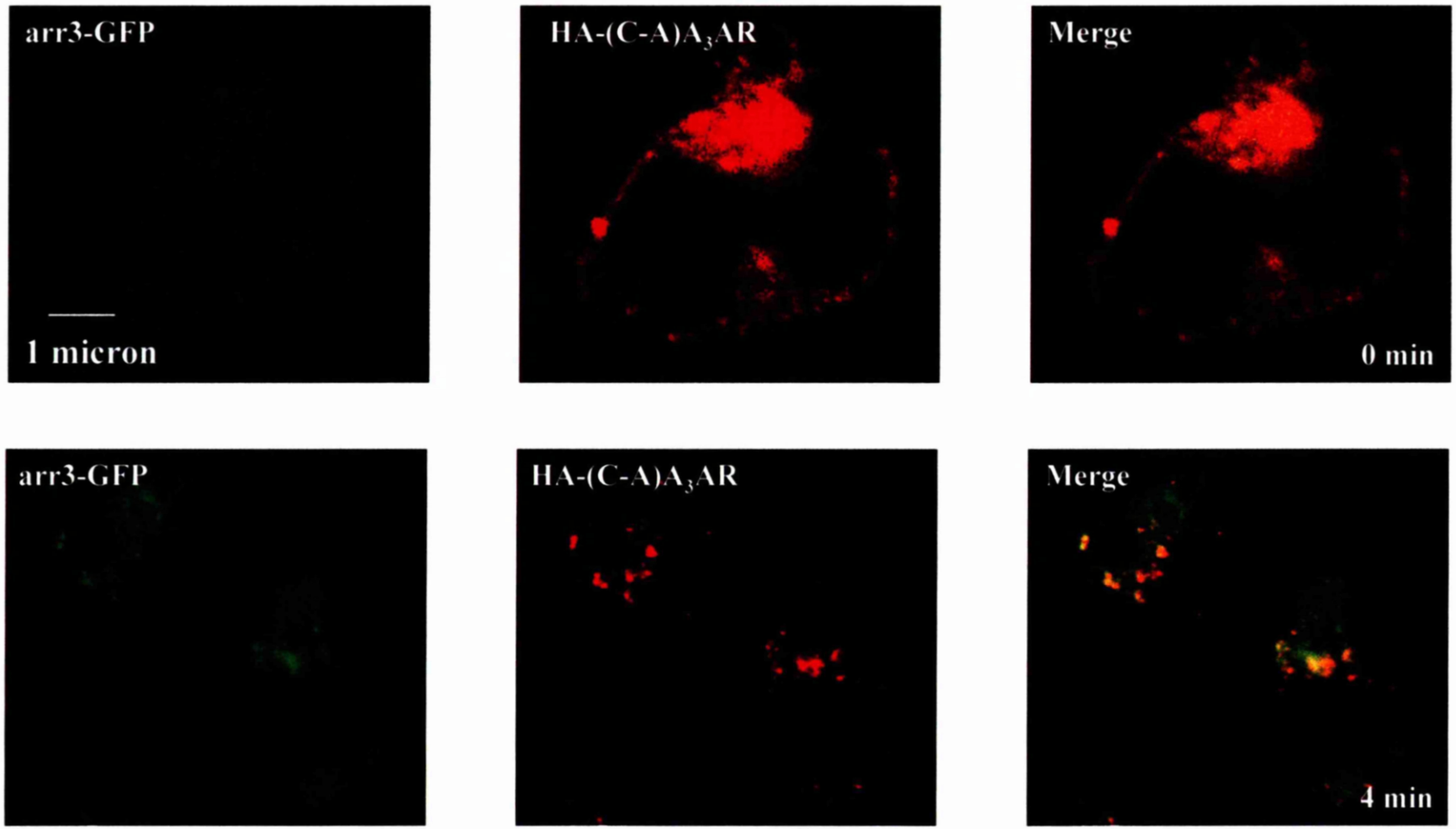
arr3-GFP
1 micron
HA-(C-A)A_3AR
Merge
0 min
arr3-GFP
HA-(C-A)A_3AR
Merge
4 min

Figure 4.14 **Confocal microscopic analysis of arr3-GFP and HA-(C-A)A_3AR cellular distribution in transiently transfected HEK 293 cells**

HEK 293 cells transiently co-transfected with HA-(C-A)A_3AR (red) and arr3-GFP (green) cDNA were stimulated with 1μM (R)-PIA over a 30 minute time period to induce (C-A)A_3AR internalisation. In unstimulated cells, HA-(C-A)A_3AR was observed predominately at the membrane with arr3-GFP present diffusely in the cytoplasm. Agonist activation induced internalisation of HA-(C-A)A_3AR from the membrane and led to the accumulation of arr3-GFP to distinct spots within the cytoplasm and at the plasma membrane (agonist-treated, green). No co-localisation of the two tagged proteins was observed upon merging of the red and green images (merge, 5 minutes). The images shown opposite are representatives of multiple experiments showing similar results.

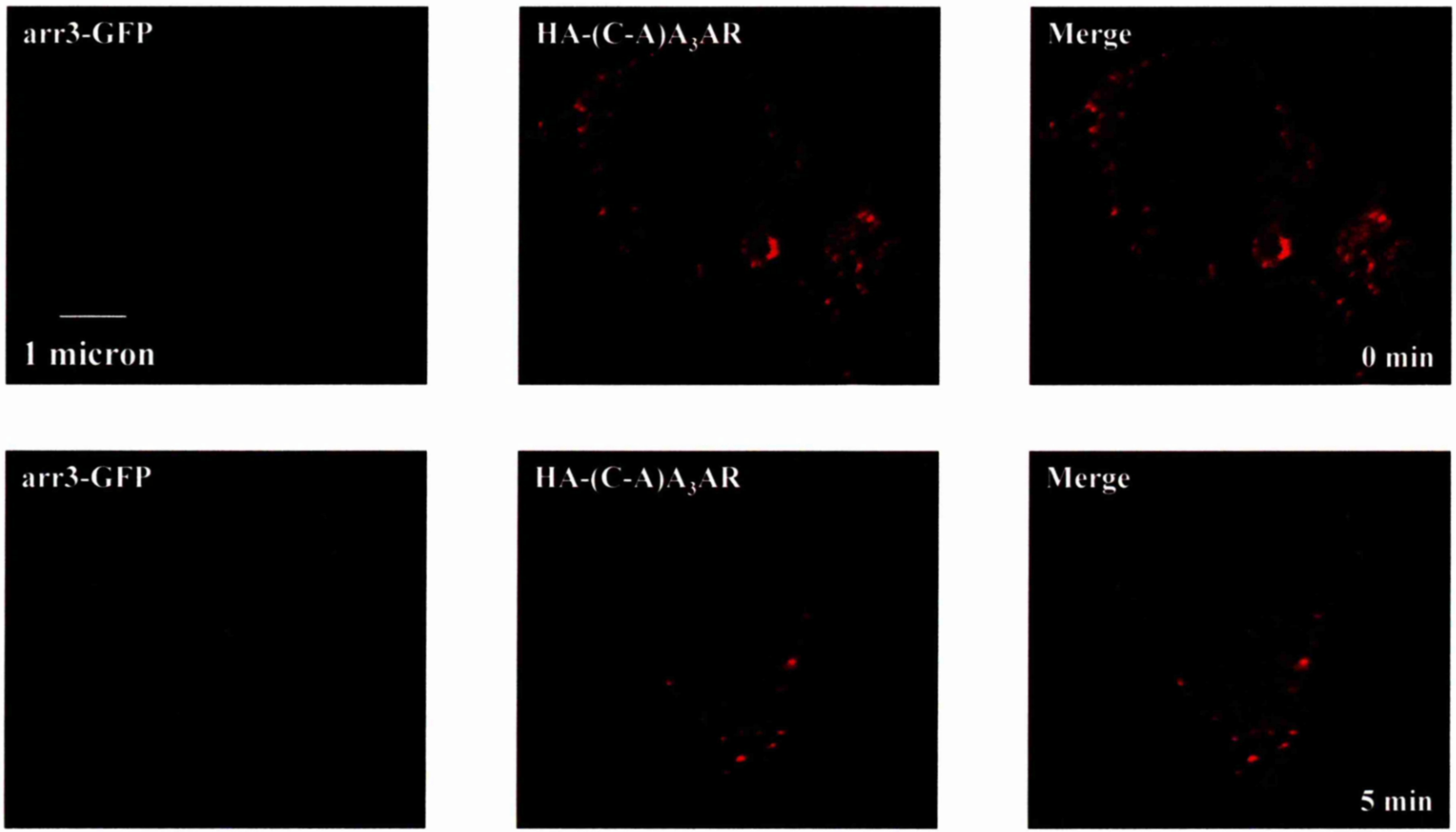
arr3-GFP
1 micron
HA-(C-A)A_3AR
Merge
0 min
arr3-GFP
HA-(C-A)A_3AR
Merge
5 min

Figure 4.15 **Confocal microscopic analysis of arr3-GFP and HA-A_1CT3AR cellular distribution in transiently transfected HEK 293 cells**

HEK 293 cells transiently co-transfected with HA-A_1CT3AR (red) and arr3-GFP (green) cDNA were stimulated with 1μM (R)-PIA over a 30 minute time period to induce A_1CT3AR internalisation. In unstimulated cells, HA-A_1CT3AR was observed predominately at the membrane with arr3-GFP present diffusely in the cytoplasm. Agonist activation induced internalisation of HA-A_1CT3AR from the membrane and led to the accumulation of arr3-GFP to distinct spots within the cytoplasm and at the plasma membrane (agonist-treated, green). No co-localisation of the two tagged proteins was observed upon merging of the red and green images (merge, 15 minutes). The images shown opposite are representatives of multiple experiments showing similar results.

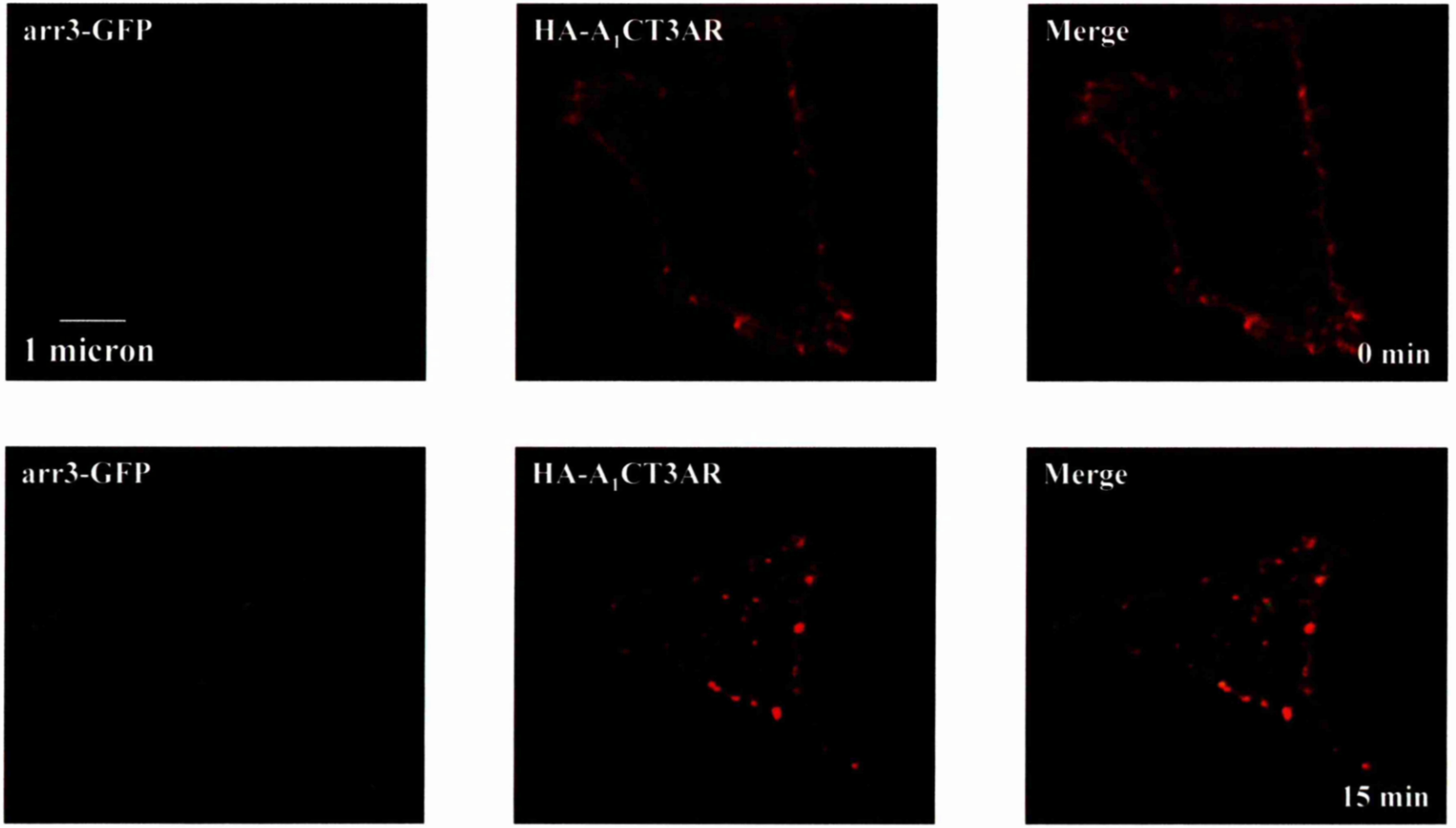
arr3-GFP
1 micron
HA-A1CT3AR
Merge
0 min
arr3-GFP
HA-A1CT3AR
Merge
15 min

Figure 4.16 **Schematic representation of the inhibition of clathrin-mediated internalisation by mutant proteins involved in clathrin-mediated endocytosis**

Over-expression of dominant-negative or mutated forms of GRK2 (GRK2[BK-CT]), arrestin2 (arr2[319-418]) and dynamin (Dyn[K44E]) have been shown to inhibit the clathrin-mediated pathway of internalisation. The diagram opposite shows the sites of interaction of these mutants within the clathrin pathway.

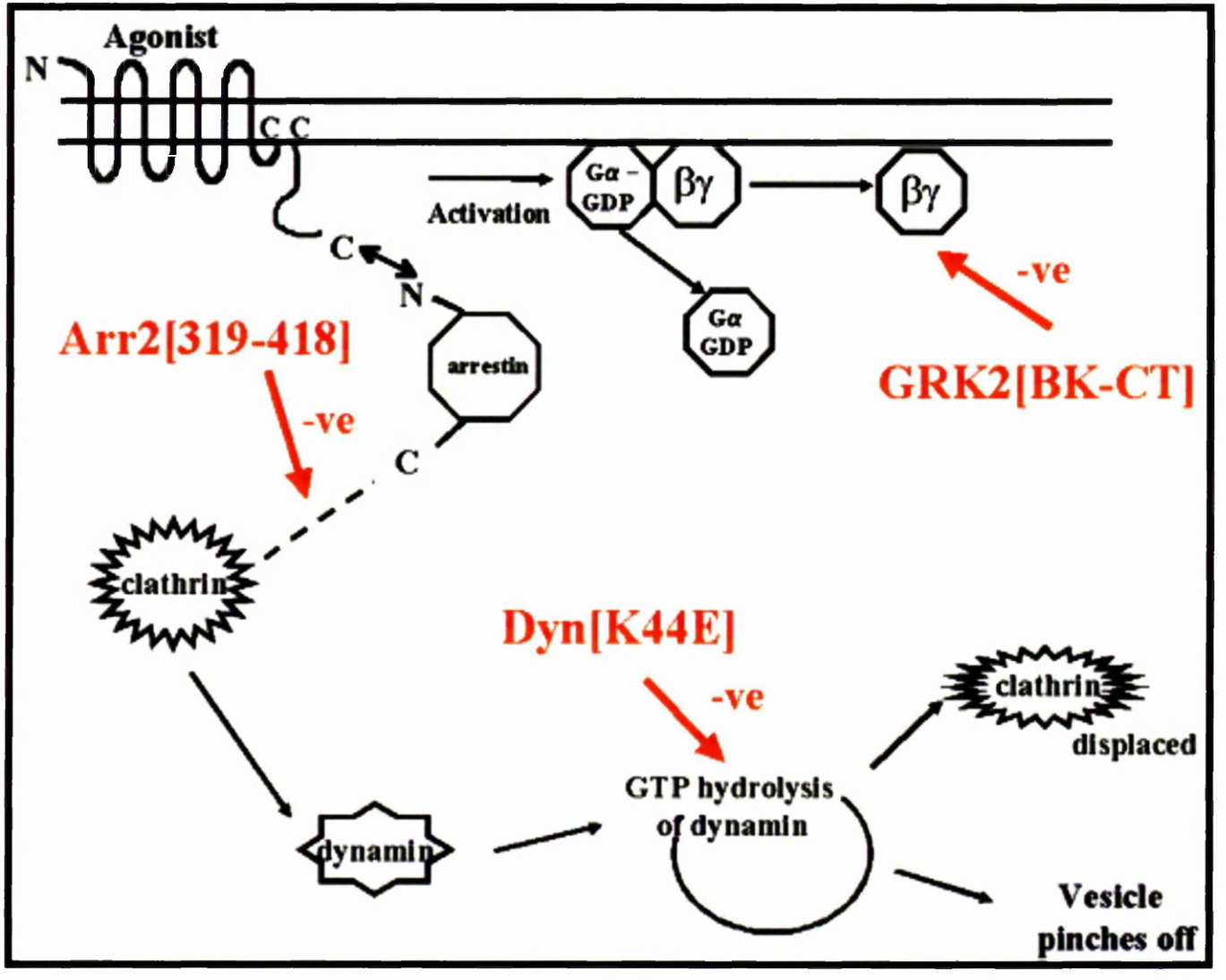
Agonist
N
C C
Activation
Gα - GDP
βγ
βγ
-ve
C
N
Gα GDP
Arr2[319-418]
arrestin
GRK2[BK-CT]
-ve
C
clathrin
Dyn[K44E]
-ve
clathrin
displaced
GTP hydrolysis of dynamin
dynamin
Vesicle pinches off

Figure 4.17 **Immunodetection of increasing concentrations of WT and mutant bovine GRK2 in transiently transfected CHO cells**

A_3AR-expressing CHO cells were transiently transfected with increasing concentrations of WT bovine GRK2 (A) and GRK2[BK-CT] cDNAs (B) ranging in concentration from 0-2.0μg/well. Cells were solubilised and the resultant protein separated by SDS-PAGE. Proteins were transferred to nitrocellulose and visualised by incubation with the GRK2-specific monoclonal antibody 3A10 followed by HRP-conjugated anti-mouse secondary antibody. Control sample used was 100ng of pure recombinant bovine GRK2. Typical data is shown from one of three experiments.

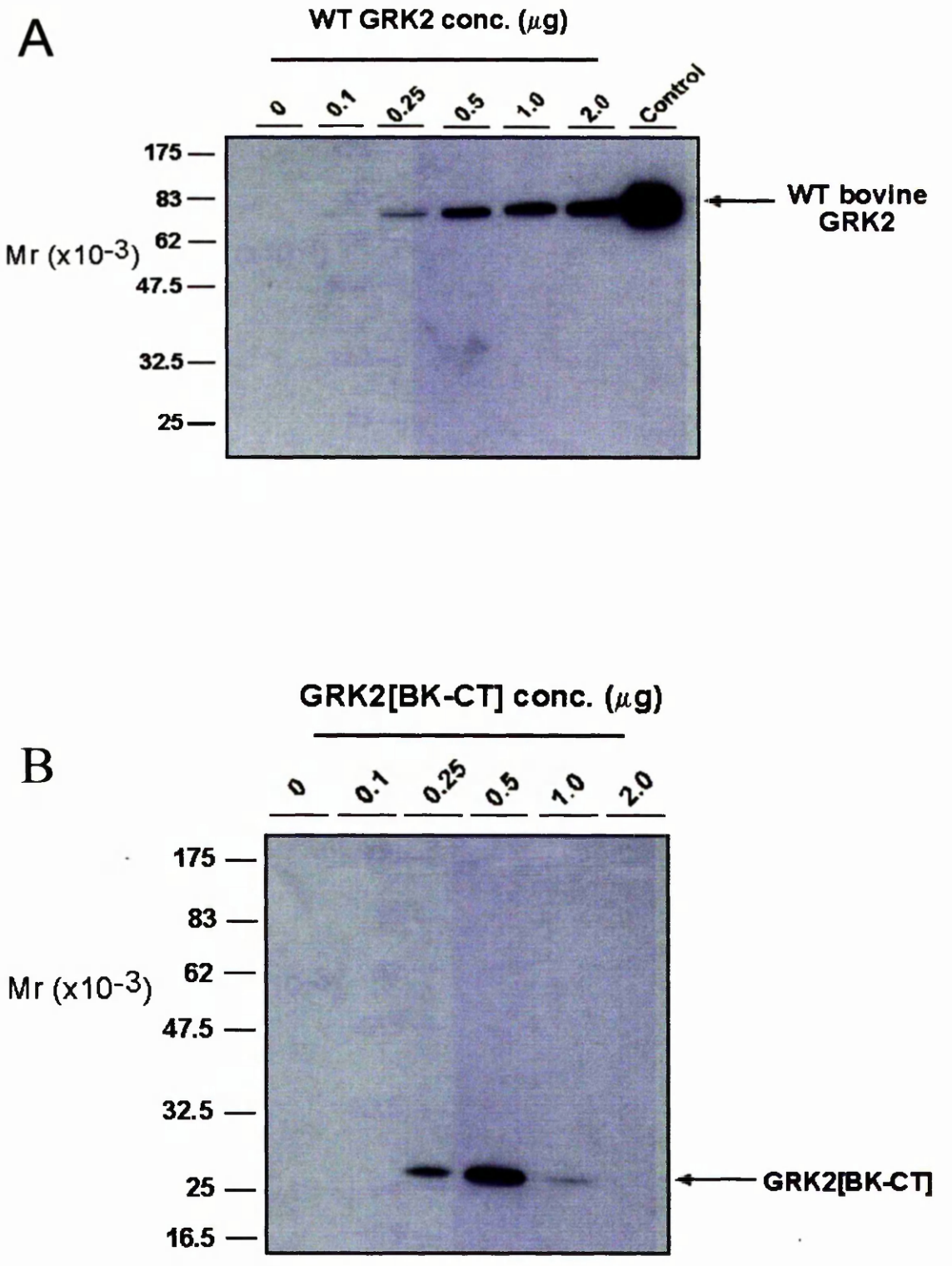
A
WT GRK2 conc. (μg)
0
0.1
0.25
0.5
1.0
2.0
Control
175
83
62
47.5
32.5
25
Mr (x10-3)
WT bovine GRK2
B
GRK2[BK-CT] conc. (μg)
0
0.1
0.25
0.5
1.0
2.0
175
83
62
47.5
32.5
25
16.5
Mr (x10-3)
GRK2[BK-CT]

Figure 4.18 Effect of increasing GRK2[BK-CT] expression on agonist-stimulated A_3AR phosphorylation

CHO cells stably expressing the A_3AR were transiently transfected with increasing concenetrations of GRK2[BK-CT] cDNA ranging from 0-0.5μg/well and left to recover overnight. Cells were labelled with ^{32}P and vehicle or (R)-PIA (final concentration of 10μM) was added for 30 minutes. Reactions were terminated and receptors solubilised as previously described. Proteins were fractionated by SDS-PAGE, the gel dried and visualised by aautoradiography. The graph shown opposite was calculated from three autoradiographs and plotted as mean ± S.E. Receptor stimulation with agonist alone was set at 100%

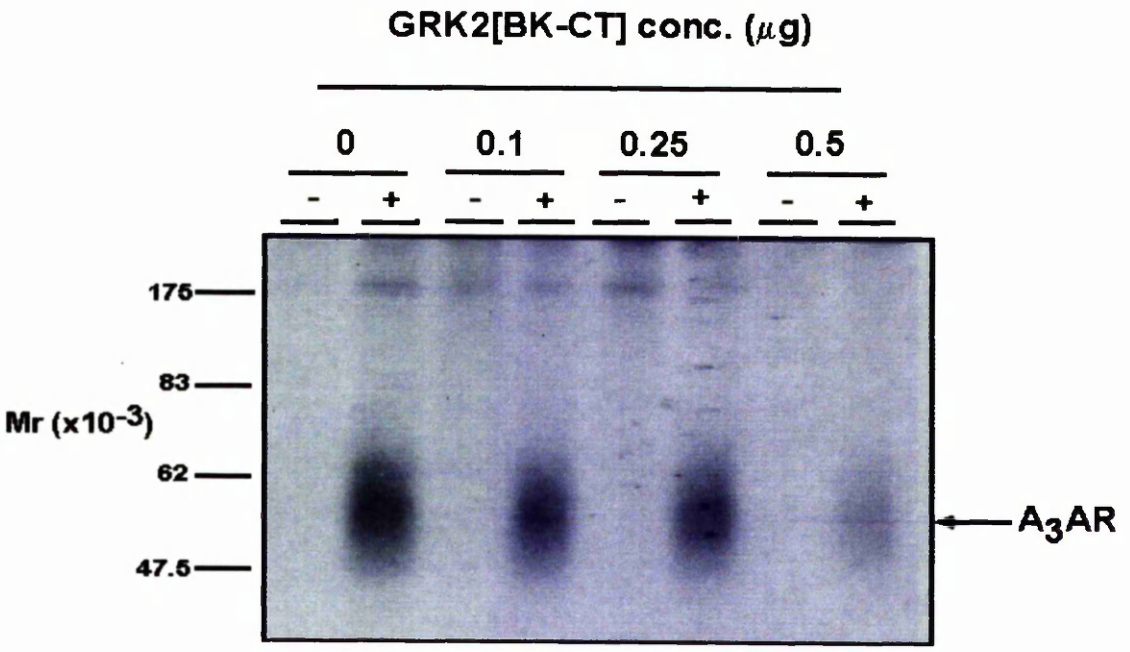
GRK2[BK-CT] conc. (μg)
0
0.1
0.25
0.5
- + - + - + - +
175
83
62
47.5
Mr (x10-3)
A3AR

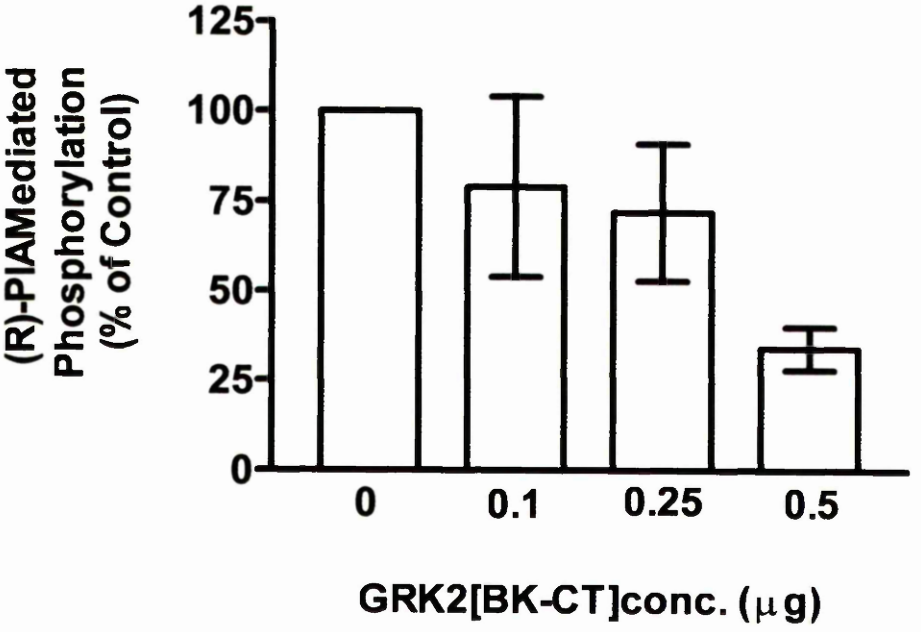
(R)-PIAMediated Phosphorylation (% of Control)
125
100
75
50
25
0
0
0.1
0.25
0.5
GRK2[BK-CT]conc. (μg)

Figure 4.19 **Confocal microscopic analysis of A_3AR-GFP internalisation in the presence of the mutant GRK2[BK-CT]**

CHO cells stably expressing A_3AR-GFP were transfected with GRK2[BK-CT] cDNA and treated with or without 1μM (R)-PIA for 30 minutes. Cells were solubilised and stained with GRK2-specific primary antibody followed by Alexa-tagged anti-mouse secondary antibody. Cells were then visualised by confocal microscopy as describe din the Methods. Images (a) and (b) show cells expressing A_3AR-GFP (green) alone with or without agonist, which were used as controls. Images (c) and (d) show A_3AR-GFP cells expressing Alexa-labelled GRK2[BK-CT] (red) with or without agonist over a 30 minute time period. Comparison of the images shows that internalisation of A_3AR-GFP appears to be unaffected by the presence of the GRK2 mutant. The images shown opposite are representative examples of multiple experiments.

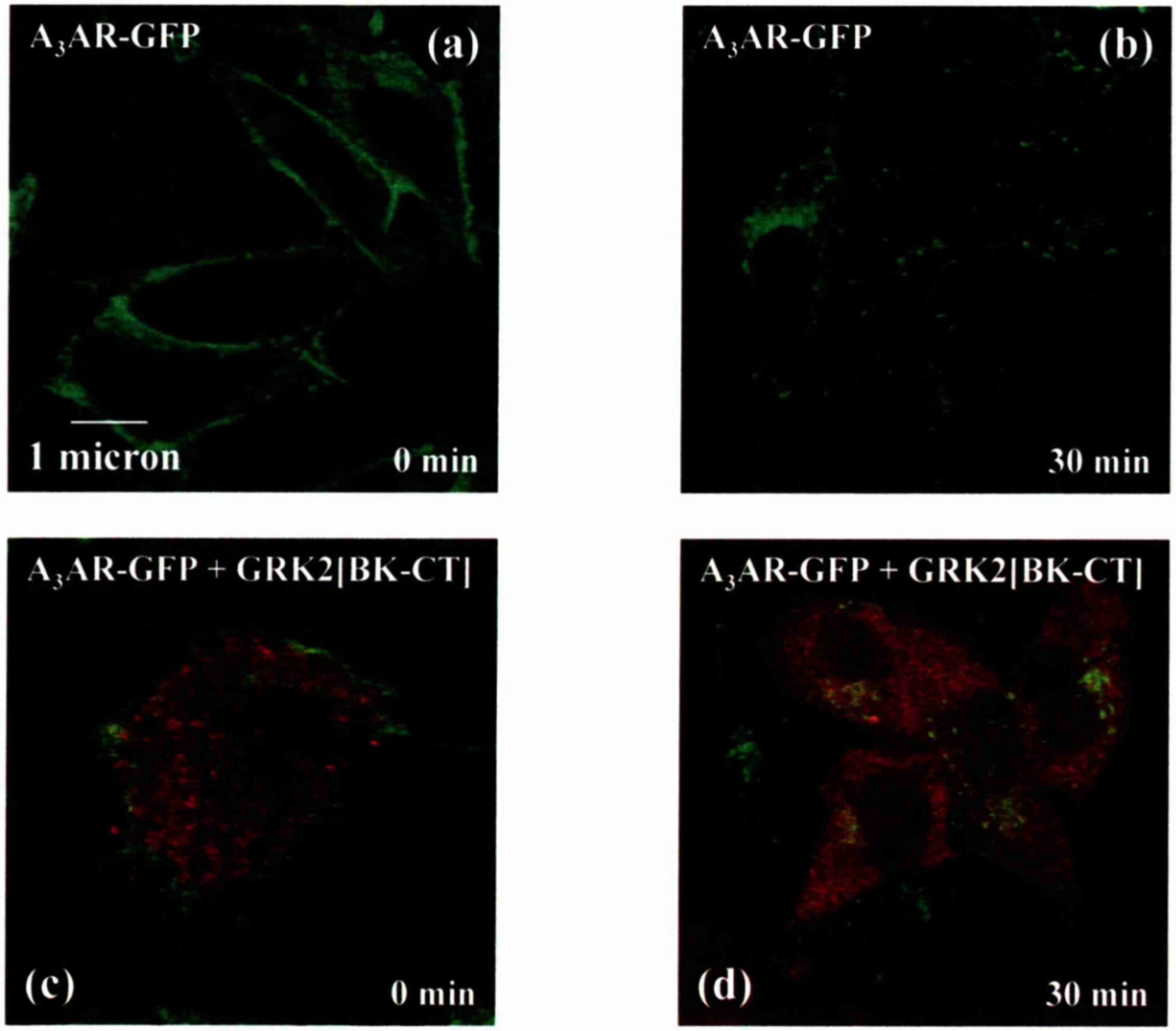
A3AR-GFP
(a)
1 micron
0 min
A3AR-GFP
(b)
30 min
A3AR-GFP + GRK2[BK-CT]
(c)
0 min
A3AR-GFP + GRK2[BK-CT]
(d)
30 min

Figure 4.20 **Immunodetection of increasing concentrations of the arrestin mutant arr2[319-418] in transiently transfected CHO cells**

A_3AR-expressing CHO cells were transiently transfected with increasing concentrations of arr2[319-418] cDNA ranging in concentration from 0-2.0μg/well. Cells were solubilised and the resultant protein separated by SDS-PAGE. Proteins were transferred to nitrocellulose and visualised by incubation with the arrestin-specific monoclonal antibody β-arrestin1 followed by HRP-conjugated anti-mouse secondary antibody. Typical data is shown from one of three experiments.

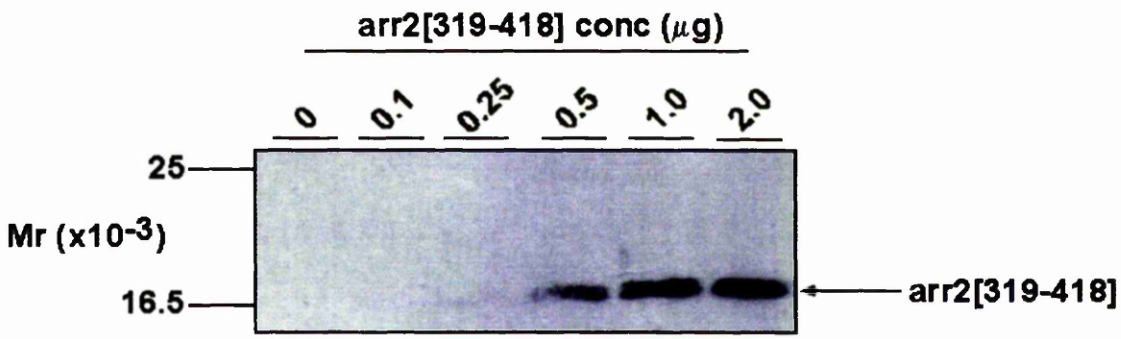
arr2[319-418] conc (μg)
0
0.1
0.25
0.5
1.0
2.0
25
Mr (x10-3)
16.5
arr2[319-418]

Figure 4.21 **Confocal microscopic analysis of A_3AR-GFP internalisation in the presence of the mutant arr2[319-418]**

CHO cells stably expressing A_3AR-GFP were transfected with arr2[319-418] cDNA and treated with or without 1μM (R)-PIA for 30 minutes. Cells were solubilised and stained with anti-arrestin primary antibody followed by Alexa-tagged anti-mouse secondary antibody as described in the Methods and visualised by confocal microscopy. arr2[319-418] (red) can be seen to be present in punctate spots throughout the cytoplasm confirming its interaction with endogenous clathrin molecules. Agonist stimulation can be seen to promote A_3AR-GFP (green) internalisation in the presence of the arr2 mutant. The images shown opposite are representative examples of multiple experiments.

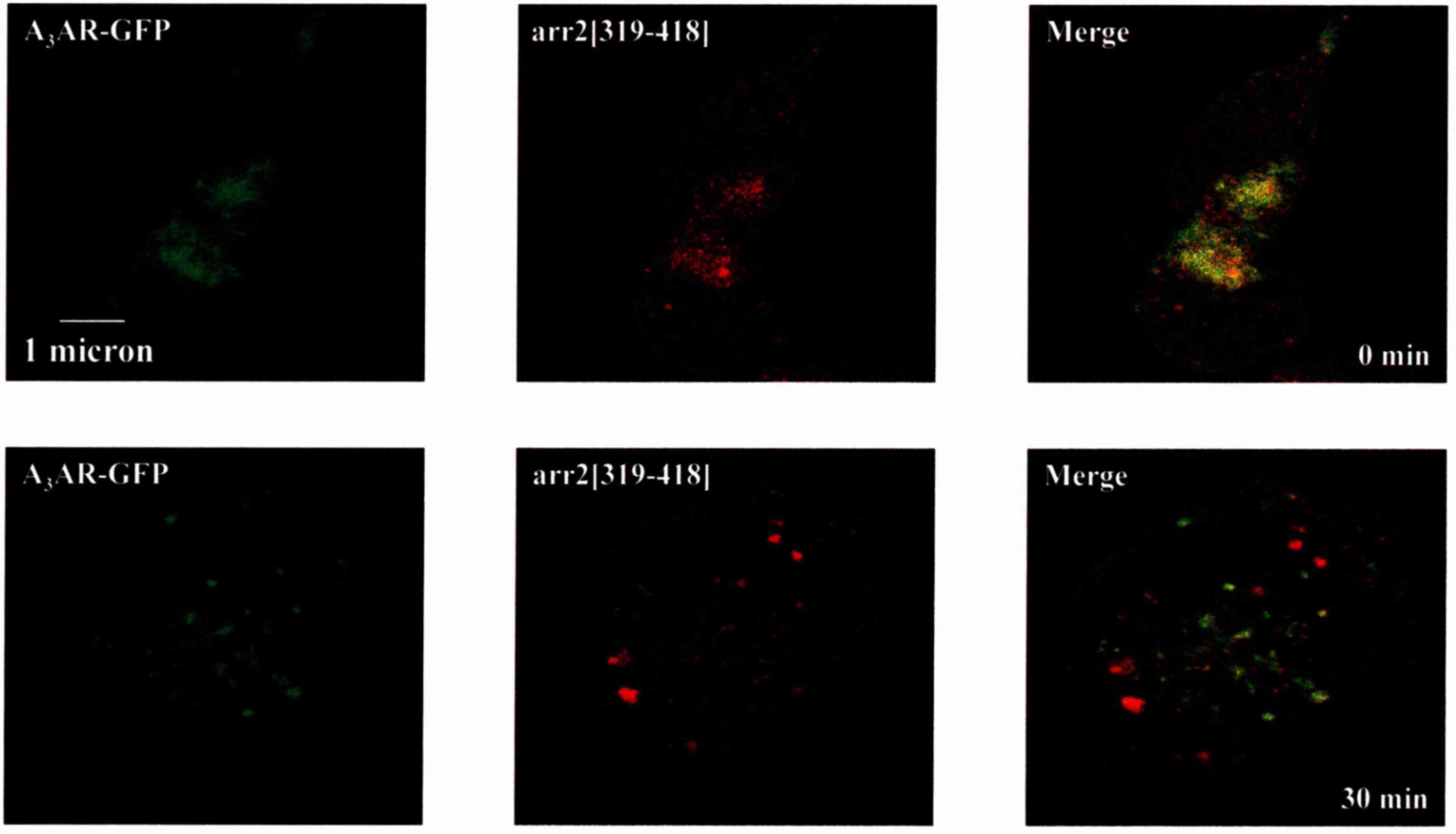
A3AR-GFP
1 micron
arr2[319-418]
Merge
0 min
A3AR-GFP
arr2[319-418]
Merge
30 min

Figure 4.22 **Confocal microscopic analysis of VSV-TRHR-GFP internalisation in the presence of the mutant arr2[319-418]**

Plain CHO cells transiently co-expressing VSV-TRHR-GFP and arr2[319-418] were treated with or without 10μM TRH for 30 minutes. Cells were solubilised and stained with anti-VSV primary antibody followed by Alexa-tagged anti-mouse secondary antibody as described in the Methods and visualised by confocal microscopy. arr2[319-418] (red) can be seen to be present in punctate spots throughout the cytoplasm confirming its interaction with endogenous clathrin molecules. Agonist stimulation can be seen to promote VSV-TRHR-GFP (green) internalisation in the presence of the arr2 mutant. The images shown opposite are representative examples of multiple experiments.

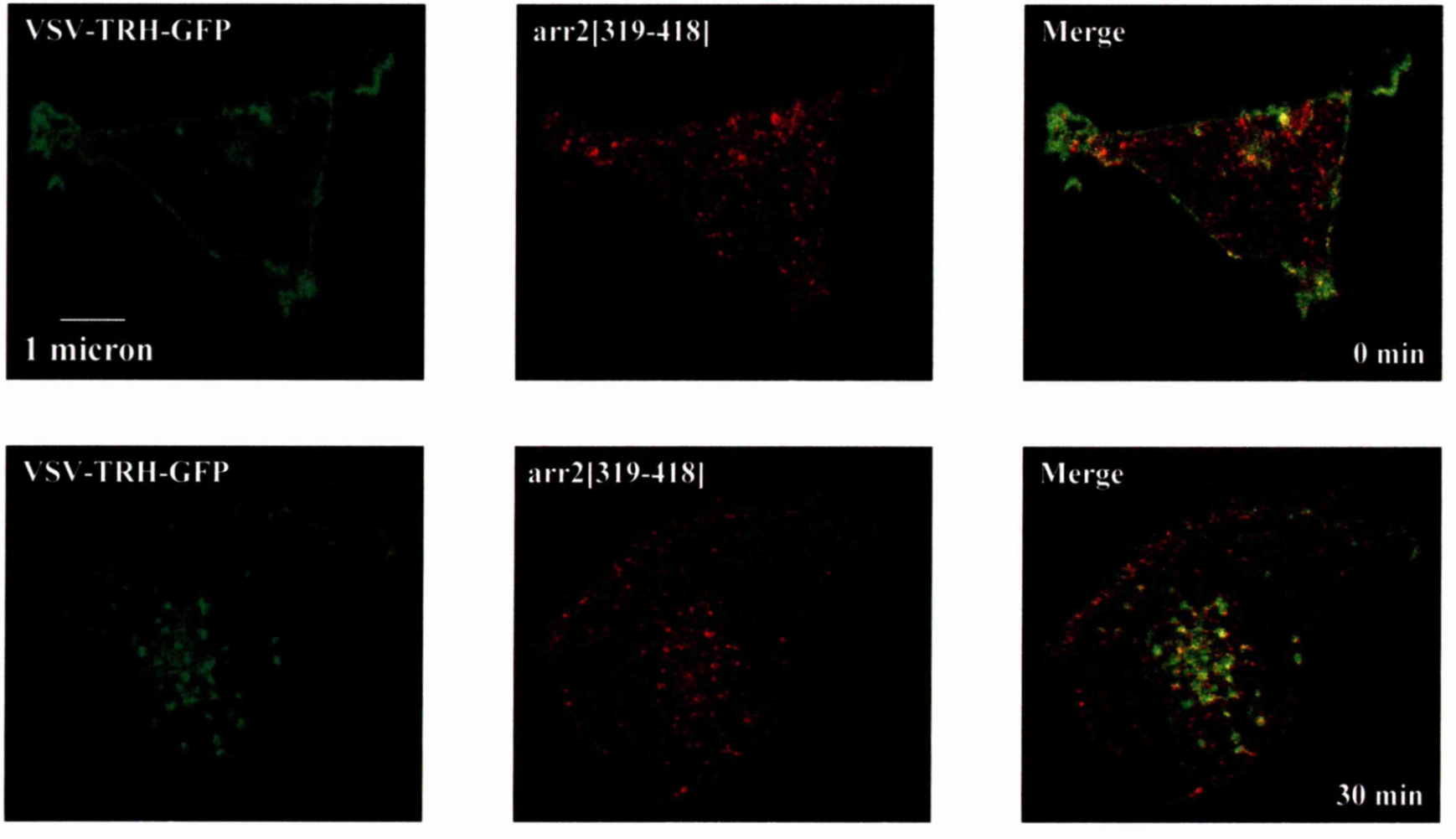
VSV-TRH-GFP
1 micron
arr2[319-418]
Merge
0 min
VSV-TRH-GFP
arr2[319-418]
Merge
30 min

Figure 4.23 **Confocal microscopic analysis of (C-A)A_3AR-GFP internalisation in the presence of the mutant arr2[319-418]**

CHO cells stably expressing (C-A)A_3AR-GFP were transfected with arr2[319-418] cDNA and treated with or without 1μM (R)-PIA for 30 minutes. Cells were solubilised and stained with anti-arrestin primary antibody followed by Alexa-tagged anti-mouse secondary antibody as described in the Methods and visualised by confocal microscopy. arr2[319-418] (red) can be seen to be present in punctate spots throughout the cytoplasm confirming its interaction with endogenous clathrin molecules. Agonist stimulation can be seen to promote (C-A)A_3AR-GFP (green) internalisation in the presence of the arr2 mutant. The images shown opposite are representative examples of multiple experiments.

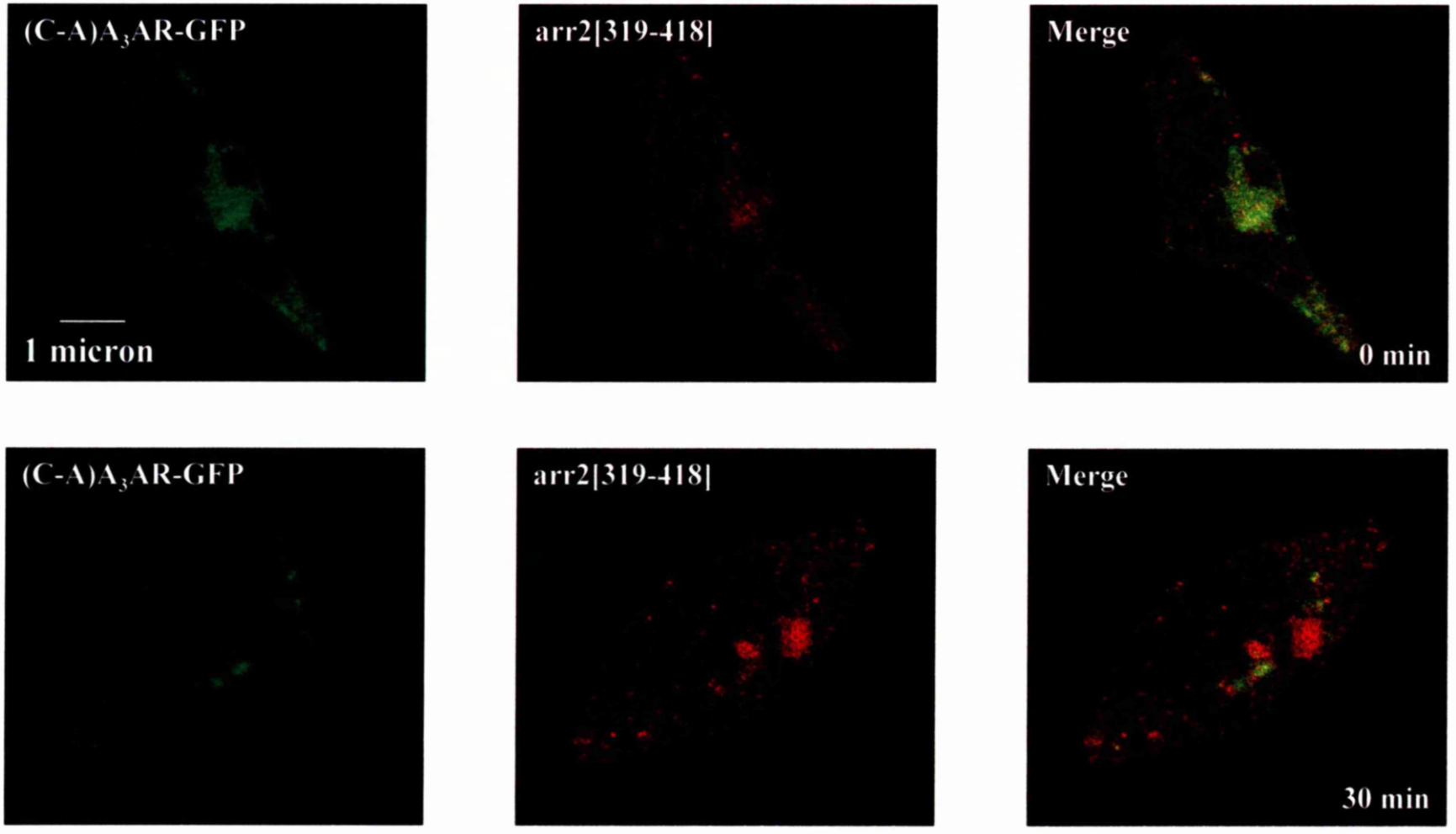
(C-A)A3AR-GFP
1 micron
arr2[319-418]
Merge
0 min
(C-A)A3AR-GFP
arr2[319-418]
Merge
30 min

Figure 4.24 **Immunodetection of increasing concentrations of myc-tagged dynamin[K44E] in transiently transfected CHO cells**

A_3AR-expressing CHO cells were transiently transfected with increasing concentrations of myc-tagged Dyamin[K44E] cDNA ranging from 0-2.0μg/well. Cells were solubilised and the resultant proteins separated by SDS-PAGE. Proteins were transferred to nitrocellulose and visualised by incubation with the myc-specific antibody 9E10 followed by HRP-conjugated anti-mouse secondary antibody. Typical data is shown from one of three experiments.

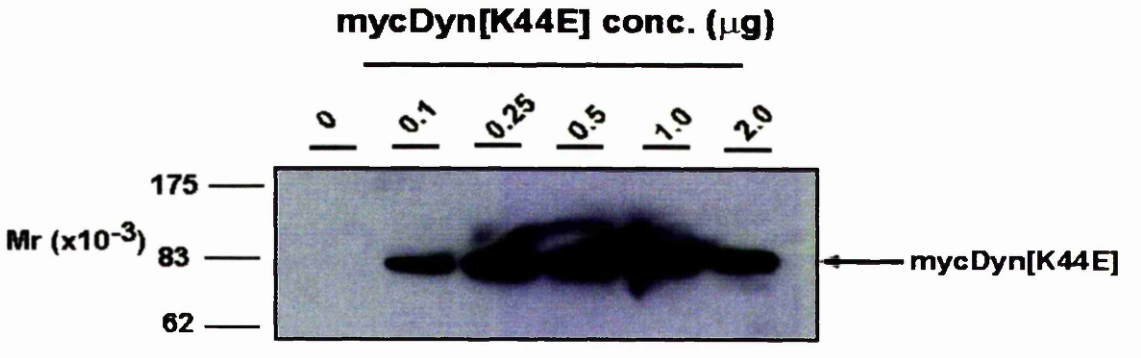
mycDyn[K44E] conc. (μg)
0
0.1
0.25
0.5
1.0
2.0
175
Mr (x10-3)
83
62
mycDyn[K44E]

Figure 4.25 **Confocal microscopic analysis of A_3AR-GFP internalisation in the presence of WT myc-dynamin**

CHO cells stably expressing A_3AR-GFP were transfected with WT myc-Dyn cDNA and treated with or without 1μM (R)-PIA for 30 minutes. Cells were solubilised and stained with anti-myc primary antibody followed by Alexa-tagged anti-mouse secondary antibody as described in the Methods and visualised by confocal microscopy. Agonist stimulation can be seen to promote A_3AR-GFP (green) internalisation in the presence of the myc-Dyn (red). The images shown opposite are representative examples of multiple experiments.

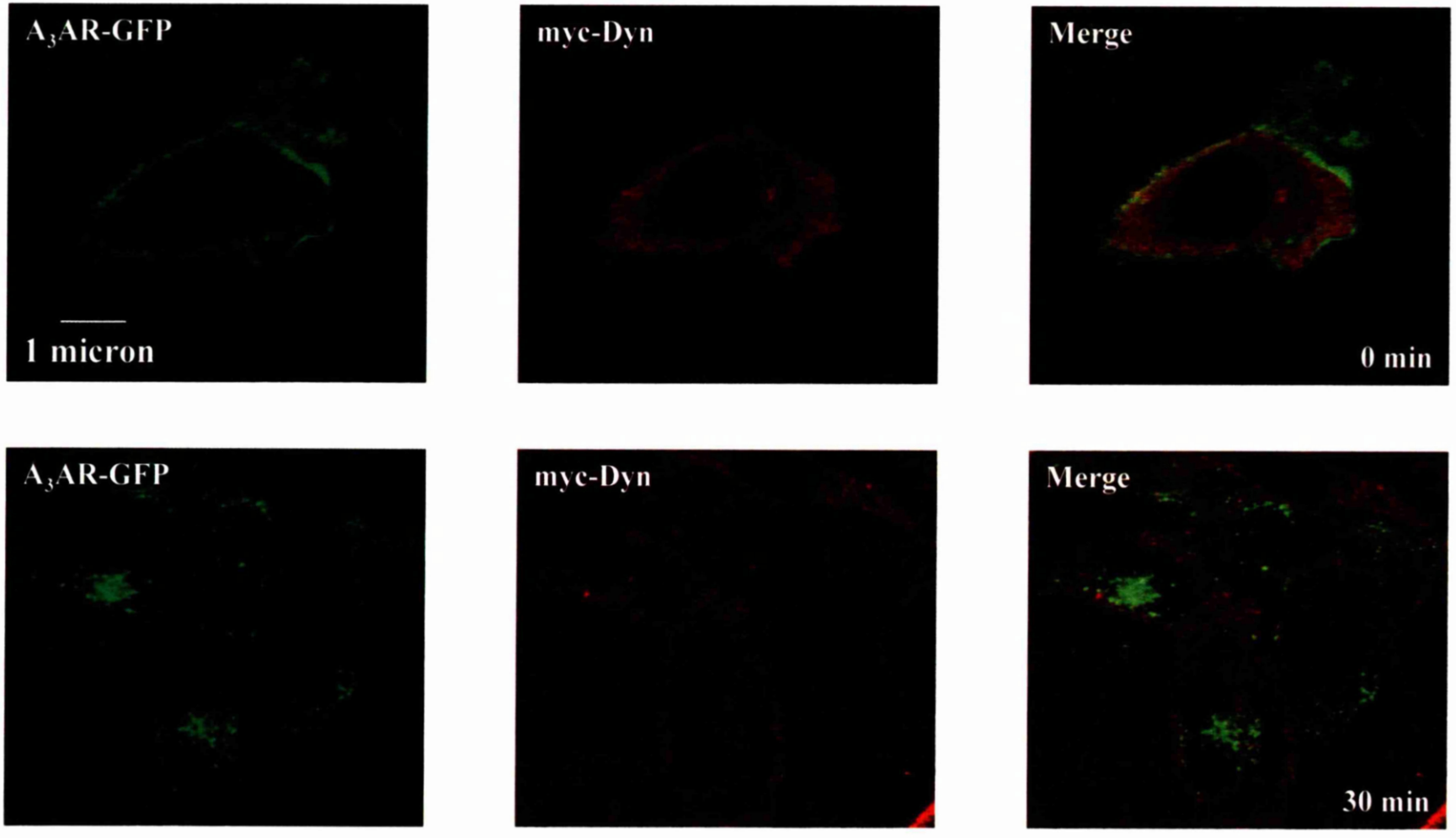
A_3AR-GFP
1 micron
myc-Dyn
Merge
0 min
A_3AR-GFP
myc-Dyn
Merge
30 min

Figure 4.26 **Confocal microscopic analysis of A_3AR-GFP internalisation in the presence of the mutant myc-dyn[K44E]**

CHO cells stably expressing A_3AR-GFP were transfected with myc-Dyn[K44E] cDNA and treated with or without 1μM (R)-PIA for 30 minutes. Cells were solubilised and stained with anti-myc primary antibody followed by Alexa-tagged anti-mouse secondary antibody as described in the Methods and visualised by confocal microscopy. Agonist stimulation can be seen to promote A_3AR-GFP (green) internalisation in the presence of the mutant dynamin (red). The images shown opposite are representative examples of multiple experiments.

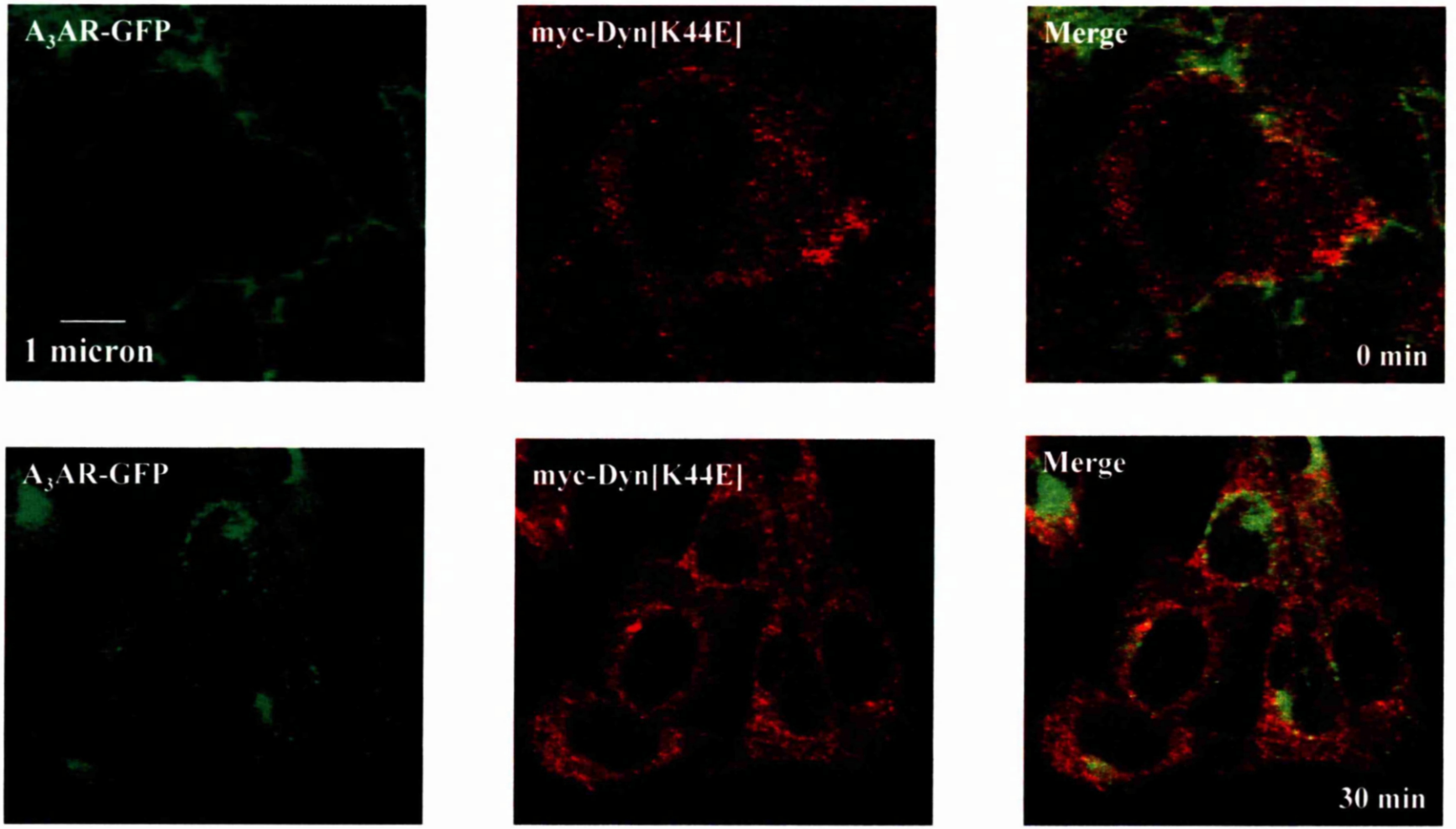
A_3AR-GFP
1 micron
myc-Dyn[K44E]
Merge
0 min
A_3AR-GFP
myc-Dyn[K44E]
Merge
30 min

Figure 4.27 **Confocal microscopic analysis of the effect of 0.4M sucrose on Alexa-Tfn internalisation and recycling**

HEK 293 cells were pre-labelled with Alexa-Tfn in the absence or presence of 0.4M sucrose for 30 minutes. Image (a) shows a normal distribution of Alexa-Tfn within the non-sucrose treated cells. Alexa-Tfn in the presence of 0.4M sucrose (b) was seen to cluster in large pools at the plasma membrane. The images shown opposite are representative examples of multiple experiments.

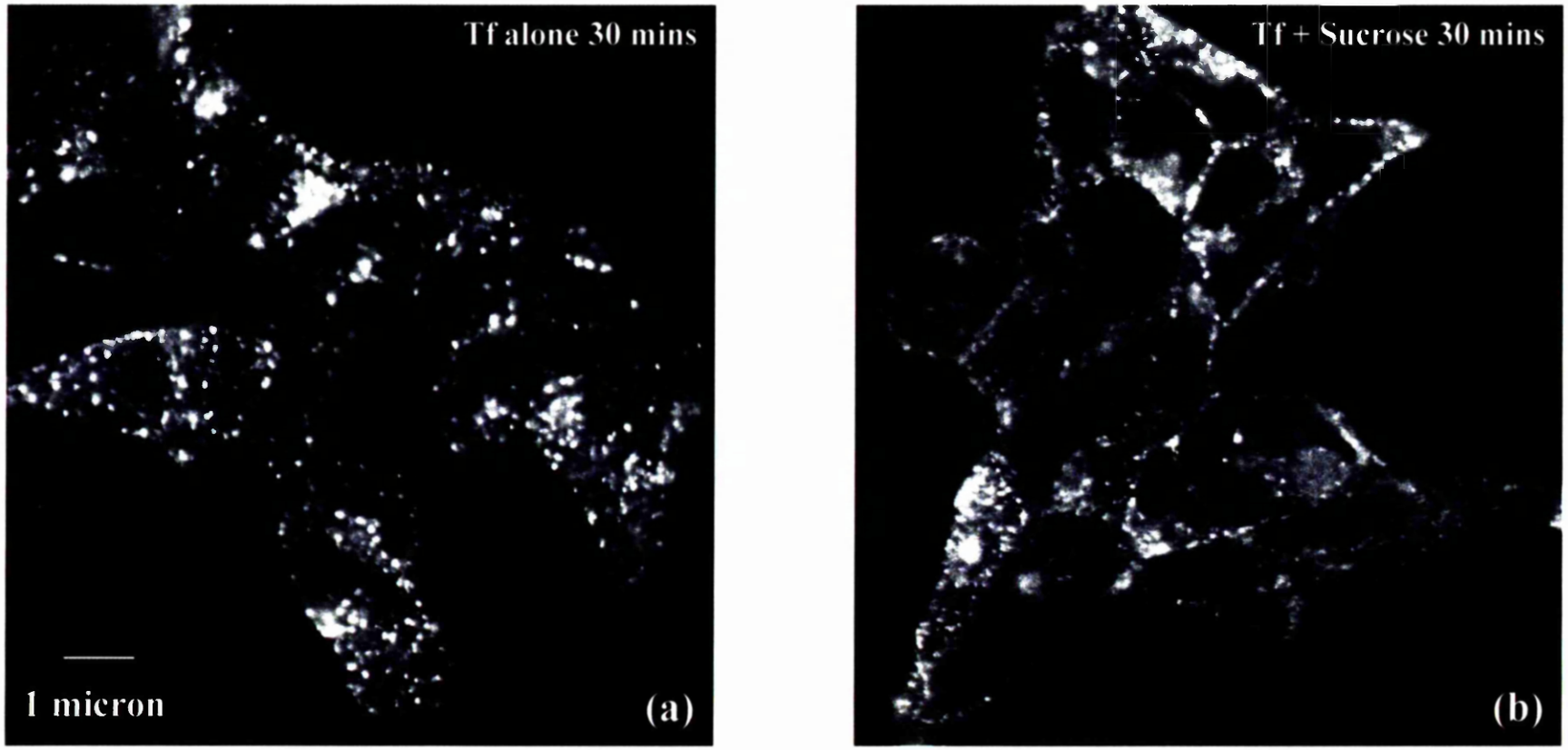
Tf alone 30 mins
1 micron
(a)
Tf + Sucrose 30 mins
(b)

Figure 4.28 **Confocal microscopic analysis of the effect of 0.4M sucrose on A_3AR-GFP internalisation**

Cells stably expressing WT A_3AR-GFP were treated in the absence or presence of 0.4M sucrose for 30 minutes. Prior to agonist stimulation, images (a) and (b) show expression of A_3AR-GFP at the plasma membrane in both the absence and presence of 0.4M sucrose. Stimulation with 1μM (R)-PIA in the absence of sucrose (c) led to normal A_3AR-GFP internalisation. The presence of 0.4M sucrose was seen to inhibit agonist-mediated internalisation of A_3AR-GFP as the receptor was retained at the plasma membrane (d). The images shown opposite are representative examples of multiple experiments.

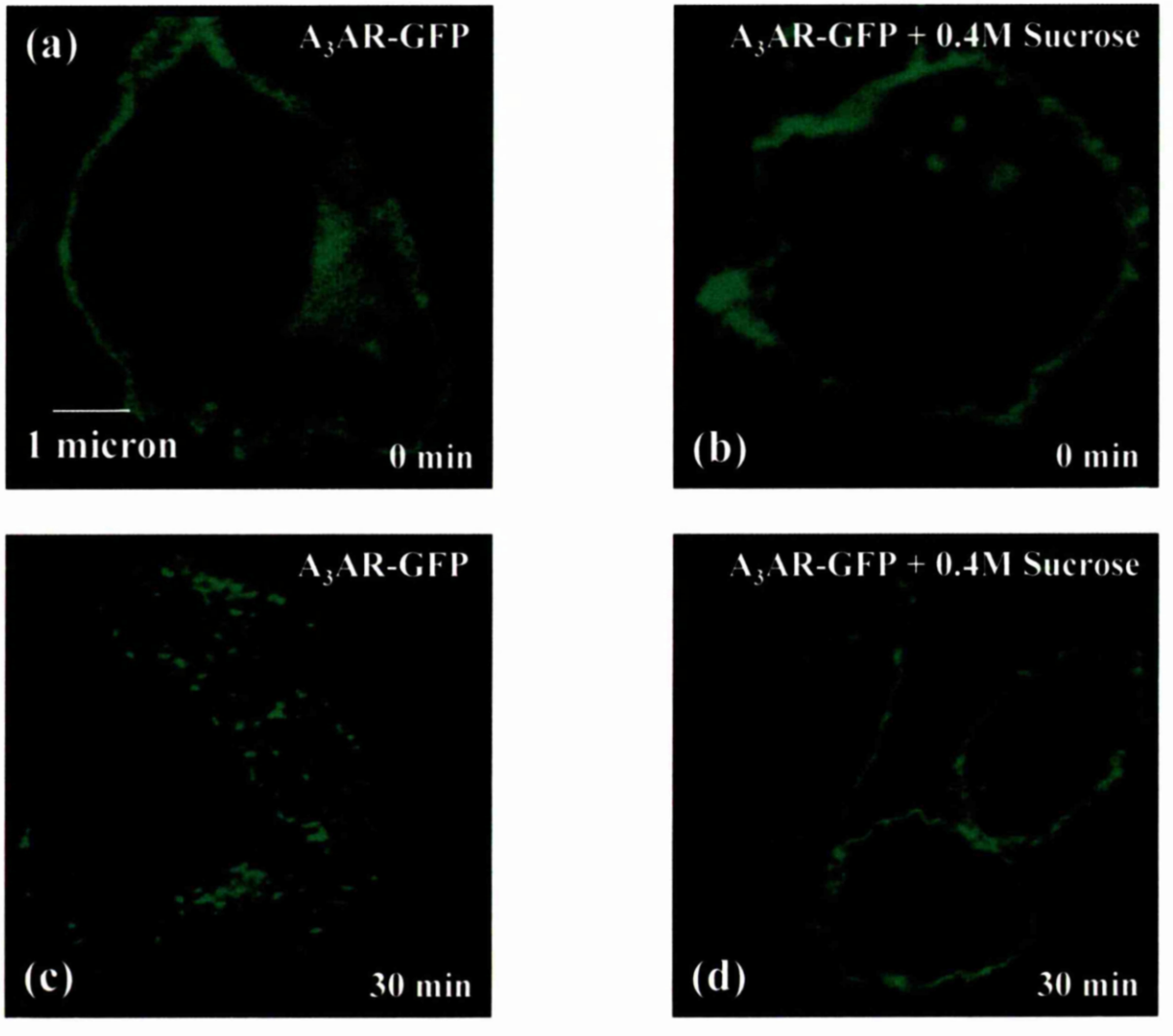
(a)
A_3AR-GFP
1 micron
0 min
A_3AR-GFP + 0.4M Sucrose
(b)
0 min
A_3AR-GFP
(c)
30 min
A_3AR-GFP + 0.4M Sucrose
(d)
30 min

Figure 4.29 **Confocal microscopic analysis of caveolin cellular distribution in HEK 293 cells transiently expressing A_3AR-GFP**

CHO cells stably expressing A_3AR-GFP were subjected to internalisation with 1μM (R)-PIA over a 30 minute period. Cells were fixed and solubilised as described in the Methods. Caveolin was detected by the use of anti-caveolin promary antibody followed by Alexa-tagged anti-mouse secondary antibody (red). Prior to agonist stimulation, A_3AR-GFP (green) and caveolin (red) were observed to overlap predominately at the membrane with very little co-localisation (yellow). Agonist activation led to internalisation of A_3AR-GFP to distinct spots in the cytoplasm with caveolin remaining at the plasma membrane. The images shown opposite are representative examples of multiple experiments.

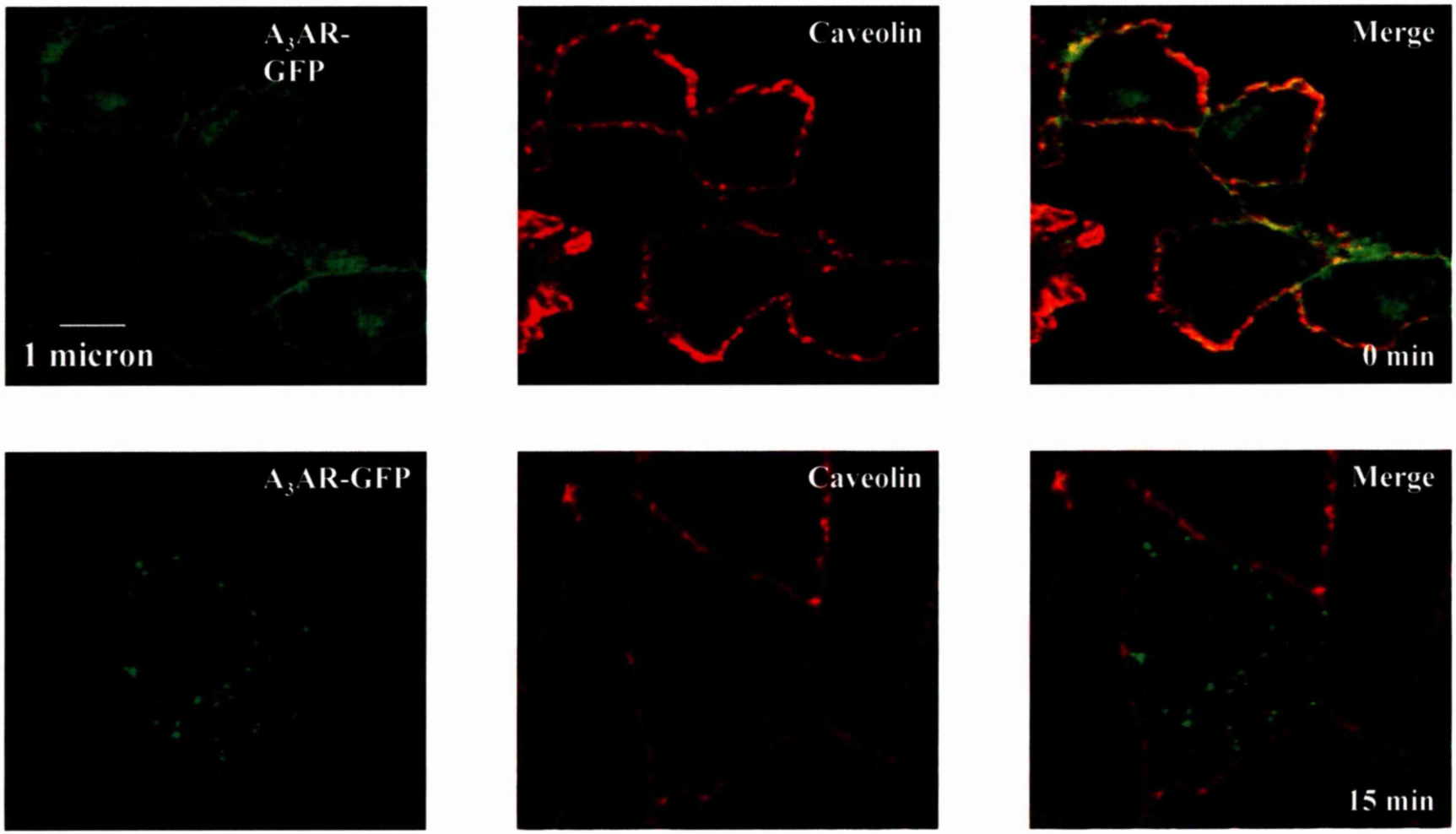
A_3AR-GFP
1 micron
Caveolin
Merge
0 min
A_3AR-GFP
Caveolin
Merge
15 min

4.3 Discussion

GPCRs play a key role in controlling regulation of numerous second messenger pathways. However, upon agonist activation, most GPCRs lose their ability to respond to the signal, a process commonly known as desensitisation. Agonist-specific desensitisation appears to be mediated primarily by two protein families: GRKs and arrestins. GRKs specifically bind to agonist-occupied receptors, promoting receptor phosphorylation that leads to arrestin binding. Arrestin binding disrupts receptor-G-protein interaction leading to functional desensitisation. Many receptors are then removed from the membrane *via* clathrin-mediated endocytosis (Krupnick and Benovic, 1998).

Several studies have suggested that agonist-induced translocation of receptors such as the β_2Ad, mACh (Koenig and Edwardson, 1996), μ and δ opioid (Keith et al., 1996) and TRH (Drmota et al., 1998) from the PM to intracellular vesicles occurs *via* the clathrin coated pit / endosomal pathway utilised by constitutively recycling receptors and growth factor receptors such as Tfn and epidermal growth factor receptor (EGFR) (Wakshull et al., 1985). Clathrin-coated pits are the primary PM specialisation involved in the uptake of a wide variety of molecules by receptor mediated endocytosis (Pearse and Crowther, 1987). Phosphorylation of receptors by GRKs serves to increase the affinity of GPCRs for arrestins, which in turn act as adapter-like molecules for receptor trafficking (Ferguson et al., 1996). Recent studies have demonstrated that arrestins can both desensitise agonist-activated GPCRs and promote their sequestration by also interacting with clathrin, the major protein component of the clathrin-based endocytic machinery (Goodman et al., 1996). With abundant data suggesting the clathrin pathway as the primary endocytosing mechanism by which GPCRs internalise, we investigated the possible involvement of this pathway in A_3AR internalisation.

In an initial attempt to determine the nature of the vesicles into which A_3AR-GFP was internalised, co-visualisation studies using Alexa-labelled Tfn were performed. These suggested that WT A_3AR, (C-A)A_3AR and A_1CT3AR were internalising *via* a pathway similar to that of Tfn and TRH due to the distinct yellow staining obtained following agonist stimulation (Figs. 4.1 – 4.5). As both Tfn and TRH receptors have been shown to internalise *via* clathrin-mediated endocytosis (Nussenzveig et al., 1993), it could be supposed that the ARs were being sequestered through a clathrin-containing pathway. However, in contrast to the TfnR, the A_3AR

is seen only to enter early endosomes upon agonist stimulation suggesting a possible interaction with other co-factors is required before internalisation can be initiated. It is not possible at this resolution to state categorically that this staining would indicate co-localisation in the same vesicles. However, it can be clearly seen that the vesicles containing the tagged proteins are at least in close proximity.

Agonist binding and subsequent internalisation of GPCRs *via* clathrin requires an auxiliary recruitment factor. In the case of the β_2AdR (Barak et al., 1997a), GnRH receptor (Vrecl et al., 1998) and TRHR (Groarke et al., 1999) this adapter has been shown to be arrestin. Phosphorylation of receptor following agonist stimulation promotes binding of arrestin which serves to uncouple the receptor from the G-protein and mobilise clathrin and other cytosolic proteins to the plasma membrane (Schmid, 1997; Fig. 4.6). Two ubiquitously expressed arrestins (arr2 and arr3) contain a region within their C-terminus that mediates binding to clathrin (Krupnick and Benovic, 1998). Arrestins 2 and 3 are 78% indentical in amino acid composition and widely expressed in tissues, but their expression level varies in a cell-type specific manner (Attramadal et al., 1992; Sterne-Marr et al., 1993). By utilising GFP-tagged chimeras of arr2 and arr3, we were able to visualise these proteins simultaneously with HA-tagged ARs and assess their involvement in agonist-mediated AR endocytosis. Agonist stimulation of β_2AdR has been shown to promote a sustained translocation of arr2 to the plasma membrane (Lin et al., 1997). Agonist stimulation did not produce arrestin translocation in cells co-transfected with arr2-GFP and either HA-A_3AR or HA-(C-A)A_3AR (Fig. 4.9 and 4.12). This lack of observable interaction could be attributed to the receptors themselves and not experimental error as THRH co-expressed with arr3-GFP was seen to co-localise as previously documented (Groarke et al., 1999). However, co-expression of arr3-GFP was seen to transiently co-localise with a small proportion of HA-tagged receptors in some cells, but more noticeable was the clustering of arr3-GFP at the plasma membrane without interaction with the receptors. This phenomenon of clustering has also been shown for arr2-GFP following stimulation of M_1 muscarinic acetlycholine and somatostatin receptors (Mundell and Benovic, 2000). A common assumption is that arrestins do not dissociate from desensitised receptors at the plasma membrane, but traffic with them into early endosomes (Ferguson et al., 1996; Krupnick and Benovic, 1998). However, recent observations have demonstrated that the fate of GPCR-arrestin complexes can differ among receptors (Zhang et al., 1999).

These data could suggest that ARs may internalise *via* an endosomal pathway that does not require arrestin or that interaction of arrestin with ARs is a rapid and transient process, therefore we do not see any interaction over the time-course investigated. One other possibility is that AR internalisation is mediated by a pathway not associated with arrestin such as caveolin or by a mechanism not yet defined.

To try to further establish any involvement of arrestins in AR sequestration, a mutant arrestin comprising of only the C-terminal tail was employed, arr2[319-418]. Previous studies have shown that the primary sites involved in arrestin interaction with phosphorylated GPCRs are localised to the NH_2-terminal half of the molecule (Krupnick et al., 1997b; Gurevich et al., 1993, 1995(a), 1995(b)). Therefore by expressing only the region of arrestin involved in clathrin binding (Krupnick et al., 1997b), it would be expected that internalisation of the ARs under investigation would be inhibited if they required arrestin proteins. As was seen in figures 4.21 and 4.22, this mutant arrestin failed to inhibit both AR and TRHR internalisation. This is in contrast to Vrecl et al. (1998) who showed inhibition of GnRH and TRH receptor internalisation in the presence of arr2[319-418]. From data obtained from Western blotting, the maximum concentration detected in our system was 0.5μg/well and was therefore used in subsequent confocal microscopy experiments. One possibility could be that the concentration of arr2[319-418] transiently expressed in the cells was insufficient to overcome the action of endogenous arrestin so that no inhibition of internalisation was observed. It was noted by Krupnick et al. (1997a) that over expression of arr2[319-418] was shown to display a constitutively punctate appearance, indicating binding to clathrin, which was also observed in our system. Having shown no distinction between the effects of WT and mutant arrestin, the possibility that confocal microscopy may not be sensitive enough to detect subtle differences, such as a small decrease in receptor internalisation, becomes apparent. One possible way to detect inhibition in sequestration brought about by the presence of arr2[319-418] could be to express increasing concentrations of arr2[319-418] in cells stably transfected with A_3ARs. Biotin-labelling and immunoprecipitation would detect loss of cell surface receptors upon agonist stimulation. This can be supported by the fact that mutant GRK2 (GRK2[BK-CT]) was seen to inhibit AR phosphorylation in a concentration-dependent manner on Western blots but was not seen to have an effect on internalisation when observed confocally. It is also known

that HEK 293 cells have a higher endogenous level of arrestin than, for example, COS cells. HEK 293 cells may require a higher concentration of mutant arrestin to inhibit the system (Ferguson et al., 1996 and Zhang et al., 1996) therefore another possibility would be to carry out this analysis in another cell type such as COS.

An essential step in many vesicle trafficking pathways is the release or budding of the vesicles from membranes. Substantial evidence suggests that dynamin oligomerisation around the necks of endocytosing vesicles and subsequent dynamin-catalysed GTP hydrolysis is responsible for membrane fission (Takei et al., 1999; Sweitzer and Hinshaw, 1998). Previous studies have indicated that expression of this mutant in HEK 293 cells stably transfected with δ-opioid receptor can inhibit agonist-induced internalisation by clathrin coated pits (Herskovits et al., 1993; van der Bliek et al., 1993 and Chu et al., 1997). In contrast to this, when co-expressed transiently with VSV-TRHR-GFP (not shown) or A_3AR-GFP, myc-Dyn[K44E] was not seen to inhibit agonist-mediated internalisation of either receptor (Fig. 4.24). This phenomenon could again be due to an insufficient level of myc-Dyn[K44E] being expressed in the cells, but it could also be possible that agonist-activated receptors are internalising *via* a different pathway when their primary route of internalisation is disrupted.

The clathrin-mediated pathway of internalisation did not appear to be inhibited by the use of dominant-negative or truncated mutants of proteins shown previously to be involved in clathrin-coated pit internalisation (Figs. 4.19, 4.21 – 4.23). Following from these data, a less subtle approach to inhibition of internalisation was taken. Daukas and Zigmond (1985) first showed that exposure of leukocytes to medium containing 0.4M sucrose caused rapid and reversible inhibition of receptor-mediated internalisation, suggesting that coated-pit function could be inhibited by hypertonicity. This effect has been shown for other receptor types including LDLR (Heuser and Anderson, 1989) and TRHR (Drmota et al., 1998). As such, there was a possibility that sucrose could also inhibit the AR system as WT and mutant A_3ARs had previously been shown to internalise to endosomes along with receptors such as Tfn which are known to internalise *via* clathrin coated vesicles (Figs. 4.2, 4.4 and 4.5). Sucrose inhibits the formation of clathrin pits by disrupting the interaction of clathrin triskelions. Control cells expressing only Alexa-Tfn showed inhibition of internalisation and recycling in the presence of 0.4 M sucrose (Fig. 4.27). CHO cells stably transfected with WT A_3AR-GFP (Fig. 4.28) also

showed an inhibition in internalisation in the presence of sucrose, suggesting that this receptor did in fact use the CCV pathway for sequestration upon agonist activation.

One other possibility is the involvement of other vesicular pathways that could be employed by the A_3AR upon agonist activation. One such pathway invloves the interaction of the activated receptors with caveolin. As stated before, caveolae are small vesicles known to be involved in the endocytosis of many different molecules. However, dual imaging of A_3AR-GFP and endogenous caveolin by confocal microscopy did not show an interaction of these two proteins either before or after agonist stimulation suggesting that caveolin plays no role in AR sequestration (Fig. 4.29). Recent work by Okamoto et al. (1998) has determined a caveolin binding motif that is present in most caveolae-associated proteins (Couet et al. 1997) such as receptors, G_α subunits and kinase domains of many protein kinases. There is no comparable site within the A_3AR, supporting the lack of interaction between the receptor and caveolin.

These data alone are inconclusive concerning the involvement of CCVs in AR internalisation, however, when taken together, these data collected thus far suggests that agonist-mediated AR sequestration is an arrestin-independent but clathrin-dependent mechanism.

Chapter 5

Study of Agonist-mediated A_3AR Down-Regulation

5.1 Introduction

Agonist stimulation leads to the desensitisation of GPCR function by three temporally distinct mechanisms: phosphorylation, internalisation and down-regulation (Gagnon et al., 1998). Down-regulation is defined as an overall decrease in receptor number in response to prolonged receptor stimulation, and can occur as a consequence of either increased lysosomal degradation of pre-existing receptors and/or reduced mRNA and receptor protein synthesis (Bouvier et al., 1989).

As can be seen in Fig. 5.1, four main pathways determine the intracellular distribution of GPCRs. Upon synthesis, new receptors are delivered from the Golgi complex to the cell surface where, in the absence of agonist, there is a slow rate of endocytosis from the membrane into endosomes. Agonist stimulation dramatically increases the rate of receptor internalisation. Upon accumulation in the endosomes, receptors such as the β_2AdR become dissociated from their ligand, dephosphorylated and recycled back to the plasma membrane for another round of agonist stimulation (Trejo and Coughlin, 1999). Following sustained agonist exposure, some receptors can be routed to lysosomes where they are degraded. Trafficking of GPCRs from endosomes to lysosomes leading to down-regulation has been described for several GPCRs, including those for thrombin (protease-activated receptor, PAR1) (Hein et al., 1994), thyrotropin (Petrou and Tashjian, 1995) and cholecystokinin (Tarasova et al., 1997).

The aim of the following experiments was to assess the consequences of chronic treatment of A_3ARs with agonist to determine whether or not this receptor follows the down-regulation pathway cited above.

5.2 Results

Firstly, to determine if prolonged agonist treatment induced down-regulation of the A_3AR, CHO cells stably expressing HA-A_3ARs were seeded into 6-well plates and treated with or without agonist over a 24 hour period. Solubilised cell extracts were analysed by immunoblotting with an anti-HA-specific antibody as described in the Methods. In the presence of 10μM NECA, HA-A_3AR protein levels were reduced by 90 ± 2% compared to non-stimulated controls ($p<0.05$) indicating a down-regulation of the total number of cellular receptors present in the cells (Fig. 5.2). To assess any effect of the GFP tag on receptor down-regulation, the same experiment was carried out using A_3AR-GFP expressing CHO cells in which they were treated in the absence or presence of 1μM (R)-PIA over a 24 hour period. Cell extracts were analysed by immunoblotting using an anti-GFP-specific antibody as previously described. Compared to non-stimulated receptors, the protein levels of agonist treated A_3AR-GFP expressing cells was reduced by 64 ± 11% ($p<0.05$; Fig. 5.3). Although less of the GFP-tagged receptor was down-regulated overall, both sets of data showed a significant difference in the levels of receptor protein in the absence and presence of agonist. GFP-tagged constructs were used in subsequent experiments for two reasons. Firstly, the antibody against GFP bound with higher affinity and greater sensitivity than the HA-specific antibody, thus requiring less protein per assay. Secondly, it was not possible to assay receptor down-regulation *via* ligand binding as receptor-ligand interactions are relatively unstable therefore we would not be detecting receptor down-regulation, more receptor-ligand uncoupling.

Having shown the A_3AR-GFP to be down-regulated in the continued presence of agonist over 24 hours, we explored the effects of increasing agonist concentration on receptor down-regulation. A_3AR-GFP expressing CHO cells were seeded into 6-well plates and treated with agonist at the concentrations indicated (Fig. 5.4). Quantitation of the blots revealed maximal receptor down-regulation (86 ± 5%, $p<0.05$) to be obtained at approximately 0.5μM. This gave an IC_{50} value for A_3AR-GFP down-regulation in the range of 0.05 to 0.5μM. When treated with low nanomolar concentrations of agonist (5nM), it was observed that there was a small, reproducible yet non-significant increase in the total amount of A_3AR-GFP protein detected in the cells ($p>0.05$, N.S.). A similar phenomenon had been observed previously when investigating the effect of increasing agonist concentration on

receptor internalisation (Chapter 3). The effect of prolonged agonist exposure on A_3AR-GFP was further investigated by exploring the time-course of this down-regulation over 24 hours. CHO cells expressing A_3AR-GFP were plated onto 6 well plates as described previously and left to recover overnight. The following day, cells were treated with or without agonist at the time points indicated and solubilised cell extracts analysed by immunoblotting as before. The greatest loss of receptor was detected between 4-12 hours of agonist exposure with a $t_{½}$ for internalisation occurring at approximately 5½ hours (Fig. 5.5). Maximal down-regulation was obtained by 12 hours of agonist exposure (87 ± 4%, $p<0.05$). Further time-course experiments narrowed this window to between 8-12 hours (Fig. 5.6).

Having detected a significant loss of overall A_3AR-GFP number in chronically agonist treated cells, we attempted to visualise this phenomenon in intact cells by confocal microscopy. A_3AR-GFP expressing cells were plated onto coverslips as described previously and treated in the presence or absence of 1μM (R)-PIA over a 24 hour period. Cells were then fixed and their subcellular distribution visualised as described in the Methods. Consistent with immunoblotting data, computational analysis that quantitatively measured the total fluorescence in selected areas containing multiple cells, confirmed that treated cells compared to untreated did in fact show a significant level of down-regulation (Fig. 5.7). This reduction in receptor levels was calculated to be 46 ± 8% ($p<0.05$) compared to untreated controls.

Once internalised, many membrane receptors and transporters including ET_B (Abe et al., 2000) and human dopamine transporter (hDAT; Daniels and Amara, 1999) transit through the endosomal/lysosomal pathway and are ultimately degraded (Chpt. 2, section 1.4.3a). Having shown that A_3AR-GFP was down-regulated in response to agonist, the next step was to try to characterise the degradation pathway utilised. Thus, CHO cells stably expressing A_3AR-GFP were seeded onto coverslips and pre-incubated for 30 minutes with LysoTracker™Red, a fluorescently labelled acidotropic probe which specifically labels acidic lysosomes (Anderson and Orci, 1988). LysoTracker was removed, the cells washed once and subsequently treated in the presence or absence of 1μM (R)-PIA over 24 hours. Cells were then fixed and visualised as described in the Methods. Confocal microscopy revealed A_3AR-GFP to be present predominantly at the plasma membrane prior to agonist treatment, with

LysoTracker™Red labelling distinct spots within the cytoplasm (Fig. 5.8, 0 minutes, merge). Following a 24 hour incubation with 1μM (R)-PIA, A_3AR-GFP had translocated from the plasma membrane to spots within the cytoplasm that were distinct from those vesicles labelled with LysoTracker™ (Fig. 5.8, 24hrs, merge), signifying no accumulation of A_3AR-GFP with lysosomes at this time point. Immunoblotting experiments showed agonist-induced down-regulation of A_3AR-GFP between 8-12 hours. Consequently the time-course of agonist treatment in the presence of LysoTracker™ was reduced to a maximum of 16 hours. Cells were treated as described previously and visualised by confocal microscopy. In the absence of agonist treatment, A_3AR-GFP was observed at the membrane with distinct lysosomal staining within the cytoplasm (Fig. 5.9, 0 minutes, merge). Agonist treatment over 16 hours failed to show co-localisation of A_3AR-GFP with lysosomes (Fig. 5.9, time points, merge).

Given the apparent lack of interaction between receptors and lysosomes, we investigated the possibility that another pathway for down-regulation was being utilised. The ubiquitin system of protein degradation controls the abundance of many critical regulatory proteins, membrane receptors, transporters and channels (Rotin et al., 2000). Protein degradation by the ubiquitin system involves two distinct and successive steps: 1) covalent attachment of a 76 amino acid polypeptide, ubiquitin, or a multi-ubiquitin chain to the end of the target protein and 2) degradation of the tagged protein by the 26S proteosome (Ciechanover, 1998). The proteosome is an essential component of the ATP-dependent proteolytic pathway in eukaryotic cells (Coux et al., 1996). The 26S proteosome (2000 kDa) is composed of a main core protease-catalytic complex (20S) flanked on both sides by 19S regulatory complexes composed of multiple ATPases. Together, this complex recognises specific ubiquitinated proteins and targets them for degradation. Ubiquitin activating enzyme (E1) catalyses the activation of ubiquitin in an ATP-dependent reaction by formation of a high-energy thiolester intermediate with ubiquitin involving an internal Cys residue. The activated ubiquitin is then transferred to a Cys residue of ubiquitin conjugating or E2 enzyme, generating another thiolester intermediate. In most cases, an E2 transfers ubiquitin to several substrate-specific E3 enzymes. E3 or ubiquitin-protein ligase enzymes link ubiquitin by its C-terminus to an ε-amino group of the substrate protein's Lys residues or with a polyubiquitin

chain already anchored to it. Formation of a substrate-E3 complex and synthesis of a substrate-anchored polyubiquitin chain causes binding of the polyubiquitinated substrate to the ubiquitin receptor subunit present in the 19S complex of the 26S proteosome. The protein is then degraded into short polypeptides by the 20S complex and the ubiquitin is recycled (Ciechanover, 1998; Hershko and Chiechanover, 1998).

To investigate any interaction between the A_3AR and down-regulation *via* the ubiquitin pathway, A_3AR-GFP-expressing CHO cells were seeded into 6-well plates and subjected to a 30 minute incubation with proteosomal (MG-132; 10μM) or lysosomal (chloroquine; 45μM and NH_4Cl; 15mM) inhibitors in the presence of ADA. Cells were then treated in the absence or presence of 1μM (R)-PIA for 24 hours in the continued presence of the inhibitors and ADA. Following agonist treatment, the cells were solubilised and receptor levels analysed by immunoblotting with anti-GFP antibody as previously described. The blots obtained showed that (R)-PIA-mediated down-regulation of A_3AR-GFP was reduced to 6 ± 5% by MG-132 and 19 ± 9% by chloroquine (Fig. 5.10). Treatment with NH_4Cl did not appear to inhibit down-regulation as the extent of receptor down-regulation was not different from that of cells treated only with ADA and agonist (59 ± 11% vs 57 ± 13% respectively; $p>0.05$, N.S.). The differences of inhibition observed between MG-132 and chloroquine treated cells were found to be statistically insignificant (6 ± 5% vs 19 ± 9%; $p>0.05$, N.S.), suggesting that MG-132 and chloroquine inhibit agonist-mediated down-regulation equally.

Down-regulation is defined as a net loss of receptor protein following agonist stimulation. This suggests that recovery from down-regulation requires new protein synthesis (Doss et al., 1981). Newly synthesised receptor proceeds from the ER to the Golgi apparatus from where it is transported to the plasma membrane. In an attempt to detect synthesis of new receptor following agonist-mediated down-regulation, A_3AR-GFP expressing cells were plated onto coverslips and left to recover overnight. The following day, the cells were treated with 1μM (R)-PIA for a 24 hour period. Cells were then fixed, solubilised and stained using Alexa^{594}-concanavalin A, a lectin that binds to α-mannopyranosyl and α-glucopyranosyl residues in the ER, or a polyclonal antibody against GM-130, a 130kDa matrix protein that has an immunogenic C-terminal that interacts with the Golgi membranes.

Cells labelled with anti-GM-130 were subsequently labelled with Alexa^{594}-conjugated anti-mouse secondary antibody as described in the Methods to allow visualisation *via* confocal microscopy. The initial images obtained did not show any co-localisation between A_3AR-GFP and either ER (Fig. 5.11) or Golgi (Fig. 5.12). The possibility that receptor synthesis was taking place only after the signal to down-regulate had been removed was investigated by plating A_3AR-GFP-expressing CHO onto coverslips and treating in the presence or absence of 1μM (R)-PIA over a 24 hour period. The following day, the medium containing agonist was replaced with fresh medium for a time course ranging from 30 minutes to 3 hours. Cells were fixed, solubilised and fluorescently labelled as previously described. From the preliminary images obtained, it was not possible to detect co-localisation of the GFP-tagged A_3AR with the ER over the time course investigated. It was observed that green fluorescence was located around the nucleus at approximately 1hr 30 minutes following agonist removal (Fig. 5.13). Comparison with the cells stained for Golgi, the green fluorescence was observed in the nuclear area along with the red Golgi marker at the 1 hour time-point (Fig. 5.14). These two stains were seen to overlap and give yellow staining in the images taken from the 1 - 1.5 hour time points, suggesting that new receptor was being synthesised.

Figure 5.1 **Schematic representation of the pathways determining GPCR subcellular distribution**

Newly synthesised receptors are subject to trafficking from the endoplasmic reticulum to the Golgi apparatus from where they are targeted to the plasma membrane in preparation for agonist activation. Upon binding of agonist, many GPCRs undergo desensitisation and subsequent sequestration into clathrin coated vesicles. Once internalised, the receptors can be dephosphorylated and recycled to the plasma membrane for another round of agonist activation or targeted for proteolytic degradation.

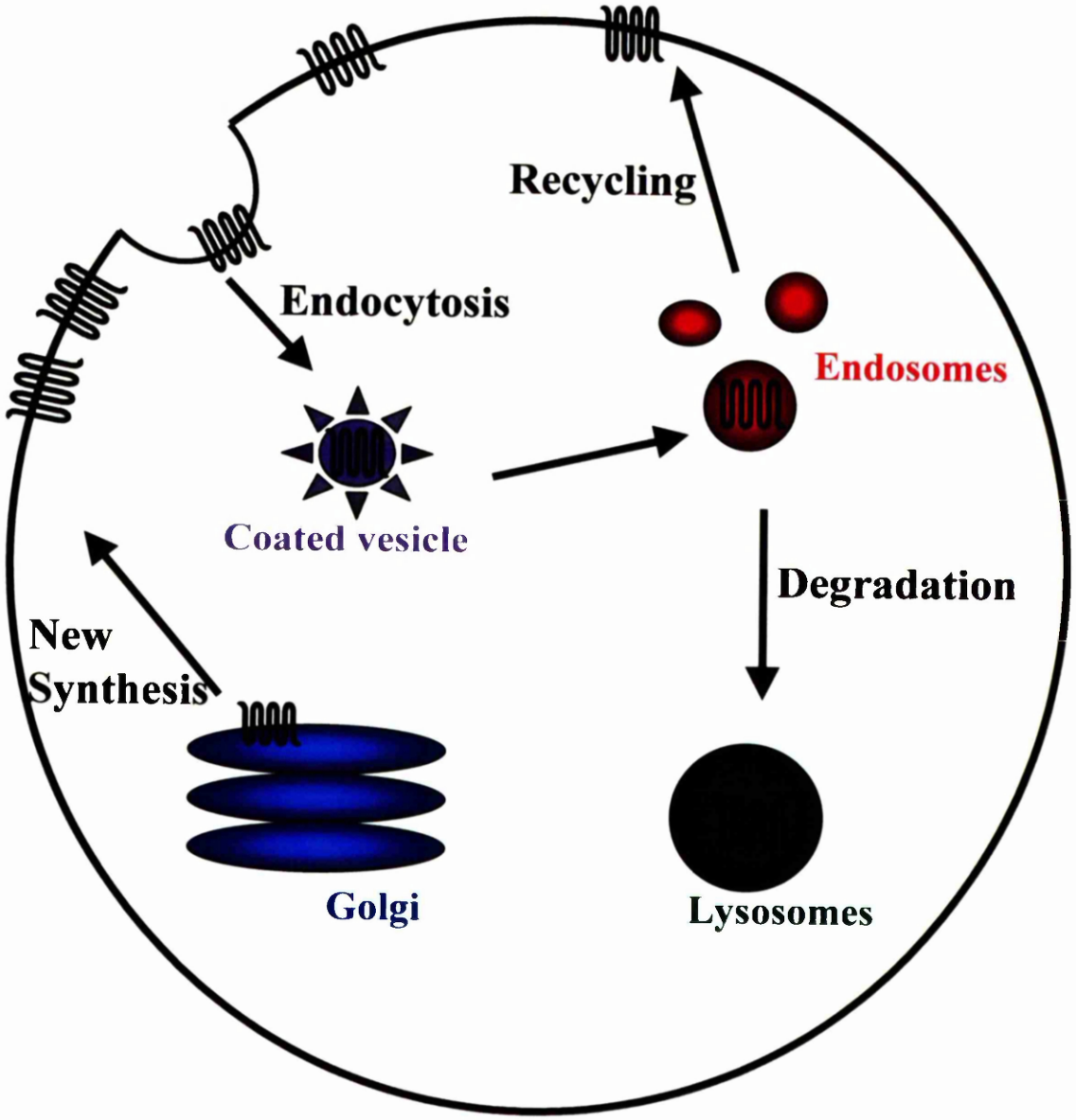
Recycling
Endocytosis
Endosomes
Coated vesicle
Degradation
New
Synthesis
Golgi
Lysosomes

Figure 5.2 Agonist-mediated down-regulation of HA-A_3AR expressed in CHO cells

CHO cells stably expressing HA-A_3AR were treated in the presence or absence of 10μM NECA over 24 hours. Cells were solubilised and the resultant protein separated by SDS-PAGE. Proteins were transferred to nitrocellulose and visualised by incubation with an anti-HA-specific antibody followed by HRP-conjugated anti-mouse secondary antibody. Blots were quantified by densitometric scanning and values represent mean ± S.E. for three experiments. The total cellular level of receptor in the absence of agonist is set at 100%.

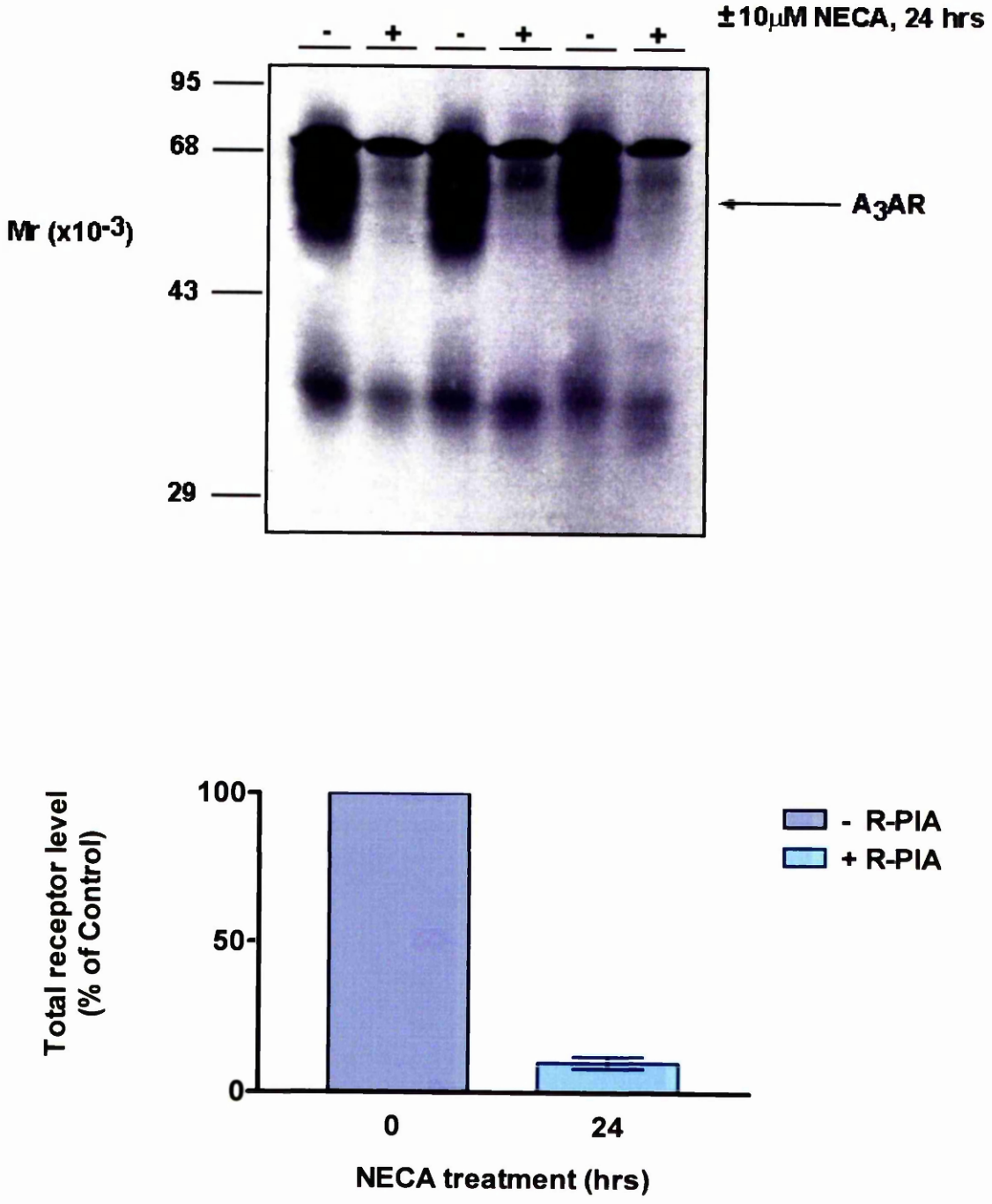
±10μM NECA, 24 hrs
- + - + - +
95
68
43
29
Mr (x10-3)
A3AR
Total receptor level (% of Control)
100
50
0
- R-PIA
+ R-PIA
0
24
NECA treatment (hrs)

Figure 5.3 **Agonist-mediated down-regulation of A_3AR-GFP expressed in CHO cells**

CHO cells stably expressing A_3AR-GFP were treated in the presence or absence of 1μM (R)-PIA over 24 hours. Cells were solubilised and the resultant protein separated by SDS-PAGE. Proteins were transferred to nitrocellulose and visualised by incubation with an anti-GFP-specific antibody followed by HRP-conjugated anti-sheep secondary antibody. Blots were quantified by densitometric scanning and values represent mean ± S.E. for three experiments. The total cellular level of receptor in the absence of agonist is set at 100%.

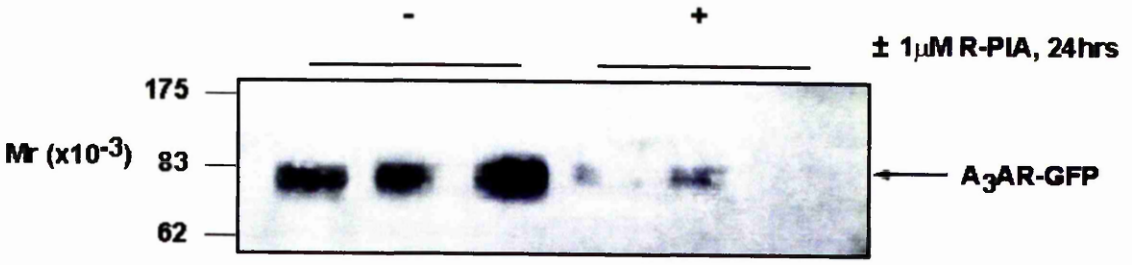
-
+
± 1μM R-PIA, 24hrs
175
Mr (x10-3)
83
62
A3AR-GFP

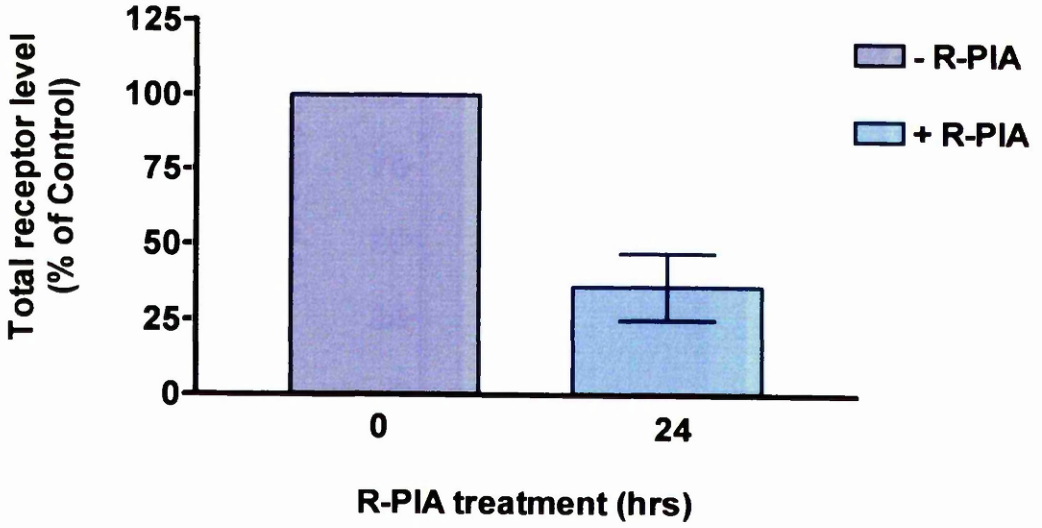
125
100
75
50
25
0
Total receptor level
(% of Control)
- R-PIA
+ R-PIA
0
24
R-PIA treatment (hrs)

Figure 5.4 Effect of increasing agonist concentration on A_3AR-GFP down-regulation

A_3AR-GFP expressing CHO cells were incubated with (R)-PIA at the concentrations indicated for 24 hours at 37°C. Cells were then solubilised and separated by SDS-PAGE before transfer to nitrocellulose. Visualisation was by incubation with anti-GFP-specific antibody followed by HRP-conjugated anti sheep secondary antibody. Blots obtained from three experiments were quantitated by densitometric scanning. The levels of cell-surface receptors in untreated cells were set at 100% and those treated only with agonist at 0%. The total levels of receptor in the agonist treated samples were normalised with respect to these limits. The figures are representative of three experiments that produced similar results.

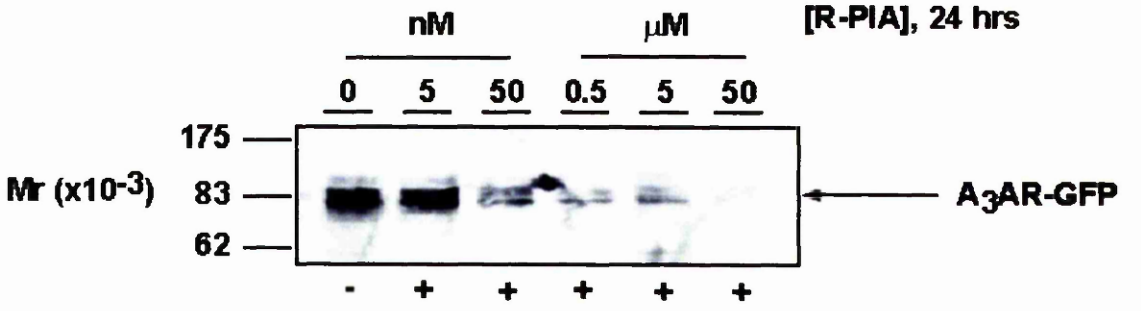
nM
μM
[R-PIA], 24 hrs
0
5
50
0.5
5
50
175
83
62
Mr (x10-3)
A3AR-GFP
-
+
+
+
+
+

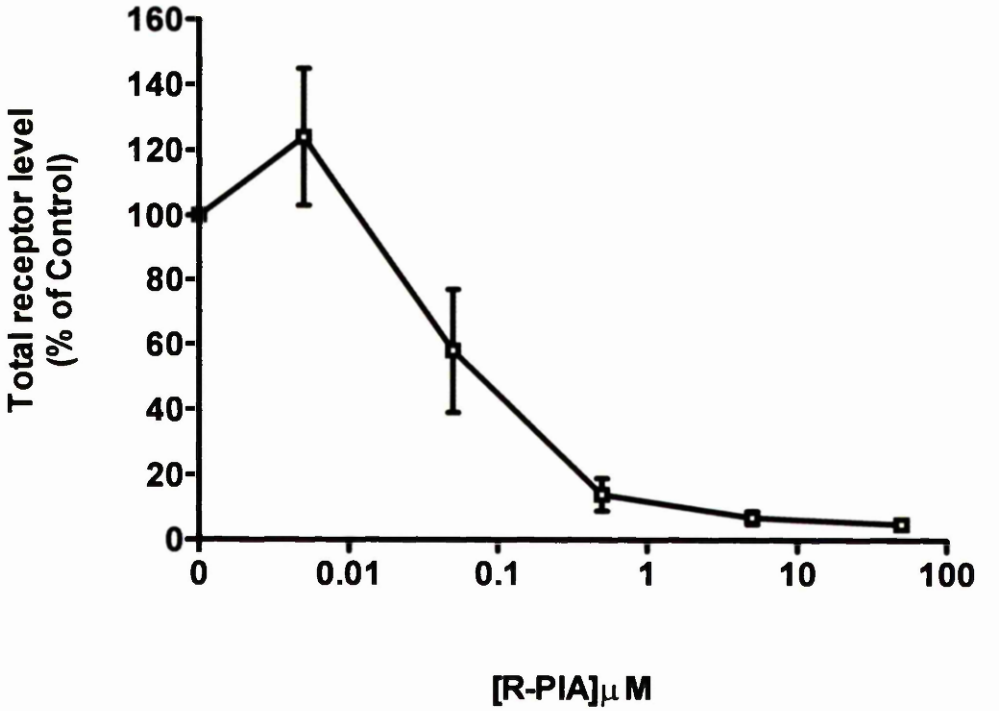
160
140
120
100
80
60
40
20
0
Total receptor level
(% of Control)
0
0.01
0.1
1
10
100
[R-PIA]μM

Figure 5.5 Time-course of agonist-mediated A_3AR-GFP down-regulation

CHO cells stably expressing A_3AR-GFP were treated in the presence or absence of 1μM (R)-PIA for the times indicated. Cells were solubilised and the resultant protein separated by SDS-PAGE. Proteins were transferred to nitrocellulose and visualised by incubation with an anti-GFP-specific antibody as described previously. Blots were quantified by densitometric scanning and values represent mean ± S.E. for three experiments. The total cellular level of receptor in the absence of agonist is set at 100%.

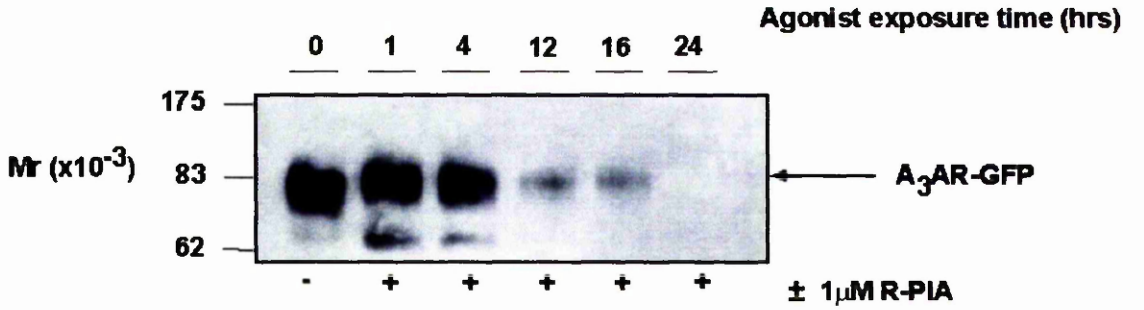
Agonist exposure time (hrs)
0
1
4
12
16
24
175
83
62
Mr (x10-3)
A3AR-GFP
-
+
+
+
+
+
± 1μM R-PIA

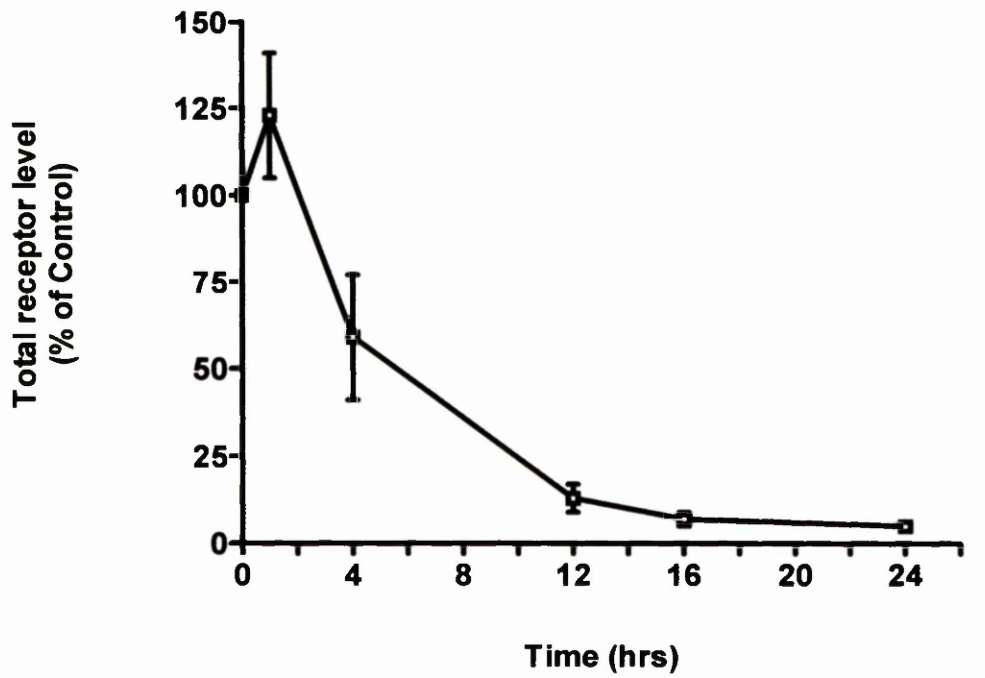
Total receptor level
(% of Control)
150
125
100
75
50
25
0
0
4
8
12
16
20
24
Time (hrs)

Fig. 5.6 Time-course of agonist-mediated A_3AR-GFP down-regulation

A_3AR-GFP expressing CHO cells were treated with or without 1μM (R)-PIA for the times indicated. Cells were then solubilised and separated by SDS-PAGE as previously described before transfer to nitrocellulose. Visualisation was by incubation with an anti-GFP-specific antibody followed by HRP-conjugated anti-sheep secondary antibody. Typical data is shown from one of three experiments.

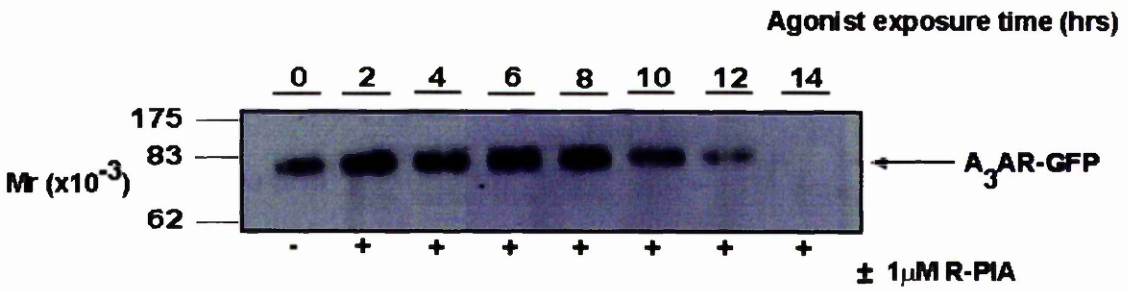
Agonist exposure time (hrs)
0
2
4
6
8
10
12
14
175
83
62
Mr (x10-3)
A3AR-GFP
-
+
+
+
+
+
+
+
± 1μM R-PIA

Fig. 5.7 Confocal microscopic analysis of (R)-PIA-mediated A_3AR-GFP down-regulation

CHO cells stably expressing A_3AR-GFP were plated onto coverslips and treated with or without 1μM (R)-PIA over 24 hours. Cells were then fixed and visualised by confocal microscopy as described in the Methods. The images represent of one of three experiments showing identical results.

The total levels of grey in each image were calculated using MetaMorph Imaging software. The total cellular level of receptor in the absence of agonist is set at 100%. Values represent mean ± S.E. for three experiments showing comparable results.

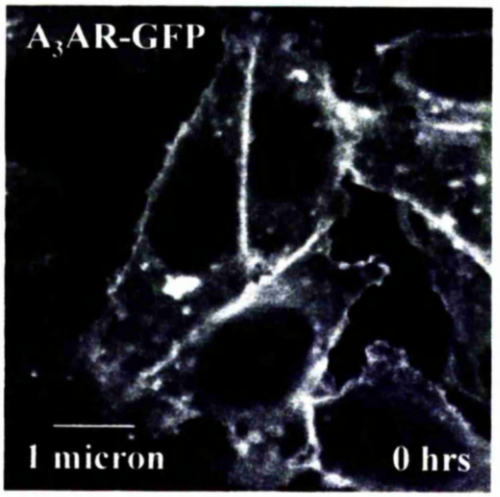
A3AR-GFP
1 micron
0 hrs

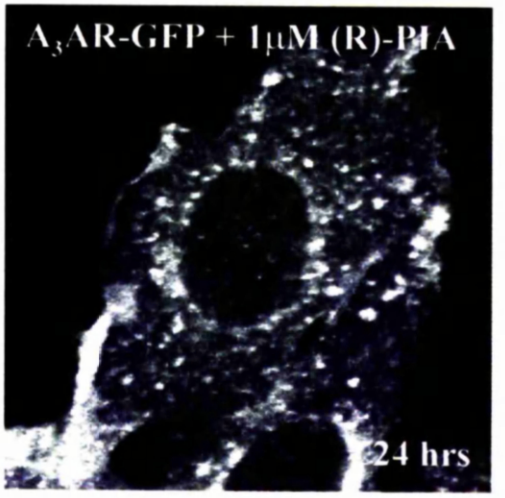
A3AR-GFP + 1μM (R)-PIA
24 hrs

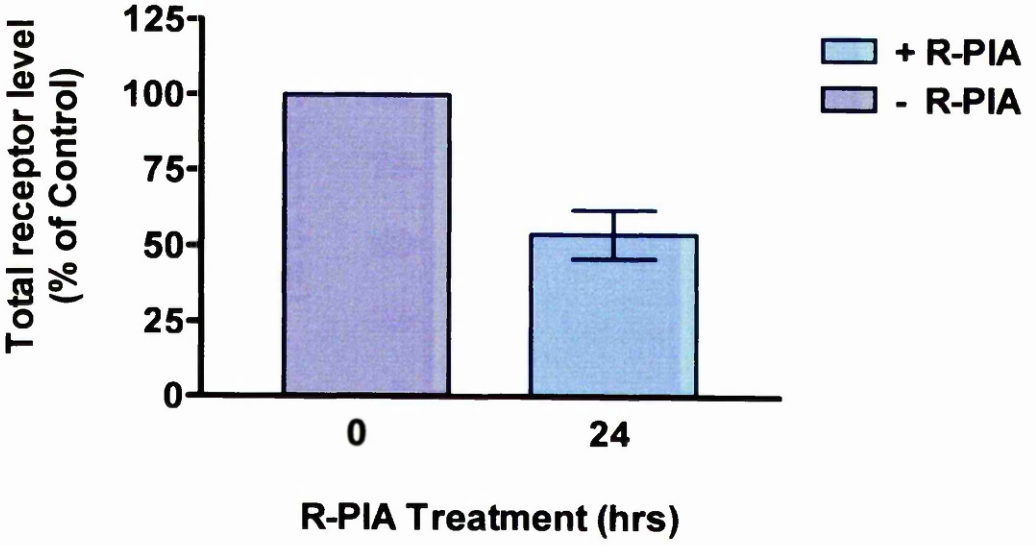
Total receptor level
(% of Control)
125
100
75
50
25
0
0
24
R-PIA Treatment (hrs)
+ R-PIA
- R-PIA

Fig. 5.8 **Confocal microscopic analysis of A_3AR-GFP and lysosomal cellular distribution following agonist stimulation**

CHO cells stably expressing A_3AR-GFP were plated onto coverslips and labelled with LysoTracker™Red for 30 minutes prior to treatment with or without 1μM (R)-PIA over a 24 hour period. Cells were fixed and visualised by confocal microscopy as described in the Methods. Agonist stimulation can be seen to promote the internalisation of A_3AR-GFP to spots within the cytoplasm distinct from those labelled with LysoTracker. Images shown represent results from three experiments showing similar results.

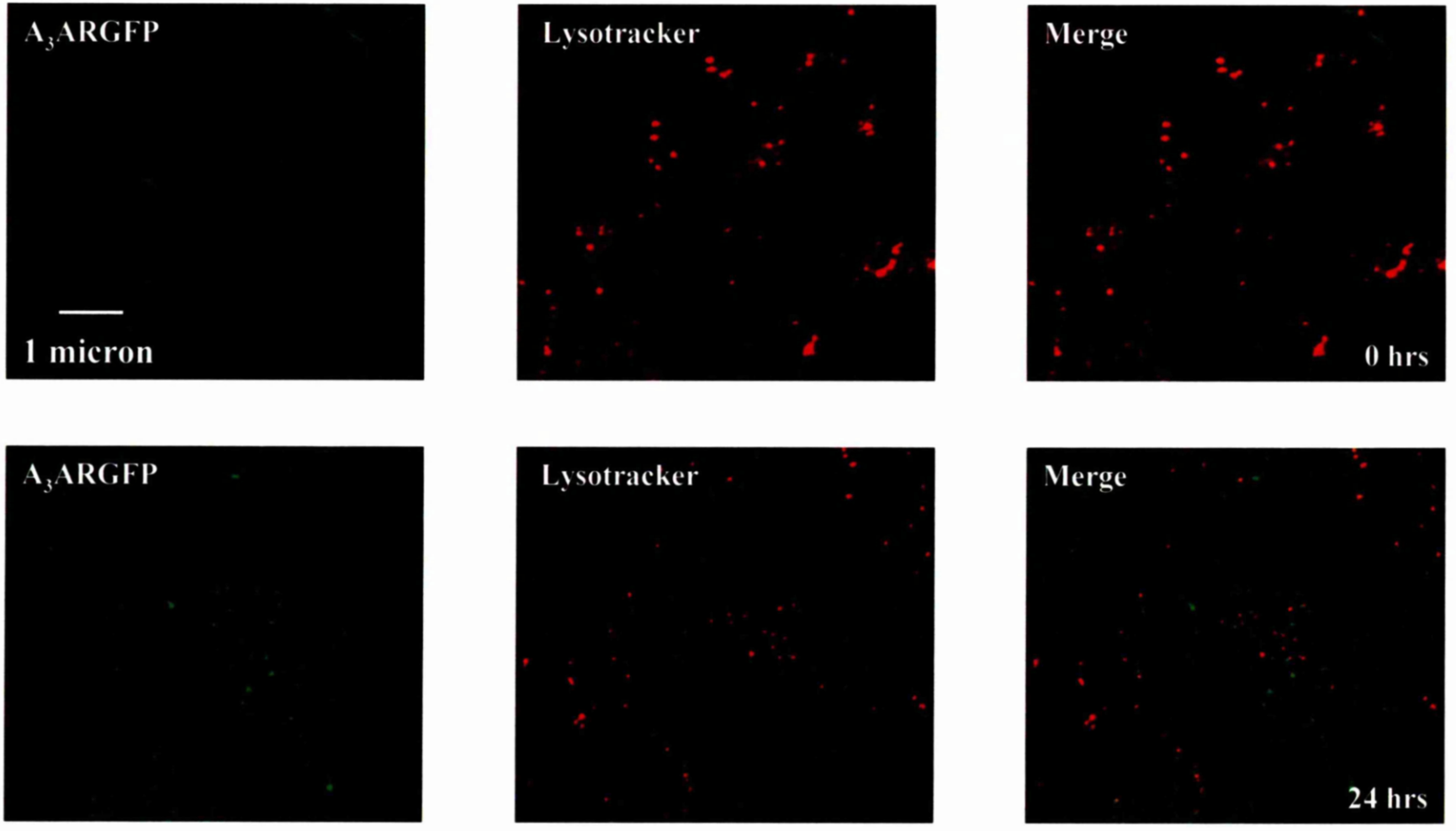
A_3ARGFP
1 micron
Lysotracker
Merge
0 hrs
A_3ARGFP
Lysotracker
Merge
24 hrs

Fig. 5.9 **Confocal microscopic analysis of A_3AR-GFP and lysosomal cellular distribution following agonist stimulation over 16 hours**

CHO cells stably expressing A_3AR-GFP were plated onto coverslips and labelled with LysoTracker™Red for 30 minutes prior to treatment with or without 1μM (R)-PIA over a 16 hour period. Cells were fixed and visualised by confocal microscopy as described in the methods. Agonist stimulation can be seen to promote the internalisation of A_3AR-GFP to spots within the cytoplasm distinct from those labelled with LysoTracker.

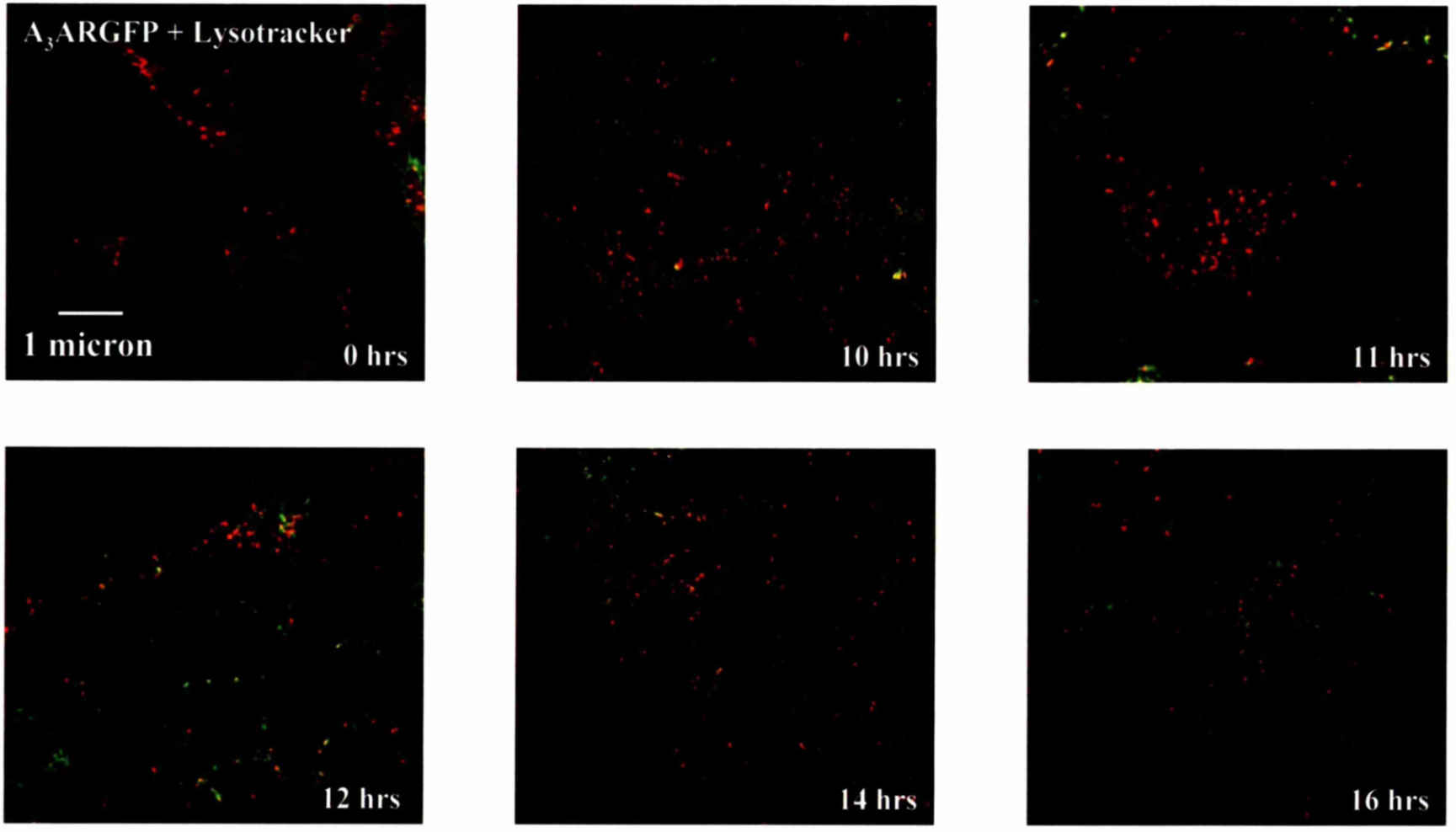
A3ARGFP + Lysotracker
1 micron
0 hrs
10 hrs
11 hrs
12 hrs
14 hrs
16 hrs

Fig. 5.10 Effects of inhibitors of proteosomal and lysosomal degradation on A_3AR-GFP down-regulation

CHO cells stably expressing A_3AR-GFP were treated with or without 1μM (R)-PIA in the presence of either proteosomal (MG-132) or lysosomal (chloroquine and NH_4Cl) inhibitors and ADA over a 24 hour period. Cells were solubilised and the resultant protein separated by SDS-PAGE. Proteins were transferred to nitrocellulose and visualised by incubation of the membrane with GFP-specific antibody followed by HRP-conjugated anti-sheep secondary antibody. Blots were quantified by densitometric scanning and values represent mean ± S.E. for three experiments. The level of receptor in the absence of agonist is set at 100%.

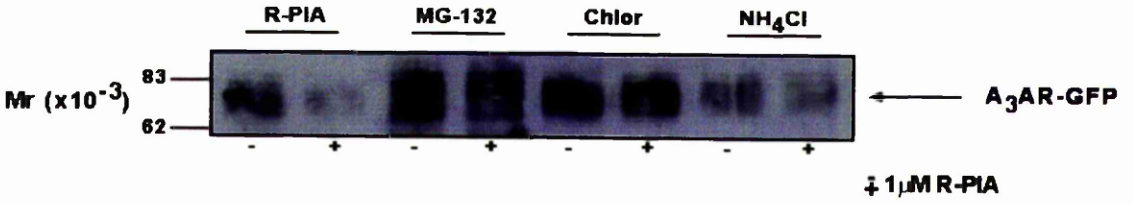
R-PIA
MG-132
Chlor
NH4Cl
Mr (x10-3)
83
62
- + - + - + - +
A3AR-GFP
± 1μM R-PIA

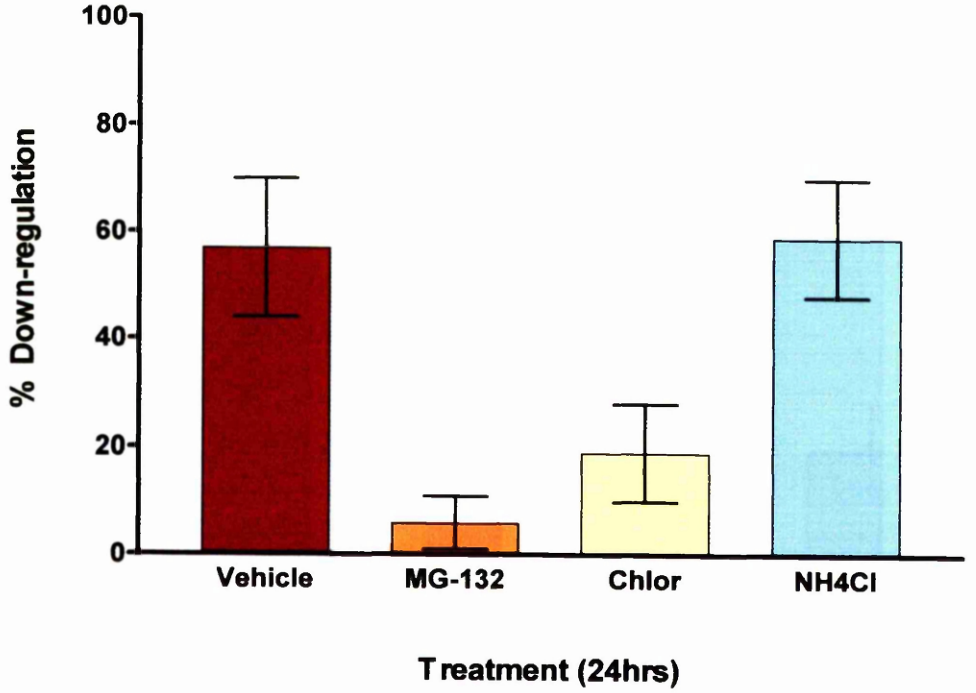
100
80
60
40
20
0
% Down-regulation
Vehicle
MG-132
Chlor
NH4Cl
Treatment (24hrs)

Fig. 5.11 **Confocal microscopic anlaysis of A_3AR-GFP cellular distribution in the presence of Alexa^{594}-concanavalin A**

A_3AR-GFP expressing CHO cells were plated onto coverslips and treated with or without 1μM (R)-PIA over a 24 hour period. Cells were then fixed, solubilised and the endoplasmic reticulum stained using Alexa^{594}-conjugated concanavalinA. Visualisation of the cells by confocal microscopy showed no overlay of A_3AR-GFP with the ER following agonist stimulation. Shown opposite are representative images from three experiments showing the same results.

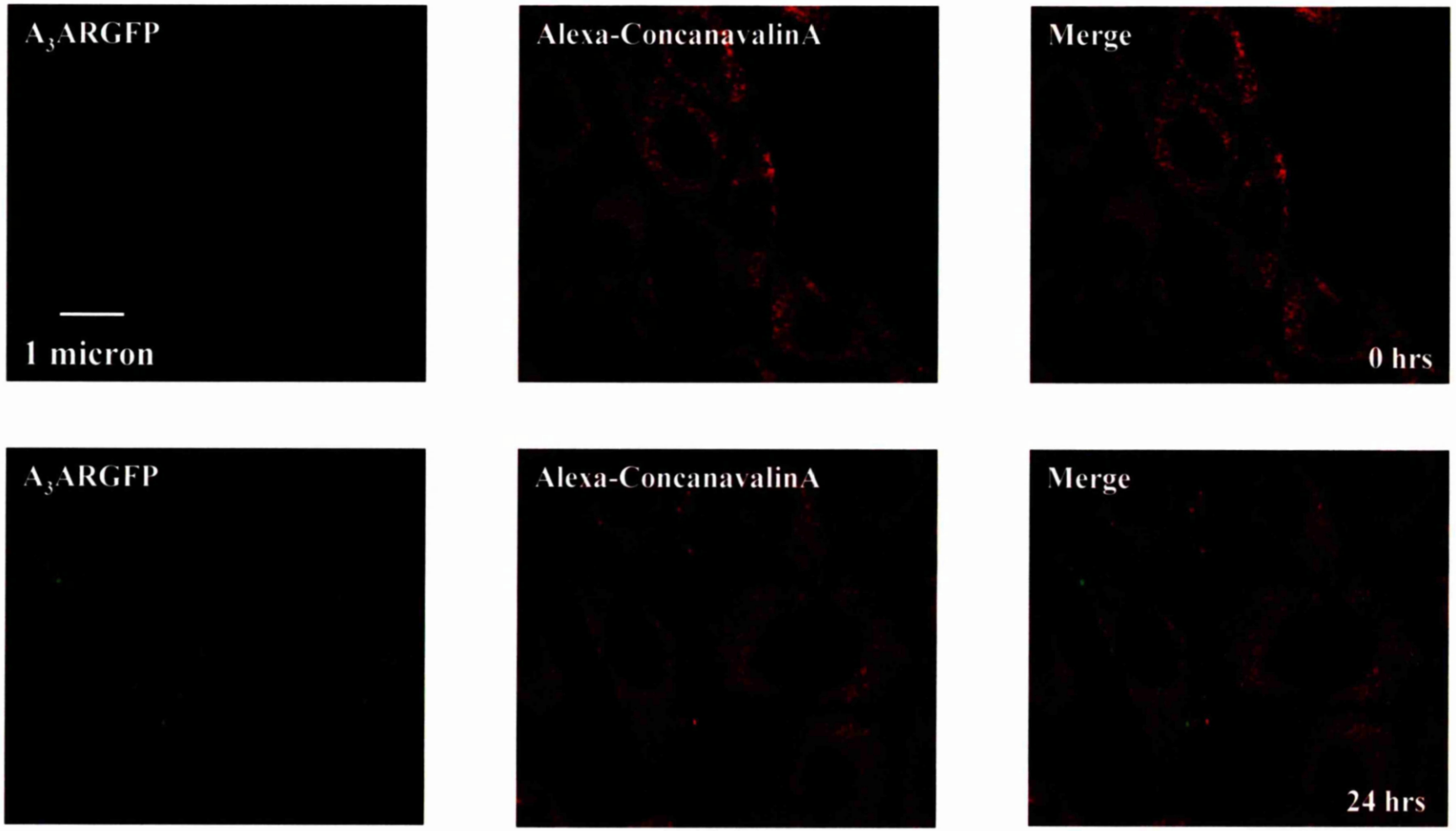
A_3ARGFP
1 micron
Alexa-ConcanavalinA
Merge
0 hrs
A_3ARGFP
Alexa-ConcanavalinA
Merge
24 hrs

Fig. 5.12 **Confocal microscopic anlaysis of A_3AR-GFP cellular distribution in the presence of the Golgi marker GM-130**

A_3AR-GFP expressing CHO cells were plated onto coverslips and treated with or without 1μM (R)-PIA over a 24 hour period. Cells were then fixed, solubilised and the Golgi apparatus stained using anti-GM-130 antibody followed by Alexa^{594}-conjugated anti-mouse secondary antibody. Visualisation of the cells by confocal microscopy showed no overlay of A_3AR-GFP with the Golgi following agonist stimulation. The images are representative of three experiments showing the same results.

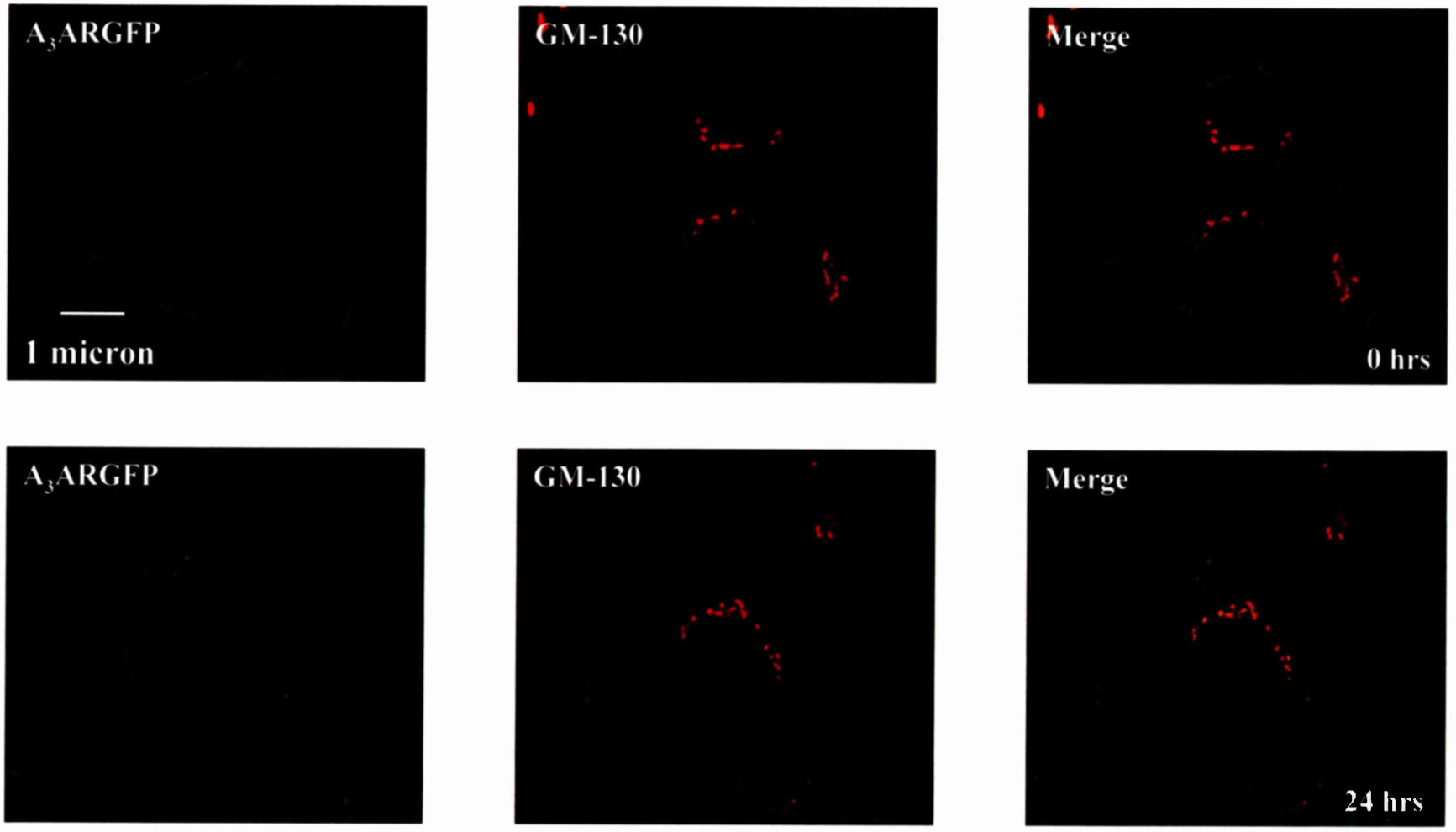
A_3ARGFP
1 micron
GM-130
Merge
0 hrs
A_3ARGFP
GM-130
Merge
24 hrs

Fig. 5.13 **Time course of A_3AR-GFP resynthesis from the ER following 24 hour agonist treatment and removal over 3 hours**

A_3AR-GFP expressing CHO cells were plated onto coverslips and treated with or without agonist over 24 hours. The following day, medium containing agonist was removed over a 3 hour period and replaced with fresh medium. The cells were then fixed and stained for ER using Alexa^{594}-conjugated concanavalin A as described in the Methods. Removal of agonist led to redistribution of A_3AR-GFP although no colocalisation was observed with the ER stain.

Shown opposite are representative examples of confocal microscopic images obtained from two experiments that showed similar results.

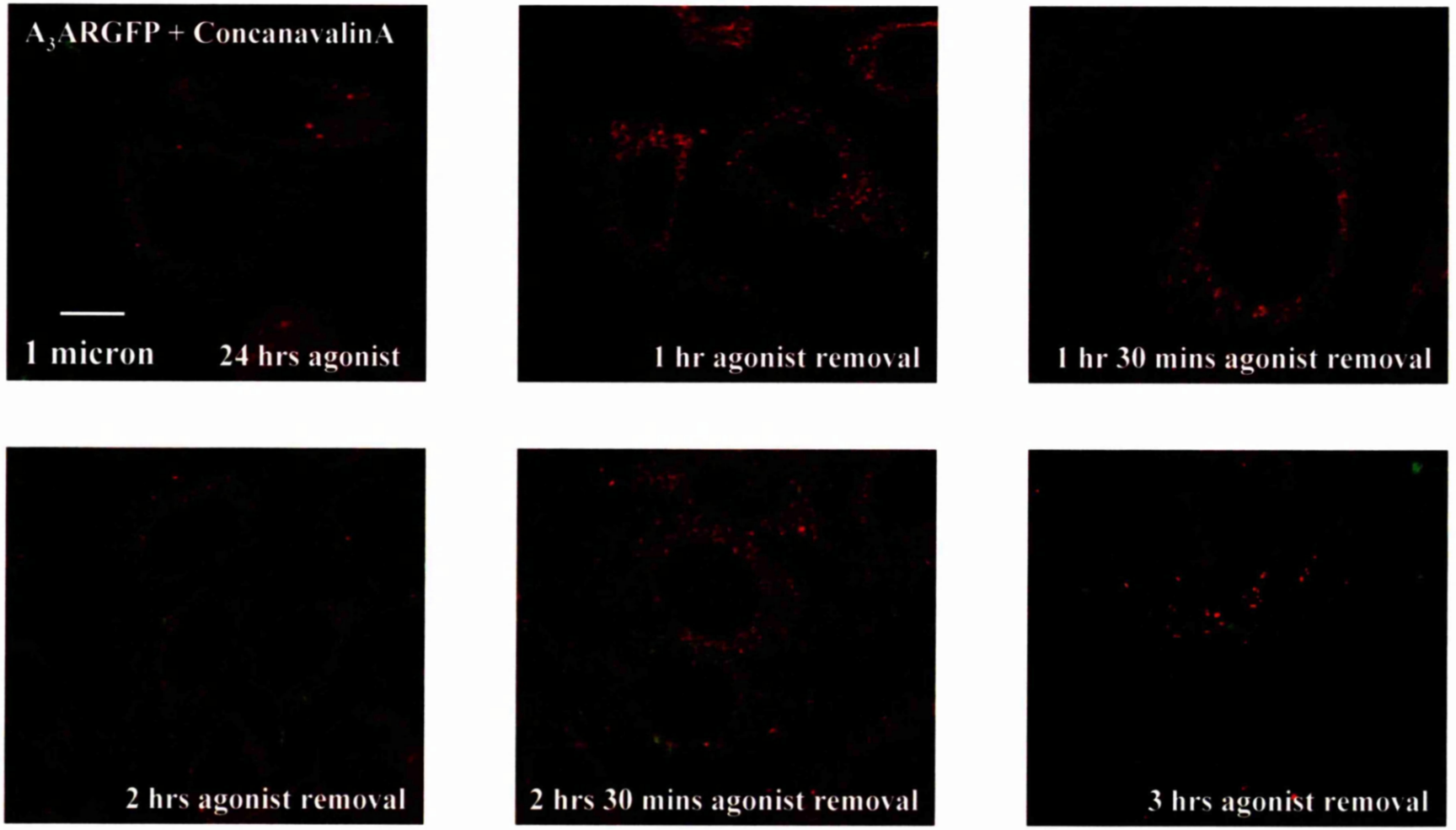
A_3ARGFP + ConcanavalinA
1 micron
24 hrs agonist
1 hr agonist removal
1 hr 30 mins agonist removal
2 hrs agonist removal
2 hrs 30 mins agonist removal
3 hrs agonist removal

Fig. 5.14 **Time course of A_3AR-GFP resynthesis from the Golgi apparatus following 24 hour agonist treatment and removal over 3 hours**

A_3AR-GFP expressing CHO cells were plated onto coverslips and treated with or without agonist over 24 hours. The following day, medium containing agonist was removed over a 3 hour period and replaced with fresh medium. The cells were then fixed and stained for Golgi using GM-130 followed by Alexa^{594}-conjugated anti-mouse secondary antibody as described in the Methods. Colocalisation of A_3AR-GFP with the Golgi was observed between 1-1.5 hours following agonist removal. Shown opposite are representative examples of confocal microscopic images obtained from two experiments that showed similar results.

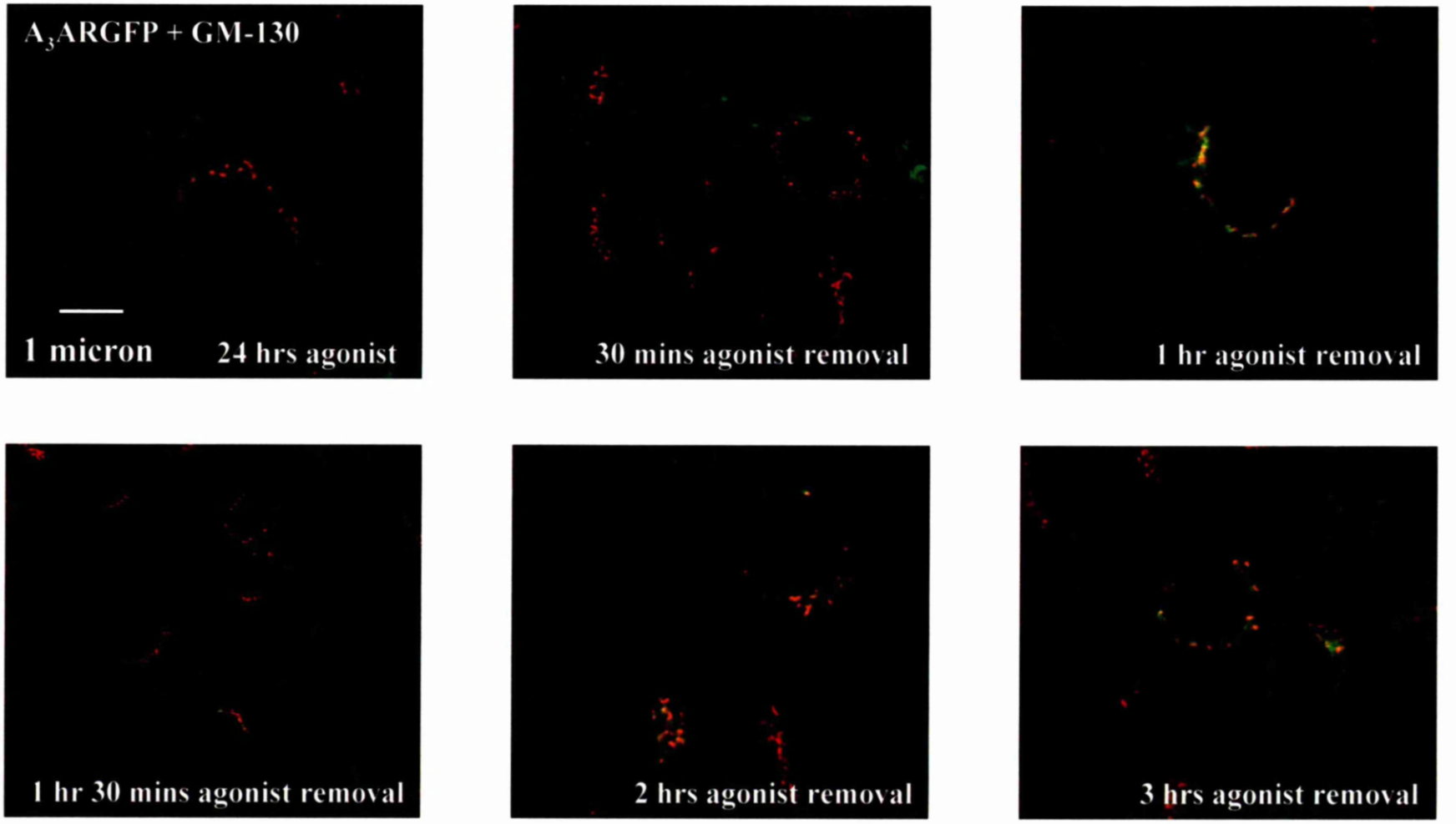
A_3ARGFP + GM-130
1 micron
24 hrs agonist
30 mins agonist removal
1 hr agonist removal
1 hr 30 mins agonist removal
2 hrs agonist removal
3 hrs agonist removal

5.3 Discussion

Down-regulation is defined as a reduction in the number of ligand binding sites detected in a total membrane fraction, which is generally induced by repeated or prolonged activation of receptors (Tsao and von Zastrow, 2000a). GPCRs regulate their physiological effects by interaction with heterotrimeric G-proteins, the duration of which is controlled by multiple processes including receptor desensitisation, sequestration and down-regulation. So far (Chpts. 3 and 4), we have shown that A_3ARs undergo desensitisation *via* phosphorylation by GRKs, and subsequent sequestration *via* an endosomal pathway in response to short-term agonist exposure. In an attempt to complete the characterisation of the A_3AR, investigation into receptor down-regulation was required.

A chronic agonist treatment (24 hours, Figs. 5.2 and 5.3) determined that the A_3AR undergoes down-regulation and that the level of degradation is elevated in response to increasing agonist concentration (Fig.5.4). It was also concluded that this degradation of A_3AR became more apparent between 8-12 hours following agonist treatment (Fig. 5.6). One question to be answered is how then are A_3ARs down-regulated? Debate still surrounds the process of GPCR down-regulation. Over-expression of dominant-negative arrestins that inhibit sequestration has been shown to reduce the rate of β_2AdR down-regulation (Gagnon et al., 1998). Mutation studies have also identified receptor mutants of the β_2AdR that do not sequester, but down-regulate more efficiently (Barak et al., 1994) as well as receptors that sequester normally but do not down-regulate (Campbell et al., 1991). Previous studies of the V2 vasopressin receptor have also demonstrated that this receptor undergoes ligand-induced endoproteolytic cleavage by a plasma membrane-associated metalloprotease (Kojro and Fahrenholz, 1995). Many GPCRs undergo ligand-induced endocytosis *via* clathrin-coated pits, a process mediated by interaction of the receptors with arrestin molecules (Goodman et al., 1998). Distinct GPCRs are significantly different in their abilities to undergo endocytosis with evidence for receptor-specific and cell-type-specific differences in the precise mechanisms used (Goodman et al., 1998; Roettger, et al., 1995; Vickery and von Zastrow, 1999). However, such diversity in the early stages of the endocytic pathway may not control the targeting of receptors to lysosomes as D_1 and D_2 receptors have been shown to exhibit similar rates of proteolytic degradation despite entering the cells *via* distinctly different

mechanisms (Vickery and von Zastrow, 1999). How then is sorting and targeting for down-regulation initiated and regulated?

Comparison of two structurally distinct GPCRs (β_2Ad and δ-opioid) by Tsao and von Zastrow (2000b) concluded that the opioid receptor was held in a different population of vesicles to the β_2 receptor upon sequestration and that this subset of endocytic vesicles was distinct from those found in the conserved recycling pathway utilised by Tfn. They also showed that β_2 receptors could be recycled to the membrane upon removal of agonist, whereas the δ-opioid receptors were retained within the vesicles (< 50% returned). This same phenomenon has been shown with the (C-A)A_3AR (Chpt. 3) suggesting that the ability of A_3ARs to be retained intracellularly, and possibly targeted for degradation following agonist removal is dependent upon the integrity of its C-terminal domain. In addition, A_3AR-GFP was seen to be retained in vesicles distinct from those labelled with lysosomal marker, possibly indicating that the pathway of down-regulation of the A_3ARs does not involve transfer to lysosomes (Figs. 5.8 and 5.9).

The concept of ARs being degraded by a pathway other than lysosomes was investigated by treating A_3AR-GFP-expressing cells with agonist in the presence of proteosomal and lysosomal inhibitors. Statistical analysis of the blots obtained revealed that the inhibition of receptor down-regulation in the presence of MG-132 and chloroquine was not significantly different from each other (Fig. 5.10). If down-regulation were taking place *via* both proteosomal and lysosomal pathways, it would then be expected that the second lysosomal inhibitor, NH_4Cl, would have a similar effect to that observed with chloroquine. However, this was not the case as NH_4Cl failed to inhibit down-regulation to any extent above only agonist treated cells. In contrast to MG-132, which is a specific proteosomal inhibitor, chloroquine and NH_4Cl have a very broad method of action. Both of these inhibitors produce their effects by raising the pH within the lysosomes causing a neutralising effect. One possible explanation for the divergent effects of NH_4Cl and chloroquine is that chloroquine may interfere with lysosomal and proteosomal degradation. Evidence to support the lack of specificity or general mechanism of action of chloroquine could be taken from its use to treat a wide range of medical conditions including malaria, leprosy and rheumatoid arthritis (Barduagni et al., 1999; Razack and Zahra, 1981; Fox, 1993). If this suggestion holds true, this could be one explanation as to why no

colocalisation of A_3AR-GFP with Alexa-labelled lysosomes was observed. One way of investigating this further would be to co-transfect non-receptor expressing cells with A_3AR-GFP and an HA-tagged ubiquitin protein and agonist treat in the absence and presence of MG-132. Any interaction of these two proteins, receptor and ubiquitin, could be detected by immunoblotting. Further analysis would involve more specific ubiquitination experiments on the A_3AR.

The colocalisation of A_3AR-GFP with Golgi marker (GM-130) following agonist removal from chronically treated cells suggests that new receptor is being synthesised through the Golgi apparatus back to the plasma membrane (Fig. 5.14). The possibility that receptor resynthesis is taking place within 1 hour of agonist removal could explain why no colocalisation was seen between A_3AR-GFP and the ER stain (Alexa^{594}-concanavalin A, Fig. 5.13). Further confocal analysis over shorter periods of time is required to allow any further conclusions to be drawn from these initial data.

In this chapter, we have shown that A_3ARs are down-regulated in response to prolonged agonist exposure and have presented initial images suggesting that removal of this stimulus causes new or recycled receptor to be transported back to the plasma membrane. However, it is currently impossible to determine whether the down-regulation pathway utilised by A_3ARs is similar to those employed by other GPCRs including β_2AdR, PAR1 and ET_BR (Kallal et al., 1998; Trejo and Coughlin, 1999; Oksche et al., 2000).

Chapter 6

Conclusions and Perspectives

The results of each individual chapter have been discussed at length elsewhere. Therefore this final discussion aims to combine the conclusions reached and consider possible therapeutic strategies that could be developed from the data obtained.

In chapter 3 it was shown that A_3AR phosphorylation and sequestration were initiated by the presence of agonist and that these phenomena were controlled primarily by the integrity of the C-terminal region. In contrast to the A_3AR, the A_1AR did not undergo significant phosphorylation and was only seen to internalise after a prolonged period of agonist treatment. Work by Liang and Jacobson (1998) showed that A_1 and A_3ARs produced cardioprotective effects within isolated cardiac ventricular cells, determined by quantitation of the percentage of cells killed and the amount of creatine kinase released into the media following stimulated ischaemia. It was established that the A_1 and A_3ARs produced a cardioprotective effect both individually and in combination, with the effect of the A_3AR being prolonged over that of A_1ARs. The cardioprotective effects of each individual receptor were blocked by receptor-selective antagonists suggesting that the A_1 and A_3ARs convey their effects *via* distinct, and as yet undesignated pathways.

Both A_1 and A_3ARs signal through G_i but produce very different effects. One reason for the effects of the A_1AR being so short-lived may be due to its inability to undergo phosphorylation and subsequently internalise following agonist activation. This lack of internalisation leaves the receptor at the membrane, possibly limiting its interaction with signalling molecules to those that are close to or membrane-bound e.g. AC and PLC. It has been suggested that GPCRs gain access to Ras-dependent signalling pathways by modulating the activity of receptor tryrosine kinases (RTKs) such as EGF and IGF-1 (Lin et al., 1998). This leads to the formation of a membrane-associated Ras activation complex that serves as a scaffold to recruit non-receptor tyrosine kinases required for down-stream signalling. Such a mechanism may explain how the non-internalising A_1AR exerts its cardioprotective effects. In contrast, the A_3AR is able to sequester into the cells, a process inhibited by dominant-negative forms of arrestin and dynamin. Treatment with these inhibitory molecules not only blocked receptor internalisation, but also had a marked effect on the MAPK signalling cascade (Daaka et al., 1998). It was found that signal transduction proceeded only as far as Raf activation, suggesting that the internalisation process is required for efficient phosphorylation of up-stream

activators of MAPK. Some GPCRs, upon agonist activation, recruit arrestin molecules to the plasma membrane leading to a functional desensitisation of receptors by uncoupling them from the G protein. In the case of the β_2AdR, this translocation of arrestin functions as an adapter protein that brings activated c-Src to the agonist-occupied receptor and targets both receptor and Src to clathrin-coated pits. Both Src binding and clathrin targeting are required for β_2AdR activation of MAPK, suggesting that receptor internalisation is required to produce a 'second wave' of signal transduction (Luttrell et al., 1999).

From the data obtained in chapter 3, this may suggest that the prolonged cardioprotective effects of the A_3AR are a consequence of its ability to undergo phosphorylation and internalisation. It may therefore be of advantage to prolong the activation of the A_1ARs during an ischaemic episode. To determine the requirement of phosphorylation in prolonged cardioprotection, cardiac cells could be transfected with either the loss of function (T-A)A_3AR mutant or the gain of function A_1CT3AR chimera and the protective effects measured as described by Liang and Jacobson (1998). Prolonging the activity of the A_1ARs could increase the protective effects of adenosine leading to a decrease in the size of the infarcted area with subsequent periods of ischaemic injury.

We have shown that mutation of the GRK phosphorylation sites in the A_3AR renders the receptor resistant to agonist-mediated phosphorylation and internalisation and that A_3AR internalisation kinetics can be conveyed to the non-phosphorylated A_1AR purely by exchange of the C-terminal tails. Investigation into the ultimate effects of these mutations on down-stream signalling events was not examined. Further studies of these mutations may prove detrimental to the overall system of cardioprotection. It should be noted that the restoration of blood flow to ischaemic tissue although supplying oxygen and nutrients, initiates a cascade of inflammatory-like processes that leads to expression of critical adhesion molecules in endothelial cells. This process brings about release of oxidants and proteases that result in damage to or death of the coronary endothelium (Jordan et al., 1999).

As with many other GPCRs, A_3ARs were shown to be desensitised in response to agonist exposure, with results from chapter 4 indicating A_3AR sequestration to follow an arrestin independent/clathrin-dependent endosomal pathway. Using the mutants described in chapter 3, it was shown that the trafficking route utilised was not altered by mutation of the receptor's predicted

palmitoylation site and that the slow-internalising A_1AR could be driven through the same pathway as WT A_3ARs, again by exchange of the C-terminal tails. There is a possibility that the initial and ensuing duration of activation of these systems is a consequence of the receptor's ability to internalise. Gene transfer of the A_1CT3AR could alter internalisation kinetics of the A_1AR. Although this may increase the duration of cardioprotection by A_1AR activation, the consequent expression of A_1CT3AR may dampen the initial A_1AR response by decreasing the chances of adenosine binding to endogenous A_1ARs. Conversely, while expression of the (C-A)A_3AR may increase onset of A_3-mediated cardioprotection, decreasing the period of time the activated receptor is present at the membrane may diminish G protein-mediated effects. We must therefore consider the advantages and disadvantages for applications of direct receptor mutation *versus* manipulation of existing signalling pathways with substrate-specific compounds.

Chapter 5 discussed the down-regulation of A_3ARs following prolonged exposure to agonist. We concluded that down-regulation occurred over an 8-12 hour period but from the data obtained, could not determine which system, lysosomal or proteosomal, was predominant. It was suggested that the C-terminal tail region directs targeting of receptors for down-regulation (Trejo and Coughlin, 1999). Down-regulation of GPCRs can occur as a consequence of either increased degradation of pre-existing receptors and/or reduced mRNA and receptor protein synthesis. This process is required in part for the regulation of GPCR signalling, it may be possible to manipulate it such that direct inhibition or activation alters the extent of down-regulation. This would have great impact on therapeutic strategies that could control the trigger that targets receptors for down-regulation thereby altering the extent to which receptors interact with ligands.

The A_3AR is the newest receptor in the adenosine family yet its presence has already been implicated in several debilitating diseases. Activation of these receptors in many cases requires a high level of adenosine (μM), concentrations that are only produced under stress conditions suggesting specificity for activation of these receptors. The mutant receptors investigated in this work may not be useful directly as regulators of A_3AR signalling, although having characterised the main regulatory functions for this specific AR, it may be possible to use this knowledge to build on the therapies already in place. Many positive therapeutic responses to adenosine have come from the inhibition of adenosine metabolism and degradation,

strategies that are currently being used in the treatment of cardiac and brain ischaemia. Prolonging the action of adenosine by inhibiting its uptake and metabolism has been documented to reduce the size of infarcted tissue and aids in recovery of cardiac function (Van Belle et al, 1993). It has also been shown to have a neuroprotective effect in the ischaemic brain, although the effects in this situation are less well documented (Ogini et al., 1997). In contrast, immune responses caused by the activation of ARs would not benefit from a prolonged presence of the causative agent. Therefore we must examine alternative therapies.

Our data have confirmed that the A_3AR undergoes agonist-mediated phosphorylation, internalisation and down-regulation over distinct time courses. If we then examine the consequence of manipulating these processes either individually or in concert with the therapies already in use, we may be able to modify the activation of specific receptors to respond to the surrounding physiological conditions. One strategy would be to carry out gene transfer of mutated receptors to the affected areas. Cardioprotection and neuroprotection are enhanced *via* a prolonged exposure of ARs to agonist. Transfer of adenovirus expressing receptors such as (T-A)A_3AR which is phosphorylation deficient, or treating with inhibitors of GRK-mediated phosphorylation (e.g. GRK2[BK-CT]) would inhibit receptor internalisation and extend the length of time that the receptor has to interact with its ligand therefore increasing its cardioprotective effects. Again the cardioprotective effects of these therapies could be determined by expressing the constructs in cardiac cells as described by Liang and Jacobson (1998). These strategies could also be coupled with ADA and adenosine kinase inhibitors to further lengthen the half-life of adenosine itself.

Allergic reactions consist of an initial response that triggers the degranulation of mast cells leading to the release of a range of chemicals that cause inflammation. This has grave consequences on the lungs where it causes constriction of the bronchiolar smooth muscle and in the heart where reperfusion after ischaemia can lead to inflammatory tissue damage. The principal site of action must therefore be inhibition of mast cell degranulation. Mast cells are found in most organs of the body, but it may be possible to administer AR antagonists to counteract the effects of increasing adenosine levels. Although only receptor-selective and not specific, antagonistic actions could be restricted to areas with increased adenosine levels. In the case of reperfusion injury, activation of A_{2A}ARs has been shown to reduce

infarction size following ischaemia, therefore it may be of advantage to inhibit A_{2A}AR sequestration and down-regulation as well as prolonging agonist activation *via* inhibitors of adenosine metabolism. The actions of A_3ARs in the pathology of human disease are still, to a certain extent, undefined. The aim of these data was to determine how A_3ARs are regulated and the possible implications for their manipulation in disease states. Although important in themselves, ARs interact with a variety of other systems to bring about their effects and any direct manipulations of these receptors may well produce both positive and negative consequences.

These data presented here have characterised only a small area of A_3AR regulation but provide a foundation for subsequent investigations. Having constructed mutant A_1 and A_3ARs that show altered regulation compared to WT, it is essential that we determine any variation in their ability to initiate intracellular signalling such as the inhibition of AC and activation of MAPK. Due to the changes in cell shape during agonist treatment (chapter 3), it would also be of interest to investigate the interaction of these receptors with other small G-proteins involved in the control of the actin cytoskeleton. Activation of Rho could be examined in cells co-expressing WT or mutant ARs and Rho by using GST-fused C21 (aa7-113 of rhotekin). This construct, which binds only to activated Rho, may be used in a pull-down assay to detect AR-mediated activation of Rho.

We failed to detect inhibition of receptor internalisation by the addition of dominant-negative forms of proteins involved in clathrin-mediated endocytosis although a decrease in receptor phosphorylation was detected in the presence of a mutant form of GRK2 (chapter 4). Further investigation of these mutants by means of immunoblotting and sensitive array scan technology using the GFP-tagged form of the WT A_3AR, may be able to detect any reduction or slowing of internalisation over time.

Down-regulation has been described for many GPCRs with the pathway utilised by the A_3AR still undetermined (chapter 5). Further characterisation of this pathway requires control experiments using receptors whose pathway of down-regulation has already been determined e.g. δ-opioid receptor that down-regulates *via* a lysosomal pathway (Tsao and von Zastrow, 2000). A consequence of down-regulation is that synthesis of new receptor and subsequent trafficking to the plasma membrane is required. Preliminary data showed that this phenomenon of receptor trafficking could be detected in cells that had undergone down-regulation then

agonist removal over a controlled time period (chapter 5). In order to detect synthesis of new receptor, cells must be examined at earlier time-points, again in the presence of a positive control. Ideally, the data obtained so far and any future work should be carried out in a cell line that endogenously expresses the A_3AR. Such cell lines have been cultured (RBL-2H3) and initial investigations are underway.

References

Abbracchio, M.P. and Burnstock, G. (1994) Purinoreceptors: are there families of P2X and P2Y purinoreceptors? *Pharmacol. and Therap.* **64**: 445-475.

Abbracchio, M.P., Brambilla, R., Ceruti, S., Kim, H.O., von Lubitz, D.K., Jacobson, K.A. and Cattabeni, F. (1995) G protein-dependent activation of phospholipase C by adenosine A_3 receptors. *Mol. Pharmacol.* **48**:1038-1045.

Abbracchio, M.P., Ceruti, S., Brambilla, R., Franceschi, C., Malorni, W., Jacobson, K.A., von Lubitz, D.K.J.E. and Cattabeni, F. (1997) Modulation of apoptosis by adenosine in the central nervous system: a possible role for the A_3 adenosine receptor. Pathophysiological significance and therapeutic implications for neurodegenerative disorders. *Ann. New York. Acad. Sci. USA* **285**: 11-22.

Abe, Y., Nakayama, K., Yamanaka, A., Sakurai, T. and Goto, K. (2000) Subtype-specific trafficking of endothelin receptors. *J. Biol. Chem.* **275**: 8664-8671.

Afify, E.A., Law, P.Y., Riedl, M., Elde, R. and Loh, H.H. (1998) Role of carboxyl terminus of μ- and δ-opioid receptor in agonist-induced down-regulation. *Mol. Brain Res.* **54**: 24-34.

Ahn, S., Maudsley, S., Luttrell, L.M., Lefkowitz, R.J. and Daaka, Y. (1998) Src-mediated tyrosine phsphorylation of dynamin is required for β2-adrenergic receptor internalisation and mitogen-activated protein kinase signalling. *J. Biol. Chem.* **274**: 1185-1188.

Al-Awqati, Q. (1986) Proton-translocating ATPases. *Ann. Rev. Cell Biol.* **2**: 179-99.

Ali, H., Richardson, R.M., Tomhave, E.D., Didsbury, J.R. and Snyderman, R. (1993) Differences in phosphorylation of formylpeptide and C5a chemoattractant receptors correlate with differences in desensitisation. *J. Biol. Chem.* **268**: 24247-24254.

Altenbach, C., Yang, K., Farrens, D.L., Farahbakhsh, Z.T., Khorana, H.G. and Hubbell, W.L. (1996) Structural features and light-dependent changes in the cytoplasmic interhelical E-F loop region of rhodopsin: a site-directed spin-labelling study. *Biochem.* **35**: 12470-12478.

Alvarez, E., Girones, N. and Davis, R.J. (1990) Inhibition of the receptor-mediated endocytosis of diferric transferrin is associated with the covalent modification of the transferrin receptor with palmitic acid. *J. Biol. Chem.* **265**: 16644-16655.

Ambrose, C., James, M., Barnes, G., Lin, C., Bates, G., Altherr, M., Duyao, M., Church, D., Wasmuth, J.J. (1992) A novel G protein-coupled receptor kinase gene cloned from 4p16.3. *Human Mol. Gene.* **1**: 697-703.

Anderson, R.G. (1993) Caveolae: where incoming and outgoing messengers meet. *Proc. Natl. Acad. Sci. USA.* **90**: 10909-10913

Anderson, R.G. and Orci, L. (1988) A view of acidic intracellular compartments. *J. Cell Biol.* **106**: 539-543.

Attramadal, H., Arriza, J.L., Aoki, C., Dawson, T.M., Codina, J., Kwatra, M.M., Snyder, S.H., Caron, M.G. and Lefkowitz, R.J. (1992) β-arrestin2, a novel member of the arrestin/β-arrestin gene family. *J. Biol.Chem.* **267**: 17882-17890.

Auchampach, J.A. and Bolli, R. (1999) Adenosine receptor subtypes in the heart: therapeutic opportunities and challenges. *Am. J. Physiol.* H1113-H1116.

Auchampach, J.A., Rizvi, A., Qui, Y., Tang, X.L., Maldonado, C., Teschner, S. and Bolli, R. (1997) Selective actiavtion of A_3 adenosine receptors with N6-(-3-iodobenzyl)adenosine-5'-N-methyluronamide protects against myocardial stunning without haemodynamic changes in conscious rabbits. *Circ. Res.* **80**: 800-809.

Baldwin, J.M. (1994) Structure and function of receptors coupled to G proteins. *Curr. Opin. Cell. Biol.* **6**: 180-190.

Barak, L.S., Ferguson, S.S.G., Zhang, J. and Caron, M.G. (1997b) A β-arrestin/green fluorescent protein biosensor for detecting G protein-coupled receptor activation. *J. Biol. Chem.* **1997**: 27497-27500.

Barak, L.S., Ferguson, S.S.G., Zhang, J., Martenson, C., Meyer, T. and Caron, M.G. (1997a) Internal trafficking and surface mobility of a functionally intact β_2-adrenergic receptor-green fluorescent protein conjugate. *Mol. Pharmacol.* **51**: 177-184.

Barak, L.S., Tiberi, M., Freedman, N.J., Kwatra, M.M., Lefkowitz, R.J. and Caron, M.G. (1994) A highly conserved tyrosine residue in G protein-coupled receptors is required for agonist-mediated β2-adrenergic receptor sequestration. *J. Biol. Chem.* **269**: 2790-2795.

Bardenheuer, H. and Schrader, J. (1986) Supply-to-demand ratio for oxygen determines formation of adenosine by the heart. *Am. J. Physiol.* **250**: H173-180.

Barduagni, P., Schwartz, U., Nyamayro, W. and Chauke, T.L. (1998) In vivo testing of the therapeutic efficacy of chloroquine on falciparum malaria infections in Chirundu, Mashonaland West, Zimbabwe. *Cent. Afr. J. Med.* **44**: 251-4

Barrington, W.W., Jacobson, K.A. and Stiles, G.L. (1990) Glycoprotein nature of the A_2-adenosine receptor binding subunit. *Mol. Pharmacol.* **38**: 177-183.

Benham, C.D. and Tsien, R.W. (1987) A novel receptor-operated Ca_{2+}-permeable channel activated by ATP in smooth muscle. *Nature (Lond)* **238**: 275-278.

Benovic, J.L. (1991a) Purification and characterisation of β-adrenergic receptor kinase. *Meth. Enzymol.* **200**: 351-362.

Benovic, J.L. and Gomez, J. (1993) Molecular cloning and expression of GRK6. A new member of the G protein-coupled receptor kinase family. *J. Biol. Chem.* **268**: 19521-19527.

Benovic, J.L., Kuhn, H., Weyand, I., Codina, J., Caron, M.G. and Lefkowitz, R.J. (1987) Functional desensitisation of the isolated β-adrenergic receptor by the β-adrenergic receptor kinase: potential role of an analogue of the retinal protein arrestin (48-kDa protein). *Proc. Natl. Acad. Sci. U.S.A.* **84**: 8879-8882.

Benovic, J.L., Mayor, F.Jr., Staniszewski, C., Lefkowitz, R.J. and Caron, M.G. (1987a) Purification and characterisation of the β-adrenergic receptor kinase. *J. Biol. Chem.* **262**: 9026-9032.

Benovic, J.L., Onorato, J.J., Arriza, J.L., Stone, W.C., Lohse, M.,Jenkins, N.A., Glibert, D.J., Copeland, N.G., Caron, M.G. and Lefkowitz, R.J. (1991b) Cloning, expression, and chromosomal localisation of β-adrenergic receptor kinase 2. A new member of the receptor kinase family. *J. Biol. Chem.* **266**: 14939-14946.

Benovic, J.L., Pike, L.J., Cerione, R.A., Staniszewski, C., Yoshimasa, T., Codina, J., Caron, M.G. and Lefkowitz, R.J. (1985) Phosphorylation of the mammalian β-adrenergic receptor by cyclic AMP-dependent protein kinase. Regulation of the rate of receptor phosphorylation and dephosphorylation by agonist occupancy and effects on coupling of the receptor to the stimulatory guanine nucleotide regulatory protein. *J. Biol. Chem.* **260**: 7094-7101.

Berne, R.M. (1980) The role of adenosine in the regulation of coronary blood flow. *Circ Res.* **47**: 807-813.

Bjorge, J.D., Jakymiw, A. and Fujita, D.J. (2000) Selected glimpses into the activation and function of Src kinase. *Oncogene* **19**: 5620-5635.

Bockaert, J. and Pin, J.P. (1999) Molecular tinkering of G protein-coupled receptors: an evolutionary success. *EMBO J.* **18**: 1723-1729.

Bokman, S.H. and Ward, W.W. (1981) Renaturation of Aequorea green-flourescent protein. *Biochem. Biophys. Res. Comms.* **101**: 1372-1380.

Bokoch, G.M., Katada, T., Northup, J.K., Hewlett, E.L. and GilmanA.G. (1983) Identification of the predominant substrate for ADP-ribosylation by islet activating protein. *J. Biol. Chem.* **258**: 2072-2075.

Bolling, S.F., Bies, L.E., Bove, E.L. and Gallagher KP. (1990) Augmenting intracellular adenosine improves myocardial recovery. *J. Thor. Cardiovasc. Surg.* **99**: 469-474.

Bourne, H.R. (1997) How receptors talk to trimeric G-proteins. *Curr. Opin. Cell Biol.* **9**: 134-142

Bourne, H.R., Sanders, D.A. and McCormick, F. (1991) The GTPase superfamily: conserved structure and molecular mechanism. *Nature* **349**: 117-127.

Bouvier, M., Collins, S., O'Dowd, B.F., Campbell, P.T., de Blasi, A., Kobilka, B.K., MacGregor, C., Irons, G.P., Caron, M.G. and Lefkowitz RJ. (1989) Two distinct pathways for cAMP-mediated down-regulation of the beta 2-adrenergic receptor. Phosphorylation of the receptor and regulation of its mRNA level. *J. Biol. Chem.* **264**: 16786-16792.

Bouvier, M., Hausdorff, W.P., De Blasi, A., O'Dowd, B.F., Kobilka, B.K., Caron, M.G. and Lefkowitz, R.J. (1988) Removal of phosphorylation sites from the β_2-adrenergic receptor delays onset of agonist-promoted desensitisation. *Nature* **333**: 370-373.

Brackett, L.E. and Daly, J.W. (1994) Functional characterisation of the A_{2B} adenosine receptor in NIH 3T3 fibroblasts. *Biochem. Pharmacol.* **47**: 801-814.

Braell, W.A., Schlossman, D.M., Schmid, S.L. and Rothman, J.E. (1984) Dissociation of clathrin coats coupled to the hydrolysis of ATP: role of an uncoating ATPase. *J. Cell Biol.* **99**: 734-741.

Brandt, D.R. and Ross, E.M. (1985) GTPase activity of the stimulatory GTP-binding regulatory protein of adenylate cyclase, Gs. Accumulation and turnover of enzyme-nucleotide intermediates. *J. Biol. Chem.* **260**: 266-272.

Brooks, J. Taylor, P.L., Saunders, P.T., Eidne, K.A., Struthers, W.J. and McNeilly, A.S. (1993) Cloning and sequencing of the sheep pituitary gonadotropin-releasing hormine receptor and changes in expression of its mRNA during the eostrous cycle. *Mol. Cell. Endocrinol.* **94**: R23-27.

Bruns, R.F., Fergus, J.H., Bedger, E.W., Bristol, J.A., Santay, L.A., Hartman, J.D., Hays, S.J. and Huang, C.C. (1987) Binding of the A_1 adenosine selective antagonist 8-cyclopentyl-1,3-dipropylxanthine to rat brain membranes. *Naun. Schmied. Arch. Pharmacol.* **335**: 59-63.

Brutsaert, D.L., Meulemans, A.L., Sipido, K.R. and Sys SU. (1988) Effects of damaging the endocardial surface on the mechanical performance of isolated cardiac muscle. *Circ. Res.* **62**: 358-366.

Buhl, A.M., Johnson, N.L., Dhanasekaran, N. and Johnson, G.L. (1995) $G\alpha_{12}$ and $G\alpha_{13}$ stimulate Rho-dependent stress fibre formation and focal adhesion assembly. *J. Biol. Chem.* **42**: 24631-24634.

Butkerait, P., Zheng, Y., Hallak, H., Graham, T.E., Miller, H.A., Burris, K.D., Molinoff, P.B. and Manning, D.R. (1995) Expression of the human 5-hydroxytryptamine$_{1A}$ receptor in Sf9 cells: reconstitution of a coupled phenotype by co-expression of mammalian G protein subunits. *J. Biol. Chem.* **270**: 18691-18699.

Campbell, P.T., Hnatowich, M., O'Dowd, B.F., Caron, M.G. and Lefkowitz, R.J. (1991) Mutations in the human β2-adrenergic receptor that impair coupling to G_s interfere with receptor down-regulation but not sequestration. *Mol. Pharmacol.* **39**: 192-198.

Carman, C.V., Barak, L.S., Chen, C., Liu-Chen, L-Y., Onorato, J.J., Kennedy, S.P., Caron, M.G. and Benovic, J.L. (2000) Mutational analysis of $G_{\beta\gamma}$ and phospholipid interaction with G protein-coupled receptor kinase 2. *J. Biol. Chem.* **275**: 10443-10452.

Carman, C.V., Lisanti, M.P. and Benovic, J.L. (1999) Regulation of G protein-coupled receptor kinases by caveolin. *J. Biol. Chem.* **274**: 8858-8864.
Casey, P.J. (1994) Lipid modifications of G proteins. *Curr. Biol.* **6**: 219-225.

Chalfie, M., Tu, Y., Euskirchen, G., Ward, W.W. and Prasher, D.C. (1994) Green fluorescent protein as a marker for gene expression. *Science* **263**: 802-805.

Chatterjee, S. and Stochaj, U. (1996) Monitoring nuclear transport in HeLa cells using the green fluorescent protein. *Biotechniques.* **21**: 62-63

Cheng, Y. and Prusoff, W.H. (1973) Relationship between the inhibition constant (K1) and the concentration of inhibitor which causes 50 per cent inhibition (I50) of an enzymatic reaction. *Biochem. Pharmacol.* **22**: 3099-3108

Chu, P., Murray, S., Lissin, D. and von Zastrow, M. (1997) δ and κ opioid receptors are differencially regulated by dynamin-dependent endocytosis when activated by the same alkaloid agonist. *J. Biol. Chem.* **272**: 27124-27130.

Ciechanover, A. (1998) The ubiquitin-proteosome pathway: on protein death and cell life. *EMBO J.* **17**: 7151-7160

Ciruela, F., Saura, C., Canela, E.I., Mallol, J., Lluis, C. and Franco, R. (1997) Ligand-induced phosphorylation, clustering, and desensitization of A1 adenosine receptors. *Mol. Pharmacol.* **52**: 788-797.

Clapham, D.E. and Neer, E.J. (1997) G protein βγ subunits. *Ann. Rev. Pharmacol. Toxicol.* **37**: 167-203.

Collis, M.G. (1989) The vasodilator role of adenosine. *Pharmacol. Therap.* **41**: 143-162.

Cormack, B.P., Valdivia, R.H. and Falkow, S. (1996) FACS-optimised mutants of the green fluorescent protein (GFP). *Gene* **173**: 33-38.

Corset, V., Nguyen-Ba-Charvet, K., Forcet, C., Moyse, E., Chetódal, A. and Mehlen, P. (2000) Netrin-1-mediated axon outgrowth and cAMP production requires interaction with adenosine A_{2B} receptor. *Nature* **407**: 747-750.

Couet, J., Li, S., Okamoto, T., Ikezu, T. and Lisanti, M.P. (1997) Identification of peptide and protein ligands for the caveolin scaffold domain: implications for the interaction of caveolin with caveolae associated proteins. *J. Biol. Chem.* **272**: 6525-6533.

Coux, O., Tanaka, K. and Goldberg, A.L. (1996) Structure and Functions of the 20S and 26S Proteasomes. *Annu. Rev. Biochem.* **65**: 801-847.

Cox, J.H., Galardy, P., Bennink, J.R. and Yewdell, J.W. (1995) Presentation of endogenous and exogenous antigens is not affected by inactivation of E_1 ubiquitin-activating enzyme in temperature-sensitive cell lines. *J. Immunol.* **154**: 511-519.

Craft, C.M., Whitmore, D.H. and Weichmann, A.F. (1994) Cone arrestin identified by targeting expression of a functional family. *J. Biol. Chem.* **269**: 4613-4619.

Cronstein, B.N., Levin, R.I., Belanoff, J., Weissmann, G. and Hirschhorn, R. (1986) Adenosine: an endogenous inhibitor of neutrophil-mediated injury to endothelial cells. *J. Clin. Invest.* **78**: 760-770.

Cyr, C.R., Rudy, B. and Kris, R.M. (1993) Prolonged desensitisation of the human endothelin A receptor in *Xenopus* oocytes: comparative studies with the human neurokinin A receptor. *J. Biol. Chem.* **268**: 26071-26074.

Daaka, Y., Luttrell, L.M. and Lefkowitz, R.J. (1997) Switching of the coupling of the β_2-adrenergic receptor to different G proteins by protein kinase A. *Nature* **390**: 88-91.

Daaka, Y., Luttrell, L.M., Ahn, S., Della Rocca, G.J., Ferguson, S.S.G., Caron, M.G. and Lefkowitz, R.J. (1998) Essential Role for G Protein-coupled Receptor Endocytosis in the Activation of Mitogen-activated Protein Kinase. *J. Biol. Chem.* **273**: 685-688.

Daaka, Y., Pitcher, J.A., Richardson, M., Stoffel, R.H., Robishaw, J.D. and Lefkowitz, R.J. (1997a) Receptor and Gβγ isoform-specific interactions with G protein-coupled receptor kinases. *Proc. Natl. Acad. Sci. U.S.A.* **94**: 2180-2185.

Dalman, H.M. and Neubig, R.R. (1991) Two peptides from the α_{2A}-adrenergic receptor alter receptor G protein coupling by distinct mechanisms. *J. Biol. Chem.* **266**: 11025-11029.

Daly, J.W., Butts-Lamb, P. and Padgett, W. (1983) Subclasses of adenosine receptors in the central nervous system: interaction with caffeine and related methylxanthines. Cell. Mol. Neurobiol. 3: 69-80.

Damaj, B.B., McColl, S.R., Neote, K., Songqing, N., Ogborn, K.T., Hébert, C.A. and Naccache, P.H. (1996) Identification of G-protein binding sites of the human interleukin-8 receptors by functional mapping of the intracellular loops. *FASEB J.* **10**: 1426

Damke, H. (1996) Dynamin and receptor-mediated endocytosis. *FEBS Letts.* **389**: 48-51.

Damke, H., Baba, T., Warnock, D.E. and Schmid, S.L. (1994) Induction of mutant dynamin specifically blocks endocytic coated vesicle formation. *J. Cell. Biol.* **127**: 915-934.

Daniels, G.M. and Amara, S.G. (1999) Regulated trafficking of the human dopamine transporter: clathrin-mediated internalisation and lysosomal degradation in response to phorbol esters. *J. Biol. Chem.* **274**: 35794-35801

Daukas, G. and Zigmond, S.H. (1985) Inhibition of receptor-mediated but not fluid-phase endocytosis in polymorphonuclear leukocytes. *J. Cell Biol.* **101**: 1673-1679.

Dautry-Varsat, A., Ciechanover, A. and Lodish, H.F. (1983) pH and the recycling of transferrin during receptor-mediated endocytosis. *Proc. Natl. Acad. Sci.* **80**: 2258-2262.

David, C., McPherson, P.S., Mundigl, O. and De Camilli, P. (1996) A role of amphiphysin in synaptic vesicle endocytosis suggested by its binding to dynamin in nerve terminals. *Proc. Natl. Acad. Sci. USA* **93**: 331-335.

Davis, C.G., Goldstein, J.L., Sudhof, T.C., Anderson, R.G.W., Russell, D.W. and Brown, M.S. (1987) Acid-dependent ligand dissociation and recycling of LDL receptor mediated by growth factor homology region. *Nature* **326**: 760-765.

Dawson, T.M., Arriza, J.L., Jaworsky, D.E., Borisy, F.F., Attramadal, H., Lefkowitz, R.J. and Ronnett, G.V. (1993) β-adrenergic receptor kinase-2 and β-arrestin-2 as mediators of odorant-induced desensitisation. *Science* **259**: 825-829.

de Deuve, C. (1963) The lysosome concept. *Lysosomes* **1-35** (Churchill, London.)

Della Rocca, G.J., Mukhin, Y.V., Garnovskaya, M.N., Daaka, Y., Clark, G.J., Luttrell, L.M., Lefkowitz, R.J. and Raymond, J.R. (1999) Serotonin 5-HT_{1A} receptor-mediated Erk activation requires calcium/calmodulin-dependent receptor endocytosis. *J. Biol. Chem.* **274**: 4749-4753.

Di Paolo, M. and Maxfield, F.R. (1984) Conformational changes in the receptors for epidermal growth factor and asialoglycoproteins induced by the mildly acidic pH found in endocytic vesicles. *J. Biol. Chem.* **259**: 9163-9171.

Dias, J.A. (1992) Recent progress in structure-function and molecular analyses of the pituitary/placental glycoprotein hormone receptors. *Biochim. Biophys. Acta* **1135**: 287-294.

Dick, L.R., Aldrich, C., Jameson, S.C., Moonmaw, C.R., Pramanik, B.C., Doyle, C.K., DeMartino, G.N., Bevan, M.J., Forman, J.M. and Slaughter, C.A. (1994) Proteolytic processing of ovalbumin and β-galactosidase by the proteasome to yield antigenic peptides. *J. Immunol.* **152**: 3884-3894.

Dickenson, J.M., Blank, J.L. and Hill, S.J. (1998) Human adenosine A_1 receptor and $P2Y_2$-purinoreceptor-mediated activation of the mitogen-activated protein kinase cascade in transfected cells. *Br. J. Pharmacol.* **124**: 1491-1499.

Diviani, D., Lattion, A-L., Larbi, N., Kanapuli, P., Pronin, A., Benovic, J.L. and Cotecchia, S. (1996) Effect of different G protein-coupled receptor kinases on phosphorylation and desensitisaiton of the α_{1B}-adrenergic receptor. *J. Biol. Chem.* **271**: 5049-5058.

Dixon, R.A., Sigal, I.S., Candelore, M.R., Register, R.B., Scattergood, W., Rands, E. and Strader, C.D. (1987) Structural features required for ligand binding to the β-adrenergic receptor. *EMBO J.* **6**:3629-3275.

Dohlman, H.G., Caron, M.G., DeBlasi, A., Frielle, T. and Lefkowitz, R.J. (1990) Role of extracellular disulphide-bonded cysteines in the ligand binding function of the β_2-adrenergic receptor. *Biochem.* **29**: 2335-2342.

Dohlman, H.G., Thorner, J., Caron, M.G. and Lefkowitz, R.J. (1991) Model systems for the study of seven-transmembrane-segment receptors. *Annu. Rev. Biochem.* **60**: 653-688.

Dolphin, A.C. and Archer, E.R. (1983) An adenosine agonist inhibits and a cyclic AMP analogue enhances the release of glutamate but not GABA from slices of rat dentate gyrus. *Neurosci. Lett.* **43**: 49-54.

Doss, R.C., Perkins, J.P. and Harden, T.K. (1981) Recovery of beta-adrenergic receptors following long term exposure of astrocytoma cells to catecholamine. Role of protein synthesis. *J. Biol. Chem.* **256**: 12281-12286.

Dougherty, C., Barucha, J., Schofield, P.R., Jacobson, K.A. and Liang, B.T. (1998) Cardiac myocytes rendered ischaemia resistant by expressing the human adenosine A_1 or A_3 receptor. *FASEB J.* **12**: 1785-1792.

Doyle, M.P., Linden, J. and Duling B.R. (1994) Nucleoside-induced arteriolar constriction: a mast cell-dependent reponse. *Am. J. Physiol.* **266**: H2042-H2050.

Drejer, J., Benveniste, H., Diemer, N.H. and Schousboe, A. (1985) Cellular origin of ischemia-induced glutamate release from brain tissue in vivo and in vitro. *J. Neurochem.* **45**: 145-151

Drmota, T., Gould, G.W. and Milligan, G. (1998) Real time visualisation of agonist-mediated redistribution and the internalisation of a green fluorescent protein-tagged form of the thyrotropin-releasing hormone receptor. *J. Biol. Chem.* **273**: 24000-24008.

Drmota, T., Novotny, J., Gould, G.W., Svoboda, P. and Milligan, G. (1999) Visualisation of distinct patterns of subcellular redistribution of the thyrotropin-releasing hormone receptor-1 and $G_{q\alpha}/G_{11\alpha}$ induced by agonist stimulation. *Biochem. J.* **340**: 529-538.

Drury, A.N. and Szent-Gyorgi A (1929) The physiological activity of adenine compounds with special reference to their action upon the mammalian heart. *J. Physiol. (Lond)* **68**: 213-237.

Dunwiddie, T.V., Diao, L., Kim, H.O., Jiang, J-L. and Jacobson, K.A. (1997) Activation of hippocampal adenosine A_3 receptors produces a desensitisation of A_1 adenosine receptor-mediated responses in rat hippocampus. *J. Neurosci.* **17**: 607-614.

Eason, M.G., Jacinto, M.T., Theiss, C.T. and Liggett, S.B. (1994) The palmitoylated cysteine of the cytoplasmic tail of the α_{2A}-adrenergic receptors confers subtype-specific agonist-promoted down-regulation. *Biochemistry* **91**: 11178-11182.

Engelman, J.A., Zhang, X-L., Galbiati, F., Volonte, D., Sotgia, F., Pestell, R.G., Minetti, C., Scherer, P.E., Okamoto, T. and Lisanti, M.P. (1998) Molecular genetics of the caveolin gene family: implications for human cancers, diabetes, alzheimer disease and muscular dystrophy. *Am. J. Hum. Genet.* **63**: 1578-1587.

Engelman, J.A., Zhang, X-L., Galbiati, F., Volonte, D., Sotgia, F., Pestell, R.G., Minetti, C., Scherer, P.E., Okamoto, T. and Lisanti, M.P. (1998) Molecular genetics of the caveolin gene family: implications for human cancers, diabetes, Alzheimer disease and muscular dystrophy. *Am. J. Hum. Genet.* **63**: 1578-1587.

Ezeamuzie, C.I. and Philips, E. (1999) Adenosine A_3 receptors on human eosinophils mediate inhibition of degranulation and superoxide anion release. *Br. J. Pharmacol.* **127**: 188-194.

Farrens, D.L., Altenbach, C., Yang, K., Hubbell, W.L. and Khorana, H.G. (1996) Requirement of rigid-body motion of transmembrane helices for light activation of rhodopsin. *Science* **274**: 768-770

Federman, A.D., Conklin, B.R., Schrader, K.A., Reed, R.R. and Bourne, H.R. (1992) Hormonal stimulation of adenylyl cyclase through G_i-protein $\beta\gamma$. *Nature* **356**: 159-161.

Felder, S., Miller, K., Moehren, G., Ullrich, A., Schlessinger, J. and Hopkins, C.R. (1990) Kinase activity controls the sorting of the epidermal growth factor receptor within the multivesicular body. *Cell* **61**: 623-634.

Fenton, R.A. and Dobson Jr., J.G. (1987) Measurement by fluorescence of interstitial adenosine levels in normoxic, hypoxic and ischaemic perfused rat hearts. *Circ. Res.* **60**: 177-184.

Feokstitov, I. and Biaggioni, I. (1995) Adenosine A_{2B} receptors evoke interleukin-8 secretion in human mast cells. An enprofylline-sensitive mechanism with implications for asthma. *J. Clin. Invest.* **96**: 1979-1986.

Feoktistov, I. and Biagionni, I. (1996) Role of adenosine in asthma. *Drug Dev. Res.* **39**: 333-336.

Ferguson, G., Watterson, K.R. and Palmer, T.M. (2000) Subtype-specific kinetics of inhibitory adenosine receptor internalisation are determined by sensitivity to phosphorylation by G protein-coupled receptor kinases. *Mol. Pharmacol.* **57**: 546-552.

Ferguson, S.S.G., Downey III, W.E., Colapietro, A-M., Barak, L.S., Menard, L. and Caron, M.G. (1996) Role of β-arrestin in mediating agonist-promoted G protein-coupled receptor internalisation. *Science* **271**: 363-365.

Fink, J.S., Weaver, D.R., Rivkees, S.A., Peterfreund, R.A., Pollack, A.E., Alder, E.M. and Reppert, S.M. (1992) Molecular cloning of the rat A_2 adenosine receptor: selective co-expression with D2 dopamine receptors in striatum. *Brain Res. Mol Brain Res.* **14**: 186-195.

Fox, R.I. (1993) Mechanisms of action of hydroxychloroquine as an antirheumatic drug. *Seminars in Arthritis and Rheumatism* **23**: 82-91

Fozard, J.R. and Carruthers, A.M. (1993) Adenosine A_3 receptor mediated hypotension in the angiotensin II-supported circulation of the pithed rat. *Br. J. Pharmacol.* **109**: 3-5.

Fraser, C.M., Chung, F.Z., Wang, C.D. and Venter, J.C. (1988) Site-directed mutagenesis of β-adenergic receptors: substitution of aspartic acid-130 by asparagine produces a receptor with high-affinity agonist binding that is uncoupled from adenylate cyclase. *Proc. Natl. Acad. Sci. USA* **85**: 5478-5482.

Fredericks, Z.L., Pitcher, J.A. and Lefkowitz, R.J. (1996) Identification of the G protein-coupled receptor kinase phosphorylation sites in the human β_2-adrenergic receptor. *J. Biol. Chem.* **271**: 13796-13803.

Fredholm, B.B., Abbracchio, M.P., Burnstock, G., Daly, J.W., Harden, T.K., Jacobson, K.A. and Leff, P. (1994) Nomenclature and classification of purinoceptors. *Pharmacol. Rev.* **46**: 143-156.

Freedman, N.J. and Lefkowitz, R.J. (1996) Desensitisation of G protein-coupled receptors. *Recent Prog. Horm. Res.* **51**: 319-351.

Freedman, N.J., Liggett, S.B., Drachamn, D.E., Pei, G., Caron, M.G. and Lefkowitz, R.J. (1995) Phosphorylation and desensitisation of the human β_1-adrenergic receptor. Involvement of G protein-coupled receptor kinases and cAMP-dependent protein kinase. *J. Biol. Chem.* **270**: 17953-17961.

Freeman, J.L.R., De La Cruz, E.M., Pollard, T.D., Lefkowitz, R.J. and Pitcher, J.A. (1998) Regulation of G protein-coupled receptor kinase 5 (GRK5) by actin. *J. Biol. Chem.* **273**: 20653-20657.

Freissmuth, M., Schutz, M. and Linder, M.E. (1991) Interactions of the bovine brain A1-adenosine receptor with recombinant G protein α-subunits. Selectivity for rGi_{α}-3. *J. Biol. Chem.* **266**: 17778-1783.

Frischknect, F., Cudmore, S., Moreau, V., Reckman, I., Röttger, S. and Way, M. (1999) Tyrosine phosphorylation is required for actin-based motility of vaccinia but not *Listeria* or *Shigella*. *Curr. Biol.* **9**: 89-92.

Frischknect, F., Cudmore, S., Moreau, V., Reckman, I., Röttger, S. and May, M. (1999) Tyrosine phosphorylation is required for actin-based motility of vaccinia but not *Listeria* or *Shigella*. *Curr. Biol.* **9**: 89-92.

Furlong, T.J., Pierce, K.D., Selbie, L.A. and Shine, J. (1992) Molecular characterisation of a human brain adenosine A_2 receptor. *Brain Res.* **15**: 62-66

Gagnon, A.W., Kallal, L. and Benovic, J.L. (1998) Role of clathrin-mediated endocytosis in agonist-induced down-regulation of the β_2-adrenergic receptor. *J. Biol. Chem.* **273**: 6976-6981

Gallo-Rodriguez, C., Ji, X.D., Melman, N., Siegman, B.D., Sanders, L.H., Orlina, J., Fischer, B., Pu, Q., Olah, M.E., van Galen, P.J., Stiles, G.L. and Jacobson, K.A. (1994) Structure-activity relationships of N6-benzyladenosine-5'-uronamides as A_3 selective adenosine agonists. *J. Med. Chem.* **37**: 636-646.

Gao, Z., Li, B.S., Day, Y.J. and Linden J. (2001) A_3 adenosine receptor activation triggers phosphorylation of protein kinase B and protects rat basophilic leukemia 2H3 cells from apoptosis. Mol. Pharmacol. 59: 76-82.

Gao, Z., Robeva, A.S. and Linden, J. (1999) Purification of A_1 adenosine receptor-G-protein complexes: effects of receptor down-regulation and phosphorylation on coupling. *Biochem. J.* **338**: 729-736.

Gerard, N.P. and Gerard, C. (1991) The chemotactic receptor for human C5a anaphylatoxin. *Nature* **349**: 614-617.

Gillespie, J.H. (1934) The biological significance of the linkages in adenosine. *J. Physiol. (London)* **80**: 45-50.

Gilman, A.G. (1987) G-proteins: transducers of receptor-generated signals. *Ann. Rev. Biochem.* **56**: 615-649.

Goodman, Jr., O.B., Krupnick, J.G., Santini, F., Gurevich, V.V., Penn, R.B., Gagnon, A.W., Keen, J.H. and Benovic, J.L. (1996) β-arrestin acts as a clathrin adaptor in endocytosis of the β_2-adrenergic receptor. *Nature* **383**: 447-450.

Goodman, O.J., Krupnick, J.G., Santini, F., Gurevich, V.V., Penn, R.B., Gagnon, A.W., Keen, J.H. and Benovic, J.L. (1998) Role of arrestins in G protein-coupled receptor endocytosis. *Adv. Pharmacol.* **42**: 429-433.

Gout, I., Dhand, R., Hiles, I.D., Fry, M.J., Panayotou, G., Das, P., Totty, N.F., Hsuan, J., Booker, G.W. (1993) The GTPase dynamin binds to and is activated by a subset of SH3 domains. *Cell.* **75**: 25-36.

Grisham, M.B., Hernandez, L.A. and Granger, D.N. (1989) Adenosine inhibits ischemia-reperfusion-induced leukocyte adherence and extravasation. *Am. J. Physiol.* **257**: H1334-1339,

Groarke, D.A., Wilson, S., Krasel, C. and Milligan, G. (1999) Visualisation of agonist-induced association and trafficking of green fluorescent protein-tagged forms of both β-arrestin1 and the thyroptropin-releasing hormone receptor. *J. Biol. Chem.* **274**: 23263-23269.

Gurevich, V.V. and Benovic, J.L. (1992) Cell-free expression of visual arrestin. Truncation mutagenesis identifies multiple domains involved in rhodopsin interaction. *J. Biol.Chem.* **267**: 21919-21923.

Gurevich, V.V. and Benovic, J.L. (1995b) Visual arrestin binding to rhodopsin. Diverse functional roles of positively charged residues within the phosphorylation-recognition region of arrestin. *J. Biol. Chem.* **270**: 6010-6016.

Gurevich, V.V., Dion, S.B., Onorato, J.J., Ptasienski, J., Kim, C.M., Sterne-Marr, R., Hosey, M.M. and Benovic, J.L. (1995a) Arrestin interactions with G protein-coupled receptors. Direct binding studies of wild type and mutant arrestins with rhodopsin, β_2-adrenergic and m2 muscarinic cholinergic receptors. *J. Biol. Chem.* **270**: 720-731.

Gurevich, V.V., Richardson, R.M., Kim, C.M., Hosey, M.M. and Benovic, J.L. (1993) J. Biol. Chem. Binding of wild type and chimeric arrestins to the M_2 muscarinic cholinergic receptor. *J. Biol. Chem.* **268**: 16879-16882.

Gutkind, J.S. (1998) The Pathways Connecting G Protein-coupled Receptors to the Nucleus through Divergent Mitogen-activated Protein Kinase Cascades *J. Biol. Chem.* **273**: 1839-1842.

Haendler, B., Hechler, U. and Schleuning, W.D. (1992) Molecular cloning of human endothelin (ET) receptors ET_A and ET_B. *J. Cardiovasc. Pharmacol.* **20**: S1-4.

Hagberg, H., Andersson, P., Lacarewicz, J., Jacobson, I., Butcher, S. and Sandberg, M. (1987) Extracellular adenosine, inosine, hypoxanthine and xanthine in relation to tissue nucleotides and purines in rat stiatum during transient ischaemia. *J. Neurochem.* **49**: 227-237.

Hallak, H., Seiler, A.E.M., Green, J.S., Ross, B.N. and Rubin, R. (2000) Association of heterotrimer G_i with insulin-like growth factor-I receptor. *J. Biol. Chem.* **275**: 2255-2258.

Hamm, H.E. (1998) The many faces of G protein signalling. *J. Biol. Chem.* **273**: 669-672.

Hausdorff, W.P., Caron, M.G. and Lefkowitz, R.J. (1990) Turning off the signal: desensitisation of β-adrenergic receptor function. *FASEB J.* **4**: 2881-2889.

Hein, L., Ishii, K., Coughlin, S.R. and Kobilka, B.K. (1994) Intracellular targeting and trafficking of thrombin receptors: a novel mechanism for resensitization of a G protein-coupled receptor. *J. Biol. Chem.* **269**: 27719-27726

Heithier, H., Frohlich, M., Dees, C., Baumann, M., Haring, M., Gierschik, P., Schlitz, E., Vaz, W.L., Hekman, M. and Helmreich, E.J. (1992) Subunit interactions of GTP-binding proteins. *Eur. J. Biochem.* **204**: 1169-1181.

Henderson, R., Baldwin, J.M., Ceska, T.A., Zemlin, F., Beckmann, E. and Downing, K.H. (1990) Model for the structure of bacteriorhodopsin based on high-resolution electron cryo-microscopy. *J. Mol. Biol.* **213**: 899-929.

Herbst, J.J., Opresko, L.K., Walsh, B.J., Lauffenburger, D.A. and Wiley, H.S. (1994) Regulation of postendocytic trafficking of the epidermal growth factor receptor through endosomal retention. *J. Biol. Chem.* **269**: 12865-12873.

Hershko, A. and Ciechanover, A. (1998) The ubiquitin system. *Annu. Rev. Biochem.* **67**: 425-79

Herskovits, J.S., Burgess, C.C., Obar, R.A. and Vallee, R.B. (1993) Effects of mutant rat dynamin on endocytosis. *J. Cell Biol.* **122**: 565-578.

Heuser, J.E. and Anderson, R.G.W. (1989) Hypertonic media inhibit receptor-mediated endocytosis by blocking clathrin-coated pit formation. *J. Cell Biol.* **108**: 389-400.

Higashijima, T., Ferguson, K.M., Smigel, M.D. and Gilman A.G. (1987) The effect of GTP and Mg^{2+} on the GTPase activity and the fluorescet properties of G_o. *J. Biol. Chem.* **262**: 757-761.

Hirasawa A. Sugawara T. Awaji T. Tsumaya K. Ito H. Tsujimoto G. (1997) Subtype-specific differences in subcellular localization of alpha1-adrenoceptors: chlorethylclonidine preferentially alkylates the accessible cell surface alpha1-adrenoceptors irrespective of the subtype. *Mol. Pharmacol.* **52**: 764-770

Hohenegger, M., Mitterauer, T., Voss, T., Nanoff, C. and Freissmuth, M. (1996) Thiophosphorylation of the G protein β subunit in human platelet membranes: evidence against a direct phosphate transfer reaction to G_α. *Mol. Pharmacol.* **49**: 73-80.

Hsu, W.H., Rudolph, U., Sanford, J., Bertrand, P., Olate, J., Nelson, C., Moss, L.G., Boyd III, A.E., Codina, J. and Birnbaumer, L. (1990) Molecular cloning of a novel splice variant of the alpha subunit of the mammalian G_o protein. *J. Biol. Chem.* **265**: 11220-11226

Huang, N-K., Lin, Y-W., Huang, C-L., Messing, R.O. and Chern, Y. (2001) Activation of protein kinase A and atypical protein kinase C by A_{2A} adenosine receptors antagonises apoptosis due to serum deprivation in PC12 cells. *J. Biol. Chem.* **276**: 13838-13846.

Hubbard, S.C. and Ivatt, R.J. (1981) Synthesis and processing of asparagine-linked oligosaccharides. *Ann. Rev. Biochem.* **50**: 555-583.

Hulme, E.C., Birdsall, N.J.M. and Buckley, N.J. (1990) Muscarinic receptor subtypes. *Annu. Rev. Pharmacol. Toxicol.* **30**: 633-673.

Hunziker, W. and Geuze, H.J. (1996) Intracellular trafficking of lysosomal membrane proteins. *Bioessays* **18**: 379-389.

Hutchinson, A.J., Williams, M., de Jesus, R., Yokoyama, R., Oei, H.H., Ghai, G.R., Webb, R.L., Zoganas, H.C., Stone, G.A. and Jarvis, M.F. (1990) 2-(Arylalkylamino)adenosine-5'-uronamides: a new class of highly selective adenosine A_2 receptor ligands. *J. Med. Chem.* **33**: 1919-1924.

Hutchinson, A.J., Williams, M., de Jesus, R., Yokoyama, R., Oei, H.H., Ghai, G.R., Webb, R.L., Zoganas, H.C., Stone, G.A. and Jarvis, M.F. (1990) 2-(Akrylalkylamino)adenosine-5'-uronamides: a new class of highly selective A_2 adenosine receptor ligands. *J. Med. Chem.* **33**: 1919-1924.

Jacobson, M.A., Johnson, R.G., Luneau, C.J. and Salvatore, C.A. (1995) Cloning and chromosomal localisation of the human A2B adenosine recepyor gene (ADORA2B) and its pseudogene. *Genomics* **27**: 374-376.

Jacobson, K.A., Nikodijevic, O., Padgett, W.L., Gallo-Rodriguez, C., Maillard, M. and Daly, J.W. (1993) 8-(3-Chlorostyryl)caffeine (CSC) is a selective A_2 adenosine antagonist *in vitro* and *in vivo*. *FEBS Letts.* **323**: 141-144.

Jacobson, K.A., Park, K.S., Jiang, J.L., Kim, Y.C., Olah, M.E., Stiles, G.L. and Ji, X.D. (1997) Pharmacological characterisation of novel A_3 adenosine receptor-selective antagonists. *Neuropharmacol.* **36**: 1157-1165.

Jacobson, K.A., Stiles, G.L. and Ji, X.D. (1992a) Chemical modification and irreversible inhibition of striatal A_{2A} adenosine receptors. *Mol. Pharmacol.* **42**: 123-133.

Jacobson, K.A., van Galen, P.J. and Williams, M. (1992b) Adenosine receptors: pharmacology, structure-activity relationships, and therapeutic potential. *J. Med. Chem.* **35**: 407-422.

Jacobson, K.A., von Lubitz, D.K.J.E., Daly, J.W. and Fredholm, B.B. (1996) Adenosine receptor ligands: differences with accute versus chronic treatment. *TiPS.* **17**: 108-113.

Jarvis, M.F., Schulz, R., Hutchinson, A.J., Do, U.H., Sills, M.A. and Williams, M. (1989) [^{3}H]CGS 21680, a selective A_2 adenosine receptor agonist directly labels A_2 receptor in rat brain. *J. Pharmacol. Expt. Ther.* **251**: 888-893.

Ji, T.H., Grossmann, M. and Ji, I. (1998) G protein coupled receptors. I. Diversity of receptor-ligand interactions. *J.Biol. Chem.* **273**: 17299-17302.

Ji, X-D., von Lubitz, D., Olah, M.E., Stiles, G.L. and Jacobson, K.A. (1994) Species differences in ligand affinity at central A_3 adenosine receptors. *Drug Dev. Res.* **33**: 51-59.

Jin, X., Shepherd, R.K., Duling, B.R. and Linden, J. (1997) Inosine binds to A3 adenosine receptors and stimulates mast cell degranulation. *J. Clin. Invest.* **100**: 2849-2857

Jones PG, Curtis CAM and Hulme EC (1995) The function of a highly-conserved arginine residue in activation of the muscarinic M1 receptor. *Eur. J. Pharmacol.* **288**: 251-257

Jordan JE. Thourani VH. Auchampach JA. Robinson JA. Wang NP. Vinten-Johansen J. (1999) A_3 adenosine receptor activation attenuates neutrophil function and neutrophil-mediated reperfusion injury. *Am. J. Physiol.* **277**: H1895-1905.

Kallal, L., Gagnon, A.W., Penn, R.B. and Benovic, J.L. (1998) Visualisation of agonist-induced sequestration and down-regulation of a green flourescent protein-tagged β_2-adrenergic receptor. *J. Biol. Chem.* **273**: 322-328.

Kanaseki, T. and Kadota, K. (1969) The "vesicle in a basket". A morphological study of the coated vesicle isolated from the nerve endings of the guinea pig brain, with special reference to the mechanism of membrane movements. *J. Cell Biol.* **42**: 202-220.

Karnik, S.S., Ridge, K.D., Bhattacharya, S. and Khorana, H.G. (1993) Palmitoylation of bovine opsin and its cysteine mutants in COS cells. *Proc. Natl. Acad. Sci. U.S.A.* **90**: 40-44.

Karnik, S.S., Sakmar, T.P., Chen, H.B. and Khorana, H.G. (1988) Cysteine residues 110 and 187 are essential for the formation of correct structure in bovine rhodopsin. *Proc. Natl. Acad. Sci. U.S.A.* **85**: 8459-8463.

Katada, T., Bokoch, G.M., Northrup, J.K., Ui, M. and Gilman, A.G. (1984) The inhibitory guanine nucleotide-binding regulatory component of adenylate cyclase. Properties and function of the purified protein. *J. Biol. Chem.* **259**: 3568-3577.

Katada, T., Bokoch, G.M., Smigel, M.D., Ui, M. and Gilman, A.G. (1984) The inhibitory guanine nucleotide-binding regulatory component of adenylate cyclase. Subunit dissociation and the inhibition of adenyalte cyclase in S49 lymphoma cyc- and wild type membranes. *J. Biol. Chem.* **259**: 3586-3595.

Katada, T., Northrup, J.K., Bokoch, G.M., Ui, M. and Gilman, A.G. (1984) The inhibitory guanine nucleotide-binding regulatory component of adenylate cyclase. Subunit dissociation and guanine nucleotide-dependent hormonal inhibition. *J. Biol. Chem.* **259**: 3578-3585.

Kawate, N. and Menon, K.M.J. (1994) Palmitoylation of leutenising hormone/human choriogonadotropin receptors in transfected cells. *J. Biol. Chem.* **269**: 30651-30658.

Keith, D.E., Murray, S.R., Zaki, P.A., Chu, P.C., Lissin, D.V., Kang, L., Evans, C.J. and von Zastrow, M. (1996) Morphine activates opioid receptors without causing their rapid internalisation. *J. Biol. Chem.* **271**: 19021-19024.

Kennedy, M.E. and Limbird, L.E. (1993) Mutations of the α_{2A}-adrenergic receptor that eliminate detectable palmitoylation do not perturb receptor-G-protein coupling. *J. Biol. Chem.* **268**: 8003-8011.

Kim, D., Lewis, D.L., Graziadei, L., Neer, E.J., Bar-Sagi, D. and Clapham, D.E. (1989) G-protein betagamma-subunits activate the cardiac muscarinic K+-channel *via* phospholipase A_2. *Nature* **337**: 557-560.

Kim, H.O., Ji, X.D., Siddiqi, S.M., Olah, M.E., Stiles, G.L. and Jakobson, K.A. (1994) 2-substitution of N6-benzyladenosine-5'-uronamides enhances selectivity for A_3 adenosine receptors. *J. Med. Chem.* **37**: 3614-3621.

Kim, Y-C., Ji, X-d., Malman, N., Linden, J. and Jacobcon, K.A. (2000) Anilide derivatives of an 8-phenylxanthine carboxylic congener are highly potent and selective antagonists at human A_{2B} adenosine receptors. *J. Med. Chem.* **43**: 1165-1172.

Kirshenbaum, L.A. (1999) Bcl-2 intersects the NFκB signalling pathway and suppresses apoptosis in ventricular myocytes. *Clin. Invest. Med.* **23**: 322-330.

Klotz, K.N., Hessling, J., Hegler, J., Owman, C., Kull, B., Fredholm, B.B. and Lohse, M.J. (1998) Comparative pharmacology of human adenosine receptor subtypes – characterisation of stably transfects receptors in CHO cells. *Naun. Schmied. Arch. Pharmacol.* **357**: 1-9.

Klotz, K.N., Lohse, M.J. and Schwabe, U. (1998) Chemical modification of A_1 adenosine receptors in rat brain membranes. Evidence for histidine in different domains of the ligand binding site. *J. Biol. Chem.* **263**: 17522-17526.

Kobilka, B. (1992) Adrenergic receptors as models for G protein-coupled receptors. *Annu. Rev. Neurosci.* **15**: 87-114.

Koch, W.J., Inglese, J., Stone, W.C. and Lefkowitz, R.J. (1993) The binding site for the bg-subunits of heterotrimeric G proteins on the b-adrenergic receptor kinase. *J. Biol. Chem.* **268**: 8256-8260.

Koenig, J.A. and Edwardson, J.M. (1996) Intracellular trafficking of the muscarinic acetylcholine receptor: importance of subtype and cell type. *Mol. Pharmacol.* **49**: 351-359.

Koenig, J.A. and Edwardson, J.M. (1997) Endocytosis and recycling of G protein-coupled receptors. *TiPS.* **18**: 276-287.

Koenig, J.H. and Ikeda, K. (1989) Disappearance and reformation of synaptic vesicle membrane upon transmitter release observed under reversible blockage of membrane retrieval. *J. Neurosci.* **9**: 3844-3860.

Kohno, Y., Ji, X-d., Mawhorter, S.D., Koshiba, M. and Jacobson, K.A. (1996) Activation of A_3 adenosine receptors on human eosinophils elevates intracellular calcium. *Blood* **88**: 3569-3574.

Kojro, E. and Fahrenholz, F. (1995) Ligand-induced cleavage of the V_2 vasopressin receptor by a plasma membrane metalloproteinase. *J. Biol. Chem.* **270**: 6476-6481.

Konig, B., Arendt, A., McDowell, Kahlert, M., Hargrave, P.A. and Hofmann, K.P. (1989) Three cytoplasmic loops of rhodopsin interact with transducin. *Proc. Natl. Acad. Sci. USA* **86**: 6878

Konig, B., Arendt, A., McDowell, J.H., Kahlert, M., Hargrave, P.A. and Hofmann, K.P. (1989) Three cytoplasmic loops of rhodopsin interact with transducin. *Proc. Natl. Acad. Sci. U.S.A.* **86**: 6878-6882.

Kornfeld, S. and Mellman, I. (1989) The biogenesis of lysosomes. *Ann. Rev. Cell Biol.* **5**: 483-525.

Koshimizu, T., Tsujimoto, G., Ono, K., Masaki, T. and Sakamoto, A. (1995) Truncation of the receptor carboxyl terminus impairs signalling but not ligand binding of human ET_B endothelin receptor. *Biochem. Biophys. Res. Commun.* **217**: 354-362.

Kowluru, A., Seavey, S.E., Rhodes, C.J. and Metz, S.A. (1996) A novel regulatory mechanism for trimeric GTP-binding proteins in the membrane and secretory granule fractions of human and rodent beta cells. *Biochem. J.* **313**: 97-107.

Kozak, M. (1989) The scanning model for translation: an update. *J. Cell Biol.* **108**: 229-241.

Krupnick, J.G. and Benovic, J.L. (1998) The role of receptor kinases and arrestins in G protein-coupled receptor regulation. *Ann. Rev. Pharmacol. Toxicol.* **38**: 289-319.

Krupnick, J.G., Goodman Jr., O.B., Keen, J.H. and Benovic, J.L. (1997b) Arrestin/clathrin interaction: localisation of the clathrin binding domain of non-visual arrestins to the carboxyl terminus. *J. Biol. Chem.* **272**: 15011-15016.

Krupnick, J.G., Santini, F., Gagnon, A.W., Keen, J.H. and Benovic, J.L. (1997a) Modulation of the arrestin-clathrin interaction in cells: characterisation of β-arrestin dominant-negative mutants. *J. Biol. Chem.* **272**: 32507-32512.

Kuhn, H., Hall, S.W. and Wilden, U. (1984) Light-induced binding of 48-kDa protein to photoreceptor membranes is highly enhanced by phosphorylation of rhodopsin. *FEBS Letts.* **176**: 473-478.

Kunapuli, P. and Benovic, J.L. (1993) Cloning and expression of GRK5: a member of the G protein-coupled receptor kinase family. *Proc. Natl. Acad. Sci. U.S.A.* **90**: 5588-5592.

Kunapuli, P., Gurevich, V.V and Benovic, J.L. (1994) Phospholipid-stimulated autophosphorylation activates the G protein-coupled receptor kinase GRK5. *J. Biol. Chem.* **269**: 10209-10212.

Lamaze, C., Chuang, T-H., Terlecky, L. J., Bokoch, G.M., Schmid, S.L. (1996) Regulation of receptor-mediated endocytosis by Rho and Rac. *Nature* **382**: 177-179

Leff, P. (1995) The two-state model of receptor activation. *TiPS* **16** :259-60.

Lefkowitz, R.J. (1992) G proteins. The subunit story thickens. *Nature* **358**: 424-426.

Lefkowitz, R.J. (1993) Turned on to ill effect. *Nature* **365**: 603-604.

Lefkowitz, R.J. (1998) G protein-coupled receptors. *J. Biol. Chem.* **273**: 18677-18680.

Li, A.H., Moro, S., Melman, N., Ji, X.D. and Jacobson, K.A. (1998) Structure-activity relationships and molecular modeling of 3,5-diacyl-2,4-dialkylpyridine derivatives as selective A_3 adenosine receptor antagonists. *J. Med. Chem.* **41**: 3186-3201

Li, J-G., Luo, L-Y., Krupnick, J.G., Benovic, J.L and Liu-Chen, L-Y. (1999) U50, 488H-induced internalisation of the human κ opioid receptor involves a β-arrestin- and dynamin-dependent mechanism. *J. Biol. Chem.* **274**: 12087-12094.

Liang, B.T. (1998b) Protein kinase C-dependent activation of K_{ATP} channel enhances adenosine-induced cardioprotection. *Biochem. J.* **336**: 337-343.

Liang, B.T. and Jacobson, K.A. (1998a) A physiological role of the adenosine A_3 receptor: sustained cardioprotection. *Proc. Natl. Acad. Sci. USA* **95**: 6995-6999.

Libert, F., Van Sande, J., Lefort, A., Czernilofsky, A., Dumont, J.E., Vassart, G., Ensinger, H.A. and Mendla, K.D. (1992) Cloning and functional characterisation of a human A_1 adenosine receptor. *Biochem. Biophys. Res. Comms.* **187**: 919-926.

Lichte, B., Vah, R.W., Meyer, H.E. and Kilimann, M.W. (1992) Amphiphysin, a novel protein associated with synaptic vesicles. *EMBO J.* **11**: 2521-2530.

Lin, F.T., Krueger, K.M., Kendall, H.E., Daaka, Y., Fredericks, Z.L., Pitcher, J.A. and Lefkowitz, R.J. (1997) Clathrin-mediated endocytosis of the beta-adrenergic receptor is regulated by phosphorylation/dephosphorylation of beta-arrestin1. J. Biol. Chem. 272: 31051-31057.

Lin, F-T., Daaka, Y. and Lefkowitz, R.J. (1998) β-arrestins regulate mitogenic signalling and clathrin-mediated endocytosis of the insulin-like growth factor I receptor. *J. Biol. Chem.* **273**: 31640-31643.

Linden, J. (1994) Cloned adenosine A_3 receptors: pharmacological properties, species differences and receptor functions. *TiPS.* **15**: 298-306.

Linden, J. (2001) Molecular approach to adenosine receptors: receptor-mediated mechanisms of tissue protection. *Ann. Rev. Pharmacol. Toxicol.* **41**: 775-787.

Linden, J., Auchampach, J.A., Jin, X. and Figler, R.A. (1998) The structure and function of A_1 and A_{2B} adenosine receptors. *Life Sci.* **62**: 1519-1524.

Linden, J., Taylor, H.E., Robeva, A.S., Tucker, A.L., Stehle, J.H., Rivkees, S.A., Fink, J.S. and Reppert, S.M. (1993) Molecular cloning and functional expression of a sheep A_3 adenosine receptor with widespread tissue distribution. *Mol. Pharmacol.* **44**: 524-532.

Liu, X. Davis, D. and Segaloff, D.L. (1993) Disruption of potential sites for N-linked glycosylation does not impair hormone binding to the lutropin/choriogonadotropin receptor if Asn-173 is left intact. *J. Biol. Chem.* **268**: 1513-1516.

Lohse MJ. Klotz KN. Schwabe U. Cristalli G. Vittori S. Grifantini M. (1988) 2-Chloro-N6-cyclopentyladenosine: a highly selective agonist at A_1 adenosine receptors. *Naunyn-Schmiedebergs Arch. of Pharmacol.* **337**: 687-689.

Lohse, M., Benovic, J.L., Codina, J., Caron, M.G. and Lefkowitz, R.L. (1990) β-arrestin: a protein that regulates β-adrenergic receptor function. *Science* **248**: 1547-1549.

Lohse, M.J., Klotz, K.N., Lidenborn-Fotinos, J., Reddington, M., Schwabe, U. and Olsson, R.A. (1987) 8-Cyclopentyl-1,3-dipropylxanthine (DPCPX)—a selective high affinity antagonist for A_1 adenosine receptors. *Naun. Schmied. Arch. Pharmacol.* **336**: 204-210.

Loisel, T.P., Adam, L., Hebert, T.E. and Bouvier, M. (1996) Agonist stimulation increases the turnover rate of β_2AR-bound palmitate and promotes receptor depalmitoylation. *Biochem.* **35**: 15923-15932.

Londos, C., Cooper, D.M. and Wolff, J. (1980) Subclasses of external adenosine receptors. *Proc. Natl. Acad. Sci. U.S.A.* **77**: 2551-2554.

Lorenz, W., Inglese, J., Palczewski, K., Onorato, J.J., Caron, M.G. and Lefkowitz, R.J. (1991) The receptor kinase family: primary structure of rhodopsin kinase reveals similarities to the β-adrenergic receptor kinase. *Proc. Natl. Acad. Sci U.S.A.* **88**: 8715-8719.

Lui, G.S., Richards, S.C., Olsson, R.A., Mullane, K., Walsh, R.S. and Downey, J.M. (1994) Evidence that the adenosine A_3 receptor may mediate the protection afforded by preconditioning in the isolated rabbit heart. *Cardiovasc. Res.* **28**: 1057-1061.

Lupica, C.R., Cass, W.A., Zahniser, N.R. and Dunwiddie, T.V. (1990) Effects of the selective adenosine A_2 receptor agonist CGS21680 on in vitro electrophysiology, cAMP formation and dopamine release in rat hippocampus and striatum. *J. Pharmacol. Expt. Ther.* **252**: 1134-1141.

Luttrell, L.M., Daaka, Y. and Lefkowitz, R.J. (1999b) Regulation of tyrosine kinase cascades by G-protein-coupled receptors. *Curr. Opin. Cell. Biol.* **11**: 177-183.

Luttrell, L.M., Daaka, Y., Della Rocca, G.J. and Lefkowitz, R.J. (1997) G Protein-coupled Receptors Mediate Two Functionally Distinct Pathways of Tyrosine Phosphorylation in Rat 1a Fibroblasts. Shc phosphorylation and receptor endocytosis corelate with activation of Erk kinases. *J. Biol. Chem.* **272**: 31648-31656.

Luttrell, L.M., Ferguson, S.S.G., Daaka, Y., Miller, W.E., Maudsley, S., Della Rocca, G.J., Lin, F-T., Kawakatsu, H., Owada, K., Luttrell, D.K., Caron, M.G. and Lefkowitz, R.J. (1999a) β-arrestin-dependent formation of β_2 adrenergic receptor-Src protein kinase complexes. *Science* **283**: 655-661.

Maenhaut, C., Van Sande, J., Libert, F., Abramowicz, M., Parmentier, M., Vanderhaegen, J.J., Dumont, J.E., Vassart, G. and Schiffmann, S. (1990) RDC8 codes for an adenosine A_2 receptor with physiological constitutive activity. *Biochem. Biophys. Res. Comms.* **173**: 1169-1178.

Mahan, L.C., McVittie, L.D., Smyk-Randall, E.M., Nakata, H., Monsma Jr., F.J., Gerfen, C.R. and Sibley, D.R. (1991) Cloning and expression of an A_1 adenosine receptor from rat brain. *Mol. Pharmacol.* **40**: 1-7.

Marquardt, D.L., Gruber, H.E. and Wasserman, S.I. (1984) Adenosine releasef rom stimualted mast cells. *Proc. Natl. Acad. Sci. USA* **81**: 6192-6196.

Marquardt, D.L., Walker, L.L. and Heinemann, S. (1994) Cloning of two adenosine receptor subtypes from mouse bone marrow-derived mast cells. *J. Immunol.* **152**: 4508-4515.

Masu, M., Tanabe, Y., Tsuchida, K., Shigemoto, R. and Nakanishi, S. (1991) Sequence and expression of a metabotropic glutamate receptor. *Nature* **349**: 760-765.

Masuda, M., Sukehiro, S., Mollhoff, T., Van Belle, H. and Flameng, W. (1993) Effect of nulcleoside transport inhibition and hypoxanthine accumulation in the ischaemic human myocardium. *Archives Internationales de Pharmacodynamie et de Therapie.* **322**: 45-54.

McLean, A.J., Bevan, N., Rees, S. and Milligan, G. (1999) Visualising differences in ligand regulation of wild-type and constitutively active mutant β_2-adrenergic-green flourescent protein fusion proteins. *Mol. Pharmacol.* **65**: 1182-1191.

McMahon, H.T., Wigge, P. and Smith, C. (1997) Clathrin interacts specifically with amphiphysin and is displaced by dynamin. *FEBS Letts.* **413**: 319-322.

Merrifield, C.J., Moss, S.E., Ballestrem, C., Imhof, B.A., Giese, G., Wunderlich, I. And Almers, W. (1999) Endocytic vesicles move at the tips of actin tails in cultured mast cells. *Nature Cell. Biol.* **1**: 72-74.

Meyerhof, W., Paust, H.J., Schonrock, C. and Richter, D. (1991) Cloning of a cDNA encoding a novel putative G-protein-coupled receptor expressed in specific rat brain regions. *DNA Cell Biol.* **10**: 689-694.

Milligan, G. and Rees, S. (1999) Chimaeric G_a proteins: their potential use in drug discovery. *TiPS* **20**:118-124.

Milligan, G., Parenti, M. and Magee, A.I. (1995) The dynamic role of palmitoylation in signal transduction. *TiBS.* **20**: 181-186.

Moffett, S., Mouillac, B, Bonin, H. and Bouvier, M. (1993) Altered phosphorylation and desensitisation patterns of a human β_2-adrenergic receptor lacking the palmitoylated Cys341. *EMBO J.* **12**: 349-356.

Mori, S., Tanaka, K., Omura, S. and Saito, Y. (1995) Degredation process of ligand-stimulated platelet-derived growth factor β-receptor involves ubiquitin-proteasome protoelytic pathway. *J. Biol. Chem.* **270**: 29447-29452.

Moriarty, T.M., Padrell, E., Carty, D.J., Omri, G., Landau, E.M. and Iyengar R. (1990) G_o protein as signal transducer in the pertussis toxin-sensitive phosphatidylinositol pathway. *Nature* **343**: 79-82.

Morise, H., Shimomura, O., Johnson, F.H. and Winant, J. (1974) Intermolecular energy transfer in the bioluminescent system of Aequorea. *Biochem.* **13**: 2656-2652.

Morris, A.J. and Scarlata, S. (1997) Regulation of effectors by G-protein α and $\beta\gamma$-subunits. Recent insights from studies of the phospholipase c-β isoenzymes. *Biochem. Pharmacol.* **54**: 429-435.

Morrison, D.F., O'Brien, P.J. and Pepperberg, D.R. (1991) Depalmitoylation with hydroxylamine alters the functional properties of rhodopsin. *J. Biol. Chem.* **266**: 20118-20123.

Mumby, S.M. (1997) Reversible palmitoylation of signalling proteins. *Curr. Op. Cell Biol.* **9**: 148-154.

Mundell, S. and Benovic, J.L. (2000) Selective regulation of endogenous G protein-coupled receptors by arrestins in HEK293 cells. *J. Biol. Chem.* **275**: 12900-12908.

Munshi, R., Pang, I.H., Sternweis, P.C. and Linden, J. (1991) A_1 adenosine receptors of bovine brain couple to guanine nucleotide-binding proteins G_{i1}, G_{i2} and G_o. *J. Biol. Chem.* **266**: 22285-22289.

Muntz, K.H., Sternweis, P.C., Gilman, A.G. and Mumby, S.M. (1992) Influence of γ subunit prenylation on association of guanine nucloetide-binding regulatory proteins with membranes. *Mol. Biol. Cell.* **3**: 49-61.

Murakami, A., Yajima, T., Sakuma, H., McLaren, M.J. and Inana, G. (1993) X-arrestin: a new retinal arrestin mapping to the X chromosome. *FEBS Letts.* **334**: 203-209.

Murga, C., Esteban, N., Ruiz-Gómez, A. and Mayor Jr., F. (1997) The basal subcellular distribution of β-adrenergic receptor kinase is independent of G-protein βγ subunits. *FEBS Letts.* **409**: 24-28.

Murga, C., Laguinge, L., Wetzker, R., Cuadrado, A. and Gutkind, J.S. (1998) Activation of Akt/protein kinase B by G protein-coupled receptors. A role for α and βγ subunits of heterotrimeric G proteins acting through phosphatidylinositol-3-OH kinaseγ. *J. Biol. Chem.* **273**: 19080-19085.

Murga, C., Ruiz-Gómez, A., García-Higuera, I, Kim, C.M., Benovic, J.L. and Mayor Jr., F. (1996) High affinity binding of β-adrenergic receptor kinase to microsomal membranes: modulation of the activity of bound kinase by heterotrimeric G-protein activation. *J. Biol. Chem.* **271**: 985-994.

Ng, G.Y. Mouillac, B., George, S.R., Caron, M., Dennis, M., Bouvier, M. and O'Dowd, B.F. (1994) Desensitization, phosphorylation and palmitoylation of the human dopamine D1 receptor. *Eur. J. Pharmacol.* **267**: 7-19

Ng, G.Y.K., George, S.R., Zastawny, R.L., Caron, M., Bouvier, M., Dennis, M. and O'Dowd, B.F. (1993) Human serotonin$_{1B}$ receptor expression in Sf9 cells - phosphorylation, palmitoylation and adenylyl cyclase inhibition. *Biochemistry* **32**: 11727-11733.

Northup, J.K., Sternweis, P.C., Smigel, M.D., Schleifer, L.S., Ross, E.M. and Gilman, A.G. (1980) Purification of the regulatory component of adenylate cyclase. *Proc. Natl. Acad. Sci. USA* **77**: 6516-6520.

Nurnberg, B., Gudermann, T. and Schultz, G. (1995) Receptors and G proteins as primary components of transmembrane signal transduction. Part 2. G proteins: structure and function. *J. Mol. Med.* **73**: 123-132.

Nussenzveig, D.R., Heinflink, M. and Gershengorn, M.C. (1993) Agonist-stimulated internalisation of the thyrotropin-releasing hormone receptor is dependent on two domains in the receptor carboxyl terminus. *J. Biol. Chem.* **268**: 2389-2392.

O'Dowd, B.F., Hnatowich, M., Caron, M.G., Lefkowitz, R.J. and Bouvier, M. (1989) Palmitoylation of the human β_2-adrenergic receptor - mutation of Cys^{341} in the carboxyl tail leads to an uncoupled non-palmitoylated form of the receptor. *J. Biol. Chem.* **264**: 7564-7569.

Ohguru, H., Fukada, Y., Takao, T., Shimonishi, Y., Yoshizawa, T. and Akino, T. (1991) Carboxyl methylation and farnesylation of transducin g-subunit synergistically enhance its coupling with metarhodopsin II. *EMBO J.* **10**: 3669-3674.

Ohyama, K., Yamano, Y., Chaki, S., Kondo, T. and Inagami, T. (1992) Domains for G-protein coupling in angiotensin II receptor type I: studies by site-directed mutagenesis. *Biochem. Biophys. Res. Commun.* **189**: 677

Okamoto, P.M., Herskovits, J.S. and Vallee, R.B. (1997) Role of the basic, prolin-rich region of dynamin in Src homology 3 binding and endocytosis. *J. Biol. Chem.* **272**: 11629-11635.

Okamoto, T. and Nishimoto, I. (1992) Detection of G protein-activator regions in M4 subtype muscarinic cholinergic and α_2-adrenergic receptors based upon characteristics in primary structure. *J. Biol. Chem.* **267**: 8342-8346.

Okamoto, T., Schlegel, A., Scherer, P.E. and Lisanti, M.P. (1998) Caveolins, a family of scaffolding proteins for organising 'pre-assembled signalling complexes' at the plasma membrane. *J. Biol. Chem.* **273**: 5419-5422.

Oksche, A., Boese, G., Horstmeyer, A., Furkert, J., Beyermann, M., Bienert, M. and Rosenthal, W. (2000) Late endosomal/lysosomal targeting and lack of recycling of ligand-occupied endothelin B receptor. *Mol. Pharmacol.* **57**: 1104-1113

Olah M.E. (1997) Identification of A_{2A} adenosine receptor domains involved in selective coupling to Gs. Analysis of chimeric A_1/A_{2A} adenosine receptors. *J. Biol. Chem.* **272**: 337-344.

Olah, M.E. and Stiles, G.L. (1995) Adenosine receptor subtypes: characterisation and therapeutic regulation. *Ann. Rev. Pharmacol. Toxicol.* **35**: 581-606.

Olah, M.E., Gallo-Rodriguez, C., Jacobson, K.A. and Stiles, G.L. (1994) ^{125}I-4-aminobenzyl-5'-methylcarboxamidoadenosine, a high affinity radioligand for the rat A_3 adenosine receptor. *Mol. Pharmacol.* **45**: 978-982.

Olah, M.E., Jacobson, K.A. and Stiles (1990) Purification and characterisation of bovine cerebral cortex A_1 adenosine receptor. *Arch. Biochem. Biophys.* **283**: 440-446.

Olah, M.E., Ren, H., Ostrowski, J., Jacobson, K.A. and Stiles, G.L. (1992) Cloning, expression and characterisation of the unique bovine A1 adenosine receptor. Studies on the ligand binding site by site-directed mutagenesis. *J. Biol. Chem.* **267**: 10764-10770.

Olate, J. and Allende, J.E. (1991) Structure and function of G proteins. *Pharmacol. &Therap.* **51**: 403-419.

Ongini, E. and Fredholm, B.B. (1996) Pharmacology of adenosine A_{2A} receptors. *TiPS* **17**: 364-372.

Ongini, E., Adami, M., Ferri, C. and Bertorelli, R. (1997) Adenosine A_{2A} receptors and neuroprotection. *Annals NY. Acad. Sci.* **825**: 30-48.

Ormo M. Cubitt AB. Kallio K. Gross LA. Tsien RY. Remington SJ. (1996) Crystal structure of the Aequorea victoria green fluorescent protein. *Science* **273**: 1392-1395.

Orsini, M.J. and Benovic, J.L. (1988) Characterisation of dominant negative arrestins that inhibit β_2-adrenergic receptor internalisaiton by distinct mechanisms. *J. Biol. Chem.* **273**:34616-34622.

Ovchinnikov Y.A., Abdulalv, N.G. and Bogachuck, A.S. (1988) Two adjacent cysteine residues in the C-terminal cytoplasmic fragment of bovine rhodopsin are palmitoylation. *FEBS Lett.* **230**: 1-5.

Owen, D.J., Wigge, P., Vallis, Y., Moore, J.D.A., Evans, P.R. and McMahon, H.T. (1998) Crystal structure of the amphiphysin-2 SH3 domain and its role in the prevention of dynamin ring formation. *EMBO J.* **17**: 5273-5285.

Palczewski, K., Pulvermuller, A., Buczylco, J. and Hofmann, K.P. (1991) Phosphorylated rhodopsin and heparin induce similar conformational changes in arrestin. *J. Biol. Chem.* **266**: 18649-18654.

Palmer, T.M. and Stiles, G.L. (1995a) Adenosine receptors. *Neuropharmacol.* **34**: 683-694.

Palmer, T.M. and Stiles, G.L. (1997) Identification of an A_{2A} adenosine receptor domain specifically responsible for mediating short-term desensitisation. *Biochem.* **36**: 832-838.

Palmer, T.M. and Stiles, G.L. (2000) Identification of the threonine residues controlling the agonist-dependent phosphorylation and desensitisation of the rat A_3 adenosine receptor. *Mol. Pharmacol.* **57**: 539-545.

Palmer, T.M., Benovic, J.L. and Stiles, G.L. (1995c) Agonist-dependent phosphorylation and desensitisation of the rat A_3 adenosine receptor: evidence for a G protein-coupled receptor kinase-mediated mechanism. *J. Biol. Chem.* **270**: 29607-29613.

Palmer, T.M., Benovic, J.L. and Stiles, G.L. (1996) Molecular basis for subtype-specific desensitisation of inhibitory adenosine receptors: analysis of a chimeric A_1-A_3 adenosine receptor. *J. Biol. Chem.* **271**: 15272-15278.

Palmer, T.M., Gettys, T.W. and Stiles, G.L. (1995b) Differential interaction with and regulation of multiple G-proteins by the rat A_3 adenosine receptor. *J. Biol. Chem.* **270**: 16895-16902.

Palmer, T.M., Gettys, T.W., Jacobson, F.A. and Stiles, G.L. (1994) Desensitisation of the canine A_{2A} adenosine receptor: delineation of multiple processes. *Mol. Pharmacol.* **45**: 1082-1094.

Palmer, T.M., Jacobson, K.A. and Stiles, G.L. (1992) Immunological identification of A_2 adenosine receptors by two antipeptide antibody preparations. *Mol. Pharmacol.* **42**: 391-397.

Palmer, T.M., Poucher, S.M., Jakobson, K.A. and Stiles, G.L. (1995c) ^{125}I-4-(2-[2-furyl][1,2,4]triazolo[2,3-a][1,3,5]triazin-5-yl-amino]ethyl)phenol, a high affinity antagonist radioligand selective for the A_{2A} adenosine receptor. *Mol. Pharmacol.* **48**: 970-974.

Pang, I.H. and Sternweis, P.C. (1990) Purification of unique α subunits of GTP-binding regulatory proteins (G proteins) by affinity chromatography with immobilized βγ subunits. *J. Biol. Chem.* **265**: 18707-18712.

Parent, J.L., Labrecque, P., Orsini, M.J. and Benovic, J.L. (1999) Internalisation of the TXA2 receptor α and β isoforms. Role of the differentially spliced COOH terminus in agonist-promoted receptor internalisation. *J. Biol. Chem.* **274**: 8941-8948.

Parent, J-L., Labrecque, P., Rochdi, M.D. and Benovic, J.L. (2001) Role of the differentially spliced carboxyl terminus in thromboxane A_2 receptor trafficking. *J. Biol. Chem.* **276**: 7079-7085.

Park, D., Jhon, D.Y., Kriz, R., Knopf, J. and Rhee, S.G. (1992) Cloning, sequencing, expression and G_q-independent activation of phospholipase C-β2. *J. Biol. Chem.* **267**: 16048-16055.

Park, D., Jhon, D.Y., Lee, C.W., Lee, K.H. and Rhee, S.G. (1993) Activation of phospholipase C isozymes by G protein βγ subunits. *J. Biol. Chem.* **268**: 4573-4576.

Parton, R.G. (1996) Caveolae and caveolins. *Curr. Op. Cell Biol.* **8**: 542-548.

Pearse, B.M. (1976) Clathrin: a unique protein associated with intracellular transfer of membrane by coated vesicles. *Proc. Natl. Acad. Sci. U.S.A.* **73**: 1255-1259.

Pearse, B.M. and Bretscher, M.S. (1981) Membrane recycling by coated vesicles. *Ann. Rev. Biochem.* **50**: 85-101.

Pearse, B.M. and Crowther, R.A. (1987) Structure and assembly of coated vesicles. *Annu. Rev. Biophys. Biophys. Chem.* **16**: 49-68.

Pearse, B.M. and Robinson, M.S. (1990) Clathrin, adaptors, and sorting. *Ann. Rev. Cell Biol.* **6**:151-171.

Peralta, E.G., Ashkenazi, A., Winslow, J.W., Smith, D.H., Ramachandran, J. and Capon, D.J. (1987) Distinct primary structures, ligand-binding properties and tissue-specific expression of four human muscarinic acetylcholine receptors. *EMBO J.* **6**: 3923-3929.

Petrou CP. Tashjian AH Jr. (1995) Evidence that the thyrotropin-releasing hormone receptor and its ligand are recycled dissociated from each other. *Biochem. J.* **306**: 107-13

Petrou, C., Chen, L. and Tashjian Jr., A.H. (1997) A receptor-G protein coupling-independent step in the internalisation of the thyrotropin-releasing hormone receptor. *J. Biol. Chem.* **272**: 2326-2333.

Pfister, C., Chabre, M., Plouet, J., Tuyen, V.V., De Kozak, Y., Faure, J.P. and Kuhn, H. (1985) Retinal S antigen identified as the 48K protein regulating light-dependent phosphodiesterase in rods. *Science* **228**: 891-893.

Phillips, W.J. and Cerione, R.A. (1992) Rhodopsin/transducin interactions. Characterisation of the binding of the transducin-βγ subunit complex to rhodopsin using fluorescence spectroscopy. *J. Biol. Chem.* **267**: 17032-17039.

Pierce, K.D., Furlong, T.J., Selbie, L.A. and Shine, J. (1992) Molecular cloning and expression of an adenosine A_{2B} receptor from human brain. *Biochem. Biophys Res Comms*. **187**: 86-93.

Pippig, S., Andexinger, S., and Lohse, M.J. (1995) Sequestration and recycling of β_2-adrenergic receptors permit receptor resensitisation. *Mol. Pharmacol.* **47**: 666-676.

Pitcher, J.A., Freedman, N.J. and Lefkowitz, R.J. (1998) G protein-coupled receptor kinases. *Ann. Rev. Biochem.* **67**: 653-692.

Pitcher, J.A., Inglese, J., Higgins, J.B., Arriza, J.L., Casey, P.J., Kim, C., Benovic, J.L., Kwatra, M.M., Caron, M.G. and Lefkowitz, R.J. (1992) Role of βγ subunits of G proteins in targeting the β-adrenergic receptor kinase to membrane-bound receptors. *Science* **257**: 1264-1267.

Pitcher, J.A., Touhara, K., Payne, E.S. and Lefkowitz, R.J. (1995) Pleckstrin homology domain-mediated membrane association and activation of the β-adrenergic receptor kinase requires coordinate interaction with $G_{\beta\gamma}$ subunits and lipid. *J. Biol. Chem.* **270**: 11707-11710.

Poucher, S.M., Keddie, J.R., Singh, P., Stoggall, S.M., Caulkett, P.W., Jones, G. and Coll, M.G. (1995) The in vitro pharmacology of ZM 241385, a potent, non-xanthine A_{2A} selective adenosine receptor antagonist. *Brit. J. Pharmacol.* **115**: 1096-1102.

Prasad, M.V.V.S., Dermott, J., Heasley, L.E., Johnson, G.L. and Dhanasekaran, N. (1995) Activation of Jun kinase/stress-activated protein kinase by GTPase-deficient mutants of $G\alpha_{12}$ and $G\alpha_{13}$. *J. Biol. Chem.* **270**: 18655-18659.

Premont, R.T., Inglese, J. and Lefkowitz, R.J. (1995) Protein kinases that phosphorylate activated G protein-coupled receptors. *FASEB J.* **9**: 175-182.

Premont, R.T., Koch, W.J., Inglese, J. and Lefkowitz, R.J. (1994) Identification, purification, and characterisation of GRK5, a member of the family of G protein-coupled receptor kinases. *J. Biol. Chem.* **269**: 6832-6841.

Prendergast, F.G. and Mann, K.G. (1978) Chemical and physical properties of aequorin and the green flourescent protein isolated from Aequorea forskalea. *Biochem.* **17**: 3448-3453.

Presley, J.F., Cloe, N.B., Schroer, T.A., Hirschberg, K., Zaal, K.J.M. and Lippincott-Schwartz, J. (1997) ER-to-golgi transport visualised in living cells. *Nature* **389**: 81-85.

Probst, W.C., Snyder, L.A., Schuster, D.I., Brosius, J. and Sealfon, S.C. (1992) Sequence alignment of the G-protein coupled receptor superfamily. *DNA Cell Biol.* **11**: 1-20.

Qualmann, B., Kessels, M.M. and Kelly, R.B. (2000) Molecular links between endocytosis and the actin cytoskeleton. *J. Cell Biol.* **150**: F111-F116.

Ralevic, V. and Burnstock, G. (1998) Receptors for purines and pyrimidines. *Pharmacol. Revs.* **50**: 413-492.

Ramkumar, V., Olah, M.E., Jacobson, K.A. and Stiles, G.L. (1991) Distinct pathways of desensitisation of A_1- and A_2-adenosine receptors in DDT1 MF-2 cells. *Mol. Pharmacol.* **40**: 639-647.

Ramkumar, V., Stiles, G.L., Beaven, M.A. and Ali, H. (1993) The A_3 adenosine receptor is the unique adenosine receptor which facilitates release of allergic mediators from mast cells. *J. Biol. Chem.* **268**: 16887-16890.

Rapoport, B., Kaufman, K.D. and Chazenbalk, G.D. (1992) Cloning of a member of the arrestin family from a human thyroid cDNA library. *Mol. Cell. Endocrinol.* **84**: R39-43.

Razack, E.M. and Zahra, A. (1981) Multi-drug treatment for reactions in leprosy. *Leprosy in India* **53**: 204-12

Reid, T., Furuyashiki, T., Ishizaki, T., Watanabe, G., Watanabe, N., Fujisawa, K., Moril, N., Madaule, P. and Narumiya, S. (1996) Rhotekin, a new putative target for rho bearing homology to a serine/threonine kinase, PKN, and rhophilin in the Rho-binding domain. *J. Biol. Chem.* **271**: 13556-13560.

Ren, H. and Stiles, G.L. (1994) Characterisation of the human A_1 adenosine receptor gene. Evidence for alternative splicing. *J. Biol. Chem.* **269**: 3104-3110.

Reppert, S.M., Weaver, D.R., Stehle, J.H. and Rivkees, S.A. (1991) Moleular cloning and characterisation of the rat A_1-adenosine receptor that is widely expressed in brain and spinal cord. *Mol. Endocrinol.* **5**: 1037-1048.

Resh, M.D. (1996) Regulation of cellular signalling by fatty acid acylation and prenylation of signal transduction proteins. *Cell. Signall.* **8**: 403-412.

Rivkees, S.A. and Reppert, S.M. (1992) RFL9 encodes an A_{2B} adenosine receptor. *Mol. Endocrinol.* **6**: 1598-1604.

Rodbell, M., Birnbaumer, L., Pohl, S.L. and Krans, H.M. (1971) The glucagon-sensitive adenylyl cyclase system in plasma membranes of rat liver. An obligatory role of guanylnucleoides in glucagon action. *J. Biol. Chem.* **246**: 1877-1882.

Roettger BF. Rentsch RU. Pinon D. Holicky E. Hadac E. Larkin JM. Miller LJ. (1995) Dual pathways of internalization of the cholecystokinin receptor. J. Cell Biol. 128: 1029-1041.

Ross, E.M. (1995) Protein modification. Palmitoylaiton in G protein signalling pathways. *Curr. Biol.* **5**: 107-109.

Rothman, J.E. and Schmid, S.L. (1986) Enzymatic recycling of clathrin from coated vesicles. *Cell* **46**: 5-9.

Rotin, D., Staub, O. and Haguenauer-Tsapis, R. (2000) Ubiquitination and endocytosis of plasma membrane proteins: role of Nedd4/Rsp5p family of ubiquitin-protein ligases. J. Memb. Biol. 176: 1-17.

Rozelle, A.L., Machesky, L.M., Yamamoto, M., Driessens, M.H.E., Insall, R.H., Roth, M.G., Luby-Phelps, K., Marriott, G., Hall., A. and Yin, H.L. (2000) Phosphatidylinositol 4,5-bisphosphate induces actin-based movement on reft-enriched vesicles through WASP-Arp2/3. *Curr. Biol.* **10**: 311-320.

Rudolphi, K.A., Schubert, P., Parkinson, F.E. and Fredholm, B.B. (1992) Neuroprotective role of adenosine in cerebral ischaemia. *TiPS* **13**: 439-445.

Sah, V.P., Seasholtz, T.M., Sagi, S.A. and Brown, J.H. (2000) The role of Rho in G protein-coupled receptor signal transduction. *Annu. Rev. Pharmacol. Toxicol.* **40**: 459-489.

Sajjadi, F.G. and Firestein, G.S. (1993) cDNA cloning and sequence analysis of the human A_3 adenosine receptor. *Biochimica et Biophysica Acta.* **1179**: 105-107.

Sajjadi, F.G., Boyle, D.L., Domingo, R.C. and Firestein, G.S. (1996) cDNA cloning and characterisation of A_3i an alternatively spliced rat A_3 adenosine receptor variant. *FEBS Letts.* **382**, 125-129.

Salvatore, C.A., Jacobson, M.A. Taylor, H.E., Linden, J. and Johnson, R.G. (1993) Molecular cloning and characterisation of the human A_3 adenosine receptor. *Proc. Natl. Acad. Sci. USA* **90**: 10365-10369.

Salvatore, C.A., Tilley, S.L., Latour, A.M., Fletcher, D.S., Koller, B.H. and Jacobson, M.A. (2000) Disruption of the A_3 adenosine receptor gene in mice and its effect on stimulated inflammatory cells. *J. Biol. Chem.* **275**: 4429-4434.

Saverse, T.M. and Fraser, C.M. (1992) *In vitro* mutagenesis and the search for structure-function relationships among G protein-coupled receptors. *Biochem. J.* **283**: 1-19.

Scheer A, Fanelli F, Costa T, De Benedetti PG and Cotecchia S (1996) Constitutively active mutants of the 1B-adrenergic receptor: Role of highly conserved polar amino acids in receptor activation. *EMBO J.* **15**: 3566-3578

Schlegel, A., Volonte, D., Engelman, J.A., Galbiati, F., Mehta, P., Zhang, X-L., Scherer, P.E. and Lisanti, M.P. (1998) Crowded little caves: structure and function of caveolae. *Cell. Signal.* **10**: 457-463.

Schmid, S.L. (1997) Clathrin-caoted vesicle formation and protein sorting: an integrated process. *Ann. Rev. Biochem.* **66**: 511-548.

Schmid, S.L. and Damke, H. (1995) Coated vesicles: a diversity of form and function. *FASEB J.* **9**:1445-1453.

Schubert, P., Heinemann, U. and Kolb, R. (1985) Differential effects of adenosine on pre-and postsynaptic calcium fluxes. Brain Res. 376: 382-386.

Schulein, R., Lorenz, D., Oksche, A., Wiesner, B., Hermosilla, R., Ebert, J. and Rosenthal, W. (1998) Polarised cell surface expression of the green flourescent-protein tagged vasopressin V_2 receptor in Madin Darby canine kidney cells. *FEBS Letts.* **441**: 170-176.

Schwartz, L.M., Myer, A., Kosz, L., Engelstein, M. and Maier, C. (1990) Activation of polyubiquitin gene expression during developmentally programmed cell death. *Neuron.* **5**: 411-419.

Segaloff, D.L. and Ascoli, M. (1992) The gonadotrophin receptors: insights from the cloning of their cDNAs. *Oxford Rev. Repro. Biol.* **14**: 141-168.

Segaloff, D.L. and Ascoli, M. (1993) The lutropin/choriogonadotropin receptor...4 years later. *Endoc. Rev.* **14**: 324-347.

Selbie, L.A. and Hill S.J. (1998) G protein-coupled receptor cross-talk: the fine-tuning of multiple receptor-signalling pathways. *TiPS* **19**: 87-93.

Sever, S., Muhlberg, A.B. and Schmid, S.L. (1999) Impairment of dynamin's GAP domain stimulates receptor-mediated endocytosis. *Nature* **398**: 481-486.

Severs, N.J. (1988) Caveolae: static inpocketings of the plasma membrane, dynamic vesicles or plain artifact? J. Cell Sci. 90: 341-348

Shaw, G. (1996) The pleckstrin homology domain: an intriguing multifunctional protein module. *Bioessays* **18**: 35-46.

Shepherd, R., Linden, J. and Duling, B.R. (1996) Adenosine-induced vasoconstriction in vivo: role of the mast cell and A_3 adenosine receptor. *Circ. Res.* **78**: 627-634.

Shibasaki, T., Moroi, K., Nishiyama, M., Zhou, J., Sakamoto, A., Masaki, T., Ito, K., Haga, T. and Kimura, S. (1999) Characterization of the carboxyl terminal-truncated endothelin B receptor coexpressed with G protein-coupled receptor kinase 2. Biochem. *Mol. Biol. Int.* **47**: 569-577.

Shichi, H. and Somers, R.L. (1978) Light-dependent phosphorylation of rhodopsin. Purification and properties of rhodopsin kinase. *J. Biol. Chem.* **253**: 7040-7046.

Shimomura, O. and Johnson, F.H. (1969) Properties of the bioluminescent protein aequorin. *Biochem.* **8**: 3991-7.

Shinohara, T., Dietzschold, B., Craft, C.M., Wistow, G., Early, J.J., Donoso, L.A., Horwitz, J. and Tao, R. (1987) Primary and secondary structure of bovine retinal S antigen. *Proc. Natl. Acad. Sci. U.S.A.* **84**: 6975-6979.

Shpetner, H.S. and Vallee, R.B. (1989) Identification of dynamin, a novel mechanochemical enzyme that mediates interactions between microtubules. *Cell* **59**: 421-432.

Sibley, D.R., Benovic, J.L., Caron, M.G. and Lefkowitz, R.J. (1987) Molecular mechanisms of beta-adrenergic receptor desensitization. Adv. Expt. Med. Biol. 221: 253-273.

Siddiqi, S.M., Jacobson, K.A., Esker, J.L., Olah, M.E., Ji, X.D., Melman, N., Tiwari, K.N., Secrist, J.A.3rd, Schneller, S.W., Cristalli, G., Stiles, G.L., Johnson, C.R. and Ijzerman, A.P. (1995) Search for new purine- and ribose-modified adenosine analogues as selective agonists and antagonists at adenosine receptors. *J. Med. Chem.* **38**:1174-1188.

Siesjo, B.K. And Bengtsson, F. (1989) Calcium fluxes, calcium antagonists, and calcium-related pathology in brain ischemia, hypoglycemia, and spreading depression: a unifying hypothesis. J. Cereb. Blood Flow Metab. 9: 127-140.

Simon, M.I., Strathmann, M.P. and Gautam, N. (1991) Diversity of G proteins in signal transduction. *Science* **252**: 802-808.

Simonds, W.F., Butrynski, J.E., Gautam, N., Unson. And Spiegel, A.M. (1991) G protein $\beta\gamma$ dimers. Membrane targeting reqiures subunt coexpression and intact γ C-A-A-X doamin. *J. Biol. Chem.* **266**: 5363-5366.

Smolenski, R.T., Kalsi, K.K., Zych, M., Kochan, Z. and Yacoub, M.H. (1998) Adenosine/ribose supply increases adenosine production and protects ATP pool in adenosine kinase-inhibited cardiac cells. *J. Mol. Cell Cardiol.* **30**: 673-683.

Stadel, J.M., Nambi, P., Shorr, R.G., Sawyer, D.F., Caron, M.G. and Lefkowitz, R.J. (1983) Catecholamine-induced desensitisation of turkey erythrocyte adenylate cyclase is assocaited with phosphorylation of the β-adrenergic receptor. *Proc. Natl. Acad. Sci. U.S.A.* **80**: 3173-3177.

Stambaugh, K., Jacobson, K.A., Jiang, J-L. and Liang, B.T. (1997) A novel cardioprotective function of adenosine A_1 and A_3 receptors during prolonged stimulated ischaemia. *Am. J. Physiol.* **273**: H501-H505.

Stehle, J.H., Rivkees, S.A., Lee, J.J., Weaver, D.R., Deeds, J.D. and Reppert, S.M. (1992) Molecular cloning and expression of the cDNA for a novel A2-adenosine receptor subtype. *Mol. Enocrinol.* **6**: 384-393.

Sterne-Marr, R., Gurevich, V.V., Goldsmith, P., Bodine, R.C., Sanders, C., Donoso, L.A. and Benovic, J.L. (1993) Polypeptide variants of β-arrestin and arrestin3. *J. Biol. Chem.* **268**: 15640-15648.

Sternweis, P.C. Northup, J.K., Hanski, E., Schleifer, L.S., Smgel, M.D. and Gilman, A.G. (1981) Purification and properties of the regulatory component (G/F) of adenylate cyclase. *Adv. Cyc. Nuc. Res.* **14**: 23-36.

Strader, C.D., Sigal, I.S. and Dixon, R.A. (1989) Mapping the functional domains of the b-adrenergic receptor. *Am. J. Resp. Cell & Mol. Biol.* **1**: 81-86.

Strasser, R.H., Sibley, D.R. and Lefkowitz, R.J. (1986) A novel catecholamine-activated adenosine cyclic 3',5'-phosphate independent pathway for β-adrenergic receptor phosphorylation in wild-type and mutant S49 lymphoma cells: mechanism of homologous desensitisation of adenylate cyclase. *Biochem.* **25**: 1371-1377.

Stryer, L. (1986) Biochemistry (4^{th} Edition). *W.H. Freeman and Co. Publishers.*

Sweitzer, S.M. and Hinshaw, J.E. (1998) Dynamin undergoes a GTP-dependent conformational change causing vesiculation. Cell. 93: 1021-9.

Takei, K., Slepnev, V.I. Haucke, V. and De Camilli, P. (1998) Functional partnership between amphiphysin and dynamin in clathrin-mediated endocytosis. Nature Cell Biol. 1: 33-39.

Tang, W.J. and Gilman, A.G. (1991) Type-specific regulation of adenylyl cyclase by g protein βγ. *Science* **254**: 1500-1503.

Tapon, N. and Hall, A. (1997) Rho, Rac and Cdc42 GTPases regulate the organisation of the cytoskeleton. *Curr. Opin. Cell. Biol.* **9**: 86-92.

Tarasova, N.I., Staubers, R.H., Choi, J.K., Hudson, E.A., Czerwinski, G., Miller, J.L., Pavlakis, G.N., Michejda, C.J. and Wank, S.A. (1997) Visualisation of G protein-coupled receptor trafficking with the aid of green fluorescent protein – endocytosis and recycling of cholycystokinin receptor type A. *J. Biol. Chem.* **272**: 14817-14824

Thourani, V.H., Nakamura, M., Ronson, R.S., Jordan, J.E., Zhao, Z-Q., Levy, J.H., Szlam, F., Guyton, R.A. and Vinten-Johansen, J. (1999) Adenosine A_3 receptor stimulation attenuates post-ischaemic dysfunction through K_{ATP} channels. *Am. J. Physiol.* **277**: H228-H235.

Tolbert, L.M. and Lameh, J. (1996) Human muscarinic cholinergic receptor Hm1 internalises *via* clathrin-coated vesicles. *J. Biol. Chem.* **271**: 17335-17342.

Townsend-Nicholson, A. and Shine, J. (1992) <Molecular cloning and characterisation of a human brain A_1 adenosine receptor. *Brain Res. Mol. Brain Res.* **16**: 365-370.

Tracey, W.R., Magee, W., Masamune, H., Kennedy, S.P., Knight, D.R., Buchholz, R.A. and Hill, R.J. (1997) Selective adenosine A_3 receptor stimulation reduces ischaemic myocardial injury in the rabbit. *Cardiovasc. Res.* **33**: 410-415.

Tracey, W.R., Magee, W., Masamune, H., Oleynek, J.J. and Hill, R.J. (1998) Selective activation of adenosine A_3 receptors with N6-(-3-chlorobenzyl)-5'-N-methylcarboxamidoadenosine (CB-MECA) provides carioprotection *via* K_{ATP} channel activation. *Cardiovasc. Res.* **40**: 138-145.

Trejo, J. and Coughlin, S.R. (1999) The cytoplasmic tails of protease-activated receptor-1 and substance-P receptor specify sorting to lysosomes versus recycling. *J. Biol. Chem.* **247**: 2216-2224.

Tsao, P. and von Zastrow, M. (2000a) Down-regulation of G protein-coupled receptors. *Curr. Opin. Cell Biol.* **10**: 365-369

Tsao, P.I. and von Zastrow, M. (2000b) Type-specific sorting of G-protein-coupled receptors after endocytosis. *J. Biol. Chem.* **275**: 11130-11140

Tsien, R.Y., Bacskai, B.J.and Adams, S.R. (1993) FRET for studying intracellular signalling. TiCB 3:242-245.

Tsien, R.Y. (1998) The green fluorescent protein. *Ann. Rev. Biochem.* **67**: 509-544.

Tucker, A.L. and Linden, J. (1993) Cloned receptors and cardiovascular responses to adenosine. *Cardiovasc. Res.* **27**: 62-67.

Tucker, A.L., Linden, J., Robeva, A.S., D'Angelo, D.D. and Lynch, K.R. (1992) Cloning and expression of a bovine adenosine A_1 receptor cDNA. *FEBS Letts.* **297**: 107-111.

Tycko, B. and Maxfield, F.R. (1982) Rapid acidification of endocytic vesicles containing α_2-macroglobulin. *Cell* **28**: 643-651.

Ulloa-Aguirre, A., Stanislaus, D., Janovic, J.A. and Conn, P.M. (1999) Structure-activity relationships of G protein-coupled receptors. *Arch. Med. Res.* **30**: 420-435.

Vallee, R.B. and Okamoto, P.M. (1995) The regulation of endocytosis: Identifying dynamin's binding partners. *TiCB* **5**: 43-47.

van Aelst, L. and D'Souza-Schorey, C. (1997) Rho GTPases and signalling networks. *Genes & Dev.* **11**: 2295-2322.

van Belle, H. (1993) Nucleoside transport inhibition: a therapeutic approach to cardioprotection *via* adenosine? *Cardiovasc. Res.* **27**: 68-76.

van Biesen, T., Hawes, B.E., Raymond, J.R., Luttrell, L.M., Koch, W.J. and Lefkowitz, R.J. (1996a) G_o-protein α-subunits activate mitogen-activated protein kinase *via* a novel protein kinase C-dependent mechanism. *J. Biol. Chem.* **271**: 1266-1269.

van Biesen, T., Luttrell, L.M., Hawes, B.E. and Lefkowitz, R.J. (1996b) Mitogenic signalling *via* G protein-coupled receptors. *Endocrin. Revs.* **17**: 698-714.

van Calker, D., Muller, M. and Hamprecht, B. (1979) Adenosine regulates *via* two different types of receptors, the accumulation of cylic AMP in cultured brain cells. *J. Neurochem.* **33**:999-1005.

van der Bliek, A.M., Redelmeier, T.E., Damke, H., Tisdale, E.J., Meyerowitz, E.M. and Schmid, S.L. (1993) Mutations in human dynamin block an intermediate stage in coated vesicle formation. *J. Cell Biol.* **122**: 553-563.

van Deurs, B., Peterson, O.W., Olsnes, S. and Sandvig, K. (1989) The ways of endocytosis. *Int. Rev. Cytol.* **117**: 131-177.

van Deurs, B., Peterson, O.W., Sandvig, K. and Olsnes, S. (1989) Endocytosis, intracellular transport and sorting of proteins. *Nordisk Medicin* **104**: 9-11.

Vickery, R.G. and von Zastrow, M. (1999) Distinct dynamin-dependent and – independent mechanisms target structurally homologous dopamine receptors to different endocytic membranes. *J. Cell Biol.* **144**: 31-43

von Heijne, G. (1990) The signal peptide. *J. Memb. Biol.* **115**: 195-201.

von Lubitz, D.K.J.E. (1997) Adenosine A_3 receptor and brain. A culprit, a hero or merely yet another receptor? *Annal. New York Acad. Sci.* **825**: 49-67.

von Lubitz, D.K.J.E., Lin, R.C-S., Popik, P., Carter, M.F. and Jacobson, K.A. (1994) Adenosine A_3 receptor stimulation and cerebral ischaemia. *Eur. J. Pharmacol.* **263**: 59-67.

von Lubitz, D.K.J.E., Lin, R.C-S., Boyd, M., Bischofberger, N. and Jacobson, K.A. (1999) Chronic administration of adenosine A_3 receptor agonist and cerebral ischaemia: neuronal and glial effects. *Eur. J. Pharmacol.* **367**: 157-163.

von Zastrow, M. and Kobilka, B.K. (1992) Ligand-regulated internalisation and endocytosis of human β_2-adrenergic receptors between the plasma membrane and endosomes containing transferrin receptors. *J. Biol. Chem.* **267**: 3530-3538.

Vrecl, M., Anderson, L., Hanyaloglu, a., McGregor, A.M., Groarke, D.A., Milligan, G., Taylor, P.L. and Eidne, K.A. (1998) Agonist-induced endocytosis and recycling of the gonadotropin-releasing hormone receptor: effect of β-arrestin on internalisation kinetics. *Mol. Endocrinol.* **12**: 1818-1829.

Wakshull, E., Hertel, C., O'Keefe, E.J. and Perkins, J.P. (1995) Cellular redistribution of beta-adrenergic receptors in a human astrocytoma cell line: a comparison with the epidermal growth factor receptor in murine fibroblasts. J. Cell. Biochem. 29: 127-41.

Wang, L.H., Sudhof, T.C. and Anderson, R.G. (1995) The appendage domain of α-adaptin is a high affinity binding site for dynamin. *J. Biol Chem.* **270**: 10079-10083.

Wedegaertner, P.B., Wilson, P.T. and Bourne, H.R. (1995) Lipid modifications of trimeric G-proteins. *J. Biol. Chem.* **270**: 503-506.

Whistler, J.L., Chuang, H-H., Chu, P., Jan, L.Y. and von Zastrow, M. (1999) Functional dissociation of u opioid receptor signalling and endocytosis: implications for the biology of opiate tolerance and addiction. *Neuron* **23**: 737-746.

Wieland, T., Nurnberg, B., Ulibarri, I., Kaldenberg-Stasch, S., Schultz G. and Jakobs, K.H. (1993) Guanine nucleotide-specific phosphate transfer by guanine nucleotide- binding regulatory protein beta-subunits. Characterization of the phosphorylated amino acid. *J. Biol. Chem.* **268**: 18111-18118.

Wigge, P. and McMahon, H.T. (1998) The amphiphysin family of proteins and their role in endocytosis at the synapse. *TiNS.* **21**: 339-344.

Wigge, P., Köhler, K., Vallis, Y., Doyle, C.A., Owen, D., Hunt, S.P. and McMahon, H.T. (1997) Amphiphysin heterodimers: potential role in clathrin-mediated endocytosis. *Mol. Biol. Cell* **8**: 2003-2015.

Wilkie, T.M., Scherle, P.A., Strathmann, M.P., Slepak, V.Z. and Simon, M.I. (1991) Characterisation of G- protein α subunits in the G_q class: expression in murine tissues and in stromal and haematopoietic cell lines. *Proc. Natl. Acad. Sci. USA* **88**: 10049-10053.

Williams, M. (1989) Adenosine antagonists. *Med. Res Revs.* **9**: 219-243.

Winegrad, S., Henrion, D., Rappaport, L. and Samual, J.L. (1999) Self-protectionby cardiac myocytes against hypoxia and hyperoxia. *Circ. Res.* **85**: 690-698.

Wu, G., Krupnick, J.G., Benovic, J.L. and Lanier, S.M. (1997) Interaction of arrestins with intracellular domains of muscarinic and α_2-adrenergic receptors. *J. Biol. Chem.* **272**: 17836-17842.

Yakel, J.L., Warren, R.A., Reppert, S.M. and North, R.A. (1993) Functional expression of adenosine A_{2B} receptor in Xenopus oocytes. *Mol. Pharmacol.* **43**: 277-280.

Yamashiro, D.J. and Maxfield, F.R. (1987) Kinetics of endosome acidification in mutant and wild-type Chinese hamster ovary cells. *J. Cell. Biol.* **105**: 2713-2721.

Yang F. Moss LG. Phillips GN Jr. (1996) The molecular structure of green fluorescent protein. *Nat. Biotech.* **14**: 1246-1251

Yang, T-T., Cheng, L. and Kain, S.R. (1996) optimised codon usage and chromophore mutations provide enhanced sensitivity with the green fluorescent protein. *Nucl. Acid Res.* **22**: 4592-4594.

Yano, M., Kanazawa, M., Terada, K., Namchai, C.,Yamaizumi, M., Hanson, B., Hoogenraad, N. and Mor, M. (1997) Visualisaiton of mitochondrial protein import in cultured mammalian cells with green fluorescent protein and effects of overexpression of the human import receptor Tom20. *J. Biol. Chem.* **272**: 8459-8465.

Yin, H.L. and Stull, J.T. (1999) Proteins that regulate dynamic actin remodelling in response to membrane signalling minireview series. *J. Biol. Chem.* **274**: 32529-32530.

Yu, S.S., Lefkowitz, R.J. and Hausdorff, W.P. (1992) β-adrenergic receptor sequestration. A potential mechanism of receptor resensitisation. *J. Biol. Chem.* **268**: 337-341.

Zhang, J., Barak, L.S., Anborgh, P.H., Laporte, S.A., Caron, M.G. and Ferguson, S.S.G. (1999) Cellular traffickingof G protein-coupled receptor/β-arrestin endocytic complexes. *J. Biol. Chem.* **274**: 10999-11006.

Zhang, J., Ferguson, S.S.G., Barak, L.S., Menard, L. and Caron, M.G. (1996) Dynamin and β-arrestin reveal distinct mechanisms for G protein-coupled receptor internalisation. *J. Biol. Chem.* **271**: 18302-18305.

Zhang, Y-Z. (1994) Novel fluorescent acidic organelle-selective dyes and mitochondrion-selective dyes that are well retained during cell fixation and permeabilisation. *Mol. Biol. Cell.* **5**: 113a-113c.

Zhong, C., Hayzer, D.J., Corson, M.A. and Runge, M.S. (1992) Molecular cloning of the rat vascular smooth muscle thrombin receptor. Evidence for *in vitro* regulation by basic fibroblast growth factor. *J. Biol. Chem.* **267**: 16975-16979.

Zhou, Q-Y., Li, M., Olah, M.E., Johnson, R.A., Stiles, G.L. and Civelli, O. (1992) Molecular cloning and characterisation of an adenosine recptor: the A_3 adenosine receptor. *Proc. Natl. Acad. Sci. USA* **89**: 7432-7436.

Zhu SZ, Wang SZ, Hu JR and Elfakahany EE (1994) An arginine residue conserved in most G-protein-coupled receptors is essential for the function of the M1 muscarinic receptor. *Mol Pharmacol.* **45**: 517-523

Zimmerman, B.J. and Granger, D.N. (1992) Reperfusion injury. *Surg. Clin. North Amer.* **72**: 65-83.

Zubay, G.L. (1998) Biochemistry (4^{th} Edition). *Wm.C. Brown Publishers.*

Appendix 1

Sample calculation for B_{max}

Bmax = nM = 0.03407

Molarity $= \frac{\text{moles}}{\text{v}}$

$\therefore$ moles = Molarity (M) x volume (L)

$= (0.03407 \times 10^{-9}) \times (250 \times 10^{-6})$

$=$ **8.5175 fmol**

Actual protein conc. $= \frac{0.500}{14}$ (dilution factor)

= 35.7µg/ml

0.15ml membranes added/tube = 0.15 x 35.7

= 5.355mg/tube

$\therefore$ 8.5175fmol in 5.355mg protein $= \frac{8.5175}{5.355}$

= 1.59 fmol/µg [= pmol/mg]

Appendix 2

Cheng-Prusoff Equation

$$K_i = \frac{EC_{50}}{1 + \frac{[Ligand]}{K_d}}$$